

**UNIVERSIDADE DE SÃO PAULO  
INSTITUTO DE QUÍMICA**

Programa de Pós-graduação em Ciências Biológicas (Bioquímica)

**LUCAS SOUZA DANTAS**

**Effect of secosterol aldehydes on Amyotrophic  
Lateral Sclerosis: study in animal model and SOD1  
aggregation *in vitro***

**Versão corrigida da Tese conforme Resolução CoPGr 5890**

**A original se encontra disponível na Secretaria de Pós-Graduação do IQ-USP**

São Paulo

Data do Depósito na SPG:  
**02/05/2018**

LUCAS SOUZA DANTAS

**Efeito de aldeídos de colesterol na Esclerose Lateral  
Amiotrófica: estudo em modelo animal e na  
agregação da SOD1 *in vitro***

*Tese apresentada ao Instituto de Química da  
Universidade de São Paulo para a obtenção do  
título de doutor em Ciências Biológicas  
(Bioquímica)*

*Orientador (a): Profa. Dra. Sayuri Miyamoto*

São Paulo  
2018

Autorizo a reprodução e divulgação total ou parcial deste trabalho, por qualquer meio convencional ou eletrônico, para fins de estudo e pesquisa, desde que citada a fonte.

Ficha Catalográfica elaborada eletronicamente pelo autor, utilizando o programa desenvolvido pela Seção Técnica de Informática do ICMC/USP e adaptado para a Divisão de Biblioteca e Documentação do Conjunto das Químicas da USP

Bibliotecária responsável pela orientação de catalogação da publicação:  
Marlene Aparecida Vieira - CRB - 8/5562

D192e	Dantas, Lucas Souza Effect of secosterol aldehydes on Amyotrophic Lateral Sclerosis: study in animal model and SOD1 aggregation in vitro / Lucas Souza Dantas. - São Paulo, 2018. 162 p.  Tese (doutorado) - Instituto de Química da Universidade de São Paulo. Departamento de Bioquímica. Orientador: Miyamoto, Sayuri  1. Aldeídos de colesterol. 2. Superóxido dismutase. 3. Esclerose Lateral Amiotrófica. I. T. II. Miyamoto, Sayuri, orientador.
-------	--



*Aos meus pais Moacir e Guiomar*

*“There should be no boundaries to human endeavor. We are all different. However bad life may seem, there is always something you can do, and succeed at. While there's life, there is hope”*

*Stephen Hawking*

## AGRADECIMENTOS

Agradeço a Deus por tudo que tenho e por ter conseguido, durante esses cinco anos, concluir mais essa etapa da minha vida profissional;

À professora Sayuri Miyamoto pela atenção e orientação durante o doutorado, além de todos os ensinamentos que me fizeram crescer profissionalmente. Obrigado por abrir as portas do laboratório e me dar a oportunidade de trabalhar na sua equipe.

Aos meus pais Moacir e Guiomar por serem os grandes responsáveis por eu chegar aonde cheguei, devo tudo isso a vocês. Agradeço também aos meus irmãos Amanda, Felipe e Flaviana e aos meus cunhados pelo apoio de sempre. Um agradecimento especial a Vó Zefa que sempre me incentivou a estudar e buscar meus objetivos. Agradeço também aos meus familiares de São Paulo que sempre me acolheram, em especial Tio Pedro, Tia Graça, Paty e Hugo. Vocês sempre serão como uma segunda família. Obrigado também a minha tia Joana pelo acolhimento e carinho.

À minha noiva Ray por estar sempre ao meu lado me apoiando em cada passo dado na minha vida. Obrigado por ser minha parceira em todos os momentos. Te amo!

Aos meus sogros Maria Perpétua e Batatinha pelo carinho e apoio de sempre. E um agradecimento especial à tia Iara por sempre me ajudar e incentivar.

Aos meus grandes amigos Adriano e Isabella pelo convívio diário desde o tempo de iniciação científica, faculdade e agora doutorado. Obrigado pela amizade, paciência e apoio durante todo esse tempo.

Aos colegas de laboratório Daniela Cunha, Patrícia Appolinário, Priscilla Derogis, Silvio Oliveira, Thiago Mattos, Nicole Noda, Alex Inague, Rodrigo de Faria, Karen Campos, Camila Roubik, Maria Fernanda e Marcos Yoshinaga pela ótima convivência, ensinamentos e discussões. Ao Marcos um agradecimento especial pela ajuda nas partes escritas. Agradeço

também aos técnicos Zilda Izzo, Adriana Wendel, Sirley Mendes, Izaura Toma, Fernando Coelho e Emerson Marques por todo o apoio e colaboração.

Aos colegas do IQ, em especial Vanderson, Chris, Adriana, Isabel, Marcela, Flávia Meotti e Albert pela amizade.

Ao professor Humberto Matos pela orientação na iniciação científica e aos amigos do LEOPAR, em especial João, Isaac, Fabiula, Daiane e Japa.

Aos professores colaboradores Ohara Augusto, Marisa Medeiros, Antônia do Amaral, e Miriam Uemi pela ajuda e contribuição no projeto.

A todos os professores e funcionários do IQ pelos serviços prestados.

Às agências de fomento CNPq, CAPES e FAPESP e à pro-reitoria de pesquisa da USP, pelo financiamento da pesquisa.



## RESUMO

DANTAS, L. S. **Efeito de aldeídos de colesterol na Esclerose Lateral Amiotrófica: estudo em modelo animal e na agregação da SOD1 *in vitro***. 2018. 162 p. Tese - Programa de Pós-Graduação em Ciências Biológicas (Bioquímica). Instituto de Química - Universidade de São Paulo - São Paulo.

Aldeídos de colesterol (Secosterol A e Secosterol B) têm sido detectados em amostras de cérebro humano e investigados em modelos de doenças neurodegenerativas como possíveis marcadores e intermediários do processo patológico. Estes oxisteróis constituem uma classe de eletrófilos derivados de lipídeos que podem modificar e induzir agregação de proteínas. A esclerose lateral amiotrófica (ELA) é um distúrbio neurodegenerativo associado ao acúmulo de agregados imunorreativos de superóxido dismutase (Cu, Zn-SOD, SOD1). O objetivo deste trabalho foi avaliar a presença de aldeídos de colesterol em ratos modelo ELA e sua capacidade de induzir a formação de agregados de SOD1 *in vitro*. Aldeídos de colesterol foram analisados no plasma, medula espinhal e córtex motor de ratos ELA. Uma quantidade elevada de Secosterol B foi detectada no córtex motor desses ratos em comparação com animais controle. Adicionalmente, os experimentos *in vitro* mostraram que Secosterol B e Secosterol A induziram a agregação da SOD1 em uma forma amiloidogênica que se liga à tioflavina T. Esta agregação não foi observada com o colesterol e os seus hidroperóxidos. Usando aldeídos de colesterol marcados com grupo alquil e um ensaio de *click chemistry*, foi observado que os agregados de SOD1 estão ligados covalentemente aos aldeídos. A modificação covalente da proteína foi confirmada por análise de MALDI-TOF, que mostrou a adição de até cinco moléculas de aldeídos de colesterol à proteína por base de Schiff. Curiosamente, a análise comparativa com outros eletrófilos derivados de lipídeos (e.g. HHE e HNE) demonstrou que a agregação de SOD1 aumentou proporcionalmente à hidrofobicidade dos aldeídos, observando-se a maior

agregação com aldeídos de colesterol. Os sítios de modificação da SOD1 foram caracterizados por nanoLC-MS/MS após digestão da proteína com tripsina, onde foram identificadas lisinas como o principal aminoácido modificado. Em geral, nossos dados mostram que a oxidação do colesterol que leva à produção de aldeídos de colesterol é aumentada no cérebro de ratos ELA e que os aldeídos altamente hidrofóbicos derivados de colesterol podem promover eficientemente modificação e agregação de SOD1.

Palavras-chave: Esclerose Lateral Amiotrófica, aldeídos de colesterol, doenças neurodegenerativas, superóxido dismutase.

## ABSTRACT

DANTAS, L. S. **Effect of secosterol aldehydes on Amyotrophic Lateral Sclerosis: study in animal model and SOD1 aggregation *in vitro***. 2018. 162 p. PhD Thesis - Graduate Program in Biochemistry. Instituto de Química - Universidade de São Paulo - São Paulo.

Secosterol aldehydes (Secosterol B and Secosterol A) have been detected in human brain samples and investigated in models of neurodegenerative diseases as possible markers and intermediates of the pathological process. These oxysterols constitute a class of lipid-derived electrophiles that can modify and induce aggregation of proteins. Amyotrophic lateral sclerosis (ALS) is a neurodegenerative disorder associated with the accumulation of immunoreactive aggregates of superoxide dismutase (Cu, Zn-SOD, SOD1). The objective of this work is to evaluate the presence of secosterol aldehydes in ALS rats and their ability to induce formation of SOD1 aggregates *in vitro*. Secosterol aldehydes were analyzed in plasma, spinal cord and motor cortex of ALS rats. A higher amount of Secosterol B was detected in the motor cortex of these rats compared to control animals. In addition, *in vitro* experiments have shown that Secosterol B and Secosterol A induce aggregation of SOD1 into an amyloidogenic form that binds to thioflavin T. This aggregation was not apparent in incubations with cholesterol and its hydroperoxides. Using alkynyl-labeled secosterol aldehydes and a click chemistry assay, it was found that the SOD1 aggregates are covalently linked to the aldehydes. Covalent modification of the protein was confirmed by MALDI-TOF analysis, which showed the addition of up to five molecules of secosterol aldehydes to the protein by Schiff base formation. Interestingly, the comparative analysis with other lipid-derived electrophiles (e.g. HHE and HNE) demonstrated that the aggregation of SOD1 increased according to the hydrophobicity of the aldehydes. Compared to the other electrophiles, a higher SOD1 aggregation was observed with secosterol aldehydes. SOD1 modification sites were characterized by nanoLC-MS/MS after

protein digestion with trypsin, revealing lysine as the major amino acid modified in these experiments. Collectively, our data show that cholesterol oxidation leads to the production of secoesterol aldehydes, which are increased in the brain of ALS rats, and that these highly hydrophobic aldehydes can efficiently promote the modification and aggregation of SOD1.

**Keywords:** Amyotrophic Lateral Sclerosis, secoesterol aldehydes, neurodegenerative diseases, superoxide dismutase.

## LIST OF ACRONYMS AND ABBREVIATIONS

$^1\text{O}_2$  - Singlet oxygen

a-Ch - Alkynyl-cholesterol

a-HNE - Alkynyl-4-hydroxynonenal

ALS - Amyotrophic lateral sclerosis

a-seco-A - alkynyl-Secosterol A

a-seco-B - alkynyl-Secosterol B

Ch - Cholesterol

ChOOH - Cholesterol hydroperoxide

CR - Congo red

Cys - Cysteine

DEC - 2,4-decadienal

DHA - Docosahexaenoic acid

DTPA - Diethylenetriaminepentaacetic acid

DTT - Dithiothreitol

HEX - 2-Hexen-1-al

HHE - 4-hydroxy Hexenal

His - Histidine

HNE - 4-hydroxy Nonenal

IAM - Iodoacetamide

IDA - Information Dependent Acquisition

LC-MS/MS - Liquid chromatography coupled to mass spectrometry

$\log P_{\text{calc}}$  - Theoretical partition coefficient

Lys - Lysine

MALDI-TOF MS - Matrix assisted laser desorption ionization - time-of-flight mass spectrometry

MDA - Malondialdehyde

NaBH<sub>4</sub> - Sodium borohydride

NON - 2,4-nonadienal

O<sub>3</sub> - Ozone

PBH - 1-Pyrenebutiric hydrazine

ROS - Reactive oxygen species

SDS-PAGE - Sodium dodecyl sulfate - polyacrylamide gel electrophoresis

SEC - Size exclusion chromatography

Seco-A - Secosterol A

Seco-B - Secosterol B

SOD1 - Superoxide Dismutase 1

TEM - Transmission electronic microscopy

ThT - Thioflavin T

TIC - Total ion chromatogram

WT - Wild type

XIC - Extracted ion chromatogram

## SUMMARY

1. INTRODUCTION.....	17
1.1 Lipid peroxidation.....	17
1.2 Lipid-derived electrophiles .....	18
1.3 Cholesterol and its oxidation products.....	22
1.4 <i>In vivo</i> formation of secosterol aldehydes .....	25
1.5 Protein modification by secosterol aldehydes .....	26
1.6 Amyotrophic Lateral Sclerosis (ALS) .....	29
1.7 SOD1 and ALS .....	30
1.8 Lipids and Neurodegenerative Diseases .....	32
1.9 Cholesterol and ALS.....	34
2. OBJECTIVES .....	36
CHAPTER 1 .....	37
<b>ABSTRACT</b> .....	38
<b>Highlights:</b> .....	39
<b>INTRODUCTION</b> .....	40
<b>MATERIALS AND METHODS</b> .....	42
1. Materials.....	42
2. ALS Rat Model .....	43
3. Quantification of Cholesterol and Secosterol Aldehydes .....	43
4. SOD1 aggregation experiments .....	43
5. Effects of pH and Secosterol Aldehyde Concentration on SOD1 Aggregation.....	44
6. Analysis of SOD1 Aggregates Morphology .....	44
7. Click Chemistry Assay.....	45
8. MALDI-TOF Analysis.....	46
9. Enzymatic Digestion of SOD1 and Peptide Analysis .....	46
<b>RESULTS</b> .....	47
1. Secosterol aldehydes are increased in the motor cortex of ALS rats .....	47
2. Secosterol aldehydes induce SOD1 aggregation <i>in vitro</i> .....	48
3. Aggregates Formed by Secosterol Aldehydes Have Amorphous Nature .....	50
4. SOD1 Aggregates are Bound to Secosterol Aldehydes .....	51
5. SOD1 is Modified Mainly at Lysine Residues.....	54
<b>DISCUSSION</b> .....	57

<b>Acknowledgments</b> .....	62
<b>References</b> .....	63
<b>Supporting information</b> .....	71
<b>CHAPTER 2</b> .....	74
<b>ABSTRACT</b> .....	75
<b>Highlights</b> .....	76
<b>INTRODUCTION</b> .....	77
<b>MATERIALS AND METHODS</b> .....	79
1. Chemicals .....	79
2. Theoretical LogP Determination .....	80
3. Incubations of SOD1 with the Aldehydes .....	80
4. Aggregate Formation Analysis by Size Exclusion Chromatography (SEC) .....	80
5. Enzymatic Digestion of SOD1 .....	81
6. Peptide Analysis by Liquid Chromatography Coupled to Mass Spectrometry (LC-MS/MS) .....	81
7. Covalent docking .....	82
8. Lipophilic surface generation .....	83
<b>RESULTS</b> .....	83
1. Aldehyde-induced SOD1 aggregation is dependent on the hydrophobicity .....	83
2. Aldehydes modify peptide residues of SOD1, especially lysines .....	84
3. Covalent docking .....	88
<b>DISCUSSION</b> .....	93
<b>Acknowledgments</b> .....	96
<b>References</b> .....	97
3. CONCLUSIONS AND FUTURE DIRECTIONS .....	147
4. REFERENCES .....	149
<b>CURRICULUM VITAE</b> .....	159

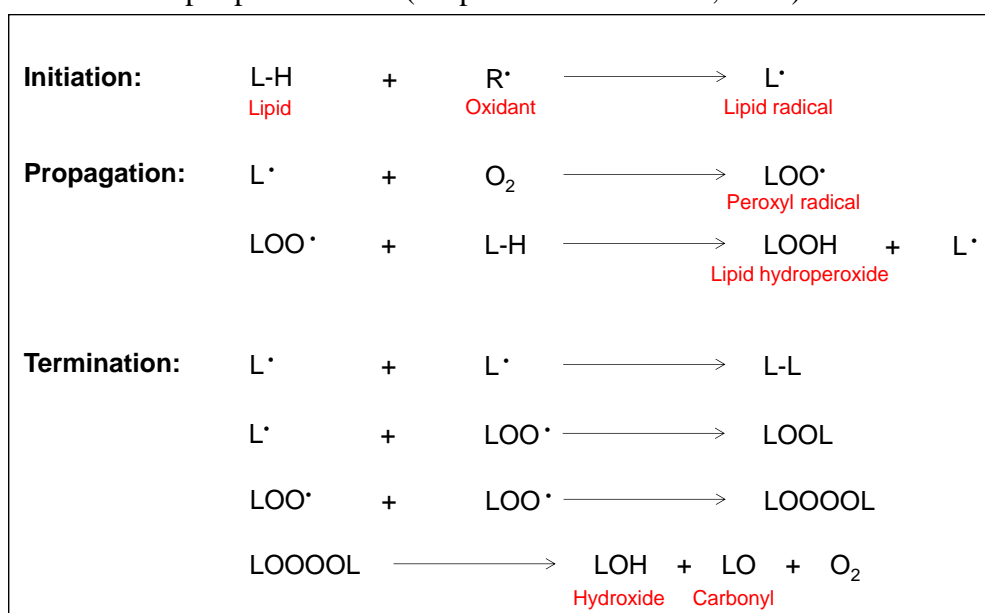


## 1. INTRODUCTION

### 1.1 Lipid peroxidation

Lipids are the major components of biological membranes and play important roles in the cell's physiology. In addition to the membrane's physical structure, they contribute to the cell homeostasis with fundamental roles such as controlling permeability and fluidity of membranes and acting as signaling molecules [1]. They are the most susceptible biomolecules to free radicals attack or oxidation by non-radical species in a process called lipid peroxidation. Such susceptibility is due to the presence of a high number of unsaturations in their structures [2-4]. Lipid peroxidation has been widely studied in the last decades and a link between this oxidative process and several diseases has been firmly established in neurodegenerative, cardiovascular and metabolic disorders [2–4]. Lipid peroxidation can be defined as a process by which oxidant species attack double bonds of lipids, thereby abstracting hydrogen and resulting in the formation of lipid-derived radicals, hydroperoxides and other oxidized products. It can be divided in three steps: (1) Initiation, (2) Propagation and (3) Termination [3,4] (Scheme 1).

**Scheme 1.** Lipid peroxidation (adapted from Yin et al., 2011).



## 1.2 Lipid-derived electrophiles

In addition to the generation of hydroperoxides, alcohols and ketones, lipid peroxidation may also yield aldehydes [3,5]. The most known and studied aldehydes are acrolein [6], malondialdehyde (MDA) [7], 4-hydroxy-2-hexenal (HHE) [8] and 4-hydroxy-2-nonenal (HNE) [9]. These lipid-derived electrophiles have been described as important intermediates in the pathogenesis of inflammatory and neurodegenerative diseases [10–16].

Acrolein can be formed endogenously by the oxidation of fatty acids from cell membranes or be consumed from dietary sources or even derived from air pollution [6]. The generation of acrolein by peroxidation of polyunsaturated fatty acids involves the formation of an intermediate hydroperoxide followed by  $\beta$ -cleavage of its correspondent alkoxy radical [17,18] (Figure 1).

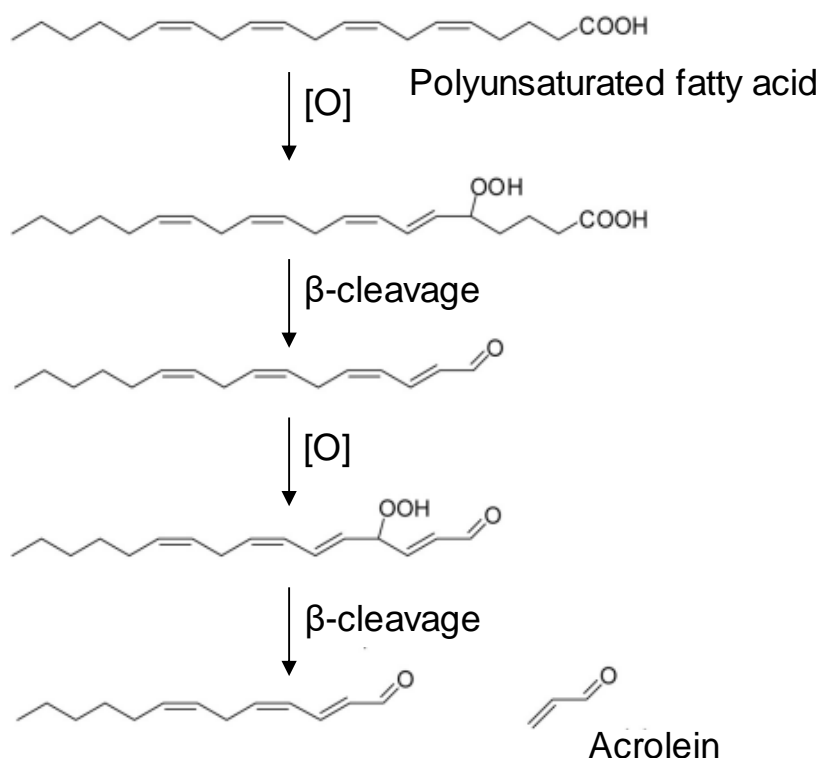


**Figure 1.** Mechanism of acrolein formation by lipid peroxidation. Acrolein is formed by  $\beta$ -cleavage of alkoxy radicals derived from lipid hydroperoxides (adapted from Stevens & Maier, 2008).

MDA is a dialdehyde considered a final product in the peroxidation of polyunsaturated fatty acids (mainly arachidonic acid) through enzymatic or non-enzymatic processes [7]. Enzymatic oxidation can be divided into two different processes, which involve the activity of the enzymes cyclooxygenase 1 (COX-1) and cyclooxygenase 2 (COX-2) [19]. In the first, arachidonic acid is oxidized by COX-1 or COX-2 yielding prostaglandin endoperoxide (PGH<sub>2</sub>), which is a precursor of inflammatory mediators, such as prostaglandin E<sub>2</sub>, thromboxane B<sub>2</sub> and others [20]. PGH<sub>2</sub> is also an unstable product that, in the presence of iron or heme group, may be degraded to MDA and secondary products (Figure 2). The second enzymatic mechanism starts with the oxidation of arachidonic acid to 5 *S*-HETE by the enzyme 5-lipoxygenase (5-LOX). This product is then a substrate of COX-2 to form a di-endoperoxide which then is degraded to MDA and other products, such as HNE (Figure 2). Non-enzymatic formation of MDA occurs when hydroperoxides derived from lipid peroxidation suffer rearrangements and additional oxidations generating bicyclic endoperoxides structurally related to prostaglandins that may undergo cleavage to produce MDA [3] (Figure 3).

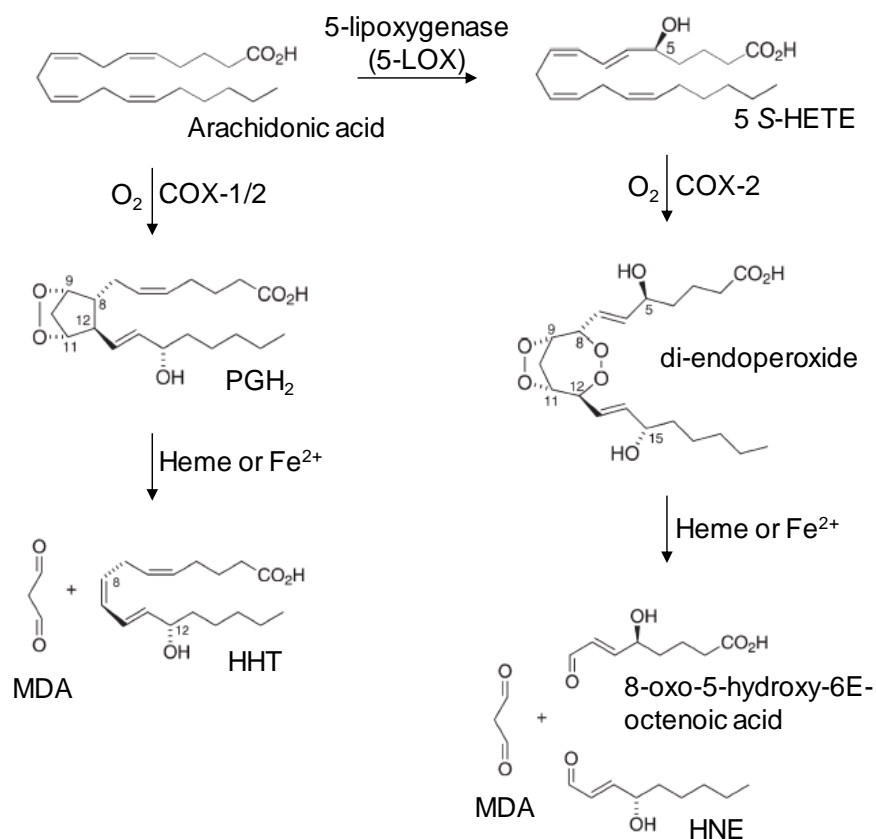


**Figure 2.** Enzymatic mechanism of MDA formation. Two different pathways are responsible for enzymatic MDA formation, both involving cyclooxygenases (COX1/2). The first with an intermediate prostaglandin endoperoxide ( $PGH_2$ ) and the second by the action of the enzyme 5-lipoxygenase (5-LOX) yielding 5 S-HETE and a di-endoperoxide as intermediate. (adapted from Griesser et al., 2009).

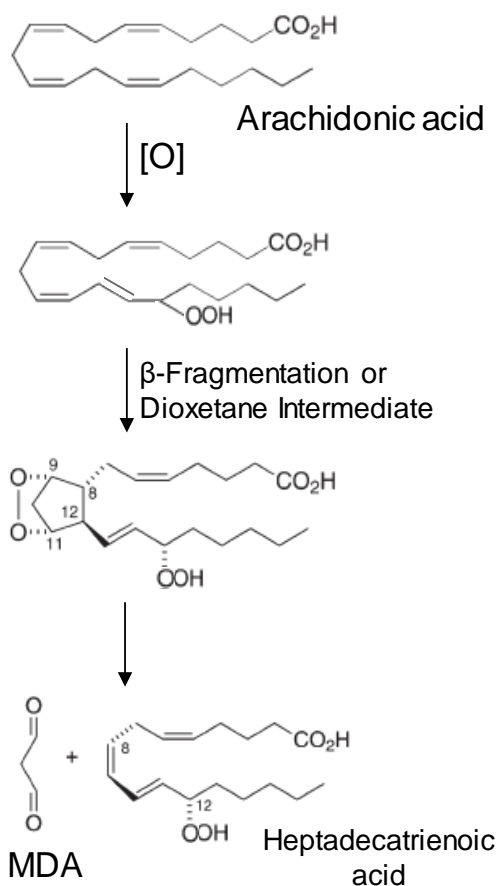


**Figure 3.** Non-enzymatic mechanism of MDA formation. Hydroperoxides derived from lipid peroxidation suffer rearrangements and additional oxidations generating bicyclic endoperoxides as intermediates. (adapted from Yin et al., 2011).

HHE and HNE are aldehydes generated during peroxidation of  $\omega$ -3 polyunsaturated fatty acids, such as docosahexaenoic acid (DHA) and eicosapentaenoic acid (EPA), and  $\omega$ -6 polyunsaturated fatty acids, mainly arachidonic acid or linoleic acid, respectively [3,8]. In addition to the mechanism illustrated in Figure 2, two other pathways are known for HHE and HNE formation: an enzymatic and a non-enzymatic (as exemplified for HNE generation from linoleic acid in Figure 4) [3,9]. The enzymatic mechanism involves the formation of a hydroperoxide in position 9 of linoleic acid (9(S)-HPODE) followed by its reduction by CYP74 and cleavage. This cleavage leads to the formation of two products, being the hydroperoxide of 9 carbons (4-HPNE) rapidly reduced to HNE. This pathway is more likely to occur in plants,

since some of the enzymes are not found in animals [3]. On the other hand, the non-enzymatic mechanism occurs with formation of hydroperoxides in position 9 and 13 by reactive oxygen species, followed by Hock cleavage steps (Figure 4). Although the mechanisms of HHE formation have not been specifically described in the literature, the pathways are considered similar to those of HNE, but starting from  $\omega$ -3 polyunsaturated fatty acids [21].

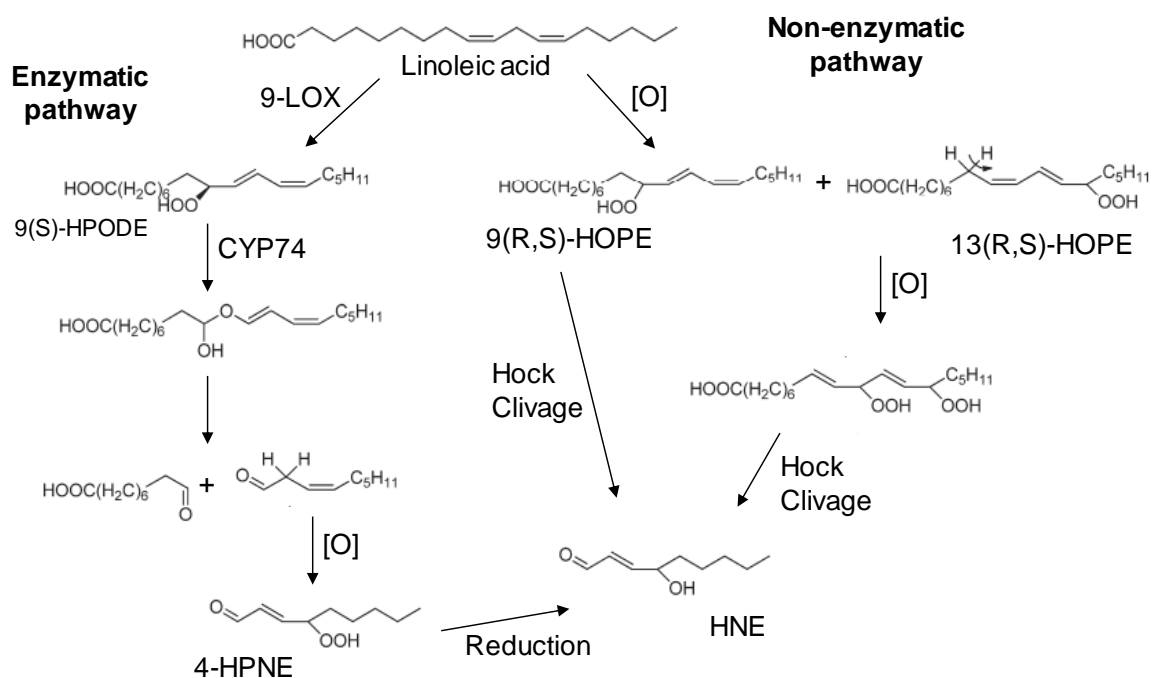


**Figure 4.** Pathways for the formation of HNE from the oxidation of  $\omega$ -6 polyunsaturated fatty acids. Enzymatic mechanism involves the enzymes 9-LOX and CYP74 yielding to a hydroperoxide of 9 carbons (4-HPNE) which is rapidly reduced to HNE. Non-enzymatic mechanism occurs with the formation of hydroperoxides as intermediates which suffer Hock cleavage to form HNE. These mechanisms also occur to HHE, initiating from  $\omega$ -3 polyunsaturated fatty acids. (adapted from Yin et al., 2011 and Uchida, 2003).

### 1.3 Cholesterol and its oxidation products

Cholesterol (cholest-5-en-3 $\beta$ -ol; Ch) is a neutral lipid found in all membrane compartments of mammalian cells. As for all unsaturated lipids, cholesterol is also susceptible to oxidation in the presence of reactive oxygen species (ROS), yielding a variety of potentially mutagenic and cytotoxic species [22–24]. Cholesterol oxidation by enzymatic and non-

enzymatic mechanisms leads to products called oxysterols. Enzymatic oxidation can occur both in the rings and in the side chain of cholesterol leading to the formation of hydroxides ( $7\alpha$ -hydroxycholesterol), ketones ( $7\alpha$ -hydroxy-4-cholesten-3-one) and epoxides ( $24(S),25$ -epoxycholesterol). Most of the enzymes involved in the enzymatic oxidation of cholesterol are enzymes from the cytochrome P450 complex and are related to cholesterol metabolism and production of bile acids [25,26]. Non-enzymatic oxidation occurs only in the cholesterol rings and is related to the reaction of cholesterol with reactive oxygen species. This non-enzymatic oxidation is further divided into two types according to the nature of the oxidant species: type I or radical autooxidation, which occurs when cholesterol is oxidized by free radicals mainly to hydroxides ( $7\beta$ -hydroxycholesterol), epoxides ( $5\beta,6\beta$ -epoxycholesterol) and ketones (7-ketocholesterol); and type II or non-radical, which occurs when oxidation occurs by non-radical oxidizing species, forming hydroperoxides ( $7\alpha$ -OOH,  $7\beta$ -OOH,  $5\alpha$ -OOH,  $6\alpha$ -OOH,  $6\beta$ -OOH) and secosterol aldehydes (Secosterol A and Secosterol B) [27–30] (Figure 5).

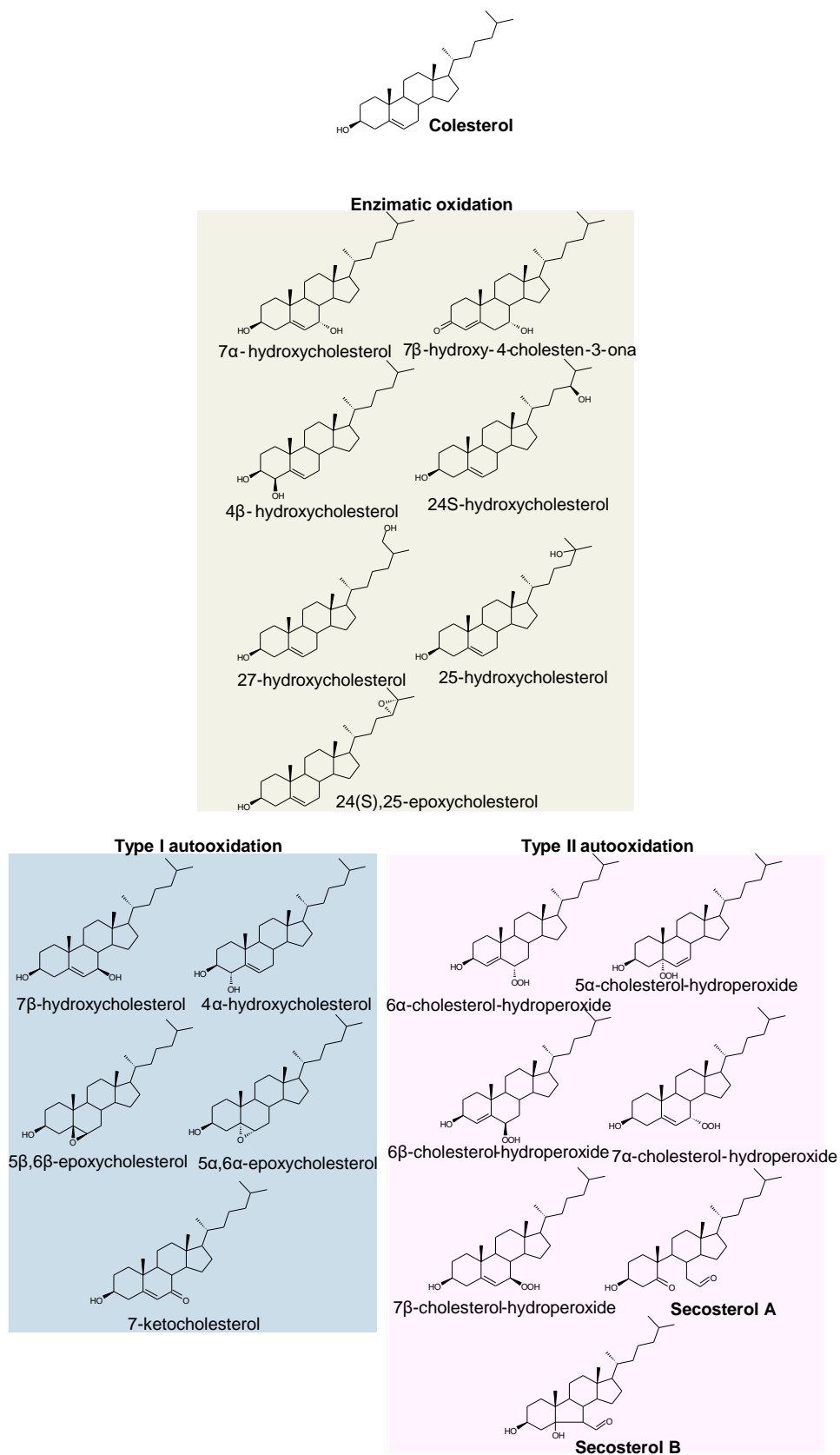


**Figure 5.** Oxysterols: products of cholesterol oxidation. Cholesterol oxidation can occur by enzymatic mechanisms and non-enzymatic mechanisms, which are divided in type I (radical oxidation) and type II (non-radical oxidation).



#### *1.4 In vivo formation of secosterol aldehydes*

Secosterol aldehydes are known to be products of a non-enzymatic oxidation of cholesterol. Wentworth and coworkers (2009) reported that secosterol A (Seco-A) is formed only when cholesterol reacts with ozone, but not with other reactive oxygen species, such as singlet oxygen, superoxide, and hydroxyl radical [31]. More recently, Tomono and colleagues reported that seco-A but not seco-B was formed in neutrophil culture through a myeloperoxidase-dependent pathway, which was significantly increased in the presence of IgG that catalyzes the formation of ozone as an oxidizer. In addition, seco-A was rapidly converted to seco-B and other metabolites in the presence of fetal bovine serum in this neutrophil experiment [32]. Elevated levels of seco-A and B were detected in plasma samples from wild type (WT) rats, but not in myeloperoxidase (MPO) deficient mice after treatment with lipopolysaccharide (LPS). The formation of these aldehydes appears to be mediated mainly by MPO-dependent ozonolysis of cholesterol in inflamed tissues [32]. On the other hand, it has been also reported that seco-B is formed not only by seco-A aldolization, but also by the Hock cleavage of 5 $\alpha$ -hydroperoxide, which is formed by the reaction of singlet oxygen with cholesterol [33,34]. In 2016, it was demonstrated that 5 $\alpha$ -hydroperoxide could also be a product of radical oxydation of cholesterol and that not only 5 $\alpha$ -hydroperoxide could form secosterols by Hock cleavage, but also hydroperoxides at the position 6, which are minor products of cholesterol radical oxidation [35]. This data suggests for the first time that secosterol aldehydes may be derived from type 1 autooxidation of cholesterol [33]. Thus, there are at least three pathways to the formation of secosterol aldehydes: an ozone-dependent, a singlet oxygen-dependent and a free radical-dependent (Figure 6).

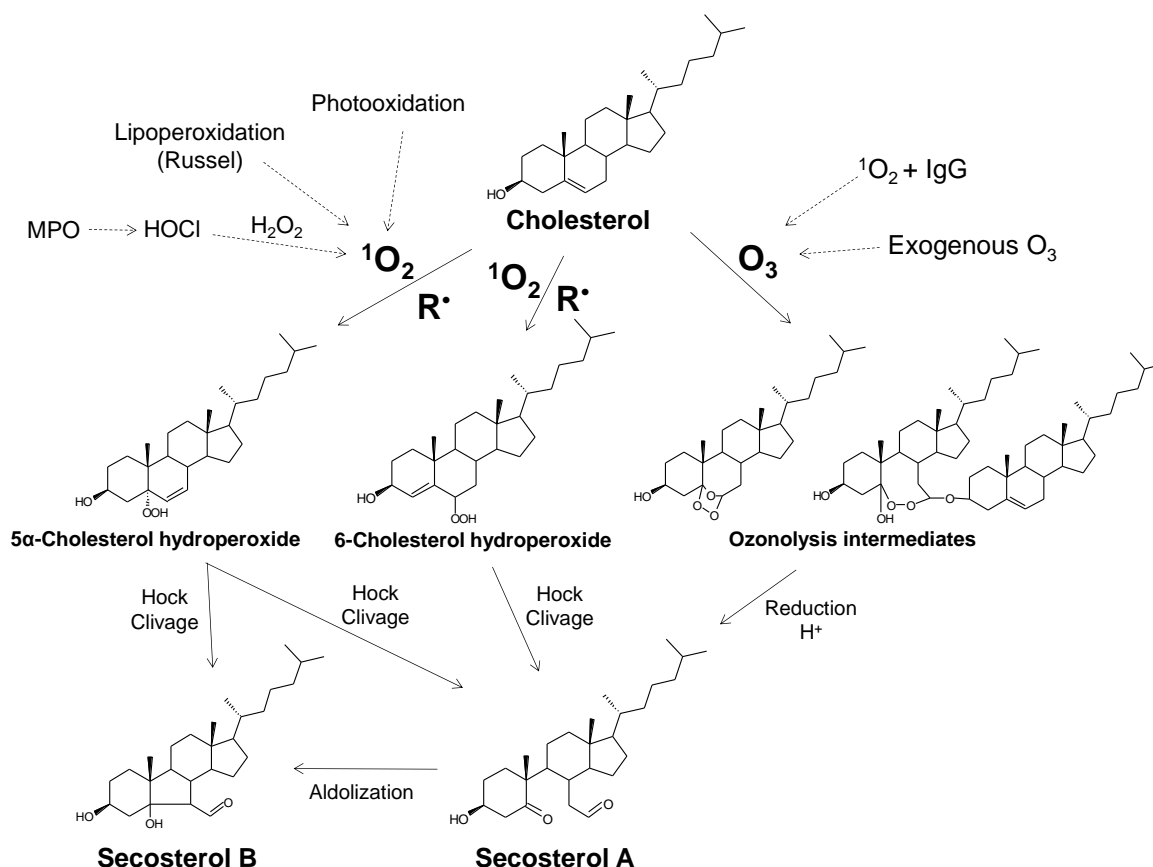


**Figure 6.** Proposed mechanisms for secosterol aldehydes formation *in vivo*. Three different pathways have been described and discussed in the literature: Oxidation of cholesterol by singlet oxygen ( $^1\text{O}_2$ ), free radicals ( $\text{R}^\bullet$ ) or ozone ( $\text{O}_3$ ).

### 1.5 Protein modification by secosterol aldehydes

Secosterol aldehydes have been detected in samples of atherosclerotic tissue and human brain as important intermediates in the pathogenesis of cardiovascular and neurodegenerative diseases. Studies have shown that these cholesterol derivatives modify specific proteins in the brain, such as the  $\beta$ -amyloid peptide by Schiff base formation with basic amino acid residues, more specifically lysines 16 and 28, as well as the N-terminal group of aspartate 1 [36]. These modifications favor the formation of neurotoxic protein aggregates linked to Alzheimer's disease. In this case, lysine 16 appears as the most vulnerable target, reacting more rapidly with

secosterol aldehydes due to its presence on the more hydrophobic fraction of the peptide [36–39].

Bosco and colleagues (2006) have shown that secosterol aldehydes concentrations are more than two-fold increased in the cerebral cortex of patients suffering of dementia related to the formation of Lewy bodies compared to healthy subjects, and that these oxidation products of cholesterol can induce  $\alpha$ -synuclein aggregation *in vitro* [40]. Similar adduct formation has been observed with bovine myelin basic protein (bMBP), which is directly related to myelin sheath adhesion and stability, as well as the sensitivity to autoimmune reactions in multiple sclerosis. Conformational changes and agglomeration of bMBP have been attributed to the covalent attachment with seco-B, leading to increased exposure of the peptide domain V86-T98 related to the immunological reaction and decreased exposure of F42 and F43 proteolytic region, an enzyme responsible for the cleavage of bMBP [41].

A study evaluating the reactivity of seco-A in human atherosclerotic tissue observed that this cholesterol-derived aldehyde induces formation of apolipoprotein CII amyloid fibers *in vitro*. Apolipoprotein CII is secreted by macrophages in the atherosclerotic process and its fibrillation is directly related to plaque formation in the disease [42]. Seco-A has also been identified as a potent inhibitor of the nitric oxide synthase (NOs) *in vitro*, which may contribute to the development of vascular and neurodegenerative diseases. The mechanism of inhibition seems to be related to the blockade of the enzyme binding site with its cofactor calmodulin through the formation of Schiff bases with lysine residues present in this region [43]. Furthermore, a relationship between inflammation and cancer has been uncovered by Nieva and coworkers (2011) showing that secosterol aldehydes are capable of inducing amyloidogenesis and dysfunction of wild-type p53 protein. Through thioflavin T assay and circular dichroism analysis, this study showed that secosterol aldehydes, but not other lipid-derived aldehydes, induce amyloidogenesis and conformational changes in p53 [44].

Interestingly, Wachtel and colleagues (2006) demonstrated that not only amino groups of proteins are capable of forming Schiff bases with seco-sterol aldehydes, but also amino groups of phospholipids polar head groups such as phosphatidylethanolamine. Through mass spectrometry, they identified the product of the reaction between 1-palmitoyl-2-oleoyl-sn-glycero-3-phosphoethanolamine (POPE) and seco-A as the mass corresponding to the sum of two reactants and loss of water, which indicates the formation of a Schiff base. The result was confirmed by a peak fragmentation profile (MS/MS) analysis corresponding to the product [45].

In a study conducted by our group [46], using SDS micelles as a mitochondrial membrane mimetic model, seco-B has been shown to covalently modify cytochrome c (CytC), a protein that participates in the electron transport chain and apoptosis. This result suggests that seco-B can promote cytochrome c anchoring in the membrane, which interferes with the apoptotic signaling. Using MALDI-TOF MS, it was possible to observe an increase of 400 Da mass in cytochrome c after incubation, equivalent to seco-B mass and water loss, which identifies Schiff bases formation. Furthermore, MS/MS data of the modified peptides identified adducts of the aldehyde with Lys 8 and Lys 22 [46].

More recently, cholesterol and its aldehydes modified with an alkynyl group (a-Ch, a-seco-A and a-seco-B) were synthesized by the group of Professor Ned Porter (Vanderbilt University) (Figure 7). Alkynyl-labeled cholesterol aldehydes represent a direct method of detecting modifications proteins by these lipids using click chemistry approach. A study with amino acids, peptides and proteins have provided evidence for the role of seco-sterol aldehydes as well as their dehydration products in the formation of protein adducts. By means of trypsin digestion and hydrophobic separation by lipid extraction and SPE, covalent modifications in

proteins such as albumin (K4, K190, K195, K199, K414, K436, K525, K534) and cytochrome c (His33) were detected by mass spectrometry and click chemistry [47].

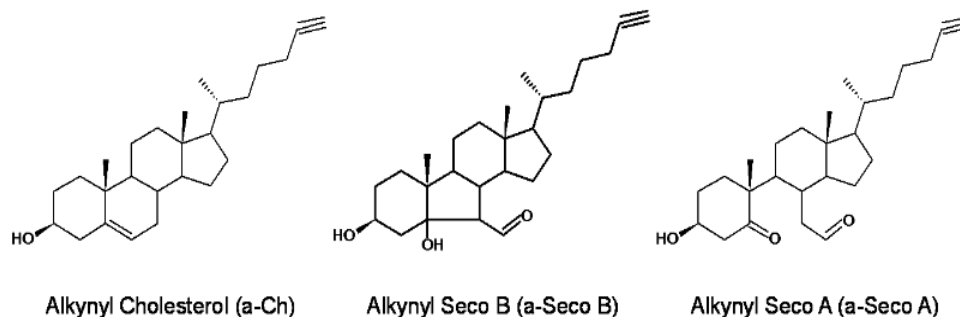


**Figure 7.** Structures of alkynyl-labeled cholesterol and secosterol aldehydes [47].

### 1.6 Amyotrophic Lateral Sclerosis (ALS)

Amyotrophic Lateral Sclerosis (ALS) or Lou Gehrig's Disease is among the most common neurodegenerative diseases manifested in adults, with an incidence of 1-2/100,000 in most populations. Typically, ALS develops between 50 and 60 years of age, with a progressive neuromuscular failure caused by the degeneration of both superior motor neurons of the cerebral cortex and lower connective neurons of the spinal cord. The latter degeneration may ultimately affect muscular fibers, causing a denervation and, consequently, atrophy. The major cause of death is by respiratory failure [48] (Figure 8).

The etiology of ALS is still unknown, but most diagnosed cases have been characterized as sporadic (sALS). However, it is estimated that 5-10% of the cases are genetic, classified as familial (fALS) [49]. In 1993, Deng and coworkers identified the first mutated gene in ALS, responsible for 20-25% of the autosomal dominant cases in fALS. This gene encodes the enzyme copper/zinc superoxide dismutase (Cu/Zn SOD, SOD1) which is located on chromosome 21, where more than 100 mutations have been identified [50].

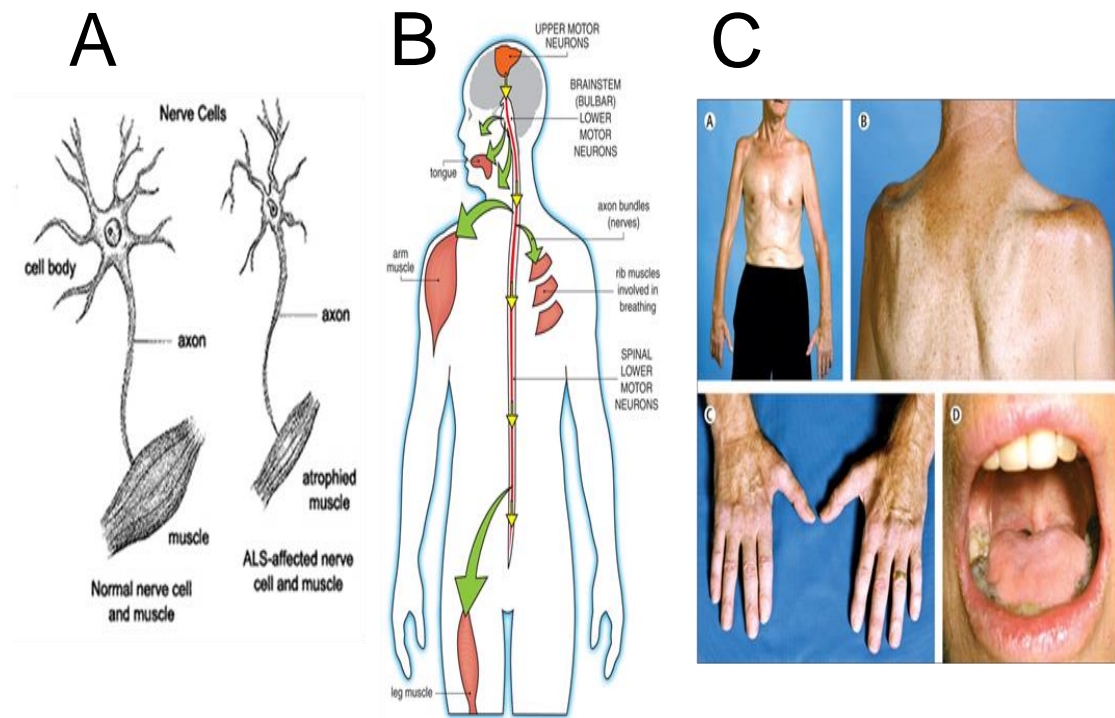


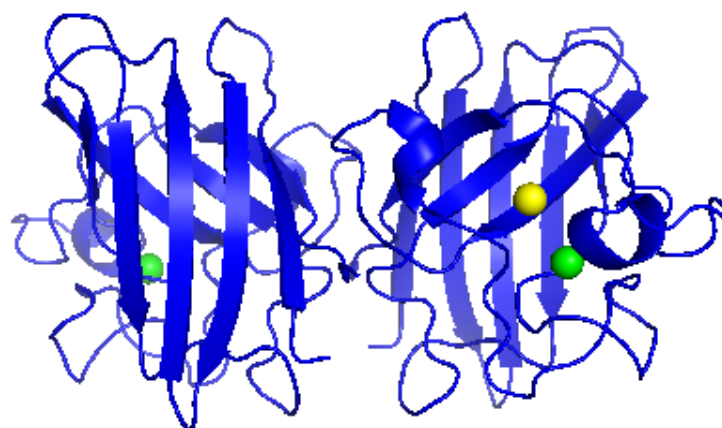
**Figure 8.** Amyotrophic Lateral Sclerosis (ALS). (A) Scheme of motor neuron death and muscle atrophy. (B) Regions affected by ALS. (C) Symptoms of ALS in a patient.

Sources: <http://www.mayo.edu/research/departments-divisions/department-neurology/programs/neuromuscular-diseases-amyotrophic-lateral-sclerosis>; <https://www.mda.org/disease/amyotrophic-lateral-sclerosis/signs-and-symptoms>; Kiernan et al., 2011.

### 1.7 SOD1 and ALS

SOD1 is an antioxidant enzyme found in the cytosol, nucleus, peroxisomes and mitochondrial intermembrane space of eukaryotic cells [51]. Like its other isoforms, SOD1 is responsible for the catalytic dismutation of the superoxide anion radical to form hydrogen peroxide and oxygen (Figure 9). These redox reactions occur in two stages involving reduction and reoxidation of copper ions at the enzymatic reactive site. Thus, the enzyme is considered to be one of the most important antioxidant defenses of the human body. On the other hand, SOD1 has been also known for its peroxidase activity both by catalyzing the reverse reaction to dismutation and by using hydrogen peroxide as a substrate to produce hydroxyl radicals through the Fenton reaction [52]. Thus, although superoxide and hydrogen peroxide are not

highly reactive, additional reactions may generate products with higher oxidizing potential. For instance, superoxide reacts rapidly with nitric oxide to produce peroxynitrite [53], which can lead to production of singlet molecular oxygen [54]. Hydrogen peroxide decomposes slowly into hydroxyl radical in a process that can be catalyzed by reduction with  $\text{Fe}^{2+}$ . Peroxynitrite, singlet molecular oxygen and hydroxyl radical are highly oxidizing agents that are prone to damage proteins, lipids and DNA. Abnormal iron increase have been detected at motor neuron degeneration sites in ALS, which may lead to lipid peroxidation [55]. In fact, patients with ALS have presented increase in the parameters related to the oxidative stress when compared to healthy subjects [56,57].



### **Cu, Zn-SOD (SOD1, 32 kDa)**

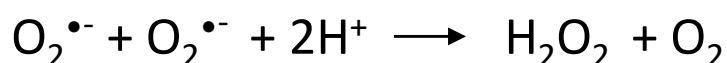


**Figure 9.** Chemical structure and SOD1 activity. Yellow balls represent copper and green balls represent zinc.

The exact molecular mechanisms of selective degeneration of motor neurons by mutant SOD1 in fALS are still unknown. It is believed that the mutation results in a gain of toxic function related to the pro-oxidant effect of the mutant SOD1 and/or the formation of cytotoxic aggregates of SOD1 [58–60]. The structural events that lead to formation of high molecular weight oligomers of SOD1 are still uncertain [61]. Some studies suggest that oxidized SOD1

WT and several of its mutants form soluble oligomers *in vitro* only when they are deficient in metal (apo form) [62]. These oligomers would be formed under aerobic conditions when proteins are maintained at 37 °C for 230 h near the physiological concentration and pH. These resulting oligomers are formed by intermolecular covalent disulfide bonds, involving the cysteines 6 and 111, and by non-covalent interactions between  $\beta$ -sheets, forming  $\beta$ -amyloid-like structures. The rate of protein oligomerization is different for the various mutants, but eventually generate the same type of soluble oligomeric species [61,63].

Kim and colleagues (2005) showed that there is induction of SOD1 aggregation in the presence of polyunsaturated fatty acids. These high molecular weight aggregates have a granular morphology and show significant cytotoxicity [60]. Lipids serve as mediators in signaling and inflammation during the progression of neurodegeneration. Although SOD1 is frequently in contact with lipids, interactions with SOD1 have not been investigated at the same intensity when compared to other proteins related to other diseases [64,65]. In a recent study conducted in our laboratory, it was shown that docosahexaenoic acid (DHA), one of the major polyunsaturated fatty acids in the brain's gray matter, possesses the ability to induce SOD1 oligomerization [66].

### *1.8 Lipids and Neurodegenerative Diseases*

Primarily in the last years, there exists an increasing number of publications relating the role of lipids in the pathology of several diseases, including neurodegenerative diseases [67–69]. If we search in science databases for the term “neurodegenerative disease” we observe a steady increase in the number of articles published from 1990 to 2017 (Figure 10A). The same increase is observed when term of the search is “lipid and neurodegenerative diseases” (Figure 10B). This trend is likely related to the fact that oxidative stress is associated with several neurodegenerative diseases [70–72], and lipid oxidation may reflect these conditions serving as



biomarkers of the diseases [10,73,74]. In this context, it has been reported increased levels of lipid-derived electrophiles, such as acrolein, MDA and HNE, in patients and animal models of Alzheimer's disease [10,75,76], Parkinson's disease [73,77,78] and ALS [79–82]. Moreover, there are a number of *in vitro* studies showing that lipid-derived electrophiles may potentially represent ligands and aggregation inducers of most protein linked to neurodegenerative diseases. For instance,  $\alpha$ -Synuclein aggregation is associated with Parkinson's disease and the process of aggregation has been reported to be induced by acrolein [14], HNE [13,83] and secosterol aldehydes [40]. Similarly, aggregation of  $\beta$ -amyloid peptide induced by these aldehydes has been found as a link to Alzheimer's disease [15,37,42].

Alterations in lipid metabolism by neurodegenerative diseases have been also the subject of many investigations [84–87]. The 24(S)-hydroxycholesterol (24-OH cholesterol) represents the major cholesterol metabolite in brain and can be used as clinical biomarker for Alzheimer's disease development. Patients diagnosed with this disease seem to present higher concentration of 24-OH cholesterol in plasma and cerebrospinal fluid compared to healthy subjects [88,89]. Alterations in the activity of the enzyme sterol O-acyltransferase 1 (ACAT1), responsible for the production of cholesteryl esters, was also suggested to play a role in Alzheimer's disease, since this enzyme activity is related to the production of  $\beta$ -amyloid peptide [90,91]. Cholesterol metabolism and its products have been also studied in other neurodegenerative diseases, such as Parkinson's disease [92], Huntington's disease [86] and ALS [93]. Sphingolipids and their metabolism is also a common subject of study in field of neurodegenerative disorders. For instance, increased ceramides levels appear as a hallmark of several neurodegenerative diseases linked to oxidative stress [94–97]. Several other lipid classes and their metabolism have been studied and seem to be related to neurodegenerative diseases, such as free fatty acids [98,99] and phospholipids [100,101]. Finally, it is worth mentioning that advances in lipidomics analysis in recent years allowed a global lipid

quantification in patients and animal models of neurodegenerative diseases, increasing the number of lipid classes and lipid-derived biomarkers involved in these disorders [102–104].

### *1.9 Cholesterol and ALS*

Cholesterol represents the major lipid in the brain [105], and not surprisingly, a significant fraction of studies showed in Figure 10B are related to the link between cholesterol metabolism and neurodegenerative diseases (Figure 10C). Part of these works was already presented in the topic “*1.5 Protein modification by secoesterol aldehydes*” where it was talked about how these cholesterol-derived electrophiles could modify and induce aggregation of specific proteins linked to neurodegenerative diseases. In “*1.9 Lipids and Neurodegenerative Diseases*” it was showed that cholesterol metabolism and oxysterols concentration have been studied in neurodegenerative diseases and seem to be associated with these disorders in some specific cases.

In ALS, a pioneer study was published in 2002, showing abnormalities in ceramide and cholesteryl ester metabolism in ALS patients and mouse model spinal cords [106]. The authors associated this result with the increase of oxidative stress in ALS [106]. On the other hand, dyslipidemia conditions such as elevated triglyceride and cholesterol serum levels have shown a significantly positive effect on survival of patients with ALS [107,108]. In addition, statin drugs (inhibitors of cholesterol biosynthesis) were suggested to play a possible role inhibiting ALS progression [109]. Collectively, however, these papers do not delineate the mechanism by which cholesterol could protect ALS development [107–109].

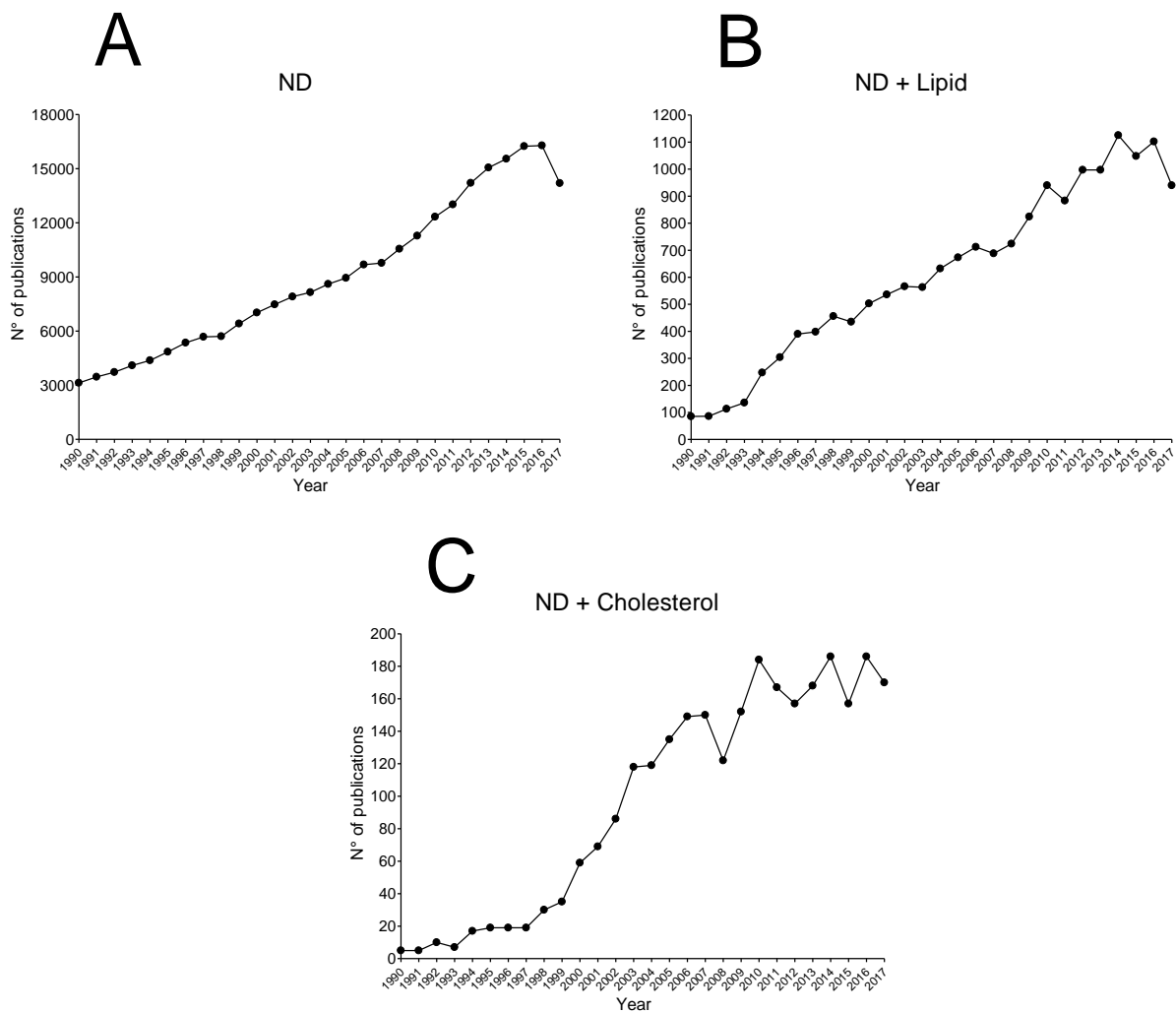


**Figure 10.** Number of publications about neurodegenerative diseases (A), lipids and neurodegenerative diseases (B) and cholesterol and neurodegenerative diseases (C) over the last 28 years. (Source: PubMed <https://www.ncbi.nlm.nih.gov/pubmed/> in April 25, 2018).

In 2017, a group from the United Kingdom quantified more than 40 different sterols in serum and cerebrospinal fluid (CSF) from ALS patients [93]. They found increased concentrations of cholesterol in CSF of ALS patients compared with control. Furthermore, specific cholesterol metabolites formed in CSF were reduced in ALS, while other metabolites imported from blood circulation were present in normal levels. This work concluded that cholesterol metabolism is altered in the brain of ALS patients, promoting an excess of

cholesterol in the CSF [93]. More recently, a specific cholesterol metabolite found in blood, 25-hydroxycholesterol, was increased in serum of ALS patients and implicated in motor neuronal death in a cell model of ALS [110].

Yet there are no studies on how cholesterol-derived electrophiles could modify and/or induce aggregation of proteins linked to ALS. Thus, in the Chapter 1 of this thesis, we have explored whether secosterol aldehydes could induce SOD1 aggregation.

## **2. OBJECTIVES**

Taking into account that neurodegenerative diseases have been associated with alterations in lipid metabolism and that lipid oxidation products may participate in the pathology of these diseases, this thesis sought to verify a possible relationship between Amyotrophic Lateral Sclerosis and aldehydes derived from cholesterol oxidation (secosterol aldehydes). The first chapter of this thesis is aimed at evaluating secosterol aldehydes concentration in an animal model for ALS (overexpressing SOD<sup>G93A</sup> mutant rats). In addition, *in vitro* experiments were performed to test whether secosterol aldehydes could modify and induce aggregation of SOD1, with subsequent characterization of possible covalent modifications.

In order to contribute to the understanding of the mechanism involved in the results of Chapter 1, the second part of this thesis (Chapter 2) compared the effect of lipid-derived aldehydes with different sizes and hydrophobicities on SOD1 aggregation. Possible modifications were characterized in detail by examining the hydrophobic surface of SOD1 and covalent docking of the aldehydes on the protein.

## CHAPTER 1

### **Cholesterol Secosterol Aldehydes Induce Covalent Modification and Aggregation of Cu,Zn-Superoxide Dismutase: Potential Implications in ALS**

Lucas S. Dantas<sup>†</sup>; Adriano de B. Chaves Filho<sup>†</sup>; Thiago C. Genaro-Mattos<sup>‡1</sup>; Keri A. Tallman<sup>‡</sup>; Ned A. Porter<sup>‡</sup>; Fernando R. Coelho<sup>†</sup>; Ohara Augusto<sup>†</sup>; and Sayuri Miyamoto<sup>\*†</sup>

<sup>†</sup>Departamento de Bioquímica, Instituto de Química, Universidade de São Paulo, São Paulo, SP, Brazil

<sup>‡</sup>Department of Chemistry, Vanderbilt Institute of Chemical Biology and Vanderbilt Kennedy Center for Research on Human Development, Vanderbilt University, Nashville, Tennessee, United States

<sup>1</sup>Current address: Munroe-Meyer Institute, University of Nebraska Medical Center, Omaha, Nebraska, United States

\*Corresponding author: Sayuri Miyamoto, Departamento de Bioquímica, Instituto de Química, Universidade de São Paulo, Avenida professor Lineu Prestes, 748, Bloco 10 Superior, sala 1074, São Paulo, SP, Brazil 05508-000.

Phone: +55113091-9113. E-mail: miyamoto@iq.usp.br.

## ABSTRACT

Amyotrophic lateral sclerosis (ALS) is a neurodegenerative disorder characterized by degeneration of upper and lower motor neurons. While the fundamental causes of the disease are still unclear, the accumulation of Cu,Zn-superoxide dismutase (SOD1) immunoreactive aggregates is associated with familial ALS cases. Cholesterol 5,6-seco-sterol aldehydes (seco-A and seco-B) constitute a class of lipid-derived electrophiles that modify proteins causing their aggregation. Here we have investigated the presence of seco-A and seco-B in ALS SOD1-G93A rats and their capacity to induce SOD1 aggregation. Cholesterol-derived aldehydes were analyzed in plasma, spinal cord and motor cortex of ALS rats at the symptomatic stage. Higher levels of seco-B were detected in the motor cortex of ALS rats compared to control animals. *In vitro* experiments showed that seco-A and seco-B induce formation of SOD1 aggregates with amorphous morphology. No effect was observed with cholesterol and its hydroperoxides. Using a click chemistry assay, we observed seco-sterol adducted-SOD1 mostly in the high molecular weight aggregate fraction with no detectable adducts in the monomer or dimer forms. SOD1-seco-sterol adducts containing up to five seco-sterol molecules were confirmed by MALDI-TOF analysis. Trypsin digestion followed by LC-MS/MS analysis showed that seco-sterols were covalently attached to Lys residues preferentially located at the electrostatic loop (Lys 122, 128 and 136) and nearby the dimer interface (Lys 3 and 9). Altogether, our results show that the levels of cholesterol aldehydes are increased in the brain cortex of symptomatic ALS rats and highlight the importance of these electrophiles in SOD1 aggregation.

**Keywords:** Amyotrophic Lateral Sclerosis, seco-sterol aldehydes, neurodegenerative diseases, superoxide dismutase, protein aggregation

**Highlights:**

- Secosterol aldehydes are increased in motor cortex of ALS rat model;
- These aldehydes modify SOD1 *in vitro*, producing high molecular weight aggregates;
- Secosterol aldehydes modifies Lys residues located at electrostatic loop and nearby the dimer interface;
- Secosterol adduction increases protein hydrophobicity and its propensity to aggregate.

## INTRODUCTION

Cholesterol is a neutral lipid found in the membranes of all mammalian cells. The central nervous system is particularly rich in cholesterol, presenting a concentration near to 20 mg/g in the brain and 40 mg/g in spinal cord, which represents about 23% of the total sterol present in the body [1]. Cholesterol, like all other unsaturated lipids, is susceptible to oxidation, giving rise to a variety of oxidized derivatives, collectively known as oxysterols [2–4]. This lipid can be oxidized by enzymatic and non-enzymatic mechanisms. Non-enzymatically, cholesterol can be oxidized by singlet molecular oxygen ( $^1\text{O}_2$ ), ozone ( $\text{O}_3$ ), and free-radicals [5–11]. Among the major products of cholesterol oxidation are the isomeric hydroperoxides ( $7\alpha\text{-OOH}$ ,  $7\beta\text{-OOH}$ ,  $5\alpha\text{-OOH}$ ,  $6\alpha\text{-OOH}$ ,  $6\beta\text{-OOH}$ ), epoxides, and aldehydes [6–8,11]. Attention has been particularly focused on cholesterol 5,6-secoesterol aldehydes (seco-A and seco-B) (Figure 1), two electrophilic oxysterols known to be formed from cholesterol oxidation intermediates formed by  $\text{O}_3$  [9,10] and  $^1\text{O}_2$  [8,11]. More recently, Zielinsk and Pratt demonstrated that these aldehydes can also arise from free radical mediated oxidation of cholesterol [12], suggesting that their formation does not require the presence of high energy oxygen intermediates (i.e.  $\text{O}_3$  or  $^1\text{O}_2$ ).

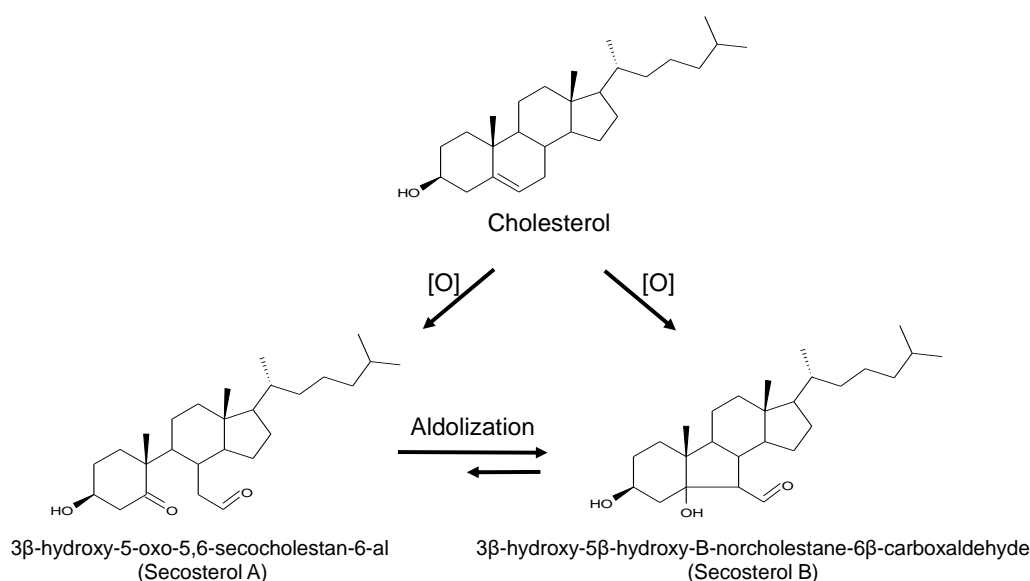


**Figure 1.** Chemical structures of Cholesterol 5,6-secoesterol aldehydes.



Secosterol aldehydes have been detected in samples of atherosclerotic tissue and human brain as important intermediates in the pathogenesis of cardiovascular [13,14] and neurodegenerative diseases [15–18]. These electrophilic oxysterol derivatives can modify specific proteins in the brain, such as  $\beta$ -amyloid peptide [15,16,19,20],  $\alpha$ -synuclein [17] and bovine myelin basic protein [18], leading to the formation of protein aggregates. In addition, secosterol aldehydes may also modify other proteins such as apoB-100 [8], p53 [16], NO synthase [9] and cytochrome c [17], resulting in structural change and function loss.

SOD1 is a soluble antioxidant enzyme present in the cytosol, nucleus, peroxisomes and mitochondrial intermembrane space of eukaryotic cells [23,24]. SOD1, as well as its other isoforms, is responsible for the catalytic dismutation of the superoxide radical anion to hydrogen peroxide and molecular oxygen. Mutations of the SOD1 gene are linked to some cases of Amyotrophic Lateral Sclerosis (ALS) [25]. ALS is a fatal neurodegenerative disease manifested in adults with an incidence of 1-2/100,000 in most populations. Typical ALS develops between 50 and 60 years of age, with progressive neuromuscular failure caused by motor neurons degeneration in the brain and spinal cord causing denervation and consequent muscle atrophy. The etiology of the disease is still unknown. Whereas the majority of diagnosed cases have been characterized of sporadic origin (sALS), it is estimated that 5-10% of the cases are genetic, classified as familiar ALS (fALS) [26]. In 1993, Deng and colleagues identified the first mutated gene in ALS, responsible for approximately 25% of autosomal dominant fALS cases. This gene encodes the enzyme SOD1 which is located on chromosome 21 [25].

Although more than 100 mutations have been identified in the SOD gene, the molecular mechanisms of selective degeneration of motor neurons in SOD1 fALS mutants are still unclear. The mutation results in a gain of toxic function, which has suggested to cause pro-oxidant effects and/or formation of cytotoxic SOD1 aggregates [27,28]. The structural events that lead to the formation of high molecular weight SOD1 oligomers have been extensively

debated [27]. These events likely involve intermolecular covalent disulfide bonds at cysteines 6 and 111, and non-covalent interactions between beta sheets, forming the  $\beta$ -amyloid-like structures [29]. A number of factors can enhance protein aggregation, including zinc-deficiency [30,31], protein oxidative modifications [28] and the interaction with membrane lipids [32–34]. Yet, the interaction between SOD1 and lipids has been underexplored as compared to key proteins involved in other diseases [35–37].

Considering the high abundance of cholesterol in brain and spinal cord [1] and the electrophilic nature of its oxidation products, we sought to investigate the presence of secosterol aldehydes in neural tissues and plasma from an ALS rat model and also to evaluate their potential to induce SOD1 aggregation. Here we found elevated amounts of secosterol aldehydes in the cerebral cortex of an ALS rat model (SOD1-G93A rats). Moreover, secosterol aldehydes dramatically enhanced SOD1 aggregation through a mechanism involving covalent modifications of Lys residues mainly at the electrostatic loop (Lys 122, 128 and 136) and at the dimer interface (Lys 3 and 9).

## MATERIALS AND METHODS

### 1. Materials

Secosterol-A (3 $\beta$ -hydroxy-5-oxo-5,6-secocholestan-6-al) was synthesized by the ozonization of cholesterol and purified as described by Wang and colleagues [38]. Secosterol-B (3 $\beta$ -hydroxy-5 $\beta$ -hydroxy-B-norcholestane-6 $\beta$ -carboxaldehyde) was synthesized by the photooxidation of cholesterol and purified as described by Uemi and colleagues [8]. SOD1 was expressed in *Escherichia coli*, purified and its apo form prepared as previously described [39]. Alkynyl lipids were synthesized as previously described [40]. Unless otherwise stated all chemicals were of the highest analytical grade and were purchased from Sigma, Merck or Fisher.

## 2. ALS Rat Model

Sprague Dawley hemizygous male rats overexpressing multiple copies (~8 copies) of G93A mutant human copper,zinc-superoxide dismutase (SOD1<sup>G93A</sup>) were obtained from Taconic (Germantown, NY). The development of characteristic symptoms of the disease was accompanied by evaluation of animals body weight and loss of limbs movement. The animals were considered symptomatic when they showed a ~20% loss of their maximum body weight accompanied by atrophy/paralysis of the limbs. Secosterol aldehydes were quantified in plasma, motor cortex and spinal cord at the symptomatic stage ( $132 \pm 12$  days).

## 3. Quantification of Cholesterol and Secosterol Aldehydes

Plasma and homogenates of motor cortex and spinal cord were subjected to lipid extraction according to the method of Bligh & Dyer (1959) [41]. Quantification of cholesterol was performed by HPLC-UV detection at 205 nm. The separation was achieved on a Kinetix C18 (50 x 4.6 mm 2.6  $\mu$ m) using an isocratic eluent of 95% methanol and 5% water. A 5  $\mu$ L aliquot was injected for analysis and cholesterol levels were calculated according to a calibration curve. The analysis of secosterol aldehydes was performed using the method previously described by our group, in which aldehydes were derivatized with a fluorescent probe 1-pyrenebutiric hydrazine (PBH) [42]. The differences between the concentration levels obtained for cholesterol and its aldehydes (mean  $\pm$  S.D.) were determined by Student's T test. A *p* value of 0.05 or less was used as the criterion for statistical significance.

## 4. SOD1 aggregation experiments

SOD1 WT (10  $\mu$ M) in apo and holo forms were incubated in 50 mM phosphate buffer pH 7.4 containing 150 mM NaCl and 100  $\mu$ M DTPA for 24 h at 37°C in the presence of 250

$\mu\text{M}$  cholesterol, cholesterol hydroperoxides, seco-A or seco-B. 250  $\mu\text{M}$  of docosahexaenoic acid (DHA) was used as a positive control [33]. For detection of SOD1 oligomers, SDS-PAGE was performed under reducing (+ $\beta$ -mercaptoethanol) and non-reducing (- $\beta$ -mercaptoethanol) conditions in a 12% polyacrylamide gel. Aliquots of samples (20  $\mu\text{L}$ ) were incubated in sample buffer (62 mM Tris-HCl, pH 6.8 containing 10% glycerol, 2% SDS, 0.01% bromophenol blue) in the absence and presence of  $\beta$ -mercaptoethanol (200 mM) for 5 minutes at 95°C and then applied on the gel. Silver nitrate was applied for gel staining. Size exclusion chromatography (SEC) was performed using the column BioSep-SEC-S3000 (300 x 7.8 mm, Phenomenex, USA). Each sample was eluted with 50 mM phosphate buffer, pH 7.4 containing 150 mM NaCl. Fluorescence detector conditions were: excitation wavelength at 280 nm and emission at 340 nm.

## **5. Effects of pH and Secosterol Aldehyde Concentration on SOD1 Aggregation**

For pH evaluation, solutions of 50 mM phosphate containing 150 mM NaCl and 100  $\mu\text{M}$  DTPA were made in different pHs: 4.7, 5.5, 6.2, 7.4, 8.4 and 10. Apo-SOD1 (10  $\mu\text{M}$ ) was incubated with cholesterol aldehydes (250  $\mu\text{M}$ ) at all pHs for 24 h at 37°C. To evaluate the effect of concentration, incubations of apo-SOD1 (10  $\mu\text{M}$ ) were performed in increasing concentrations from 10 to 250  $\mu\text{M}$  cholesterol aldehydes for 24 h at 37°C. Aggregate analysis was performed by SEC.

## **6. Analysis of SOD1 Aggregates Morphology**

The increase of hydrophobicity at the protein surface was monitored by following the increase in fluorescence of thioflavin T (ThT). After 24 h of incubation, 10  $\mu\text{M}$  ThT was added to the samples and after 15 min at 37°C, fluorescence was recorded on a plate reader (TECAN, Switzerland) with excitation at 440 nm and emission at 485 nm. To evaluate whether SOD1

aggregates were formed by amyloid fibers, congo red (CR) assay was performed. This reagent suffers a red shift on its absorbance peak after binding to amyloid fibers. For the analysis, the incubations were mixed with 6  $\mu$ M CR in 5 mM phosphate buffer pH 7.4. A positive control was an incubation of  $\alpha$ -synuclein with seco-A, which has been known to form amyloid fibrils [17]. Spectrophotometric analyses were carried out in a Varian model Cary 50 Bio spectrophotometer. Aggregate morphology was also analyzed by transmission electron microscopy (TEM) as described previously [43].

## 7. Click Chemistry Assay

Apo-SOD1 (10  $\mu$ M) was incubated with 1 mM alkynyl lipids (a-HNE, a-Ch, a-seco-A and a-seco-B) in 50 mM phosphate buffer pH 8.4 containing 150 mM NaCl and 100  $\mu$ M DTPA for 24 h at 37°C. The samples were then reduced with 5 mM sodium borohydride for 1h at room temperature to stabilize possible adducts, and finally neutralized with 10% HCl. The following click reagents were added to each of the samples: azido-biotin reagent (0.2 mM), tris(3-hydroxypropyltriazolylmethyl)amine (THPTA) ligand (0.2 mM), copper sulfate (1 mM), and sodium ascorbate (1 mM), and the samples were vortexed and allowed to stir for 2 h in the dark at room temperature. Biotinylated samples were resolved by SDS-PAGE as described above. The protein was transferred electrophoretically to a polyvinylidene fluoride membrane (Life Technologies, Grand Island, NY) and probed with streptavidin conjugated with the Alexa Fluor 680 fluorophore (Life Technologies). Biotinylated proteins were visualized using the Odyssey Infrared Imaging System and Odyssey software according to the manufacturer (Licor, Lincoln, NE).

## 8. MALDI-TOF Analysis

Apo-SOD1 (10  $\mu$ M) was incubated with 1 mM cholesterol, seco-A or seco-B in 50 mM phosphate buffer pH 8.4 containing 150 mM NaCl and 100  $\mu$ M DTPA for 24h at 37°C. The samples were then reduced with 5 mM sodium borohydride for 1h at room temperature to stabilize possible adducts. After that, the protein was denatured at 95°C for 5 min and the aggregates were reduced with 1 M dithiothreitol (DTT) for 1h at room temperature. Methanol (750  $\mu$ L) was added to the samples, which were left on ice for 20 min to precipitate SOD1. After centrifugation at 10000 rpm for 5 min, the precipitate was suspended in 100  $\mu$ L of 0.1% trifluoroacetic acid for MALDI-TOF analysis. Samples were mixed in a 1:4 (v/v) ratio with a saturated solution of  $\alpha$ -cyano-4-hydroxycinnamic acid (HCCA) in 50% acetonitrile/0.1% aqueous trifluoroacetic acid (1:1, v/v). Approximately 1  $\mu$ L of the resulting mixture was spotted onto a MALDI target and analyzed by MALDI-TOF MS. The analyses were performed in the linear, positive ion mode in an UltrafleXtreme spectrometer (Bruker Daltonics, Germany) using an acceleration voltage of 25 kV. The resulting spectra were analyzed by flexAnalysis software (Bruker Daltonics, Germany).

## 9. Enzymatic Digestion of SOD1 and Peptide Analysis

SOD1 samples incubated in the presence of cholesterol and aldehydes were first reduced with 5 mM sodium borohydride for 1 h at room temperature. After that, cysteine residues were reduced with 5 mM DTT (dithiotreitol) and alkylated with 15 mM iodoacetamide. Then, samples were digested for 18 h with proteomic grade trypsin (Promega) in a 1:100 (w/w) ratio at 37 °C with aid of RapiGest SF Surfactant (Waters). The resulting peptides were analyzed by LC-MS/MS using a nanoAcquity UPLC system (Waters, United States) with an ACQUITY UPLC-C18 (20 mm x 180  $\mu$ m; 5  $\mu$ m) coupled to a TripleTOF 6600 mass spectrometer (Sciex, United States). Elution was used with mobile phase A (0.1% formic acid in water) and B (0.1%

formic acid in acetonitrile) at a flow rate of 0.4  $\mu$ L/min with the followed gradient: 1 to 35% B from 0 to 60 min; 35 to 90% B from 60 to 61 min; isocratic elution with 90% B from 61 to 73 min; 90 to 1% B from 73 to 74 min. Nano-electrospray ion source was operated at 2.4 kV. Software used for acquisition and data processing were Analyst TF and PeakView, respectively. For the analysis of protein modification, MASCOT software (Matrix Science Ltd., London, United Kingdom) was used with mass tolerance of 10 ppm for MS experiments and 0.05 Da for MS/MS experiments. Search configuration was set to have variable modifications of +57.0214 Da for carbamidomethyl to Cys, +400.3341 Da for Michael addition of secosterols to Cys, Lys and His, and +402.3497 Da for Schiff base adduction of secosterols to Lys.

## RESULTS

### 1. Secosterol aldehydes are increased in the motor cortex of ALS rats

First, we sought to investigate the presence of secosterol aldehydes in neural tissues and plasma of an ALS rat model (SOD1-G93A rats). For this purpose, we collected motor cortex, spinal cord and plasma from the rats at the symptomatic stage. We detected significant amounts of seco-B but no detectable levels of seco-A. This is consistent with seco-A rapid conversion to seco-B in aqueous solution [17]. Thus, we considered the concentrations found for seco-B in our samples as the sum of seco-A and seco-B. Importantly, secosterol aldehydes were significantly increased in the motor cortex of ALS animals compared to controls (Figure 2B). Significant differences were not apparent in plasma and spinal cord samples (Figure 2A and C). No difference was observed in cholesterol concentration in any tissues (caption of Figure 2).

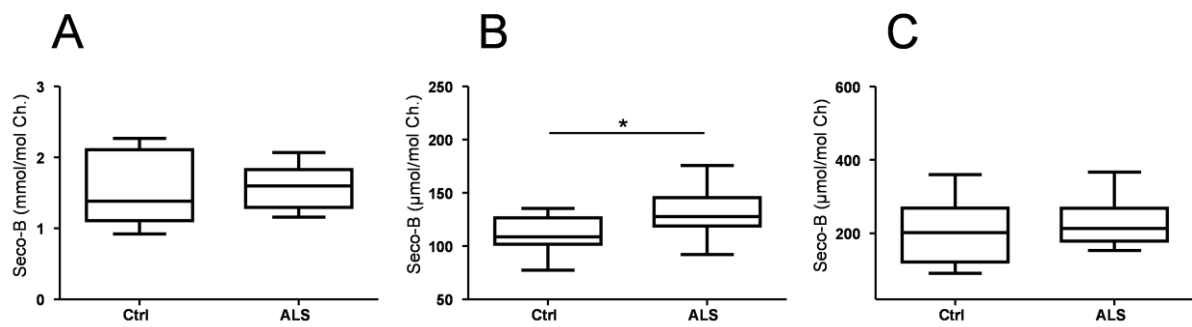


**Figure 2. Quantification of seco-sterol B in plasma (A), motor cortex (B) and spinal cord (C) of the amyotrophic lateral sclerosis (ALS) rat model.** Rats were sacrificed at symptomatic period of ALS (~130 days) and lipids were extracted to analyze cholesterol and seco-B as described in the Experimental Procedures. The ratio of seco-sterol B/cholesterol in lipids obtained from plasma (A), from the motor cortex (B) and from spinal cords (C) is shown. No difference was observed in cholesterol concentration in any tissues (Plasma: Ctrl  $4.19 \pm 0.55$  nmol/mg protein, ALS  $4.21 \pm 0.69$  nmol/mg protein; Motor cortex: Ctrl  $0.69 \pm 0.16$   $\mu$ mol/mg protein, ALS  $0.68 \pm 0.17$   $\mu$ mol/mg protein; Spinal cord: Ctrl  $0.55 \pm 0.09$   $\mu$ mol/mg protein, ALS  $0.56 \pm 0.04$   $\mu$ mol/mg protein). The shown values correspond to the mean  $\pm$  standard deviation values obtained from 10 animals for each group; T test was performed as statistical analysis; \* $p < 0.05$ .

## 2. Secosterol aldehydes induce SOD1 aggregation *in vitro*

The higher levels of seco-B in the motor cortex of ALS rats led us to investigate its ability to promote SOD1 aggregation. Interestingly, seco-A and seco-B dramatically enhanced the formation of high molecular weight SOD1 aggregates ( $> 100$  kDa), which appeared as a smear at the top of non-reducing SDS-PAGE (Figure 3A). The same trend was not observed in incubations containing cholesterol (Ch), cholesterol hydroperoxide (ChOOH) or solvent (10% methanol or isopropanol), although the later showed oligomerization to some extent (Figure S1). The aggregating effect was observed for both apo and holo-SOD1 forms, pointing to a highly destabilizing nature of the modifications promoted by seco-sterol aldehydes. Notably,



under reducing conditions, all high molecular weight bands disappeared, showing that SOD1 aggregates are mainly maintained by intermolecular disulfide crosslinking (Figure 3A).

Next, we confirmed the formation of SOD1 aggregates by size exclusion chromatography (SEC) analysis (Figure 3B). As expected, high molecular weight aggregates were only observed when SOD1 was incubated with secosterol aldehydes, but not with intact cholesterol or solvent. Interestingly, aggregation preferentially occurred with consumption of SOD1 monomer, consistent with previous studies showing high propensity of SOD1 monomers to aggregate [44].

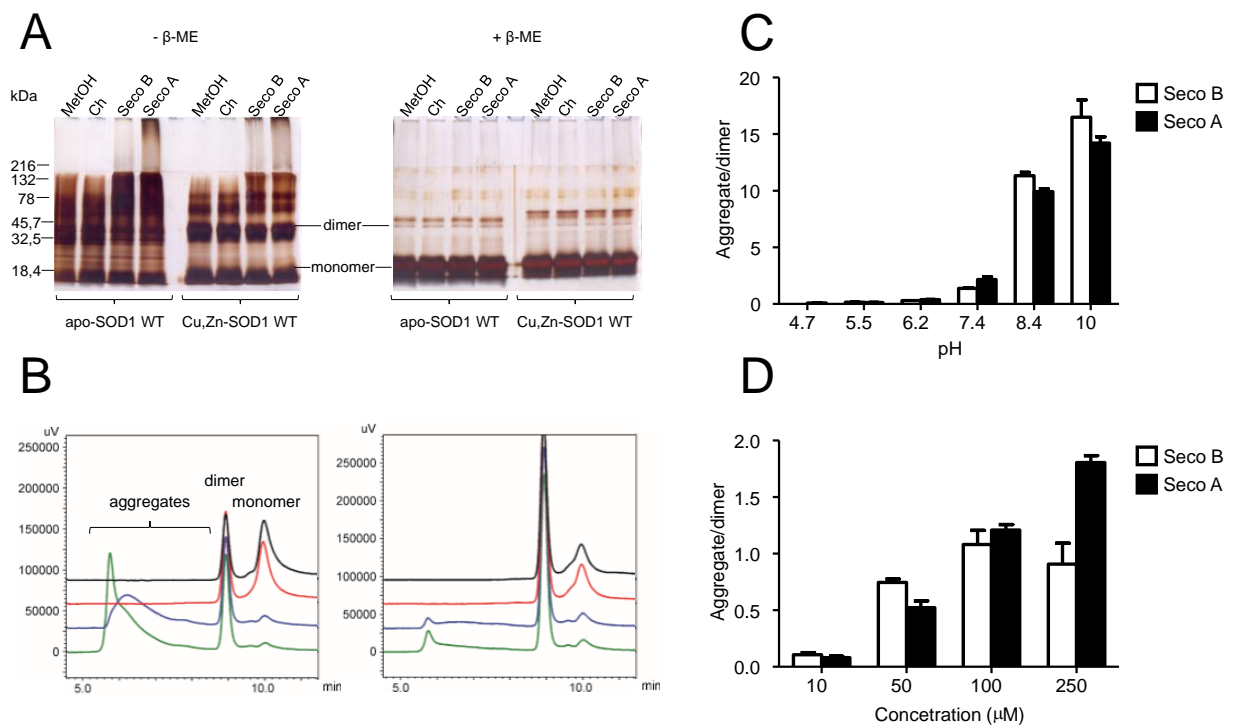


**Figure 3. Oligomerization of SOD1 in the presence of cholesterol (Ch) and its derivatives (seco-A, seco-B and ChOOH).** (A) Comparison of secosterol aldehydes (250  $\mu$ M) effect under apo- and Cu, Zn-SOD1 (holo form) (10  $\mu$ M) oligomerization by SDS-PAGE. (B) Analysis of apo-SOD1 (left panel) and Cu, Zn-SOD1 (right panel) incubation with isopropanol (black line), cholesterol (red line), seco B (blue line) and seco-A (green line) by size exclusion chromatography (SEC). (C) Graph representing the formation of apo-SOD1 WT aggregates in pH dependence test. (D) Graph representing the formation of apo-SOD1 WT aggregates in secosterol aldehydes concentration dependence test. Experiments were performed at least three times.

SOD1 aggregation induced by secosterol aldehydes was pH dependent (Figure 3C). Aggregation was greatly enhanced at neutral to alkaline pH but did not occur at acidic conditions (pH<7). We also tested different concentrations of the aldehyde. Aggregation was observed at concentrations as low as 10  $\mu$ M (aldehyde:protein, 1:1 molar ratio) and increased almost linearly up to 250  $\mu$ M reaching a plateau with seco-B at 100  $\mu$ M (Figure 3D). Time-dependent analysis showed a rather fast aggregation kinetics reaching a plateau after 12 to 24h, with seco A and B, respectively (Figure S2).

### **3. Aggregates Formed by Secosterol Aldehydes Have Amorphous Nature**

Alterations in protein conformation leading to exposure of protein hydrophobic residues can trigger the formation of  $\beta$ -amyloid type aggregates [29,45]. To check the morphology of SOD1 aggregates we first conducted dye binding experiments with thioflavin T (ThT). Experiments with apo and holo forms of SOD1 WT treated with aldehydes showed a 2-3 fold enhancement of ThT fluorescence after 24 h incubation, indicating the formation of amyloid-like structures (Figure 4A). However, a Congo Red (CR) binding experiment did not show changes in the absorbance, nor the characteristic red spectral shift typically observed for amyloid fibrils (Figure 4B, alpha-synuclein was used as positive control for amyloid fibrils). Thus, to clarify the morphological nature of SOD1 aggregates we also performed TEM analysis. In agreement with CR results, TEM images showed the presence of aggregates displaying amorphous morphology (Figure 4C).

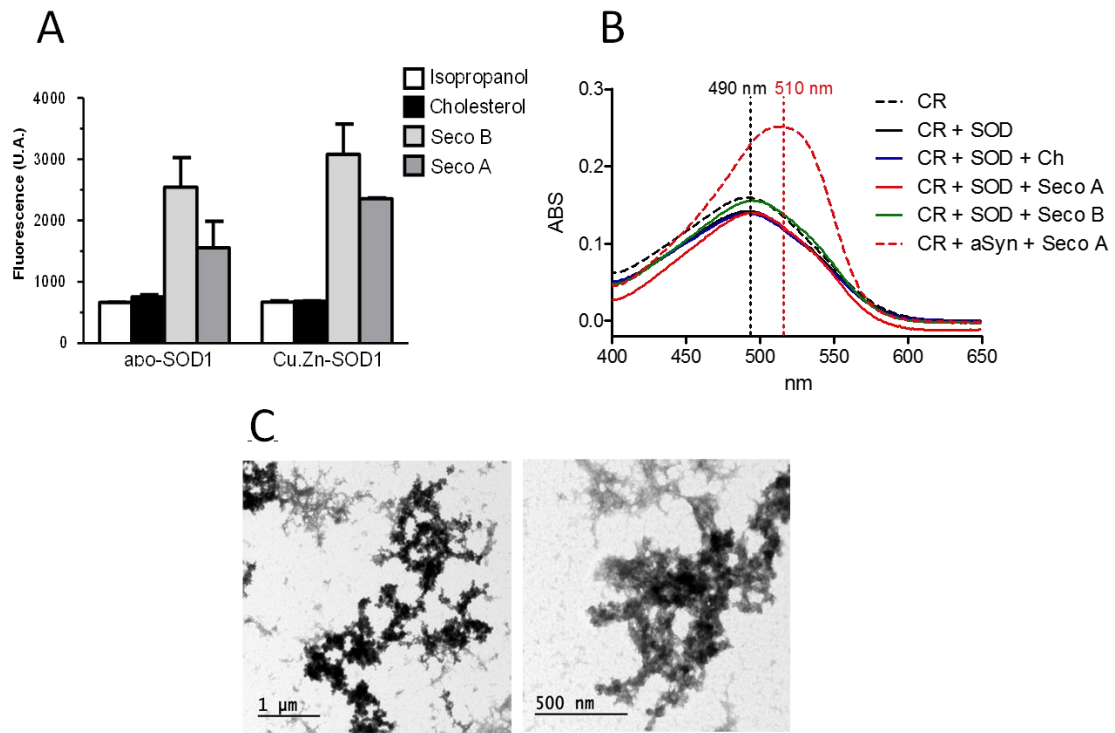


**Figure 4. Nature of SOD1 aggregates formed in the presence of cholesterol secosterol aldehydes.** (A) Effect of secosterol aldehydes on the exposition of hydrophobic residues of SOD1 by thioflavin T assay. (B) Congo red assay of SOD1 incubated with cholesterol secosterol aldehydes. Incubation of  $\alpha$ -synuclein with seco A was used as positive control. (C) Transmission electronic microscopy (TEM) of the apo-SOD1 WT incubated with seco-B.

#### 4. SOD1 Aggregates are Bound to Secosterol Aldehydes

As a way to detect SOD1-secosterol adducts we used clickable alkynyl derivatives [40]. SOD1 was incubated in the presence of alkynyl tagged-Cholesterol (a-Ch, Control), -seco-A (a-Seco-A), -seco-B (a-Seco-B) and -4-hydroxy-2-nonenal (a-HNE) (Figure 5A). The latter is a highly reactive short chain electrophile that was used for comparative purposes. In this assay, alkynyl lipids attached to proteins can be identified with the azido-biotin reagent via Huisgen-Sharpless cycloaddition and subsequently detected with a fluorescent streptavidin conjugate [40] (Figure S3). Interestingly, incubations of apo-SOD1 with alkynyl tagged secosterol aldehydes (a-seco-A and a-seco-B) showed intense labeling only in the high molecular weight

region at non reducing gels with no detectable adducted monomers or dimers (Figure 5C). Labeled monomeric and dimeric SOD1 forms became visible only after reduction with beta-mercaptoethanol (Figure 5C). Conversely, a-HNE showed intense labeling spread over almost the entire gel (Figure 5C) probably reflecting its high electrophilic nature. Of note, a-HNE-SOD1 adducts did not promote intense formation of high molecular weight aggregates (Figure 5B). This result implies that modifications induced by a-HNE are less likely to promote aggregation when compared to secosterol aldehydes.

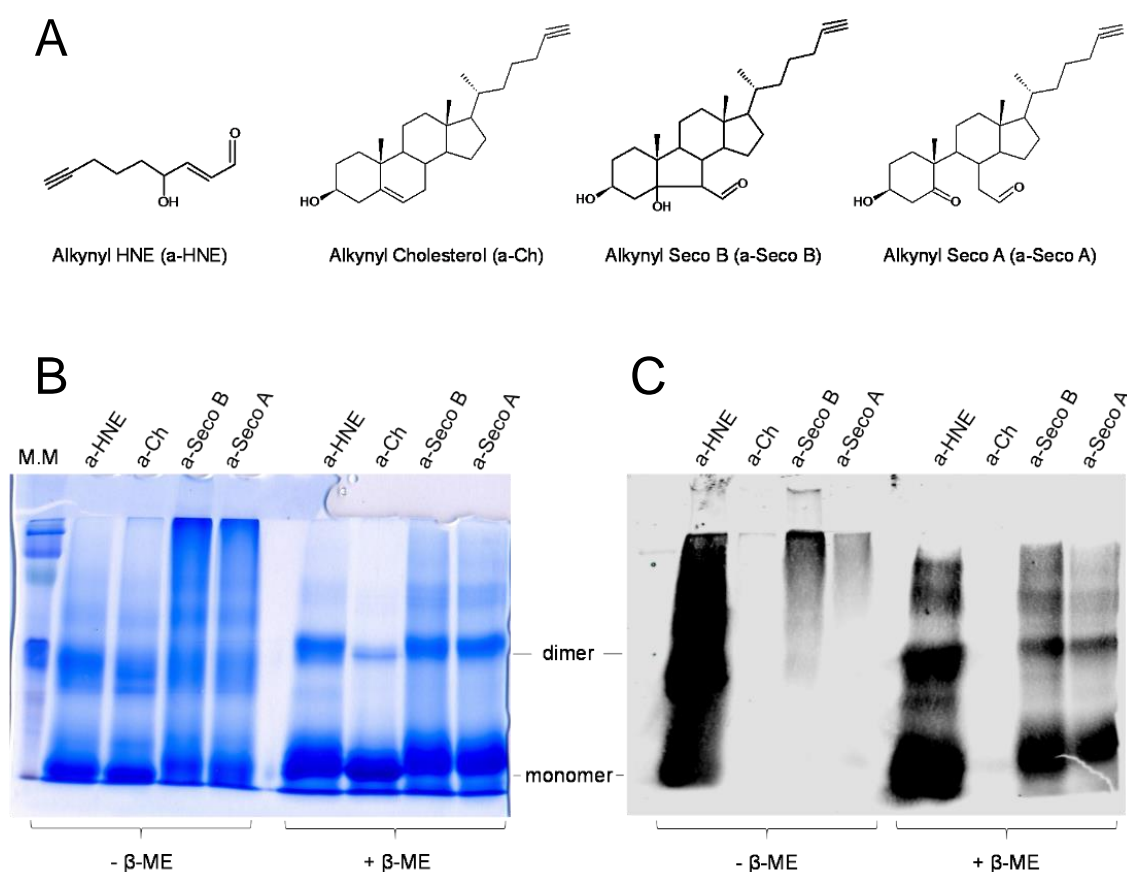


**Figure 5. Adduction of SOD1 by alkynyl-HNE and alkynyl-secosterol aldehydes.** (A) Alkynyl lipid structures. (B) SDS-PAGE of the apo-SOD1 WT incubations with a-lipids in non-reducing and reducing conditions stained with Coomassie. (C) View of apo-SOD1 modification by a-lipids using streptavidin-fluorophore by click chemistry. SOD1 modified by alkynyl lipid was labeled with biotin and stained with streptavidin conjugated with the Alexa Fluor 680 fluorophore.

To characterize the secosterol-SOD1 adducts, aggregated samples were reduced by DTT and analyzed by MALDI-TOF mass spectrometry. The MS spectrum showed the presence of up to five modifications in the protein, differing from the intact protein by the addition of 402 Da (Figure 6C and D). Such mass difference is consistent with the formation of Schiff base adducts between the secosterol aldehyde (M=418 Da) and basic amino acid residues, such as lysine, after a reduction step with sodium borohydride.

Taken together, these results suggest that secosterol aldehydes produce covalently modified SOD1-adducts that are much more prone to undergo oligomerization when compared to HNE.

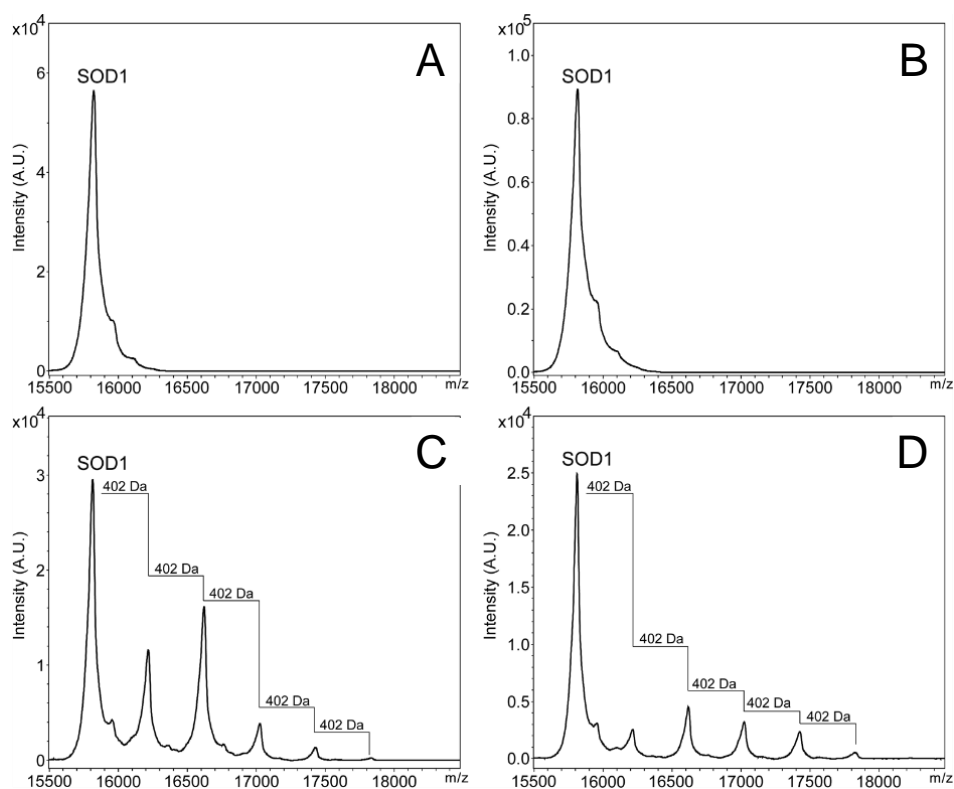


**Figure 6. SOD1-secosterol covalent adducts detected by MALDI-TOFMS.** Covalent adducts were analyzed after 24 h incubation of the protein in the absence (A) or presence of cholesterol (B), cholesterol aldehydes Seco-B (C) or Seco-A (D). After incubation, Schiff base adducts were reduced by NaBH<sub>4</sub> and SOD1 aggregates were disrupted by the addition of DTT, alkylated with IAM and then analyzed by MALDI-TOFMS.

## 5. SOD1 is Modified Mainly at Lysine Residues

To identify the sites of covalent adduction by secosterol aldehydes, SOD1 aggregates were digested by trypsin and submitted to nano-LC-MS/MS. Protein sequencing by Mascot software gave a coverage greater than 99 %. Among modified residues we found the carbamidomethylated cysteine residues at Cys6, Cys57, Cys111 and Cys146. Moreover, it was possible to identify six secosterol Schiff-base adducts (peptides with mass shift of 402.3497 Da) on six Lys residues, namely: Lys3, Lys9, Lys30, Lys122, Lys128 and Lys136.

Modified residues were found in the following peptides: 1) Lys 3 at the peptide <sup>1</sup>ATK\*AVC'VLK<sup>9</sup>; 2) Lys 9 at the peptide <sup>4</sup>AVC'VLK\*GDGPVQGIINFEQK<sup>23</sup>; 3) Lys 30 at the peptide <sup>24</sup>ESNGPVK\*VWGSIK<sup>36</sup>; 4) Lys 122 at the peptide <sup>116</sup>TLVVHEK\*ADDLGK<sup>128</sup>; 5) Lys 128 at the peptide <sup>123</sup>ADDLGK\*GGNEESTK<sup>136</sup>; and 6) Lys 136 at the peptide <sup>129</sup>GGNEESTK\*TGNAGSR<sup>143</sup>. All MS/MS analysis presented mass error below 5 ppm (Figure 7; Table S1, Supporting Information). MS/MS spectra obtained for each modified peptide showed characteristic fragments indicative of secosterol-Lys adduction (Figure 7). Interestingly, secosterol-adducted peptides eluted at very long retention times (60-70 min) when compared to the unmodified peptides that eluted between 20-50 min (Figure 8). This chromatographic behavior is correlated to the hydrophobicity of the aldehydes, which contributes to their potential to induce protein aggregation.

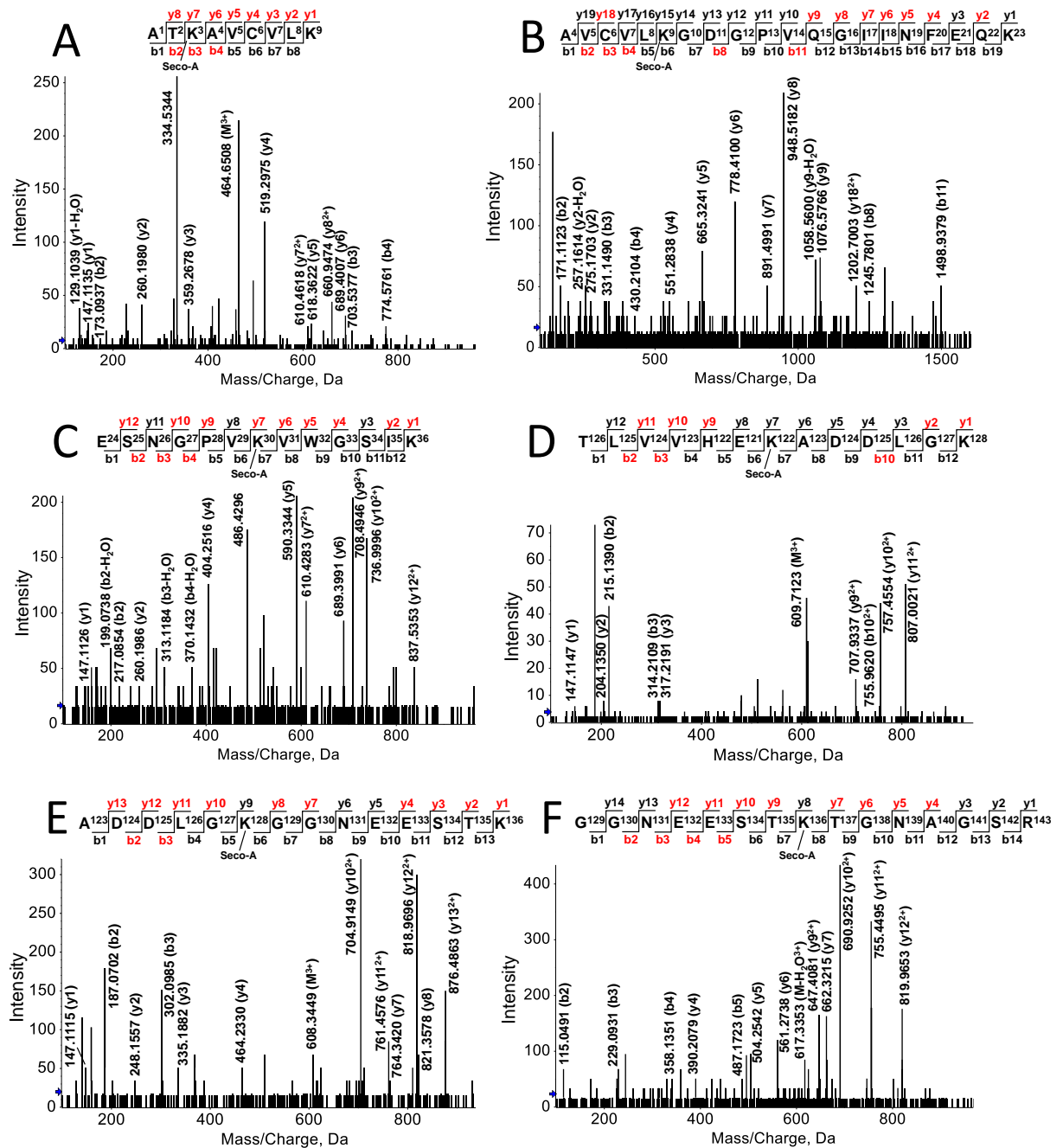


**Figure 7. MS/MS of the peptides resulting from the tryptic digestion of SOD1 after incubation with Seco-A.** Incubations contained 10  $\mu$ M SOD1 with 250  $\mu$ M Seco-A in 50 mM phosphate pH 8.4. Spectra are representative of, at least, 3 different experiments. (A) MS/MS of the peptide referent to the Lys 3. (B) MS/MS of the peptide referent to the Lys 9. (C) MS/MS of the peptide referent to the Lys 30. (D) MS/MS of the peptide referent to the Lys 122. (E) MS/MS of the peptide referent to the Lys 128. (F) MS/MS of the peptide referent to the Lys 136. This data is also representative to Seco-B, which had identical result. See Table S1 for more details concerning the tryptic digestion of SOD1.

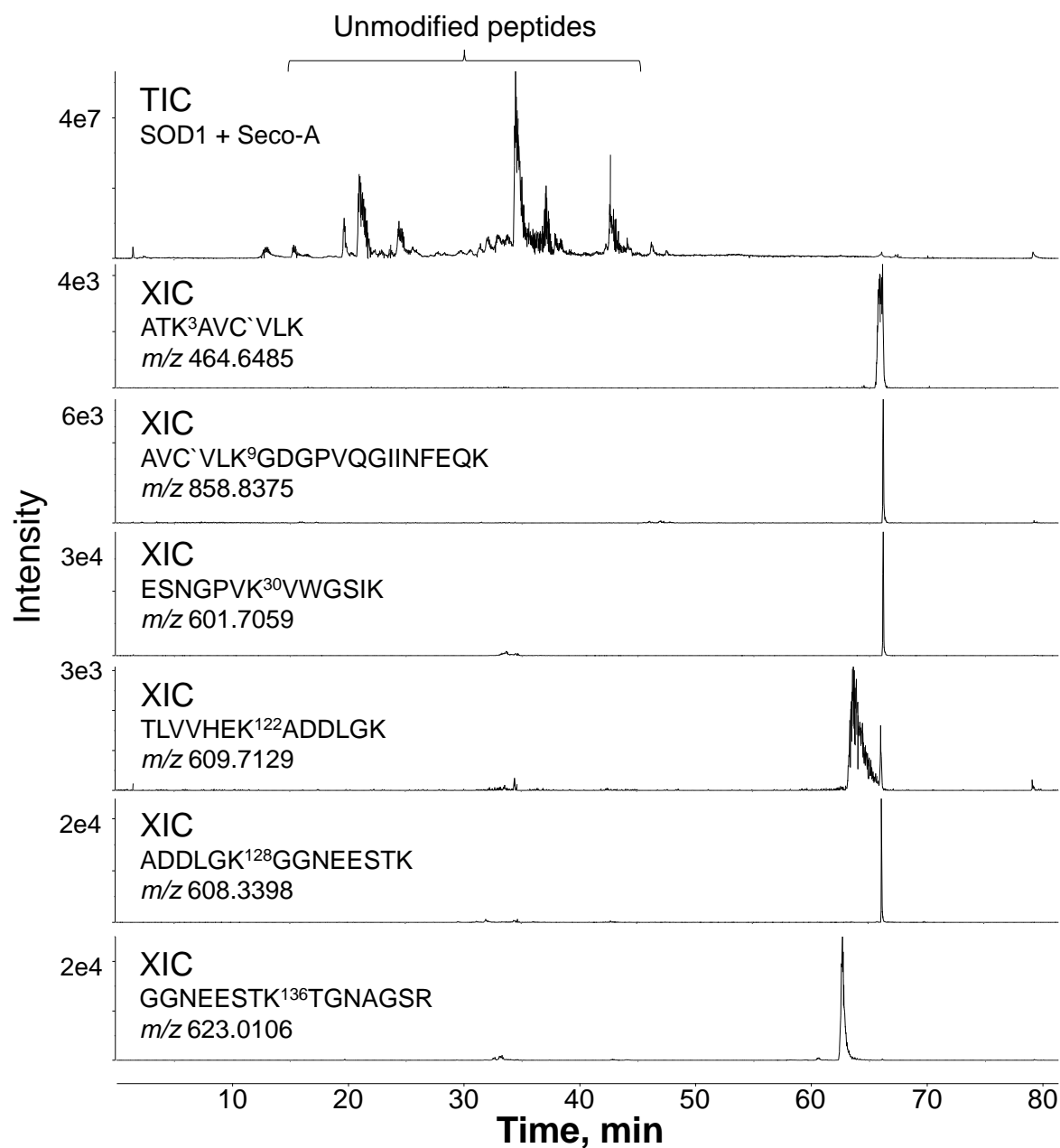


**Figure 8. Total ion chromatogram (TIC) of the tryptic digestion of SOD1 after incubation with Seco-A and extracted ion chromatogram (XIC) of each modified peptide.** Incubations contained 10  $\mu$ M SOD1 with 250  $\mu$ M Seco-A in 50 mM phosphate pH 8.4. Chromatograms are representative of, at least, 3 different experiments. This data is also representative to Seco-B, which had identical result. See Table S1 for more details concerning the tryptic digestion of SOD1.



## DISCUSSION

Neurodegenerative diseases are known to be associated with redox stress, which increases the production of lipid-derived electrophiles [46,47]. Among the targets of these reactive products, proteins are likely the most susceptible to covalent modifications because their nucleophilic residues are easily attacked by aldehydes and other electrophiles [48–50]. Levels of secosterol aldehydes are reported to be increased in several models of neurodegenerative diseases, and they are reported to contribute to disease pathology inducing protein modification and aggregation [17–20].

We showed that secosterol-B levels are increased in the motor cortex of the G93A ALS rat model as compared to controls, but not in the spinal cord (Figure 2). The higher concentration of secosterols in the cortex probably reflects their increased production and/or decreased efficiency of aldehyde detoxification in this tissue. In any case, accumulated secosterol aldehydes can potentially contribute to cerebral upper motor neuron death. Considering that neuronal death in ALS occurs at both motor cortex and spinal cord [31], it was somehow surprising that increased aldehyde levels were not detected in the spinal cord. At least two explanations for this are possible. The first is that aldehydes were quantified as free aldehydes and aldehydes that could be covalently bound to biomolecules were not monitored. Secondly, neuronal death occurs mostly in the anterior region of the spinal cord [26], from which the aldehydes could have been diluted since our analysis used the entire spinal cord. These factors might have hindered detection of secosterol aldehydes in the analyzed tissues and may explain why we did not see differences in the spinal cord.

Taking into account the ubiquitous presence of secosterol aldehyde in neuronal tissues and its accumulation in brain cortex of ALS rats, we asked the question whether they could induce SOD1 aggregation. Interestingly, secosterol aldehydes significantly enhanced SOD1 aggregation of both apo- and holo-forms. As expected, aggregation was greater in the apo-

SOD1 compared to holo, in agreement with studies showing higher structural instability of the metal-deficient form [27,29]. Indeed, studies have shown that apo-SOD1 in solution shows increased conformational dynamics and local unfolding [29,51], making it highly prone to aggregation. Usually *in vitro* apo-SOD1 aggregation under quiescent conditions takes days or weeks to occur. Yet aggregation in the presence of secosterol aldehydes was greatly accelerated reaching a plateau at 12-24 h. This can be due to the hydrophobic nature of secosterol, which probably increases protein unfolding and aggregation. SEC analysis also showed preferential consumption of SOD1 monomers during the aggregation process (Figure 3B). This result is consistent with previous studies showing higher propensity of the monomeric form to undergo aggregation [52,53].

SOD1 aggregation can be accelerated *in vitro* by incubating the protein at pH values below 6. Rakhit and coworkers demonstrated a propensity of zinc-deficient SOD1 to aggregate in acidic conditions [28]. To better characterize the secosterol aldehyde-induced SOD1 aggregation, we decided to vary some conditions, such as pH and secosterol concentration. Incubations of apo-SOD1 with secosterol aldehydes tested at different pHs (4.7; 5.5; 6.2; 7.4; 8.4 and 10) showed that aggregation is considerably increased above pH 7.4 (Figure 3C). It is well known that the reactivity of thiols is increased in its deprotonated form ( $-S^-$ ) and that the thiol group is mildly acidic. The pKa value of the thiol group is dependent on the structure of the enzyme and its local environment, but in general the pKa of thiols in peptides is usually around 9, whereas in proteins the values can be as low as 3.5 [54]. So, the increased aggregation observed at higher pH could be explained by the increase of thiolate levels on the protein, making it more prone to the formation of intermolecular disulfide cross-links under oxidative conditions. However, protein aggregation was not apparent when the same assay was performed with apo-SOD1 WT with cholesterol, even at high pH values (data not shown), showing that increased pH alone does not induce protein aggregation. The pH is not only important for thiol

group reactivity, but also instrumental for the interaction between aldehyde and protein amino groups. Schiff base formation in proteins is favored at basic pH, that facilitates the nitrogen deprotonation from amino acids such as lysine, leading to exposure of their unpaired electrons [55]. Thus, our findings highlight the importance of pH to increase the reaction between secosterol aldehydes and SOD1 and also to promote disulfide crosslinking.

Secosterol aldehyde-induced protein aggregation has been correlated to its ability to form covalent bonds with basic amino acid residues [15,16,18,22]. In this context, it is suggested that secosterol aldehyde adduction to SOD1 may induce protein conformational changes, exposing non-polar domains or hydrophobic patches, which enhances their propensity to aggregation. This conformational change can also expose free cysteines and promote aberrant intermolecular disulfide bonds and protein aggregation, favoring formation of  $\beta$ -amyloid type structures [32]. Data derived from the thioflavin T assay (Figure 4A) confirmed exposition of hydrophobic domains, typically observed for amyloid fibrils. However, Congo red and TEM identified aggregates of amorphous nature (Figure 4B and C), a morphology found in previous studies on SOD1 aggregation promoted by lipids [32–34]. More importantly, the aggregates observed here resemble those aggregates found in ALS patients [56,57] and in early aggregates found in animal and *in vitro* models [58,59].

We used two different strategies to detect SOD1 modifications: the click chemistry assay (Figure 5) and MALDI-TOF-MS analysis (Figure 6). The first one has been constantly used as an efficient tool for detecting adducts of lipid-derived electrophiles, including secosterol aldehydes, in proteins *in vitro* and in complex samples [40,60,61]. This assay was important to detect secosterol aldehyde-modified SOD1 species in SDS-PAGE gels. Using this approach, secosterol adducted-SOD1 was detected only in the high molecular weight region, with no apparent detection of modified SOD1 monomers, dimers or trimers. The data suggest that secosterol adduction generates modified intermediates that readily undergo aggregation. Of

note, MALDI-TOF analysis showed up to five simultaneous secosterol additions to the protein, greatly enhancing protein hydrophobicity and aggregation. The mass difference between the additions was 402 Da, consistent with secosterol adduction to Lys residues by Schiff base formation.

Adducted SOD1 was further digested and analyzed by nano-LC-MS/MS. We have identified modifications on six Lys residues (Lys 3, Lys 9, Lys 30, Lys 122, Lys 128 and Lys 136) out of the eleven residues in each SOD1 chain (Figure 7). These residues are located in regions of SOD1 that have been described to be critical to aggregation, namely the electrostatic loop (loop VII; residues 120-143) and the dimer interface [62,63] (Figure 9). Loop VII in apo-SOD1 wild type and its mutants display the most dynamic structural alterations before global unfolding and aggregation [64,65]. Thus, we hypothesize that secosterol adduction to Lys122, Lys128 and Lys136 greatly increases overall SOD1 hydrophobicity and aggregation. Secosterol adduction was also found at Lys3 and Lys9, located nearby the dimer interface. Based on the reactive lysine locations, we can think of two scenarios for adduction. The Lys residues are covalently modified after monomerization or before monomerization. In the latter situation, we can expect that secosterol adduction will contribute to dimer disruption, increasing monomerization and aggregation.

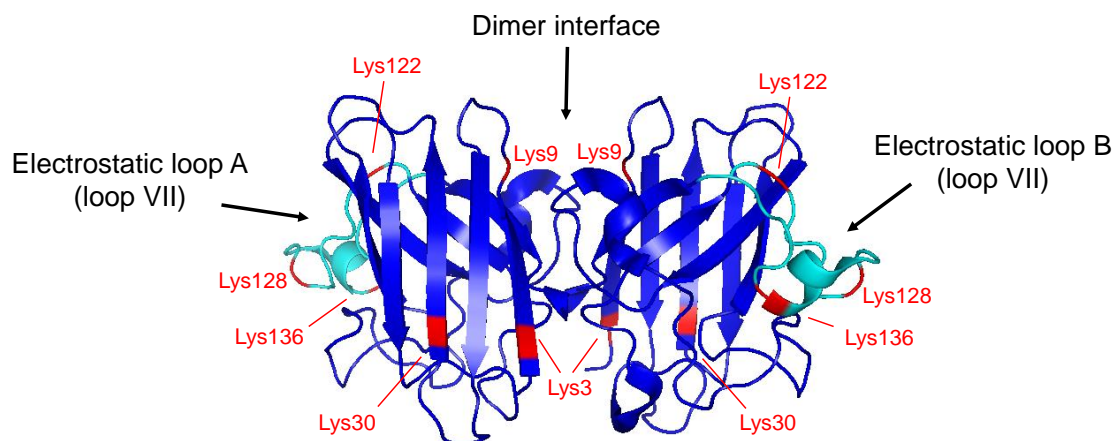


**Figure 9. Quaternary structure of SOD1.** Modified lysines are labeled in red and the electrostatic loops are labeled in cyan. The structure was drawn in Pymol software. Figure obtained from PDB <https://www.rcsb.org/3ecu>.

Exposing hydrophobic surfaces is likely to be one of the critical factors involved in the formation and stability of SOD1 aggregates [32–34]. In our work, SOD1 aggregation induced by secosterols was followed by increased hydrophobic surface, confirmed by the thioflavin T assay (Figure 4A). This phenomenon could be simply related to the intrinsic hydrophobic nature of the secosterols that dramatically increases the hydrophobicity of protein regions where they are covalently attached. It should be noted that peptides linked to secosterols eluted much later in reversed-phase chromatography (Figure 8). Alternatively, secosterol adduction could contribute to the unfolding process leading to the exposition of protein hydrophobic patches. Together, the increased hydrophobicity associated with the exposition of hydrophobic residues can greatly contribute to SOD1 destabilization and aggregation.

In conclusion, our data suggest that both apo- and holo-SOD1 can be target for secosterol aldehyde-induced aggregation. This effect added to the fact that these aldehydes are increased in the brain of an ALS rat model suggest that they may contribute to the pathological mechanism of the disease. Secosterol aldehyde-induced protein modification enhanced protein hydrophobicity, leading to the formation of high molecular weight aggregates. Taken together, our findings contribute to understand of how SOD1 forms aggregates in the presence of

hydrophobic surfaces, corroborating with similar studies in presence of lipid membranes and fatty acids. Furthermore, this work adds to evolving notion that secoesterol aldehydes can have a significantly detrimental effect by their adduction to biomolecules.

**Acknowledgments:** This work was supported by Fundação de Amparo à Pesquisa do Estado de São Paulo (FAPESP, CEPID-Redoxoma 13/07937-8 and 10/50891-0), Conselho Nacional de Desenvolvimento Científico e Tecnológico (CNPq, Universal 424094/2016-9), NAP-Redoxoma, Pro-Reitoria de Pesquisa USP and CAPES. The Ph.D. scholarship of L.S.D. was supported by CNPq.

## References

- [1] J.M. Dietschy, S.D. Turley, *Thematic review series: Brain Lipids*. Cholesterol metabolism in the central nervous system during early development and in the mature animal, *J. Lipid Res.* 45 (2004) 1375–1397. doi:10.1194/jlr.R400004-JLR200.
- [2] L.L. Smith, Review of progress in sterol oxidations: 1987-1995, *Lipids*. 31 (1996) 453–487. doi:10.1007/BF02522641.
- [3] V. Mutemberezi, O. Guillemot-Legris, G.G. Muccioli, Oxysterols: From cholesterol metabolites to key mediators, *Prog. Lipid Res.* 64 (2016) 152–169. doi:10.1016/j.plipres.2016.09.002.
- [4] W.J. Griffiths, Y. Wang, An update on oxysterol biochemistry: New discoveries in lipidomics, *Biochem. Biophys. Res. Commun.* (2018) 1–6. doi:10.1016/j.bbrc.2018.02.019.
- [5] L.L. Smith, J.I. Teng, M.J. Kulig, F.L. Hill, Sterol metabolism. 23. Cholesterol oxidation by radiation-induced processes, *J Org Chem.* 38 (1973) 1763–1765. [http://www.ncbi.nlm.nih.gov/entrez/query.fcgi?cmd=Retrieve&db=PubMed&dopt=Citation&list\\_uids=4709674](http://www.ncbi.nlm.nih.gov/entrez/query.fcgi?cmd=Retrieve&db=PubMed&dopt=Citation&list_uids=4709674).
- [6] A.W. Girotti, New trends in photobiology. Photosensitized oxidation of cholesterol in biological systems: Reaction pathways, cytotoxic effects and defense mechanisms, *J. Photochem. Photobiol. B Biol.* 13 (1992) 105–118. doi:10.1016/1011-1344(92)85050-5.
- [7] W. Korytowski, a W. Girotti, Singlet oxygen adducts of cholesterol: photogeneration and reductive turnover in membrane systems., *Photochem. Photobiol.* 70 (1999) 484–489.
- [8] M. Uemi, G.E. Ronsein, S. Miyamoto, M.H.G. Medeiros, P. Di Mascio, Generation of cholesterol carboxyaldehyde by the reaction of singlet molecular oxygen [ $O_2(1\Delta(g))$ ] as well as ozone with cholesterol., *Chem. Res. Toxicol.* 22 (2009) 875–84. doi:10.1021/tx800447b.
- [9] A.D. Wentworth, B.-D. Song, J. Nieva, A. Shafton, S. Tripurenani, P. Wentworth Jr., The ratio of cholesterol 5,6-secoosterols formed from ozone and singlet oxygen offers insight into the oxidation of cholesterol in vivo, *Chem. Commun.* (2009) 3098. doi:10.1039/b821584g.

- [10] S. Tomono, N. Miyoshi, H. Shiokawa, T. Iwabuchi, Y. Aratani, T. Higashi, H. Nukaya, H. Ohshima, Formation of cholesterol ozonolysis products in vitro and in vivo through a myeloperoxidase-dependent pathway, *J. Lipid Res.* 52 (2011) 87–97. doi:10.1194/jlr.M006775.
- [11] P.D. Brinkhorst J, Nara SJ, Hock cleavage of cholesterol 5alpha-hydroperoxide: an ozone-free pathway to the cholesterol ozonolysis products identified in arterial plaque and brain tissue., *J Am Chem Soc.* 130 (2008) 12224–5.
- [12] Z.A.M. Zielinski, D.A. Pratt, Cholesterol Autoxidation Revisited: Debunking the Dogma Associated with the Most Vilified of Lipids, *J. Am. Chem. Soc.* 138 (2016) 6932–6935. doi:10.1021/jacs.6b03344.
- [13] P. Wentworth, J. Nieva, C. Takeuchi, R. Galve, A.D. Wentworth, R.B. Dilley, G.A. DeLaria, A. Saven, B.M. Babior, K.D. Janda, A. Eschenmoser, R.A. Lerner, Evidence for ozone formation in human atherosclerotic arteries., *Science.* 302 (2003) 1053–6. doi:10.1126/science.1089525.
- [14] Y.-L. Lai, S. Tomono, N. Miyoshi, H. Ohshima, Inhibition of endothelial- and neuronal-type, but not inducible-type, nitric oxide synthase by the oxidized cholesterol metabolite secosterol aldehyde: Implications for vascular and neurodegenerative diseases, *J. Clin. Biochem. Nutr.* 50 (2011) 84–89. doi:10.3164/jcbtn.11-31.
- [15] K. Usui, J.D. Hulleman, J.F. Paulsson, S.J. Siegel, E.T. Powers, J.W. Kelly, Site-specific modification of Alzheimer's peptides by cholesterol oxidation products enhances aggregation energetics and neurotoxicity., *Proc. Natl. Acad. Sci. U. S. A.* 106 (2009) 18563–8. doi:10.1073/pnas.0804758106.
- [16] J.C. Scheinost, H. Wang, G.E. Boldt, J. Offer, P. Wentworth, Cholesterol seco-sterol-induced aggregation of methylated amyloid- $\beta$  peptides - Insights into aldehyde-initiated fibrillization of amyloid- $\beta$ , *Angew. Chemie - Int. Ed.* 47 (2008) 3919–3922. doi:10.1002/anie.200705922.
- [17] D. a Bosco, D.M. Fowler, Q. Zhang, J. Nieva, E.T. Powers, P. Wentworth, R. a Lerner, J.W. Kelly, Elevated levels of oxidized cholesterol metabolites in Lewy body disease brains accelerate alpha-synuclein fibrilization., *Nat. Chem. Biol.* 2 (2006) 249–253. doi:10.1038/nchembio782.
- [18] N.K. Cygan, J.C. Scheinost, T.D. Butters, P. Wentworth, Adduction of cholesterol 5,6-secosterol aldehyde to membrane-bound myelin basic protein exposes an



- immunodominant epitope, *Biochemistry*. 50 (2011) 2092–2100.  
doi:10.1021/bi200109q.
- [19] J. Bieschke, Q. Zhang, E.T. Powers, R.A. Lerner, J.W. Kelly, Oxidative metabolites accelerate Alzheimer's amyloidogenesis by a two-step mechanism, eliminating the requirement for nucleation, *Biochemistry*. 44 (2005) 4977–4983.  
doi:10.1021/bi0501030.
- [20] Q. Zhang, E.T. Powers, J. Nieva, M.E. Huff, M.A. Dendle, J. Bieschke, C.G. Glabe, A. Eschenmoser, P. Wentworth, R.A. Lerner, J.W. Kelly, Metabolite-initiated protein misfolding may trigger Alzheimer's disease., *Proc. Natl. Acad. Sci. U. S. A.* 101 (2004) 4752–7. doi:10.1073/pnas.0400924101.
- [21] J. Nieva, B.D. Song, J.K. Rogel, D. Kujawara, L. Altobel, A. Izharrudin, G.E. Boldt, R.K. Grover, A.D. Wentworth, P. Wentworth, Cholesterol secosterol aldehydes induce amyloidogenesis and dysfunction of wild-type tumor protein p53, *Chem. Biol.* 18 (2011) 920–927. doi:10.1016/j.chembiol.2011.02.018.
- [22] T.C. Genaro-Mattos, P.P. Appolinário, K.C.U. Mugnol, C. Bloch, I.L. Nantes, P. Di Mascio, S. Miyamoto, Covalent binding and anchoring of cytochrome c to mitochondrial mimetic membranes promoted by cholesterol carboxyaldehyde, *Chem. Res. Toxicol.* 26 (2013) 1536–1544. doi:10.1021/tx4002385.
- [23] A. Okado-Matsumoto, I. Fridovich, Subcellular distribution of superoxide dismutases (SOD) in rat liver. Cu,Zn-SOD in mitochondria, *J. Biol. Chem.* 276 (2001) 38388–38393. doi:10.1074/jbc.M105395200.
- [24] L.A. Sturtz, K. Diekert, L.T. Jensen, R. Lill, V.C. Culotta, A fraction of yeast Cu,Zn-superoxide dismutase and its metallochaperone, CCS, localize to the intermembrane space of mitochondria. A physiological role for SOD1 in guarding against mitochondrial oxidative damage, *J. Biol. Chem.* 276 (2001) 38084–38089.  
doi:10.1074/jbc.M105296200.
- [25] H. Deng, A. Hentati, J. Tainer, Z. Iqbal, A. Cayabyab, W. Hung, E. Getzoff, P. Hu, B. Herzfeldt, R. Roos, A. Et, Amyotrophic lateral sclerosis and structural defects in Cu,Zn superoxide dismutase, *Science* (80-. ). 261 (1993) 1047–1051.  
doi:10.1126/science.8351519.
- [26] P.N. Leigh, L.C. Wijesekera, Motor neuron disease: Focusing the mind on ALS:

- updated practice parameters, *Nat. Rev. Neurol.* 6 (2010) 191–192.  
doi:10.1038/nrneurol.2010.33.
- [27] L. Banci, I. Bertini, M. Boca, S. Girotto, M. Martinelli, J.S. Valentine, M. Vieru, SOD1 and amyotrophic lateral sclerosis: Mutations and oligomerization, *PLoS One*. 3 (2008) 1–8. doi:10.1371/journal.pone.0001677.
- [28] R. Rakhit, P. Cunningham, A. Furtos-Matei, S. Dahan, X.F. Qi, J.P. Crow, N.R. Cashman, L.H. Kondejewski, A. Chakrabartty, Oxidation-induced misfolding and aggregation of superoxide dismutase and its implications for amyotrophic lateral sclerosis, *J. Biol. Chem.* 277 (2002) 47551–47556. doi:10.1074/jbc.M207356200.
- [29] L. Banci, I. Bertini, M. Boca, V. Calderone, F. Cantini, S. Girotto, M. Vieru, Structural and dynamic aspects related to oligomerization of apo SOD1 and its mutants., *Proc. Natl. Acad. Sci. U. S. A.* 106 (2009) 6980–6985. doi:10.1073/pnas.0809845106.
- [30] J.P. Crow, J.B. Sampson, Y. Zhuang, J. a Thompson, J.S. Beckman, Decreased zinc affinity of amyotrophic lateral sclerosis-associated superoxide dismutase mutants leads to enhanced catalysis of tyrosine nitration by peroxynitrite., *J. Neurochem.* 69 (1997) 1936–1944. doi:10.1046/j.1471-4159.1997.69051936.x.
- [31] K.A. Trumbull, J.S. Beckman, A role for copper in the toxicity of zinc-deficient superoxide dismutase to motor neurons in amyotrophic lateral sclerosis., *Antioxid. Redox Signal.* 11 (2009) 1627–39. doi:10.1089/ars.2009.2574.
- [32] Y.J. Kim, R. Nakatomi, T. Akagi, T. Hashikawa, R. Takahashi, Unsaturated fatty acids induce cytotoxic aggregate formation of amyotrophic lateral sclerosis-linked superoxide dismutase 1 mutants, *J. Biol. Chem.* 280 (2005) 21515–21521. doi:10.1074/jbc.M502230200.
- [33] P.P. Appolinário, D.B. Medinas, A.B. Chaves-Filho, T.C. Genaro-Mattos, J.R.R. Cussiol, L.E.S. Netto, O. Augusto, S. Miyamoto, Oligomerization of Cu,Zn-superoxide dismutase (SOD1) by Docosahexaenoic acid and its hydroperoxides in vitro: Aggregation dependence on fatty acid unsaturation and thiols, *PLoS One*. 10 (2015) 1–15. doi:10.1371/journal.pone.0125146.
- [34] I. Choi, Y. In Yang, H.D. Song, J.S. Lee, T. Kang, J.J. Sung, J. Yi, Lipid molecules induce the cytotoxic aggregation of Cu/Zn superoxide dismutase with structurally disordered regions, *Biochim. Biophys. Acta - Mol. Basis Dis.* 1812 (2011) 41–48. doi:10.1016/j.bbadis.2010.09.003.

- [35] H. Karube, M. Sakamoto, S. Arawaka, S. Hara, H. Sato, C.H. Ren, S. Goto, S. Koyama, M. Wada, T. Kawanami, K. Kurita, T. Kato, N-terminal region of  $\alpha$ -synuclein is essential for the fatty acid-induced oligomerization of the molecules, *FEBS Lett.* 582 (2008) 3693–3700. doi:10.1016/j.febslet.2008.10.001.
- [36] G. De Franceschi, E. Frare, L. Bubacco, S. Mammi, A. Fontana, P.P. de Laureto, Molecular Insights into the Interaction between  $\alpha$ -Synuclein and Docosahexaenoic Acid, *J. Mol. Biol.* 394 (2009) 94–107. doi:10.1016/j.jmb.2009.09.008.
- [37] K. Broersen, D. Van Den Brink, G. Fraser, M. Goedert, B. Davletov,  $\alpha$ -Synuclein Adopts an  $\alpha$ -Helical Conformation in the Presence of Polyunsaturated Fatty Acids To Hinder Micelle Formation, *Biochemistry.* 45 (2006) 15610–15616. doi:10.1021/bi061743l.
- [38] K. Wang, E. Bermúdez, W. a Pryor, The ozonation of cholesterol: separation and identification of 2,4-dinitrophenylhydrazine derivatization products of 3 beta-hydroxy-5-oxo-5,6-secocholestan-6-al., *Steroids.* 58 (1993) 225–9. <http://www.ncbi.nlm.nih.gov/pubmed/8356575>.
- [39] L.T. Benov, W.F. Beyer, R.D. Stevens, I. Fridovich, Purification and characterization of the Cu,Zn SOD from *Escherichia coli*, *Free Radic. Biol. Med.* 21 (1996) 117–121. doi:10.1016/0891-5849(95)02217-1.
- [40] K. Windsor, T.C. Genaro-Mattos, S. Miyamoto, D.F. Stec, H.Y.H. Kim, K.A. Tallman, N.A. Porter, Assay of protein and peptide adducts of cholesterol ozonolysis products by hydrophobic and click enrichment methods, *Chem. Res. Toxicol.* 27 (2014) 1757–1768. doi:10.1021/tx500229h.
- [41] E.G. Bligh, W.J. Dyer, A rapid method of total lipid extraction and purification., *Can. J. Biochem. Physiol.* 37 (1959) 911–917. doi:dx.doi.org/10.1139/cjm2014-0700.
- [42] F. V. Mansano, R.M.A. Kazaoka, G.E. Ronsein, F.M. Prado, T.C. Genaro-Mattos, M. Uemi, P. Di Mascio, S. Miyamoto, Highly sensitive fluorescent method for the detection of cholesterol aldehydes formed by ozone and singlet molecular oxygen, *Anal. Chem.* 82 (2010) 6775–6781. doi:10.1021/ac1006427.
- [43] F.R. Coelho, A. Iqbal, E. Linares, D.F. Silva, F.S. Lima, I.M. Cuccovia, O. Augusto, Oxidation of the tryptophan 32 residue of human superoxide dismutase 1 caused by its bicarbonate-dependent peroxidase activity triggers the non-amyloid aggregation of the

- enzyme, *J. Biol. Chem.* 289 (2014) 30690–30701. doi:10.1074/jbc.M114.586370.
- [44] L. McAlary, J.A. Aquilina, J.J. Yerbury, Susceptibility of mutant SOD1 to form a destabilized monomer predicts cellular aggregation and toxicity but not in vitro aggregation propensity, *Front. Neurosci.* 10 (2016) 1–16. doi:10.3389/fnins.2016.00499.
- [45] C. Münch, J. O'Brien, A. Bertolotti, Prion-like propagation of mutant superoxide dismutase-1 misfolding in neuronal cells., *Proc. Natl. Acad. Sci. U. S. A.* 108 (2011) 3548–53. doi:10.1073/pnas.1017275108.
- [46] B. Uttara, A. V Singh, P. Zamboni, R.T. Mahajan, Oxidative stress and neurodegenerative diseases: a review of upstream and downstream antioxidant therapeutic options., *Curr. Neuropharmacol.* 7 (2009) 65–74. doi:10.2174/157015909787602823.
- [47] T. Moos, E.H. Morgan, The metabolism of neuronal iron and its pathogenic role in neurological disease review, *Ann. N. Y. Acad. Sci.* 1012 (2004) 14–26. doi:10.1196/annals.1306.002.
- [48] L.M. Sayre, D. Lin, Q. Yuan, X. Zhu, X. Tang, Protein adducts generated from products of lipid oxidation: focus on HNE and ONE., *Drug Metab. Rev.* 38 (2006) 651–675. doi:10.1080/03602530600959508.
- [49] P.A. Grimsrud, H. Xie, T.J. Griffin, D.A. Bernlohr, Oxidative stress and covalent modification of protein with bioactive aldehydes, *J. Biol. Chem.* 283 (2008) 21837–21841. doi:10.1074/jbc.R700019200.
- [50] T. Shibata, K. Shimizu, K. Hirano, F. Nakashima, R. Kikuchi, T. Matsushita, K. Uchida, Adductome-based identification of biomarkers for lipid peroxidation, *J. Biol. Chem.* 292 (2017) 8223–8235. doi:10.1074/jbc.M116.762609.
- [51] F. Ding, Y. Furukawa, N. Nukina, N. V. Dokholyan, Local unfolding of Cu, Zn superoxide dismutase monomer determines the morphology of fibrillar aggregates, *J. Mol. Biol.* 421 (2012) 548–560. doi:10.1016/j.jmb.2011.12.029.
- [52] R. Rakhit, J.P. Crow, J.R. Lepock, L.H. Kondejewski, N.R. Cashman, A. Chakrabarty, Monomeric Cu,Zn-superoxide Dismutase Is a Common Misfolding Intermediate in the Oxidation Models of Sporadic and Familial Amyotrophic Lateral Sclerosis, *J. Biol. Chem.* 279 (2004) 15499–15504. doi:10.1074/jbc.M313295200.

- [53] V.K. Mulligan, A. Kerman, S. Ho, A. Chakrabartty, Denaturational Stress Induces Formation of Zinc-Deficient Monomers of Cu,Zn Superoxide Dismutase: Implications for Pathogenesis in Amyotrophic Lateral Sclerosis, *J. Mol. Biol.* 383 (2008) 424–436. doi:10.1016/j.jmb.2008.08.024.
- [54] K.G. Reddie, K.S. Carroll, Expanding the functional diversity of proteins through cysteine oxidation, *Curr. Opin. Chem. Biol.* 12 (2008) 746–754. doi:10.1016/j.cbpa.2008.07.028.
- [55] M.A.G. del Vado, A.F.R. Cardona, G.R.E. Gorostidi, M.C.G. Martinez, J.S. Blanco, F.G. Blanco, Determination of the rates of formation and hydrolysis of the Schiff bases of pyridoxal with polyallylamine, *J. Mol. Catal. A. Chem.* 101 (1995) 137–142. doi:10.1016/1381-1169(95)00074-7.
- [56] A. Kerman, H.N. Liu, S. Croul, J. Bilbao, E. Rogaeva, L. Zinman, J. Robertson, A. Chakrabartty, Amyotrophic lateral sclerosis is a non-amyloid disease in which extensive misfolding of SOD1 is unique to the familial form, *Acta Neuropathol.* 119 (2010) 335–344. doi:10.1007/s00401-010-0646-5.
- [57] S. Kato, M. Takikawa, K. Nakashima, A. Hirano, D.W. Cleveland, H. Kusaka, N. Shibata, M. Kato, I. Nakano, E. Ohama, New consensus research on neuropathological aspects of familial amyotrophic lateral sclerosis with superoxide dismutase 1 (SOD1) gene mutations: inclusions containing SOD1 in neurons and astrocytes., *Amyotroph. Lateral Scler. Other Motor Neuron Disord.* 1 (2000) 163–184. doi:10.1080/14660820050515160.
- [58] V.K. Mulligan, A. Kerman, R.C. Laister, P.R. Sharda, P.E. Arslan, A. Chakrabartty, Early steps in oxidation-induced SOD1 misfolding: Implications for non-amyloid protein aggregation in familial ALS, *J. Mol. Biol.* 421 (2012) 631–652. doi:10.1016/j.jmb.2012.04.016.
- [59] Y.M. Hwang, P.B. Stathopoulos, K. Dimmick, H. Yang, H.R. Badieli, M.S. Tong, J.A.O. Rumfeldt, P. Chen, V. Karanassios, E.M. Meiering, Nonamyloid aggregates arising from mature copper/zinc superoxide dismutases resemble those observed in amyotrophic lateral sclerosis, *J. Biol. Chem.* 285 (2010) 41701–41711. doi:10.1074/jbc.M110.113696.
- [60] A.M. Speen, H.Y.H. Kim, R.N. Bauer, M. Meyer, K.M. Gowdy, M.B. Fessler, K.E. Duncan, W. Liu, N.A. Porter, I. Jaspers, Ozone-derived oxysterols affect liver X

- receptor (LXR) signaling: A potential role for lipid-protein adducts, *J. Biol. Chem.* 291 (2016) 25192–25206. doi:10.1074/jbc.M116.732362.
- [61] W.N. Beavers, K.L. Rose, J.J. Galligan, M.M. Mitchener, C.A. Rouzer, K.A. Tallman, C.R. Lamberson, X. Wang, S. Hill, P.T. Ivanova, H.A. Brown, B. Zhang, N.A. Porter, L.J. Marnett, Protein Modification by Endogenously Generated Lipid Electrophiles: Mitochondria as the Source and Target, *ACS Chem. Biol.* 12 (2017) 2062–2069. doi:10.1021/acschembio.7b00480.
- [62] Y. Furukawa, K. Kaneko, K. Yamanaka, N. Nukina, Mutation-dependent polymorphism of Cu,Zn-superoxide dismutase aggregates in the familial form of amyotrophic lateral sclerosis, *J. Biol. Chem.* 285 (2010) 22221–22231. doi:10.1074/jbc.M110.113597.
- [63] Y. Shi, R.A. Mowery, J. Ashley, M. Hentz, A.J. Ramirez, B. Bilgicer, H. Slunt-Brown, D.R. Borchelt, B.F. Shaw, Abnormal SDS-PAGE migration of cytosolic proteins can identify domains and mechanisms that control surfactant binding, *Protein Sci.* 21 (2012) 1197–1209. doi:10.1002/pro.2107.
- [64] L. Banci, I. Bertini, O. Blazevits, F. Cantini, M. Lelli, C. Luchinat, J. Mao, M. Vieru, NMR characterization of a “fibril-ready” state of demetallated wild-type superoxide dismutase, *J. Am. Chem. Soc.* 133 (2011) 345–349.
- [65] K.S. Molnar, N.M. Karabacak, J.L. Johnson, Q. Wang, A. Tiwari, L.J. Hayward, S.J. Coales, Y. Hamuro, J.N. Agar, A common property of amyotrophic lateral sclerosis-associated variants. Destabilization of the copper/zinc superoxide dismutase electrostatic loop, *J. Biol. Chem.* 284 (2009) 30965–30973. doi:10.1074/jbc.M109.023945.

## Supporting information

### Cholesterol Secosterol Aldehydes Induce Covalent Modification and Aggregation of Cu,Zn-Superoxide Dismutase: Potential Implications in ALS

Lucas S. Dantas<sup>†</sup>; Adriano de B. Chaves Filho<sup>†</sup>; Thiago C. Genaro-Mattos<sup>†1</sup>; Keri A. Tallman<sup>†</sup>; Ned A. Porter<sup>†</sup>; Fernando R. Coelho<sup>†</sup>; Ohara Augusto<sup>†</sup>; and Sayuri Miyamoto<sup>\*,†</sup>

#### 1. Supplementary figures and tables

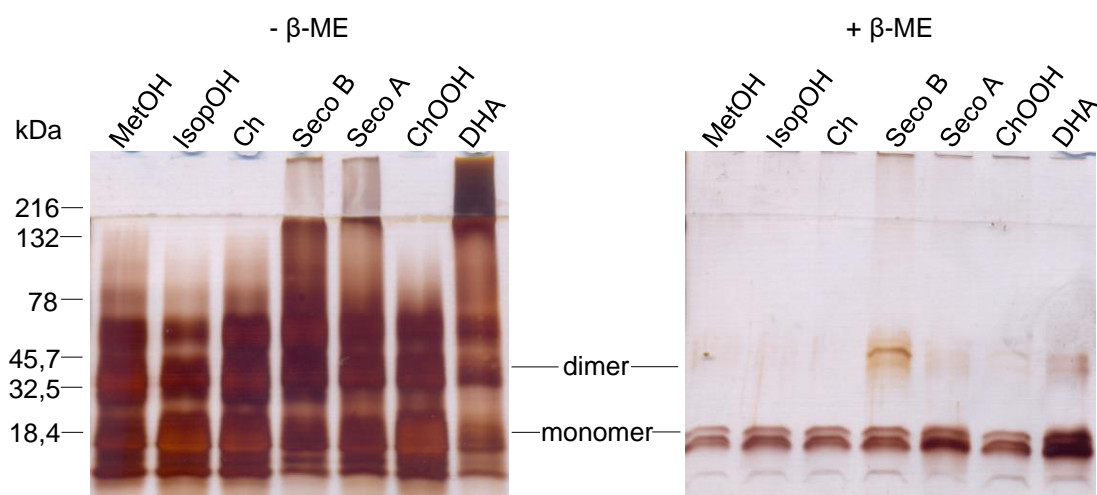


**Figure S1.** SDS-PAGE of apo-SOD1 WT incubated in the presence of cholesterol, seco-A, seco-B, ChOOH or DHA under nonreducing ( $-\beta$ -ME) or reducing conditions ( $+\beta$ -ME).

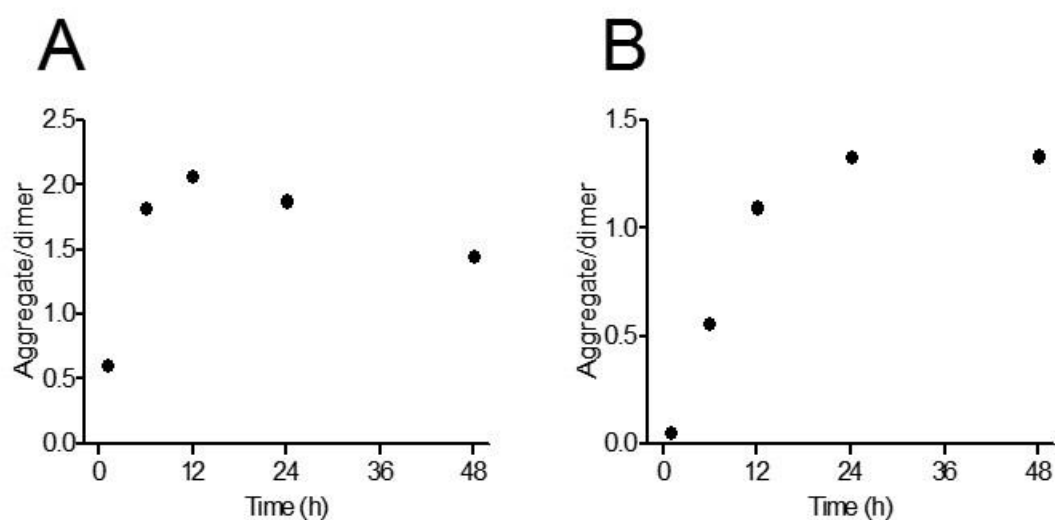


**Figure S2.** Kinetics of apo-SOD1 aggregation monitored by size exclusion chromatography (SEC). Apo-SOD1 WT (10  $\mu$ M) was incubated in the presence of 250  $\mu$ M secosterol-A (A) and secosterol-B (B) at 37°C for 48h. Aliquots at 0, 1, 8, 12, 24 and 48 hours were analyzed by SEC with fluorescence detection. Aggregation was measured by the ratio between area of the aggregate and area of dimer.

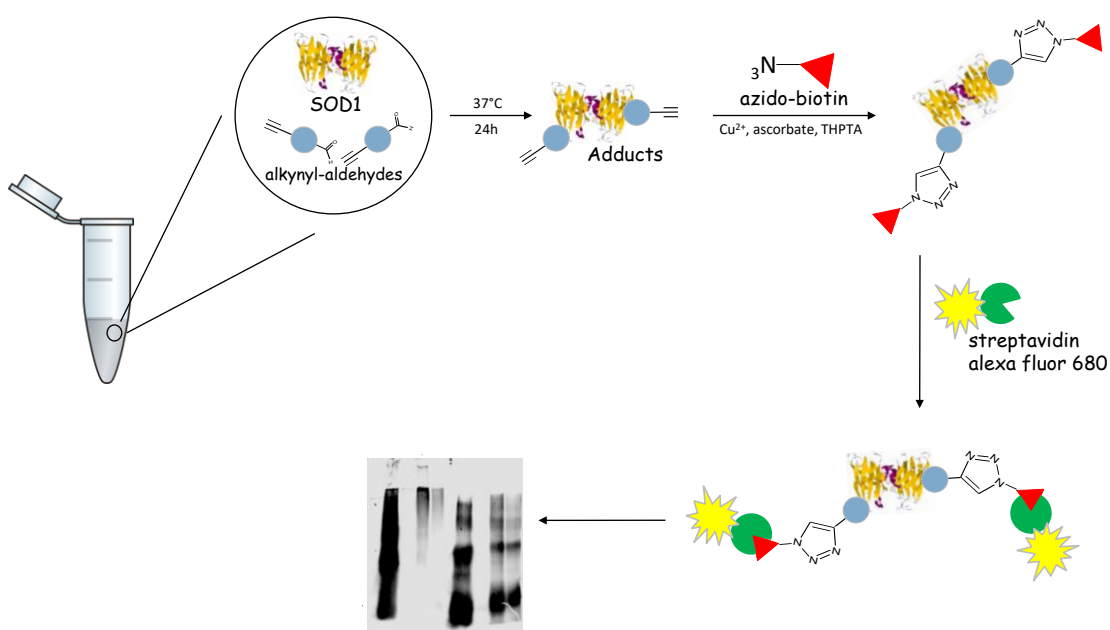


**Figure S3.** Scheme of click chemistry assay.



**Table S1.** SecoA/B-modified peptides identified by LC-MS/MS after digestion with trypsin.

Sequence	Residue	Unmodified (m/z)	Expected	Observed (Seco-A/Seco-B)	Error (ppm)
ATK*AVC'VLK	Lys3	330.5319 (3+)	464.6485 (3+)	464.6475/464.6468 (3+)	-2.1/-3.6
AVC'VLK*GDGPVQGII NFEQK	Lys9	724.7209 (3+)	858.8375 (3+)	858.8398/858.8399 (3+)	2.6/2.7
ESNGPVK*VWGSIK	Lys30	467.5893 (3+)	601.7059 (3+)	601.7057/601.7055 (3+)	-0.3/-0.6
TLVVHEK*ADDLGK	Lys122	475.5963 (3+)	609.7129 (3+)	609.7144/609.7149 (3+)	2.4/3.2
ADDLGK*GGNEESTK	Lys128	474.2232 (3+)	608.3398 (3+)	608.3398/608.3400 (3+)	0.0/0.3
GGNEESTK*TGNAGSR	Lys136	488.8940 (3+)	623.0106 (3+)	623.0132/623.0129 (3+)	4.1/3.6

\* Aldehyde adduct

' Carbamidomethyl adduct

## CHAPTER 2

### **Lipid-derived electrophiles induce covalent modification and aggregation of Cu,Zn-superoxide dismutase in a hydrophobicity-dependent manner**

Lucas S. Dantas<sup>†</sup>, Lucas G. Viviani<sup>†</sup>, Leandro de Rezende<sup>†</sup>, Fernando R. Coelho<sup>†</sup>, Ohara Augusto<sup>†</sup>, Marisa H. G. de Medeiros<sup>†</sup>, Antonia T. Amaral<sup>†</sup> and Sayuri Miyamoto<sup>\*,†</sup>

<sup>†</sup>Departamento de Bioquímica, Instituto de Química, Universidade de São Paulo, São Paulo, SP, Brazil

\*Corresponding Author: Sayuri Miyamoto, Departamento de Bioquímica, Instituto de Química, Universidade de São Paulo, Avenida professor Lineu Prestes, 748, Bloco 10 Superior, sala 1074, São Paulo, SP, Brazil 05508-000.

Phone: +55113091-9113. E-mail: miyamoto@iq.usp.br

## ABSTRACT

Unsaturated lipids are highly susceptible to oxidation induced by reactive oxygen species and enzymes, leading to the formation of lipid hydroperoxides, ketones, alcohols and aldehydes. Reactive aldehydes can modify macromolecules such as proteins, resulting in loss of function and/or aggregation. Accumulation of copper, zinc-superoxide dismutase (Cu,Zn-SOD, SOD1) immunoreactive aggregates is associated with some cases of amyotrophic lateral sclerosis (ALS). The mechanism by which SOD1 forms those aggregates in motor neurons is still unclear, although recent studies have shown that it may be linked to lipids and membranes. This study aimed to evaluate the potential of different lipid-derived electrophiles to induce formation of SOD1 aggregates *in vitro*. 4-hydroxyhexenal ( $\log P_{\text{calc}}=0.30$ ), 4-hydroxynonenal ( $\log P_{\text{calc}}=1.73$ ), 2-Hexen-1-al ( $\log P_{\text{calc}}=1.67$ ), 2,4-nonadienal ( $\log P_{\text{calc}}=3.01$ ), 2,4-decadienal ( $\log P_{\text{calc}}=3.50$ ) and cholesterol secosterol aldehydes ( $\log P_{\text{calc}}=6.45/6.48$ ) were incubated with SOD1 at 37°C for 24h. Size exclusion chromatography confirmed that these aldehydes induce SOD1 aggregation. More importantly, we were able to demonstrate that SOD1 aggregation increases proportionally to the hydrophobicity of the aldehydes ( $r^2=0.977$ ). Further analysis of digested SOD1 derived from our *in vitro* incubations by nanoLC-MS/MS revealed that SOD1 was covalently modified by aldehydes mainly at lysine residues. Covalent docking showed that hydrophobic residues on the lysines surroundings may contribute to the recruitment of the aldehydes and thus form hydrophobic interactions which could be important to aggregate formation. Our data suggest that the hydrophobicity of lipid-derived electrophiles may play significant roles in protein aggregation, which might be critical to the pathology of neurodegenerative diseases.

**Keywords:** Superoxide dismutase, reactive aldehydes, amyotrophic lateral sclerosis.

**Highlights:**

- Hydrophobicity of the ligands is essential to the induction of SOD1 aggregation;
- Lysines are the main targets for modification by lipid-derived aldehydes;
- Hydrophobic amino acids in the lysine surroundings recruit the aldehydes;

## INTRODUCTION

Oxidative stress has been regarded to play an important role in neurodegenerative diseases [1–4]. Increased concentrations of redox biomarkers such as lipid peroxidation products and oxidized proteins in blood and brain of patients and rodent models have been associated with Alzheimer's disease [5–7], Parkinson's disease [8,9], Amyotrophic Lateral Sclerosis (ALS) [10,11] and other neurological disorders [12,13]. Lipids, which are usually polyunsaturated in mammalian cells, are one of the most susceptible biomolecules to oxidation by reactive oxygen species [14]. The oxidation of lipids leads to the formation of several electrophiles compounds that are capable of modifying proteins and other components of the cell [15,16]. Among the products of lipid peroxidation, the most important are hydroperoxides, alcohols, ketones and aldehydes [15,16].

Although diverse in sizes and structures, lipid aldehydes are highly reactive with nucleophilic compounds such as protein and DNA, generally leading to irreversible damages [15,16]. Among the aldehydes formed by the oxidation of fatty acids, acrolein, malondialdehyde (MDA), 4-hydroxy-2-hexenal (HHE) and 4-hydroxy-2-nonenal (HNE) are the best known [18–20].

$\alpha,\beta$ -Unsaturated aldehydes (acrolein, HHE and HNE) can form adducts with nucleophilic residues of proteins by two different mechanisms: (1) Michael addition at the double bond with lysine, histidine or cysteine residues or (2) Schiff base formation at the carbonyl group with lysines [15,21]. Several modifications of proteins by these lipid-derived electrophiles have already been studied, including  $\alpha$ -synuclein [22–25],  $\beta$ -amyloid peptide [26,27] and superoxide dismutase (SOD1) [28], all of them associated with the pathology of neurodegenerative diseases.

Cholesterol is another lipid present in massive amounts in the neurons and glial cells [29]. Cholesterol may undergo oxidative damage yielding highly hydrophobic aldehydes called

cholesterol secosterol aldehydes (seco-A and seco-B) [30–32]. These hydrophobic aldehydes react mainly by Schiff base formation with lysine residues and their reactivities were already investigated with  $\alpha$ -synuclein [33],  $\beta$ -amyloid peptide [34,35], myelin basic protein (MBP) [36]. In a recent work conducted by our group, we demonstrated that secosterol aldehydes were increased in brain of ALS rats and could induce SOD1 aggregation by forming adducts with specific lysine residues [37]. Collectively, the above-mentioned results indicate that secosterol aldehydes play an important role in the induction of protein aggregation.

To further understand this process, in the present study, the effects of some lipid-derived electrophiles with different hydrophobicities (Figure 1) were investigated on the modification and induction of aggregation of SOD1. SOD1 is an antioxidant enzyme responsible for the dismutation of the superoxide radical anion ( $O_2^{\bullet-}$ ) [38–40]. Mutations on the SOD1 gene have been linked to the development of familial ALS. Most of these mutations result in pro-oxidant effects of SOD1 and lead to formation of high molecular weight SOD1 oligomers stabilized by covalent disulfide bonds between cysteines 6 and 111, and non-covalent interactions like  $\beta$ -amyloid structures [41–43]. The molecular mechanism which leads to the formation of SOD1 aggregates is not clearly understood, but some studies, including recent works developed by our group [37,44], suggest that SOD1 has a trend to form high molecular weight oligomers when in contact with lipids and hydrophobic surfaces [45,46]. In this paper, we demonstrated that the hydrophobicity of electrophiles is critical for protein modification and aggregation.

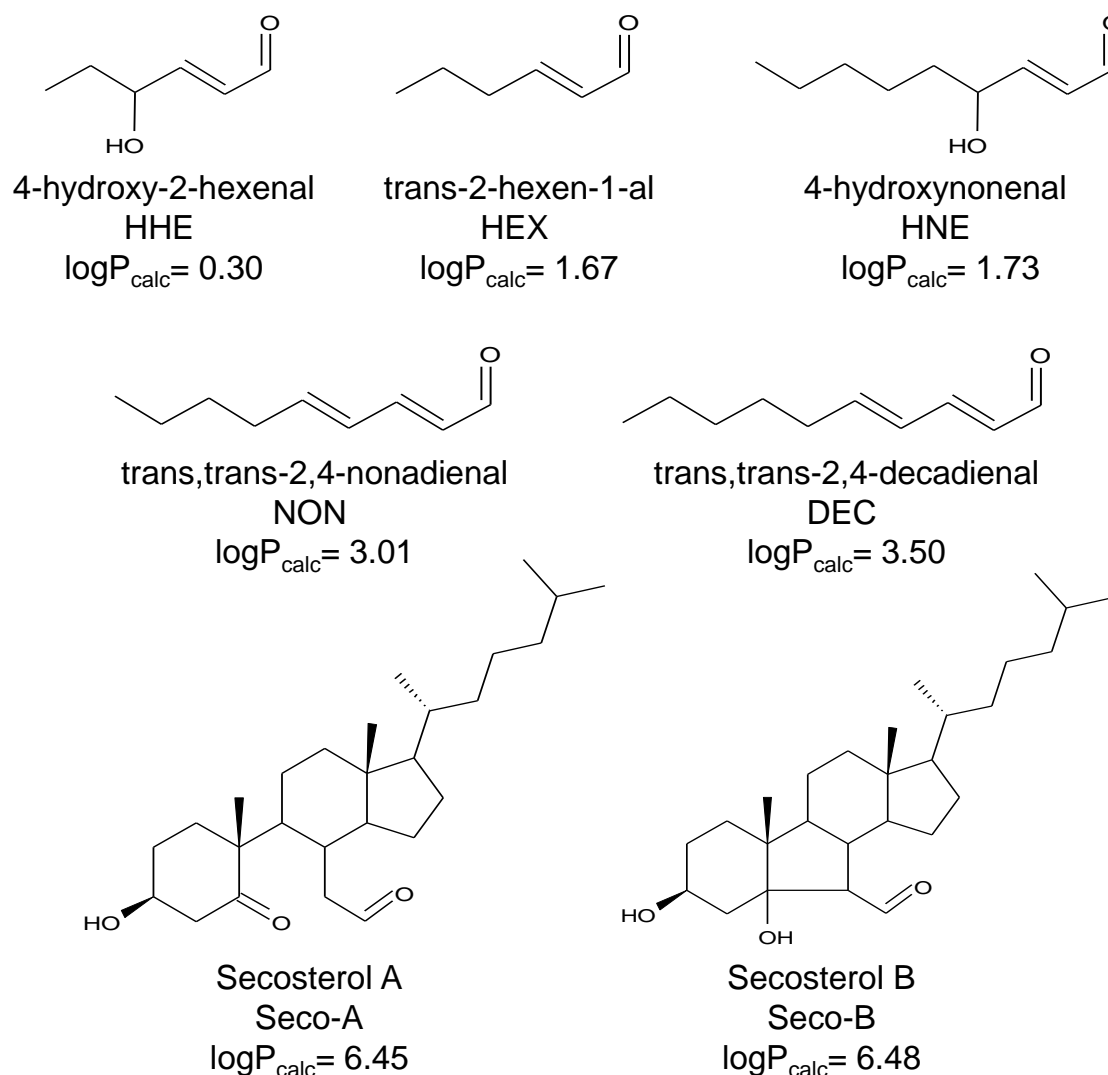


**Figure 1.** Structures and calculated partition coefficient ( $\log P_{\text{calc}}$ ) of lipid-derived electrophiles.

## MATERIALS AND METHODS

### 1. Chemicals

HHE (4-hydroxy-2-hexenal) and HNE (4-hydroxy-2-nonenal) were purchased from Cayman Chemical (Ann Arbor, MI). Hexenal (Trans-2-Hexen-1-al), Nonadienal (trans,trans-2,4-nonadienal) and Decadienal (trans,trans-2,4-decadienal) were purchased from Sigma (St. Louis, MO). Secosterol A (3 $\beta$ -hydroxy-5-oxo-5,6-secocholestan-6-al) was synthesized by ozonization and purified as described by Wang and colleagues [47]. Secosterol B (3 $\beta$ -hydroxy-

5 $\beta$ -hydroxy-B-norcholestane-6 $\beta$ -carboxaldehyde) was synthesized by photooxidation and purified as described by Uemi and colleagues [31]. SOD1 (superoxide dismutase 1) was expressed in *Escherichia coli*, purified and its apo form prepared as described by Benov and coworkers [48]. Unless otherwise stated all chemicals were of the highest analytical grade and were purchased from Sigma, Merck or Fisher.

## 2. Theoretical LogP Determination

Aldehyde hydrophobicity was determined using theoretical LogP (LogP<sub>calc</sub>) calculated by MoKa<sup>TM</sup> software [49].

## 3. Incubations of SOD1 with the Aldehydes

Apo form of SOD1 (10  $\mu$ M) was incubated in 50 mM phosphate buffer pH 7.4 containing 150 mM NaCl and 100  $\mu$ M DTPA in the presence of 250  $\mu$ M HHE, HNE, hexenal, nonadienal, decadienal, secosterol A or secosterol B at 37 °C during 24h under gentle agitation. 10% isopropanol was used as control.

## 4. Aggregate Formation Analysis by Size Exclusion Chromatography (SEC)

10  $\mu$ L of each incubation was analyzed by SEC using fluorescence detection with excitation wavelength at 280 nm and emission at 340 nm. Samples were eluted with 50 mM phosphate buffer, pH 7.4 containing 150 mM NaCl in the column BioSep-SEC-S3000 (300 x 7.8 mm, Phenomenex, USA) at 0.5 mL/min. Aggregate formation was evaluated and quantified by the ratio between area of aggregates and area of the dimer.



## 5. Enzymatic Digestion of SOD1

Incubations of SOD1 with aldehydes were first reduced with 5 mM sodium borohydride ( $\text{NaBH}_4$ ) for 1h at room temperature to stabilize the Schiff base adducts. Then samples were treated with 5 mM DTT (dithiotreitol) for 30 min at 60 °C to reduce disulfide bonds, followed by alkylation of cysteine residues with 15 mM iodoacetamide for 30 min at room temperature. After that, SOD1 samples were digested with proteomic grade trypsin (Promega) for 18h in a 1:100 (w/w) ratio at 37 °C in the presence of RapiGest SF Surfactant (Waters).

## 6. Peptide Analysis by Liquid Chromatography Coupled to Mass Spectrometry (LC-MS/MS).

Peptides resulting from tryptic digestion were analyzed using a nanoAcquity UPLC system (Waters, United States) with an ACQUITY UPLC-C18 (20 mm x 180  $\mu\text{m}$ ; 5  $\mu\text{m}$ ) coupled to a TripleTOF 6600 mass spectrometer (Sciex, United States). Samples were eluted at a flow rate of 0.4  $\mu\text{L}/\text{min}$  with mobile phase A (0.1% formic acid in water) and B (0.1% formic acid in acetonitrile) with the following gradient: 1 to 35% B from 0 to 60 min; 35 to 90% B from 60 to 61 min; isocratic elution with 90% B from 61 to 73 min; 90 to 1% B from 73 to 74 min. Nanoelectrospray ion source was operated at 2.4 kV. Mass spectrometer operated in IDA mode. MS1 spectra were analyzed in the range 300–2,000 Da with accumulation time of 100 ms. The 25 most intense ions with charge state 2–5 that exceeded 150 counts per second were selected for MS2, which was analyzed in the range 100–2,000 Da for 25 ms. The precursor ions were dynamically excluded from reselection for 4 s. Analyst TF software (Sciex, United States) was used for data acquisition and PeakView software (Sciex, United States) for data processing. For the analysis of protein sequence and modification, MASCOT software (Matrix Science Ltd., London, United Kingdom) was used. The modifications were searched based on the

possibilities of Schiff base formation to lysine residues after reduction with NaBH<sub>4</sub> (HHE: +98.0731 Da; HNE: +140.1201 Da; HEX: +82.0782 Da; NON: +122.1095 Da; DEC: +136.1252 Da; and Secosterols: +402.3497 Da) as well as Michael addition to lysine, histidine and cysteine residues (HHE: +114.0680 Da; HNE: +156.1150 Da; HEX: +98.0731 Da; NON: +138.1044 Da; DEC: +152.1201 Da; and Secosterols: +400.3341 Da). Carbamidomethyl (+57.0214 Da) was also considered as a possible modification of cysteine residues. The mass tolerance was 10 ppm for MS experiments and 0.05 Da for MS/MS experiments.

## 7. Covalent docking

Covalent docking was performed using GOLD docking suite version 5.2 (The Cambridge Crystallographic Data Centre) [50]. GOLD program assumes that there is just one atom linking the ligand to the protein. For each docking run, the nitrogen atom of lysine side chain was defined as the link atom for the covalent bond. An angle-bending potential has been incorporated into the fitness function to ensure that the geometry of the bound ligand is correct. Ten docking runs were performed for each ligand, using standard default settings and scoring function ChemPLP [51] to ranking the docking pose solutions. Prior to docking, ligand structures were minimized with Sybyl-X 2.1.1 software (Certara L.P., St Louis, MO). Energy minimization was done according to the Powell method, being stopped when the energy difference between interactions was lower than 0.05 kcal.mol<sup>-1</sup>.Å<sup>-1</sup>. Protein structure (SOD1, PDB: 3ECU, 1.9 Å resolution) was also prepared for docking using Sybyl-X 2.1.1. All hydrogen atoms were added, and predominant protonation states for amino acids side chains were set at pH 7.4. All water molecules were removed from the original pdb file.

## 8. Lipophilic surface generation

Lipophilic potential surface was generated using MOLCAD [52], at the Connolly surfaces, under Sybyl-X 2.1.1.

## RESULTS

### 1. Aldehyde-induced SOD1 aggregation is dependent on the hydrophobicity

To compare the effect of lipid-derived electrophiles in aggregating SOD1, human recombinant SOD1 was incubated with aldehydes of different sizes and polarities. After 24h, the incubations were analyzed by SEC (Figure 2A). The chromatogram shows a single peak at 8.5 min, which corresponds to the SOD1 dimer and a region from 5 to 7.5 min that represents the large protein aggregates (Figure 2A). The peak areas were calculated and used for aggregate quantification, which was expressed by aggregate/dimer ratio. Correlation analysis of SOD1 aggregation and LogP of aldehydes revealed a correlation coefficient of 0.977 (Figure 2B). The results indicate that HHE, HNE and hexenal did not induce SOD1 aggregation when compared to the solvent control. A consistent increase in SOD1 aggregate formation was observed following the order nonadialenal < decadialenal < Seco A = Seco B, which corresponds to the hydrophobicity order of the studied aldehydes (Figure 2B).

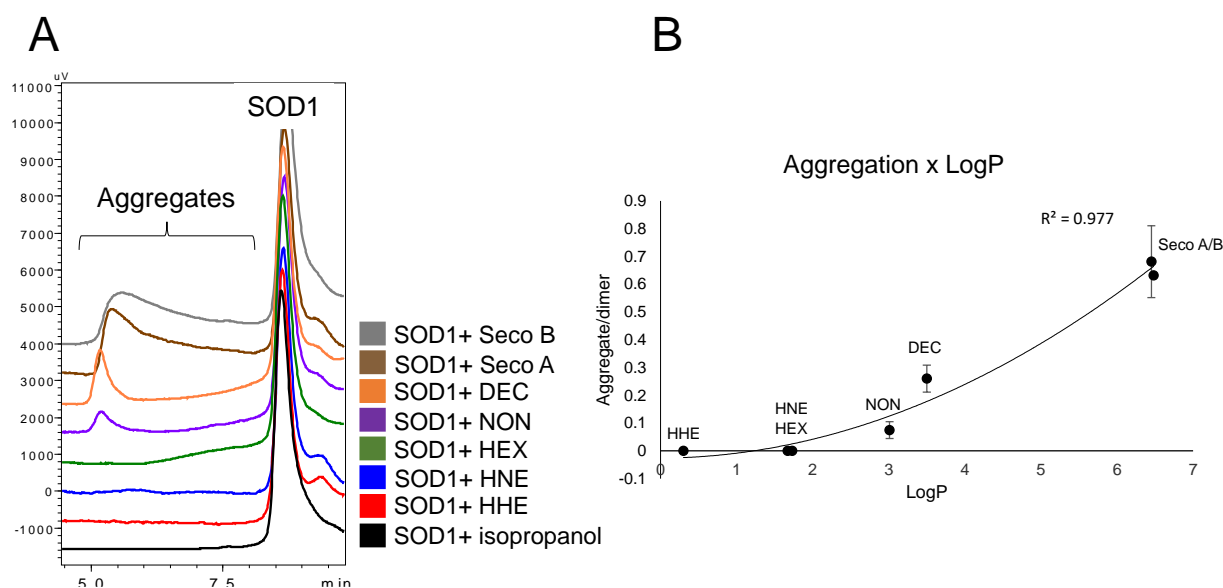


**Figure 2. SOD1 aggregation is dependent of the ligand hydrophobicity.** (A) Size exclusion chromatography (SEC) of SOD1 incubations with lipid-derived electrophiles. 10  $\mu$ M apo-SOD1 was incubated with 250  $\mu$ M aldehydes at 37°C for 24h. 10  $\mu$ L of each incubation was analyzed by SEC using fluorescence detection with excitation wavelength at 280 nm and emission at 340 nm. (B) Plot of aggregate formation (aggregate area/dimer area) versus logP of the aldehydes. Correlation showed a  $R^2 = 0.977$ .

## 2. Aldehydes modify peptide residues of SOD1, especially lysines

To characterize the structural modification of SOD1 induced by the lipid-derived electrophiles, peptides resulted from the tryptic digestion were analyzed by nanoLC-MS/MS. Data was then processed in the databank MASCOT to confirm the SOD1 sequence and to search for possible modifications, with an identification coverage greater than 99%. Among the modified residues, we found the carbamidomethyl addition at Cys6, Cys57, Cys111 and Cys146.

The modifications of aldehydes were evaluated according to two possibilities: adducts by Schiff base formation or Michael addition. Adducts of secosterol aldehydes with SOD1 occurred exclusively by Schiff base formation, while Michael addition was also possible for

the other studied aldehydes (Tables S1-6, supporting information). From the 11 lysines present in SOD1, 6 were modified by all of the aldehydes: Lys3, Lys9, Lys30, Lys122, Lys128 and Lys136 (Figure 3), whereas Lys23 was only modified by HHE. Moreover, Lys70 and Lys75 were also found to be modified by HNE and hexenal, as displayed in Figure 3B.

Some histidine residues, especially His120, were also modified only by those that could form Michael addition (Figure 3B). Interestingly, Cys6, the most reactive cysteine in SOD1, was found modified by the aldehydes, except HNE and secosterols. Since this cysteine participates on formation of disulfide crosslinks in the aggregation process [43], the apparent lack of SOD1 aggregation with some aldehydes can be explained by Cys6 modification. Besides this cysteine, Cys57 and Cys 111 were modified by the smallest aldehydes (HHE and HEX), whereas Cys 146 by HEX, NON and DEC (Figure 3B). MS/MS spectra of each modified peptide are shown in supplemental information.

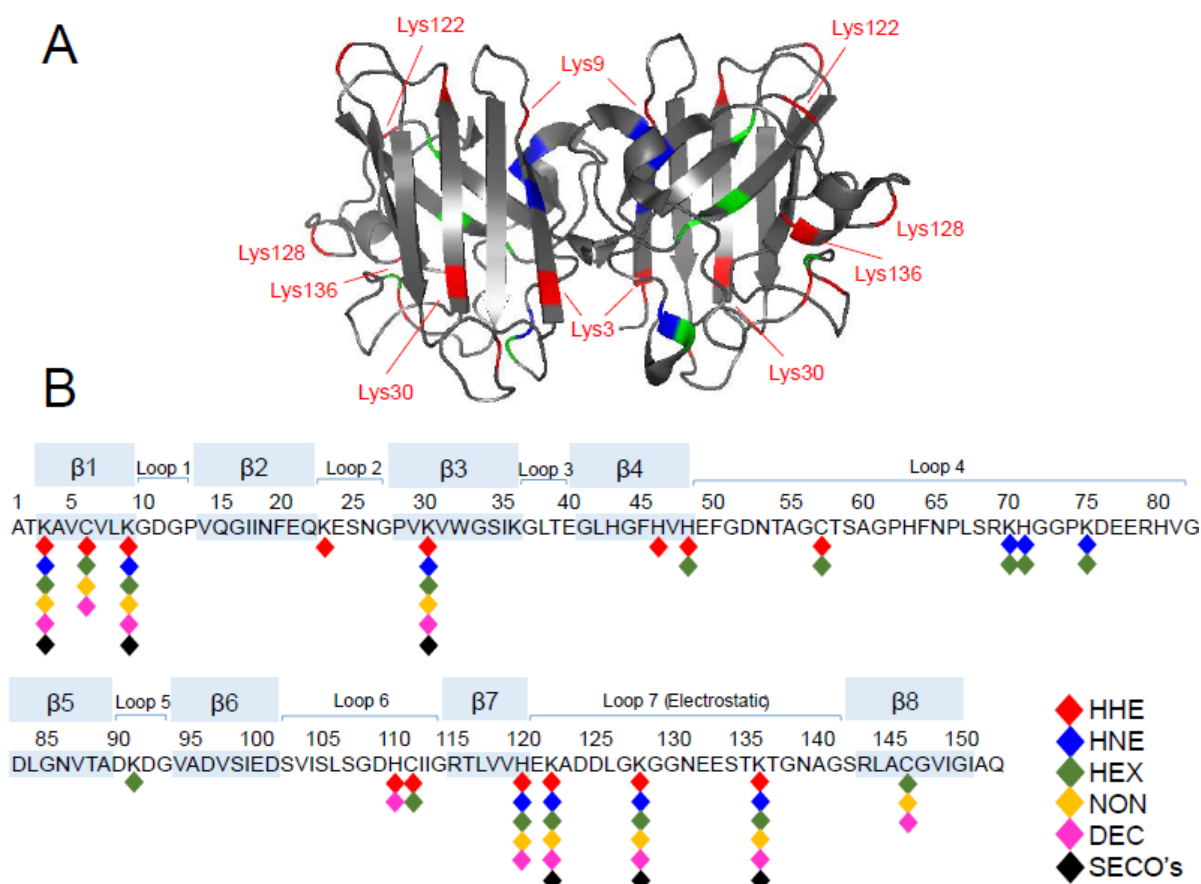


**Figure 3. Lipid-derived electrophiles covalently modify mostly lysine residues in SOD1.**

(A) Protein quaternary structure of SOD1. Lysine residues are highlighted in red, cysteine residues in blue and histidine residues in green (B) Linear sequence of SOD1. Modified residues are attached to the representative color for each aldehydes. Figure obtained from PDB <https://www.rcsb.org/3ecu>.

The modification of peptides by aldehydes chiefly affects the polarity of adducts, reflected in their very distinct retention times in the LC-MS analysis. For instance, the modifications of peptide A<sup>1</sup>TKAVCVLK<sup>9</sup> by each aldehyde at the Lys3 (illustrated in Figure 4) follow a pattern consistent with an increase in retention time with the hydrophobicity of the ligand aldehyde. These results suggest that aldehydes may directly influence the hydrophobicity of the region where they are bound to the peptides.

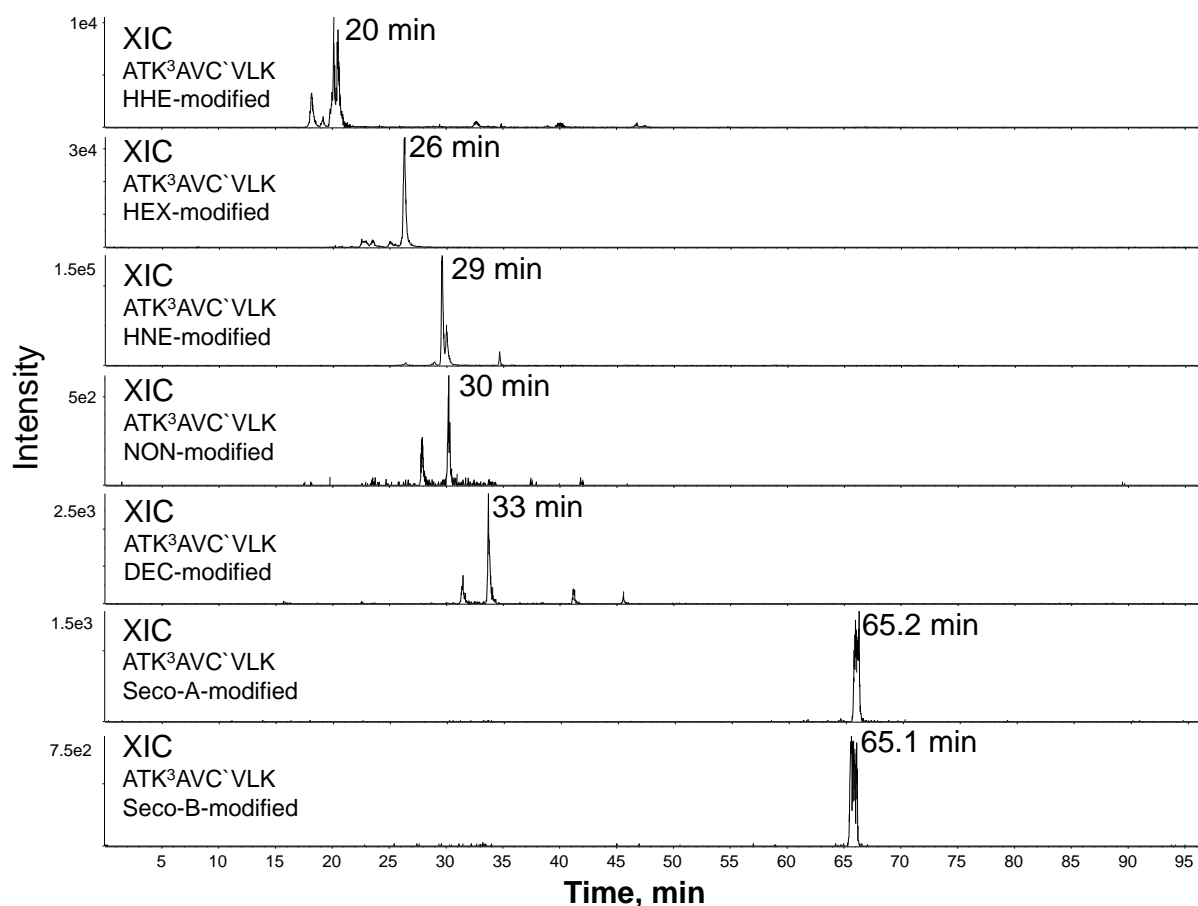


**Figure 4. Aldehyde hydrophobicity is reflected in the retention time of modified peptides.**

Peptides resulted from tryptic digestion were analyzed using a nanoAcquity UPLC system with an ACQUITY UPLC-C18 (20 mm x 180  $\mu$ m; 5  $\mu$ m) coupled to a TripleTOF 6600 mass spectrometer (Sciex, United States). Figure represents the extracted ion chromatogram (XIC) for the peptide ATK<sup>3</sup>AVCVLK modified by each aldehyde.

Analyzing the consumption of the unmodified peptides resulted from trypsin digestion, it was possible to see that HHE was the most reactive aldehyde, consuming 60% of the peptides in the reaction compared to the control. HEX, HNE, NON and DEC presented similar reactivity (20-30% of consumption of the peptides) and secosterol aldehydes were the less reactive, consuming about 10% of unmodified peptides (Figure 5). This result shows that, although the most hydrophobic aldehydes react less with SOD1, they were the most efficient to induce the

protein aggregation, indicating that hydrophobicity of the electrophile is more important for aggregation than the reactivity of the aldehyde.

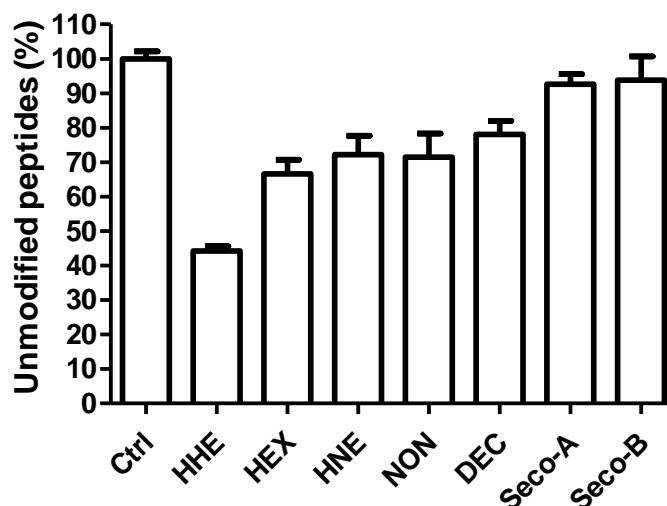


**Figure 5. Consumption of SOD1 unmodified peptides by lipid-derived electrophiles.** Areas of the peptides resulted from tryptic digestion were analyzed using MultiQuant software. Data represent the sum of areas of unmodified peptides normalized by the area of total ion chromatogram (TIC). The result was converted in percentage relative to the control.

### 3. Covalent docking

To get more insights into the protein-ligand interactions likely to occur between the aldehydes and residues surrounding the SOD1 lysines identified as major modification sites (Lys3, Lys9, Lys30, Lys122, Lys128 and Lys136), covalent docking was performed, using GOLD 5.2. With this purpose, all the aldehydes were independently docked into the binding sites located around each of these lysine residues. The non-covalent interactions between the aldehydes and the amino acids around the lysine residues found by the docking are specifically shown in table S7. It is possible to see that most of those contacts represent hydrophobic interactions with some specific residues around each lysine, such as Val5 and Ala152 near to the Lys3, Ile17 near to the Lys9, Trp32 near to the Lys30, Ala123 near to the Lys122, Leu126 near to the Lys128 and Thr137 near to the Lys136. Taking into account all these interaction



between the aldehydes and amino acids residues, we provide a score of the covalent docking. The result shows that the most hydrophobic aldehydes present a high number of interaction with the amino acid residues, probably due their high propensity to form hydrophobic interaction. This data is more prominent for the secosterol aldehydes (Table 1).

**Table 1.** Covalent docking score for the interactions aldehyde-Lys.

	<b>K3</b>	<b>K9</b>	<b>K30</b>	<b>K122</b>	<b>K128</b>	<b>K136</b>	<b>Total score</b>
<b>HHE</b>	71,8	73,4	67,5	68,0	77,6	65,4	423,64
<b>HEX</b>	69,9	72,3	67,9	66,5	72,3	61,7	410,59
<b>HNE</b>	78,1	83,3	73,2	74,1	82,8	74,2	465,56
<b>NON</b>	73,0	83,3	72,4	75,0	77,7	67,3	448,79
<b>DEC</b>	76,3	85,5	73,4	76,8	80,5	68,1	460,63
<b>Seco-A</b>	84,2	88,6	95,7	85,2	83,1	81,5	518,30
<b>Seco-B</b>	80,1	85,5	79,9	89,0	90,1	84,3	508,90

Docking results were then carefully analysed by visual inspection of the suggested top-ranked poses for the secosterol aldehydes (Figure 6). Lipophilic potential surfaces of SOD1 binding sites were also calculated using MOLCAD. The colour for lipophilic potential ranges from brown (highest lipophilic area of surface) to blue (highest hydrophilic area of surface). Predicted binding modes for seco-A and seco-B, covalently bound to Lys3, suggest that hydrophobic contacts are likely to be established between the sterol scaffold of these aldehydes and residues from both dimer subunits, including Val5-A, Ile17-A, Trp32-A 2.7 Å from the C-terminal Gln153-B carboxylate group, thus probably allowing a hydrogen-bond to be formed (Figure 6A and B). According to docking prediction, seco-A and seco-B, covalently bound to Lys-9, occupy a predominantly hydrophobic pocket located at the dimer interface, as evidenced by the brown areas in the lipophilic potential map (Figures 6C and D). In addition, seco-A hydroxyl group is oriented towards a hydrophilic region (blue-coloured) occupied by Asp11-B

side chain. The calculated distance between the hydroxyl oxygen and O $\delta$ 2 from Asp11-B carboxylate group is 2.5 Å, suggesting a hydrogen bond between these two atoms. Figures 6E and F show the top-ranked poses of seco-A and seco-B, respectively, covalently bound to Lys-30. These docking poses are placed in a cavity complementary in shape to the respective aldehyde structures, which is observed entirely at one of the dimer subunits, being composed by hydrophobic residues (Trp32 and Pro28) as well as by charged residues (Glu21, Lys23 and Glu100). Binding sites located around Lys122, Lys128 and Lys136 are predominantly formed by polar and charged residues (Figures 6G-L), most of which are part of the SOD1 electrostatic loop (Glu121-Ser142).

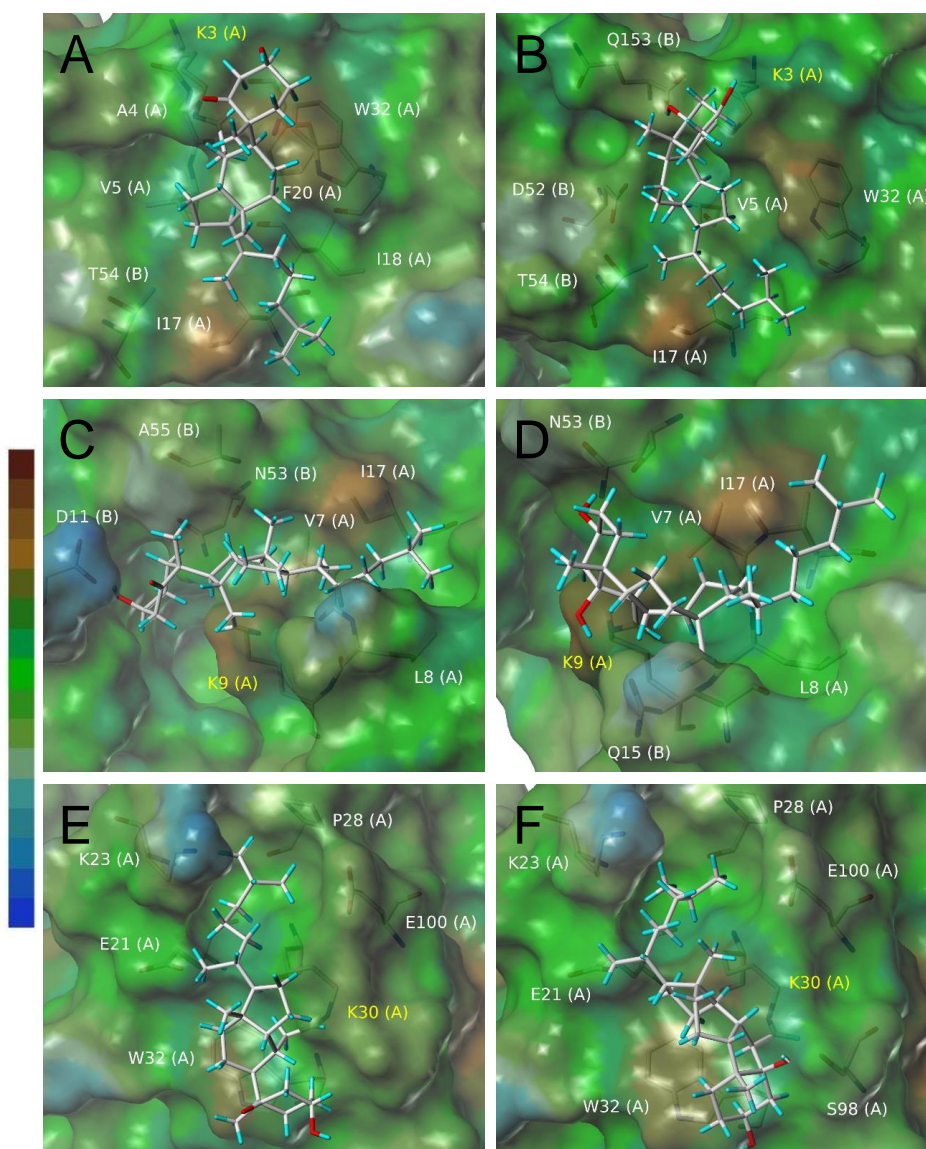


**Figure 6A-F.** Covalent docking solutions of seco-A and seco-B into the binding sites located around the SOD1 lysine residues modified by aldehydes (Lys3, Lys9 and Lys30). Lipophilic potential surfaces of the binding sites, calculated by MOLCAD, are also shown. The colour ramp for lipophilic potential ranges from brown (highest lipophilic area of surface) to blue (highest hydrophilic area of surface). Seco-A and seco-B, as well as the most relevant aminoacids, are shown as sticks and colored by atom type. For clarity, only hydrogen atoms of seco-A and seco-B are shown. **(A)** Seco-A covalently docked into the binding site around Lys3; **(B)** Seco-B covalently docked into the binding site around Lys3; **(C)** Seco-A covalently docked into the binding site around Lys9; **(D)** Seco-B covalently docked into the binding site around Lys9; **(E)** Seco-A covalently docked into the binding site around Lys30; **(F)** Seco-B covalently docked into the binding site around Lys30.

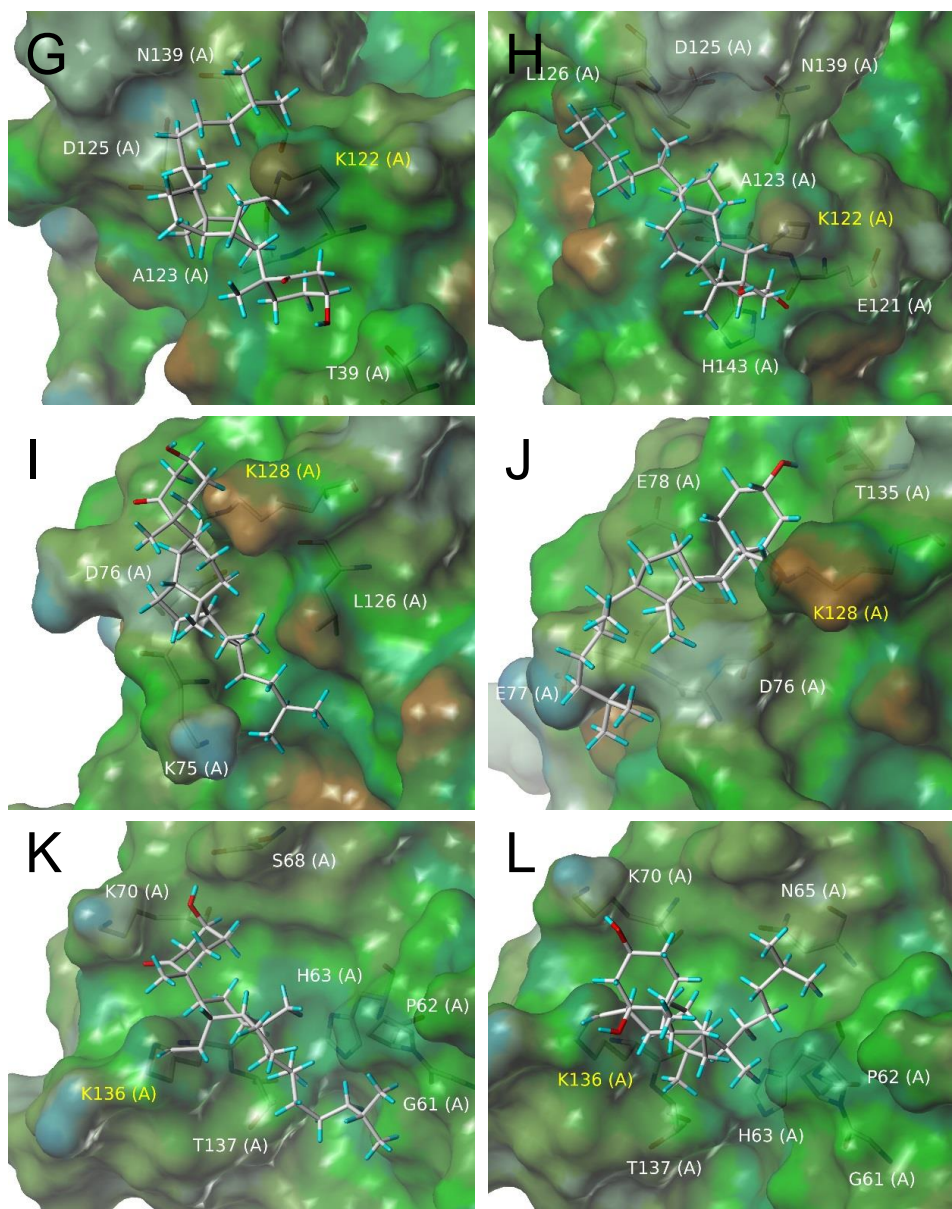


**Figure 6G-L.** Covalent docking solutions of seco-A and seco-B into the binding sites located around the SOD1 lysine residues modified by aldehydes (Lys122, Lys128 and Lys136). Lipophilic potential surfaces of the binding sites, calculated by MOLCAD, are also shown. The colour ramp for lipophilic potential ranges from brown (highest lipophilic area of surface) to blue (highest hydrophilic area of surface). Seco-A and seco-B, as well as the most relevant aminoacids, are shown as sticks and colored by atom type. For clarity, only hydrogen atoms of seco-A and seco-B are shown. **(G)** Seco-A covalently docked into the binding site around Lys122; **(H)** Seco-B covalently docked into the binding site around Lys122; **(I)** Seco-A covalently docked into the binding site around Lys128; **(J)** Seco-B covalently docked into the binding site around Lys128; **(K)** Seco-A covalently docked into the binding site around Lys136; **(L)** Seco-B covalently docked into the binding site around Lys136.

## DISCUSSION

Aldehydes derived from lipids are the end products of lipid oxidation and exhibit high reactivity with proteins and other macromolecules [15,16,30]. In the last few years, several studies have evaluated the effect of these lipid-derived electrophiles on cell physiology. Using shotgun proteomics and click chemistry, these studies have identified the main target peptides for the electrophiles, in addition to the consequence of adduct formation for cell homeostasis [53–57]. Furthermore, quantification of aldehyde-adducts has been proposed as a better tool for identification of oxidative stress biomarkers than free aldehydes, given their stability for quantification [58]. Considering the increased concentrations of lipid-derived electrophiles in neurodegenerative diseases [6,33,37,59] and their association with the pathogenesis of these disorders [22,24,25,27,60,61], our study compared the effect of different aldehydes in the induction of protein SOD1 aggregation.

Previous studies have investigated SOD1 modifications by electrophiles, such as acrolein and advanced glycation endproducts [28,62]. In the study by Kang [28], high concentrations of acrolein were shown to inhibit SOD1 activity by modification of Ser, His, Arg, Thr and Lys aminoacids. In the study conducted by Kato and co-workers [62], SOD1 aggregates immunoreactive for AGES antibodies were found in patients with ALS and mice expressing human SOD1 with G85R mutation. Both studies suggest that electrophiles may play significant roles in SOD1 homeostasis. Here, we not only demonstrated that electrophiles can modify and induce SOD1 aggregation, but our data also revealed that this effect is dependent on their hydrophobicity (Figure 2). This corroborates with our theory that when these aldehydes modify SOD1, they increase the hydrophobic surface of the protein and cause structural alterations in the protein favoring disulphide bridge formation and protein aggregation. Similarly, Liu and co-workers [27] found out that  $\beta$ -amyloid peptide misfolding and fibrillogenesis is promoted by HNE but not by HHE, which is a less hydrophobic aldehyde.



Several studies have identified nucleophilic lysines as major targets of aldehydes modification in proteins [33,34,51,52]. In this study with SOD1, we identified modifications on several Lys residues as well (Figure 3). The most common modified residues were Lys 3, 9, 30, 122, 128 and 136 that were found bonded to all tested aldehydes. These lysines are present in regions of SOD1 known to be important in the process of aggregation [65,66]. Ataya and coworkers showed that Lys136 is present in the most hydrophobic region of SOD1 [67]. This data suggests that Lys136 can be important in the process of SOD1 aggregation mediated by lipid aldehydes, and explains the reason why all aldehydes used in our study modified this residue (Figure 3). It is important to notice that the effect observed on SOD1 aggregation is not linked to the reactivity of the aldehydes but just to their hydrophobicity. Indeed, HHE was the most reactive aldehyde (Figure 5), but it didn't show any significant affect on the protein aggregation. On the other hand secosterol aldehydes were observed to be less reactive than other aldehydes (Figure 5), however they showed more effect on the SOD1 aggregation compared to the others (Figure 2). In addition, modification of cysteine residues by some aldehydes (HHE, HEX, NON and DEC) could also impact their role in SOD1 aggregation, since cysteine residues are critical to disulfide crosslinks and thus directly influencing formation and stability of the aggregates.

Acylation and acetylation of lysine residues in SOD1 have been described as potencial mechanisms for inhibition of protein aggregation [68,69]. These studies attribute the inhibitor effect of covalent modification to the increase of net surface potential and repulsion between cellular membranes and SOD1. These factors are thought to disrupt the formation of ThT-linked SOD1 fibrils [68,69]. Our data revealed that small aldehydes such as HHE and hexenal do not have any effect in SOD1 aggregation. Although their inhibitor effect was not tested in our *in vitro* aggregation model, covalent modification in lysines by these less hydrophobic aldehydes could alternatively provide a protective effect, since they block the charge of lysines,

influencing the surface potential of SOD1. On the other hand, palmitoylation of SOD1 in cysteine residues has been shown to induce association of the protein to membranes, which can increase the propensity to form aggregates [70]. This is an additional evidence showing that SOD1 interacting with lipids and membranes can be important for the aggregation process, which have been described by several works [37,44–46]. In addition to our previous results showing that secosterol aldehydes could induce SOD1 aggregation [37], in the present study we confirmed the essential role of ligand hydrophobicity to protein aggregation. We thought that the best way to show it was to compare SOD1 aggregation propensity in the presence of different aldehydes with crescent hydrophobicities. Our data also highlight the possible harmful role of lipid-derived electrophiles on protein aggregation and consequently in neurodegenerative diseases.

Covalent docking might explain the direction of the aldehydes to the specific lysines which were their target in SOD1 (Lys3, Lys9, Lys30, Lys122, Lys128, Lys136). Although there are other residues that can be modified by these aldehydes, including other lysines (Lys23, Lys70 and Lys75), some histidines (His46, His48, His71, His110 and His 120) and cysteines (Cys6, Cys57, Cys111 and Cys146), those specific lysines were modified in common by all aldehydes, specially the most hydrophobic ones, which only modified these six sites (Figure 3). Detailed inspection in the surroundings of those lysines reveals that some hydrophobic residues, such as valine, alanine, tryptophan and isoleucine (Table S7, supporting information), may play important roles directing aldehydes to the binding site. First, hydrophobic residues could recruit aldehydes for these areas by interacting with their hydrophobic surface. And secondly, when aldehydes covalently bind lysine residues, the local hydrophobic interactions with these apolar amino acids could change the native structure of SOD1, exposing reactive cysteines to form disulfide crosslinks that are responsible for aggregate formation. In Figure 6, we identified hydrophobic areas in the surroundings of the modified lysines (labeled in brown) where

aldehydes could effectively interact with these residues. The idea that these hydrophobic interactions occur between aldehydes and apolar residues of SOD1 could explain aggregate induction, clearly evidenced by covalent docking scores (Table 1). Our data thus suggest that the aldehyde hydrophobicity is directly linked to non-covalent interactions with SOD1, which critically influences protein aggregation.

There are an increasing number of studies demonstrating the importance of lipids in neurodegenerative diseases. In this context, our *in vitro* study shed light on a critical link between oxidative stress and protein aggregation, which is putatively associated with the pathology of these disorders. Our data specifically bear evidence that electrophile hydrophobicity is critical to ligand-induced SOD1 aggregation. In this respect, we highlight secosterol aldehydes with higher potential to induce SOD1 aggregation compared to the most commonly studied aldehydes such as HNE and HHE (Figure 2). Given the massive abundance of cholesterol in brain tissues [71] and the solid link between cholesterol metabolism and neurodegenerative diseases [72,73], *in vivo* experiments with cells or animal models may provide additional clues on the role of highly hydrophobic secosterol aldehydes in protein aggregation.

**Acknowledgments:** This work was supported by Fundação de Amparo à Pesquisa do Estado de São Paulo (FAPESP, CEPID-Redoxoma 13/07937-8 and 10/50891-0), Conselho Nacional de Desenvolvimento Científico e Tecnológico (CNPq, Universal 424094/2016-9), NAP-Redoxoma, Pro-Reitoria de Pesquisa USP and CAPES. The Ph.D. scholarship of L.S.D. was supported by CNPq.



## References

- [1] B. Uttara, A. V Singh, P. Zamboni, R.T. Mahajan, Oxidative stress and neurodegenerative diseases: a review of upstream and downstream antioxidant therapeutic options., *Curr. Neuropharmacol.* 7 (2009) 65–74. doi:10.2174/157015909787602823.
- [2] A.H. Bhat, K.B. Dar, S. Anees, M.A. Zargar, A. Masood, M.A. Sofi, S.A. Ganie, Oxidative stress, mitochondrial dysfunction and neurodegenerative diseases; a mechanistic insight, *Biomed. Pharmacother.* 74 (2015) 101–110. doi:10.1016/j.biopha.2015.07.025.
- [3] J. Li, W. O, W. Li, Z.-G. Jiang, H. Ghanbari, Oxidative Stress and Neurodegenerative Disorders, *Int. J. Mol. Sci.* 14 (2013) 24438–24475. doi:10.3390/ijms141224438.
- [4] R. Thanan, S. Oikawa, Y. Hiraku, S. Ohnishi, N. Ma, S. Pinlaor, P. Yongvanit, S. Kawanishi, M. Murata, Oxidative stress and its significant roles in neurodegenerative diseases and cancer, *Int. J. Mol. Sci.* 16 (2014) 193–217. doi:10.3390/ijms16010193.
- [5] M. Padurariu, A. Ciobica, L. Hritcu, B. Stoica, W. Bild, C. Stefanescu, Changes of some oxidative stress markers in the serum of patients with mild cognitive impairment and Alzheimer's disease, *Neurosci. Lett.* 469 (2010) 6–10. doi:10.1016/j.neulet.2009.11.033.
- [6] T.I. Williams, B.C. Lynn, W.R. Markesbery, M.A. Lovell, Increased levels of 4-hydroxynonenal and acrolein, neurotoxic markers of lipid peroxidation, in the brain in Mild Cognitive Impairment and early Alzheimer's disease, *Neurobiol. Aging*. 27 (2006) 1094–1099. doi:10.1016/j.neurobiolaging.2005.06.004.
- [7] M.A. Lovell, Biomarkers of lipid peroxidation in Alzheimer disease (AD): an update, *Arch. Toxicol.* 89 (2016) 1035–1044. doi:10.1007/s00204-015-1517-6.Biomarkers.
- [8] a Yoritaka, N. Hattori, K. Uchida, M. Tanaka, E.R. Stadtman, Y. Mizuno, Immunohistochemical detection of 4-hydroxynonenal protein adducts in Parkinson disease., *Proc. Natl. Acad. Sci. U. S. A.* 93 (1996) 2696–2701. doi:10.1073/pnas.93.7.2696.
- [9] C.C. de Farias, M. Maes, K.L. Bonifácio, C.C. Bortolasci, A. de Souza Nogueira, F.F. Brinholi, A.K. Matsumoto, M.A. do Nascimento, L.B. de Melo, S.L. Nixdorf, E.L. Lavado, E.G. Moreira, D.S. Barbosa, Highly specific changes in antioxidant levels and lipid peroxidation in Parkinson's disease and its progression: Disease and staging biomarkers and new drug targets, *Neurosci. Lett.* 617 (2016) 66–71. doi:10.1016/j.neulet.2016.02.011.
- [10] W. Pedersen, W. Fu, J. Keller, Protein modification by the lipid peroxidation product 4-hydroxynonenal in the spinal cords of amyotrophic lateral sclerosis patients, *Ann.* (1998) 819–824. doi:10.1002/ana.410440518.
- [11] F.J. Miana-Mena, C. González-Mingot, P. Larrodé, M.J. Muñoz, S. Oliván, L. Fuentes-Broto, E. Martínez-Ballarín, R.J. Reiter, R. Osta, J.J. García, Monitoring systemic oxidative stress in an animal model of amyotrophic lateral sclerosis, *J. Neurol.* 258 (2011) 762–769. doi:10.1007/s00415-010-5825-8.
- [12] T.T. Reed, Lipid peroxidation and neurodegenerative disease, *Free Radic. Biol. Med.*

- 51 (2011) 1302–1319. doi:10.1016/j.freeradbiomed.2011.06.027.
- [13] M.-R. Cho, J.-H. Han, H.-J. Lee, Y.K. Park, M.-H. Kang, The role of lipid peroxidation in neurological disorders, *J. Clin. Biochem. Nutr.* 56 (2015) 49–56. doi:10.3164/jcbtn.14.
  - [14] L. Xu, T.A. Davis, N.A. Porter, Rate constants for peroxidation of polyunsaturated fatty acids and sterols in solution and in liposomes, *J. Am. Chem. Soc.* 131 (2009) 13037–13044. doi:10.1021/ja9029076.
  - [15] K. Uchida, Aldehyde adducts generated during lipid peroxidation modification of proteins, *Free Radic. Res.* 49 (2015) 896–904. doi:10.3109/10715762.2015.1036052.
  - [16] M. Medeiros, Exocyclic DNA adducts as biomarkers of lipid oxidation and predictors of disease. Challenges in developing sensitive and specific methods for clinical studies, *Chem Res Toxicol.* 2009 Mar 16;22(3):419-25. doi: 10.1021/tx800367d.
  - [17] A. Ayala, M.F. Muñoz, S. Argüelles, Lipid peroxidation: Production, metabolism, and signaling mechanisms of malondialdehyde and 4-hydroxy-2-nonenal, *Oxid. Med. Cell. Longev.* 2014 (2014). doi:10.1155/2014/360438.
  - [18] D. Del Rio, A.J. Stewart, N. Pellegrini, A review of recent studies on malondialdehyde as toxic molecule and biological marker of oxidative stress, *Nutr. Metab. Cardiovasc. Dis.* 15 (2005) 316–328. doi:10.1016/j.numecd.2005.05.003.
  - [19] E.K. Long, M.J. Picklo, Trans-4-hydroxy-2-hexenal, a product of n-3 fatty acid peroxidation: Make some room HNE..., *Free Radic. Biol. Med.* 49 (2010) 1–8. doi:10.1016/j.freeradbiomed.2010.03.015.
  - [20] A. Moghe, S. Ghare, B. Lamoreau, M. Mohammad, S. Barve, C. McClain, S. Joshi-Barve, Molecular mechanisms of acrolein toxicity: Relevance to human disease, *Toxicol. Sci.* 143 (2015) 242–255. doi:10.1093/toxsci/kfu233.
  - [21] H. Esterbauer, R.J. Schaur, H. Zollner, Chemistry and biochemistry of 4-hydroxynonenal, malonaldehyde and related aldehydes, *Free Radic. Biol. Med.* 11 (1991) 81–128. doi:10.1016/0891-5849(91)90192-6.
  - [22] A. Ambaw, L. Zheng, M.A. Tambe, K.E. Strathearn, G. Acosta, S.A. Hubers, F. Liu, S.A. Herr, J. Tang, A. Truong, E. Walls, A. Pond, J.-C. Rochet, R. Shi, Acrolein-mediated neuronal cell death and alpha-synuclein aggregation: Implications for Parkinson's disease, *Mol. Cell. Neurosci.* 88 (2018) 70–82. doi:10.1016/j.mcn.2018.01.006.
  - [23] P.R. Angelova, M.H. Horrocks, D. Klenerman, S. Gandhi, A.Y. Abramov, M.S. Shchepinov, Lipid peroxidation is essential for  $\alpha$ -synuclein-induced cell death, *J. Neurochem.* 133 (2015) 582–589. doi:10.1111/jnc.13024.
  - [24] E.-J. Bae, D.-H. Ho, E. Park, J.W. Jung, K. Cho, J.H. Hong, H.-J. Lee, K.P. Kim, S.-J. Lee, Lipid Peroxidation Product 4-Hydroxy-2-Nonenal Promotes Seeding-Capable Oligomer Formation and Cell-to-Cell Transfer of  $\alpha$ -Synuclein, *Antioxid. Redox Signal.* 18 (2013) 770–783. doi:10.1089/ars.2011.4429.
  - [25] Z. Qin, D. Hu, S. Han, S.H. Reaney, D.A. Di Monte, A.L. Fink, Effect of 4-hydroxy-2-nonenal modification on  $\alpha$ -synuclein aggregation, *J. Biol. Chem.* 282 (2007) 5862–5870. doi:10.1074/jbc.M608126200.

- [26] M.I. Ellis G, Fang E, Maheshwari M, Roltsch E, Holcomb L, Zimmer D, Martinez D, Lipid oxidation and modification of amyloid- $\beta$  (A $\beta$ ) in vitro and in vivo., *J Alzheimers Dis.* 22(2) (2010) 593–607.
- [27] L. Liu, H. Komatsu, I.V.J. Murray, P.H. Axelsen, Promotion of Amyloid ?? Protein Misfolding and Fibrillogenesis by a Lipid Oxidation Product, *J. Mol. Biol.* 377 (2008) 1236–1250. doi:10.1016/j.jmb.2008.01.057.
- [28] J.H. Kang, Modification and inactivation of Cu,Zn-superoxide dismutase by the lipid peroxidation product, acrolein, *BMB Rep.* 46 (2013) 555–560. doi:10.5483/BMBRep.2013.46.11.138.
- [29] Z.A.M. Zielinski, D.A. Pratt, Cholesterol Autoxidation Revisited: Debunking the Dogma Associated with the Most Vilified of Lipids, *J. Am. Chem. Soc.* 138 (2016) 6932–6935. doi:10.1021/jacs.6b03344.
- [30] N. Miyoshi, L. Iuliano, S. Tomono, H. Ohshima, Implications of cholesterol autoxidation products in the pathogenesis of inflammatory diseases, *Biochem. Biophys. Res. Commun.* 446 (2014) 702–708. doi:10.1016/j.bbrc.2013.12.107.
- [31] M. Uemi, G.E. Ronsein, S. Miyamoto, M.H.G. Medeiros, P. Di Mascio, Generation of cholesterol carboxyaldehyde by the reaction of singlet molecular oxygen [ $O_2$  (1 $\Delta$ (g))] as well as ozone with cholesterol., *Chem. Res. Toxicol.* 22 (2009) 875–84. doi:10.1021/tx800447b.
- [32] P. Wentworth, J. Nieva, C. Takeuchi, R. Galve, A.D. Wentworth, R.B. Dilley, G.A. DeLaria, A. Saven, B.M. Babior, K.D. Janda, A. Eschenmoser, R.A. Lerner, Evidence for ozone formation in human atherosclerotic arteries., *Science.* 302 (2003) 1053–6. doi:10.1126/science.1089525.
- [33] D. a Bosco, D.M. Fowler, Q. Zhang, J. Nieva, E.T. Powers, P. Wentworth, R. a Lerner, J.W. Kelly, Elevated levels of oxidized cholesterol metabolites in Lewy body disease brains accelerate alpha-synuclein fibrilization., *Nat. Chem. Biol.* 2 (2006) 249–253. doi:10.1038/nchembio782.
- [34] K. Usui, J.D. Hulleman, J.F. Paulsson, S.J. Siegel, E.T. Powers, J.W. Kelly, Site-specific modification of Alzheimer's peptides by cholesterol oxidation products enhances aggregation energetics and neurotoxicity., *Proc. Natl. Acad. Sci. U. S. A.* 106 (2009) 18563–8. doi:10.1073/pnas.0804758106.
- [35] J.C. Scheinost, H. Wang, G.E. Boldt, J. Offer, P. Wentworth, Cholesterol seco-sterol-induced aggregation of methylated amyloid- $\beta$  peptides - Insights into aldehyde-initiated fibrillization of amyloid- $\beta$ , *Angew. Chemie - Int. Ed.* 47 (2008) 3919–3922. doi:10.1002/anie.200705922.
- [36] N.K. Cygan, J.C. Scheinost, T.D. Butters, P. Wentworth, Adduction of cholesterol 5,6-seco-sterol aldehyde to membrane-bound myelin basic protein exposes an immunodominant epitope, *Biochemistry.* 50 (2011) 2092–2100. doi:10.1021/bi200109q.
- [37] L.S. Dantas, A. de B. Chaves-Filho, T.C. Genaro-Mattos, N.A. Porter, F.R. Coelho, O. Augusto, M.H.G. Medeiros, S. Miyamoto, Cholesterol Secosterol Aldehydes Induce Covalent Modification and Aggregation of Cu,Zn-Superoxide Dismutase, *Free Radic. Biol. Med.* In press (2018).

- [38] J.M. McCord, I. Fridovich, Superoxide dismutase. An enzymic function for erythrocuprein (hemocuprein)., *J. Biol. Chem.* 244 (1969) 6049–55.  
<http://www.ncbi.nlm.nih.gov/pubmed/5389100> (accessed September 13, 2016).
- [39] A. Okado-Matsumoto, I. Fridovich, Subcellular distribution of superoxide dismutases (SOD) in rat liver. Cu,Zn-SOD in mitochondria, *J. Biol. Chem.* 276 (2001) 38388–38393. doi:10.1074/jbc.M105395200.
- [40] L.A. Sturtz, K. Diekert, L.T. Jensen, R. Lill, V.C. Culotta, A fraction of yeast Cu,Zn-superoxide dismutase and its metallochaperone, CCS, localize to the intermembrane space of mitochondria. A physiological role for SOD1 in guarding against mitochondrial oxidative damage, *J. Biol. Chem.* 276 (2001) 38084–38089. doi:10.1074/jbc.M105296200.
- [41] J.S. Valentine, P.A. Doucette, S. Zittin Potter, Copper-Zinc Superoxide Dismutase and Amyotrophic Lateral Sclerosis, *Annu. Rev. Biochem.* 74 (2005) 563–593. doi:10.1146/annurev.biochem.72.121801.161647.
- [42] R. Rakhit, P. Cunningham, A. Furtos-Matei, S. Dahan, X.F. Qi, J.P. Crow, N.R. Cashman, L.H. Kondejewski, A. Chakrabartty, Oxidation-induced misfolding and aggregation of superoxide dismutase and its implications for amyotrophic lateral sclerosis, *J. Biol. Chem.* 277 (2002) 47551–47556. doi:10.1074/jbc.M207356200.
- [43] L. Banci, I. Bertini, M. Boca, S. Girotto, M. Martinelli, J.S. Valentine, M. Vieru, SOD1 and amyotrophic lateral sclerosis: Mutations and oligomerization, *PLoS One.* 3 (2008) 1–8. doi:10.1371/journal.pone.0001677.
- [44] P.P. Appolinário, D.B. Medinas, A.B. Chaves-Filho, T.C. Genaro-Mattos, J.R.R. Cussiol, L.E.S. Netto, O. Augusto, S. Miyamoto, Oligomerization of Cu,Zn-superoxide dismutase (SOD1) by Docosahexaenoic acid and its hydroperoxides in vitro: Aggregation dependence on fatty acid unsaturation and thiols, *PLoS One.* 10 (2015) 1–15. doi:10.1371/journal.pone.0125146.
- [45] I. Choi, Y. In Yang, H.D. Song, J.S. Lee, T. Kang, J.J. Sung, J. Yi, Lipid molecules induce the cytotoxic aggregation of Cu/Zn superoxide dismutase with structurally disordered regions, *Biochim. Biophys. Acta - Mol. Basis Dis.* 1812 (2011) 41–48. doi:10.1016/j.bbadis.2010.09.003.
- [46] Y.J. Kim, R. Nakatomi, T. Akagi, T. Hashikawa, R. Takahashi, Unsaturated fatty acids induce cytotoxic aggregate formation of amyotrophic lateral sclerosis-linked superoxide dismutase 1 mutants, *J. Biol. Chem.* 280 (2005) 21515–21521. doi:10.1074/jbc.M502230200.
- [47] K. Wang, E. Bermúdez, W. a Pryor, The ozonation of cholesterol: separation and identification of 2,4-dinitrophenylhydrazine derivatization products of 3 beta-hydroxy-5-oxo-5,6-secocholestan-6-al., *Steroids.* 58 (1993) 225–9. <http://www.ncbi.nlm.nih.gov/pubmed/8356575>.
- [48] L.T. Benov, W.F. Beyer, R.D. Stevens, I. Fridovich, Purification and characterization of the Cu,Zn SOD from *Escherichia coli*, *Free Radic. Biol. Med.* 21 (1996) 117–121. doi:10.1016/0891-5849(95)02217-1.
- [49] F. Milletti, L. Storchi, G. Sforna, G. Cruciani, New and original pKa prediction method using grid molecular interaction fields, *J. Chem. Inf. Model.* 47 (2007) 2172–2181. doi:10.1021/ci700018y.

- [50] M.L. Verdonk, J.C. Cole, M.J. Hartshorn, C.W. Murray, R.D. Taylor, Improved Protein – Ligand Docking Using GOLD, *Proteins Struct. Funct. Bioinforma.* 623 (2003) 609–623. doi:10.1002/prot.10465.
- [51] O. Korb, T. Stützle, T.E. Exner, Empirical scoring functions for advanced Protein-Ligand docking with PLANTS, *J. Chem. Inf. Model.* 49 (2009) 84–96. doi:10.1021/ci800298z.
- [52] W. Heiden, G. Moeckel, J. Brickmann, A new approach to analysis and display of local lipophilicity/hydrophilicity mapped on molecular surfaces, *J. Comput. Aided. Mol. Des.* 7 (1993) 503–514. doi:10.1007/BF00124359.
- [53] C. Wang, E. Weerapana, M.M. Blewett, B.F. Cravatt, A chemoproteomic platform to quantitatively map targets of lipid-derived electrophiles, *Nat. Methods.* 11 (2014) 79–85. doi:10.1038/nmeth.2759.
- [54] Y. Isobe, Y. Kawashima, T. Ishihara, K. Watanabe, O. Ohara, M. Arita, Identification of Protein Targets of 12/15-Lipoxygenase-Derived Lipid Electrophiles in Mouse Peritoneal Macrophages Using Omega-Alkynyl Fatty Acid, *ACS Chem. Biol.* (2018) acschembio.7b01092. doi:10.1021/acschembio.7b01092.
- [55] S.G. Codreanu, J.C. Ullery, J. Zhu, K.A. Tallman, W.N. Beavers, N.A. Porter, L.J. Marnett, B. Zhang, D.C. Liebler, Alkylation Damage by Lipid Electrophiles Targets Functional Protein Systems, *Mol. Cell. Proteomics.* 13 (2014) 849–859. doi:10.1074/mcp.M113.032953.
- [56] A.T. Jacobs, L.J. Marnett, Systems analysis of protein modification and cellular responses induced by electrophile stress, *Acc Chem Res.* 43 (2010) 673–683. doi:10.1021/ar900286y.
- [57] W.N. Beavers, K.L. Rose, J.J. Galligan, M.M. Mitchener, C.A. Rouzer, K.A. Tallman, C.R. Lamberson, X. Wang, S. Hill, P.T. Ivanova, H.A. Brown, B. Zhang, N.A. Porter, L.J. Marnett, Protein Modification by Endogenously Generated Lipid Electrophiles: Mitochondria as the Source and Target, *ACS Chem. Biol.* 12 (2017) 2062–2069. doi:10.1021/acschembio.7b00480.
- [58] T. Shibata, K. Shimizu, K. Hirano, F. Nakashima, R. Kikuchi, T. Matsushita, K. Uchida, Adductome-based identification of biomarkers for lipid peroxidation, *J. Biol. Chem.* 292 (2017) 8223–8235. doi:10.1074/jbc.M116.762609.
- [59] M.A. Lovell, C. Xie, W.R. Markesbery, Acrolein is increased in Alzheimer’s disease brain and is toxic to primary hippocampal cultures, *Neurobiol. Aging.* 22 (2001) 187–194. doi:10.1016/S0197-4580(00)00235-9.
- [60] J. Nieva, B.D. Song, J.K. Rogel, D. Kujawara, L. Altobel, A. Izharudin, G.E. Boldt, R.K. Grover, A.D. Wentworth, P. Wentworth, Cholesterol secosterol aldehydes induce amyloidogenesis and dysfunction of wild-type tumor protein p53, *Chem. Biol.* 18 (2011) 920–927. doi:10.1016/j.chembiol.2011.02.018.
- [61] Q. Zhang, E.T. Powers, J. Nieva, M.E. Huff, M.A. Dendle, J. Bieschke, C.G. Glabe, A. Eschenmoser, P. Wentworth, R.A. Lerner, J.W. Kelly, Metabolite-initiated protein misfolding may trigger Alzheimer’s disease., *Proc. Natl. Acad. Sci. U. S. A.* 101 (2004) 4752–7. doi:10.1073/pnas.0400924101.
- [62] S. Kato, S. Horiuchi, J. Liu, D.W. Cleveland, N. Shibata, K. Nakashima, R. Nagai, A.

- Hirano, M. Takikawa, M. Kato, I. Nakano, E. Ohama, Advanced glycation endproduct-modified superoxide dismutase-1 (SOD1)-positive inclusions are common to familial amyotrophic lateral sclerosis patients with SOD1 gene mutations and transgenic mice expressing human SOD1 with a G85R mutation, *Acta Neuropathol.* 100 (2000) 490–505. doi:10.1007/s004010000226.
- [63] T.C. Genaro-Mattos, P.P. Appolinário, K.C.U. Mugnol, C. Bloch, I.L. Nantes, P. Di Mascio, S. Miyamoto, Covalent binding and anchoring of cytochrome c to mitochondrial mimetic membranes promoted by cholesterol carboxyaldehyde, *Chem. Res. Toxicol.* 26 (2013) 1536–1544. doi:10.1021/tx4002385.
- [64] K. Windsor, T.C. Genaro-Mattos, S. Miyamoto, D.F. Stec, H.Y.H. Kim, K.A. Tallman, N.A. Porter, Assay of protein and peptide adducts of cholesterol ozonolysis products by hydrophobic and click enrichment methods, *Chem. Res. Toxicol.* 27 (2014) 1757–1768. doi:10.1021/tx500229h.
- [65] Y. Furukawa, K. Kaneko, K. Yamanaka, N. Nukina, Mutation-dependent polymorphism of Cu,Zn-superoxide dismutase aggregates in the familial form of amyotrophic lateral sclerosis, *J. Biol. Chem.* 285 (2010) 22221–22231. doi:10.1074/jbc.M110.113597.
- [66] Y. Shi, R.A. Mowery, J. Ashley, M. Hentz, A.J. Ramirez, B. Bilgicer, H. Slunt-Brown, D.R. Borchelt, B.F. Shaw, Abnormal SDS-PAGE migration of cytosolic proteins can identify domains and mechanisms that control surfactant binding, *Protein Sci.* 21 (2012) 1197–1209. doi:10.1002/pro.2107.
- [67] F.S. Ataya, D. Fouad, E. Al-Olayan, A. Malik, Molecular cloning, characterization and predicted structure of a putative copper-zinc SOD from the camel, *Camelus dromedaries*, *Int. J. Mol. Sci.* 13 (2012) 879–900. doi:10.3390/ijms13010879.
- [68] S. Rasouli, A. Abdolvahabi, C.M. Croom, D.L. Plewman, Y. Shi, J.I. Ayers, B.F. Shaw, Lysine acylation in superoxide dismutase-1 electrostatically inhibits formation of fibrils with prion-like seeding, *J. Biol. Chem.* 292 (2017) 19366–19380. doi:10.1074/jbc.M117.805283.
- [69] A. Abdolvahabi, Y. Shi, N.R. Rhodes, N.P. Cook, A.A. Martí, B.F. Shaw, Arresting amyloid with coulomb's law: Acetylation of ALS-linked SOD1 by aspirin impedes aggregation, *Biophys. J.* 108 (2015) 1199–1212. doi:10.1016/j.bpj.2015.01.014.
- [70] S.E. Antinone, G.D. Ghadge, T.T. Lam, L. Wang, R.P. Roos, W.N. Green, Palmitoylation of superoxide dismutase 1 (SOD1) is increased for familial amyotrophic lateral sclerosis-linked SOD1 mutants, *J. Biol. Chem.* 288 (2013) 21606–21617. doi:10.1074/jbc.M113.487231.
- [71] J.M. Dietschy, S.D. Turley, *Thematic review series: Brain Lipids*. Cholesterol metabolism in the central nervous system during early development and in the mature animal, *J. Lipid Res.* 45 (2004) 1375–1397. doi:10.1194/jlr.R400004-JLR200.
- [72] J. Abdel-Khalik, E. Yutuc, P.J. Crick, J.-Å. Gustafsson, M. Warner, G. Roman, K. Talbot, E. Gray, W.J. Griffiths, M.R. Turner, Y. Wang, Defective cholesterol metabolism in amyotrophic lateral sclerosis, *J. Lipid Res.* 58 (2017) 267–278. doi:10.1194/jlr.P071639.
- [73] S. Kim, M. Noh, H. Kim, S. Cheon, K. Mi, J. Lee, E. Cha, K.S. Park, K. Lee, S.H. Kim, 25-Hydroxycholesterol is involved in the pathogenesis of amyotrophic lateral

sclerosis, 8 (2017) 11855–11867. doi:10.18632/oncotarget.14416.

## **Supporting information**

### **Lipid-derived electrophiles induce covalent modification and aggregation of Cu,Zn-superoxide dismutase in a hydrophobicity-dependent manner**

Lucas S. Dantas<sup>†</sup>, Lucas G. Viviani<sup>†</sup>, Leandro de Rezende<sup>†</sup>, Fernando R. Coelho<sup>†</sup>, Ohara Augusto<sup>†</sup>, Marisa H. G. de Medeiros<sup>†</sup>, Antonia T. Amaral<sup>†</sup> and Sayuri Miyamoto<sup>\*,†</sup>

#### **1. Supplementary figures and tables**



**Table S1.** HHE-modified peptides identified by LC-MS/MS after digestion with trypsin.

Sequence	Residue	Unmodified (m/z)	Expected	Observed	Error (ppm)
ATK*AVC'VLK	Lys3 (SB)	495.2942 (2+)	544.3308 (2+)	544.3296 (2+)	-2.2
AVC*VLK*GDGPVQGIIN FEQK	Cys6 (MA) Lys9 (SB)	705.7137 (3+)	776.4275 (3+)	776.4263 (3+)	-1.5
AVC'VLK*GDGPVQGIIN FEQK	Lys9 (SB)	724.7209 (3+)	757.4120 (3+)	757.4167 (3+)	6.2
AVC'VLK*GDGPVQGIIN FEQK	Lys9 (MA)	724.7209 (3+)	762.7436 (3+)	762.7466 (3+)	3.9
GDGPVQGIINFEQK*ESN GPVKVWGSIK	Lys23 (SB)	961.8382 (3+)	994.5292 (3+)	994.5345 (3+)	5.3
ESNGPVK*VWGSIK	Lys30 (SB)	467.5893 (3+)	500.2803 (3+)	500.2812 (3+)	1.7
GLTEGLHGFH*VHEFGD NTAGC'TSAGPHFNPLSR	His46 (MA)	693.3264 (5+)	727.5444 (5+)	727.5507 (5+)	8.6
GLTEGLHGFHVH*EFGD NTAGC'TSAGPHFNPLSR	His48 (MA)	693.3264 (5+)	727.5444 (5+)	727.5498 (5+)	7.4
GLTEGLHGFHVHEFGDN TAGC*TSAGPHFNPLSR	Cys57 (MA)	693.3264 (5+)	716.1401 (5+)	716.1453 (5+)	7.2
DGVADVSIEDSVISLSGD H*CIIGR	His110 (MA)	819.7357 (3+)	857.7584 (3+)	857.7620 (3+)	4.1
DGVADVSIEDSVISLSGD HC*IIGR	Cys111 (MA)	819.7357 (3+)	857.7584 (3+)	857.7615 (3+)	3.6
TLVVH*EK	His120 (MA)	275.8325 (3+)	313.8552 (3+)	313.8536 (3+)	-5.0
TLVVHEK*ADDLGK	Lys122 (SB)	475.5963 (3+)	508.2874 (3+)	508.2860 (3+)	-2.7
ADDLGK*GGNEESTK	Lys128 (SB)	474.2232 (3+)	506.9143 (3+)	506.9146 (3+)	0.5
GGNEESTK*TGNAGSR	Lys136 (MA)	488.8940 (3+)	526.9167 (3+)	526.9160 (3+)	-1.3

SB: Schiff Base

MA: Michael Addition

\* Aldehyde adduct

' Carbamidomethyl adduct

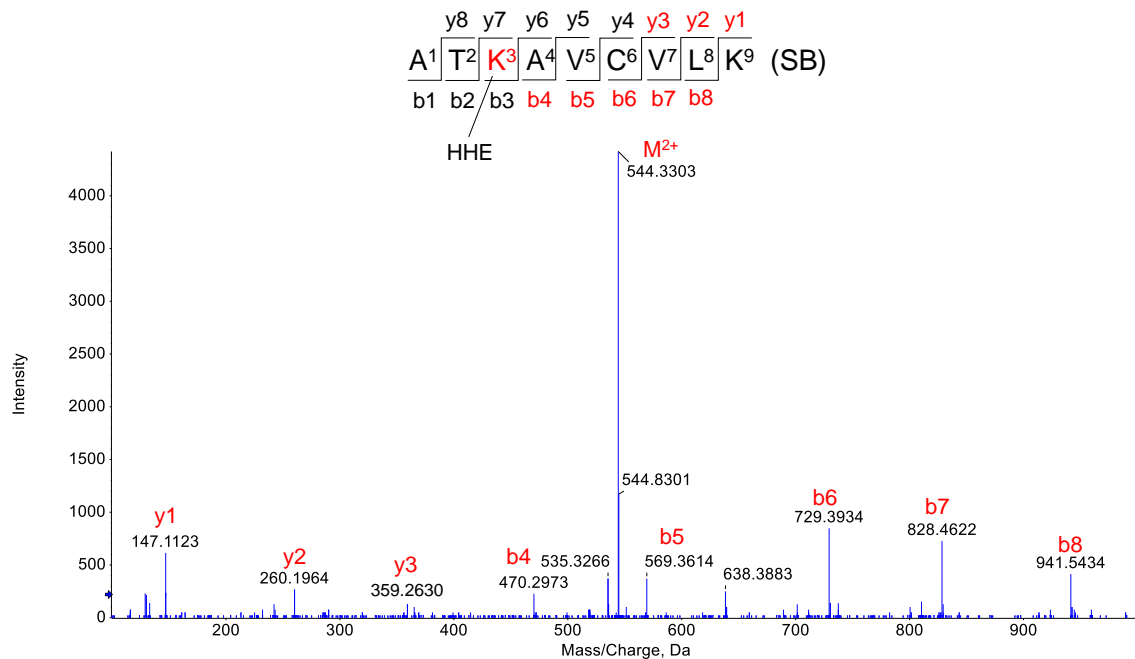


**Figure S1.** MS/MS of the peptide A<sup>1</sup>TKAVCVLK<sup>9</sup> modified by HHE at Lys3 by Michael Addition.

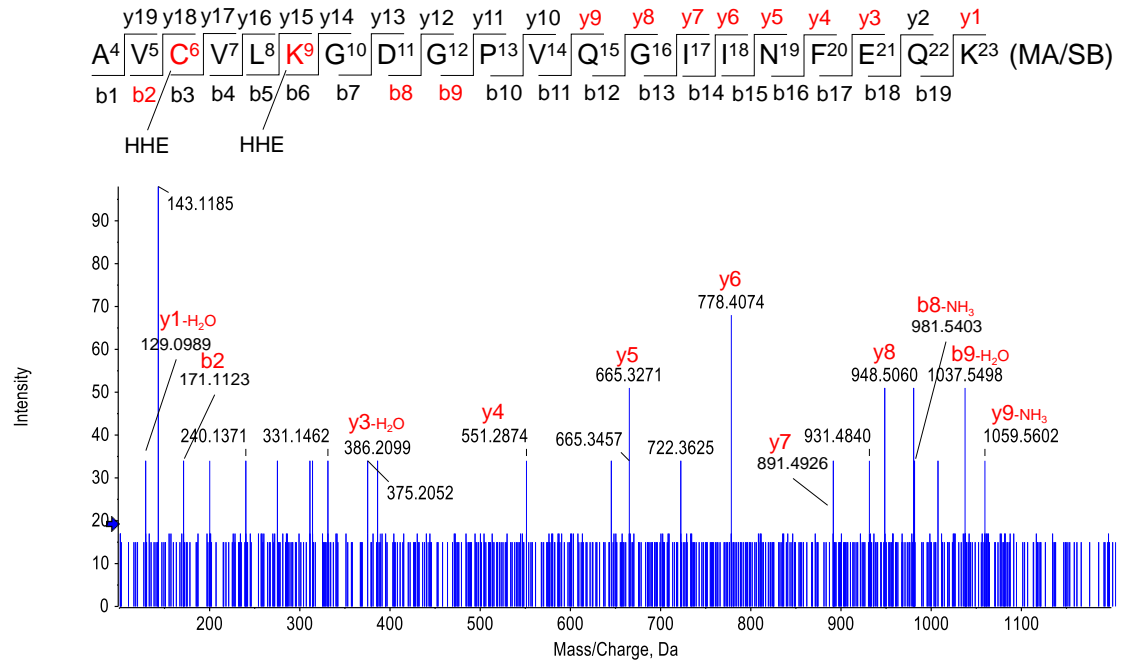


**Figure S2.** MS/MS of the peptide A<sup>4</sup>VCVLKGDGPVQGIINFEQK<sup>23</sup> modified by HHE at Cys6 by Michael Addition and Lys9 by Schiff base formation.

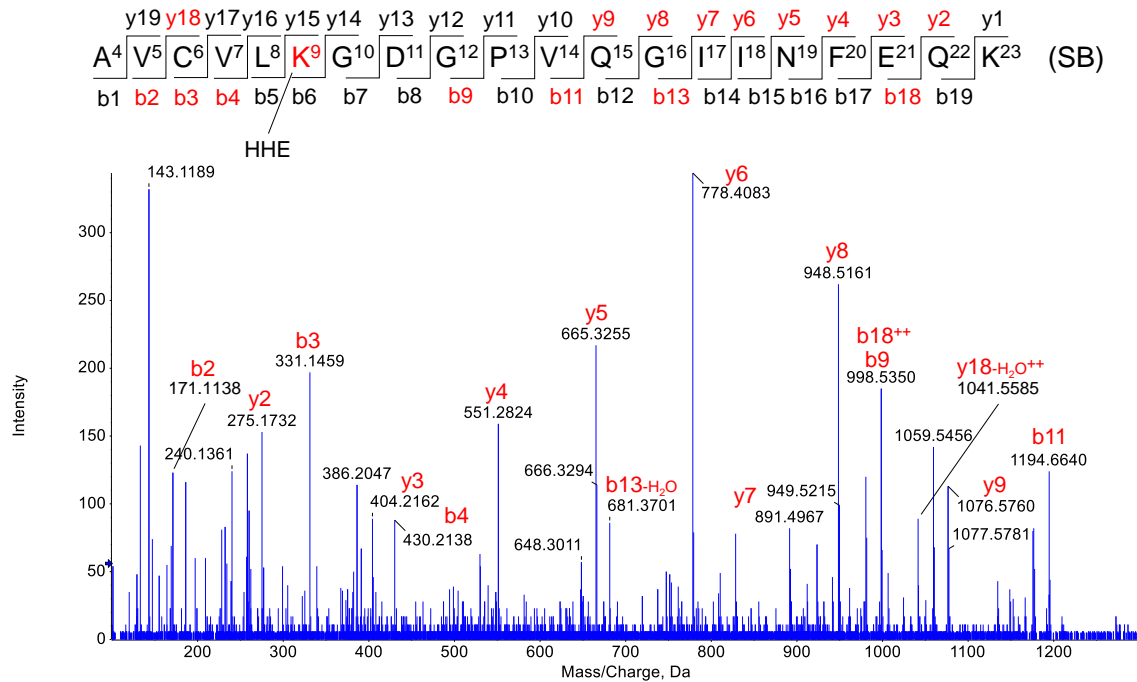


**Figure S3.** MS/MS of the peptide  $A^4VCVLKGDGPVQGIINFEQK^{23}$  modified by HHE at Lys9 by Schiff base formation.

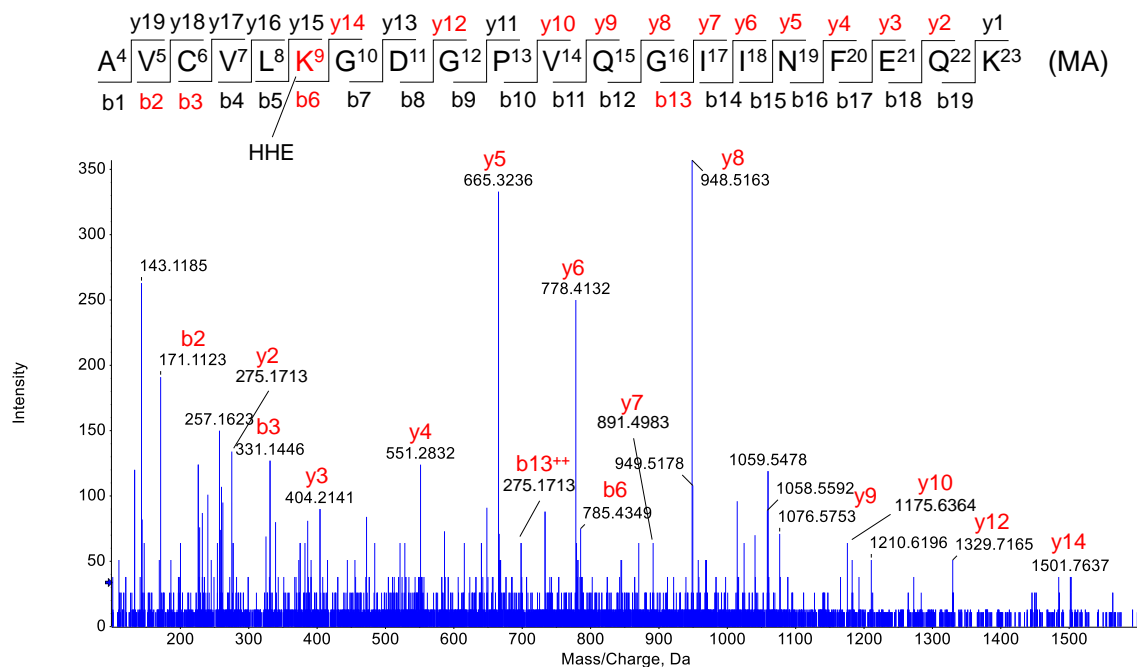


**Figure S4.** MS/MS of the peptide  $A^4VCVLKGDGPVQGIINFEQK^{23}$  modified by HHE at Lys9 by Michael Addition.

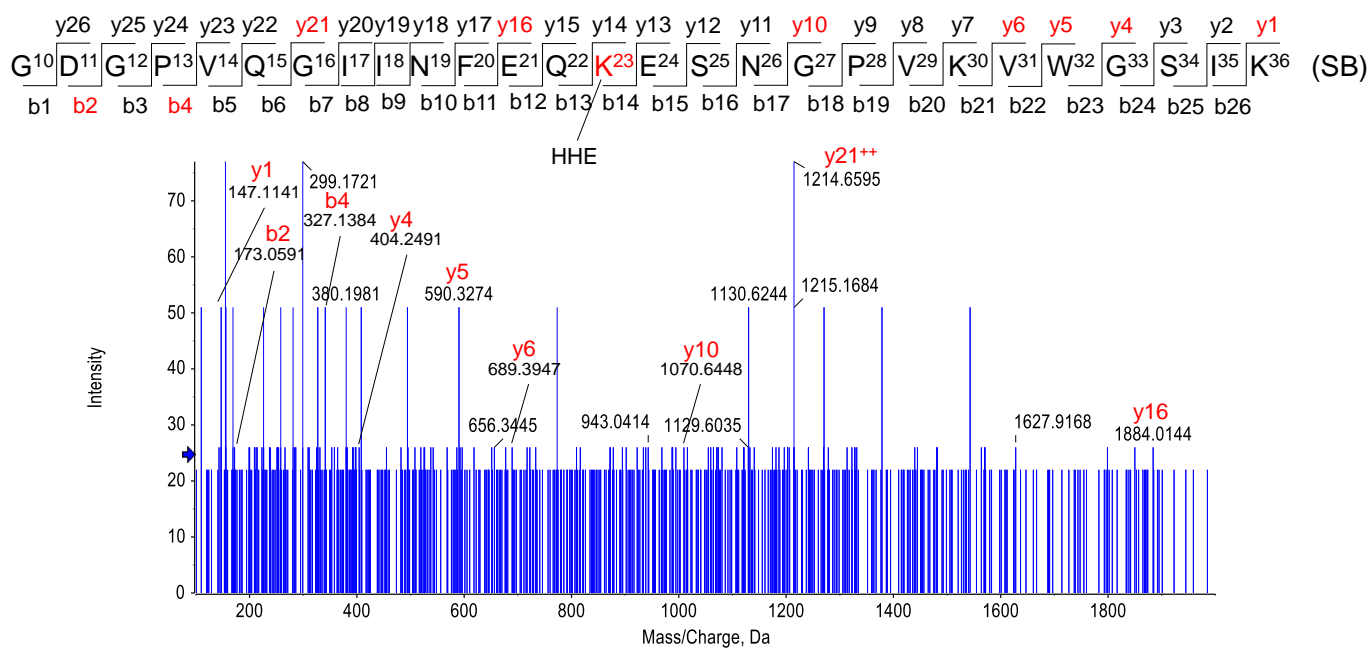


**Figure S5.** MS/MS of the peptide  $G^{10}DGPVQGIINFEQKESNGPVKVGSIK^{36}$  modified by HHE at Lys23 by Schiff base formation.

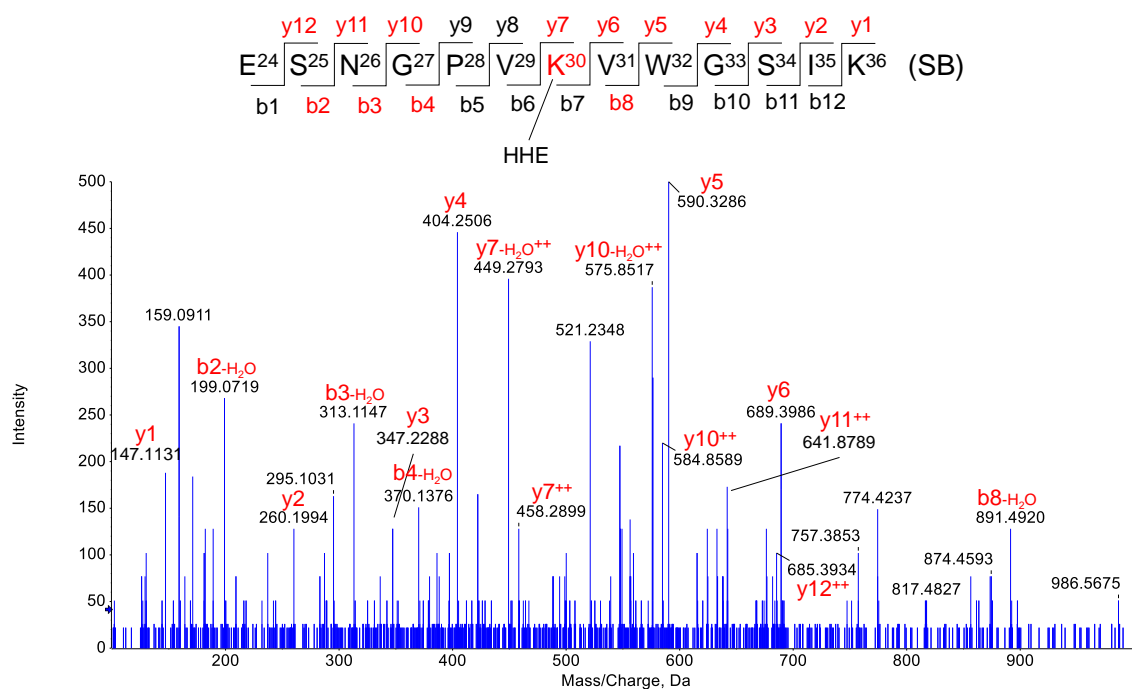


**Figure S6.** MS/MS of the peptide  $E^{24}SNGPVKVGSIK^{36}$  modified by HHE at Lys30 by Schiff base formation.

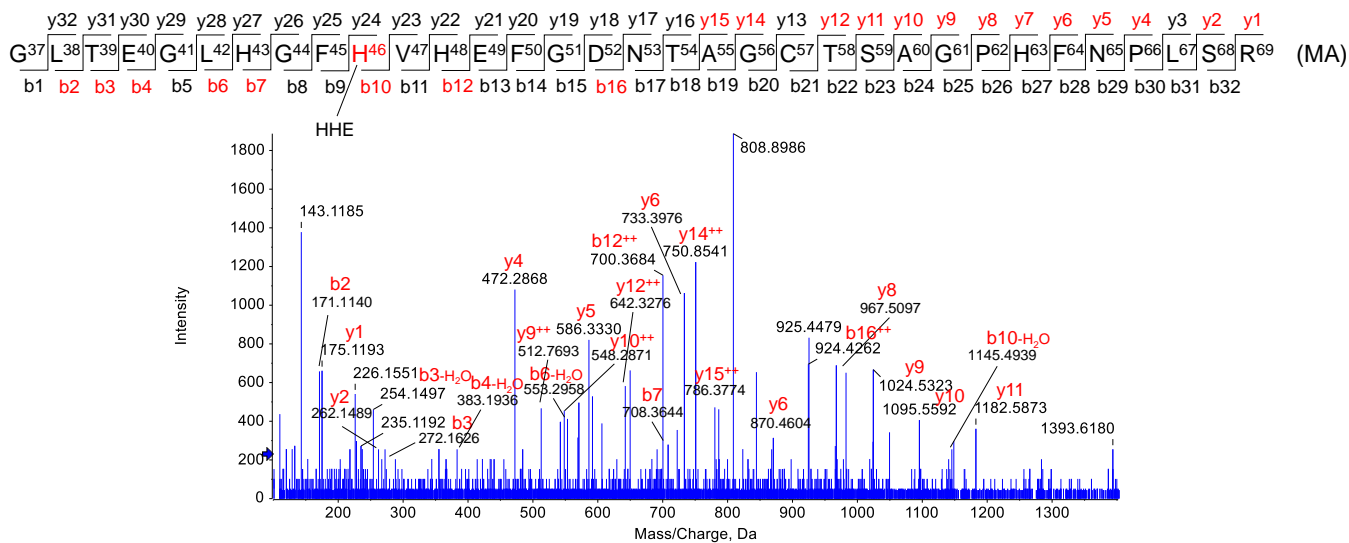


**Figure S7.** MS/MS of the peptide G<sup>37</sup>LTEGLHGFHVHEFGDNTAG CTSAGPHFNPLSR<sup>69</sup> modified by HHE at His46 by Michael Addition.

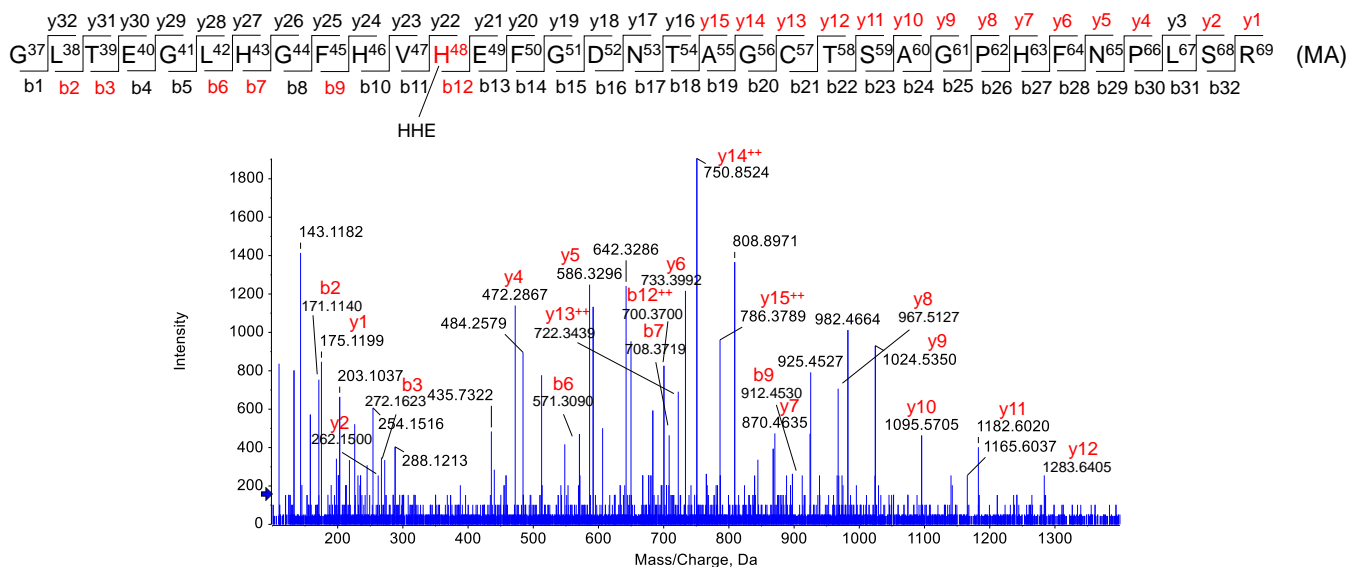


**Figure S8.** MS/MS of the peptide G<sup>37</sup>LTEGLHGFHVHEFGDNTAG CTSAGPHFNPLSR<sup>69</sup> modified by HHE at His48 by Michael Addition.

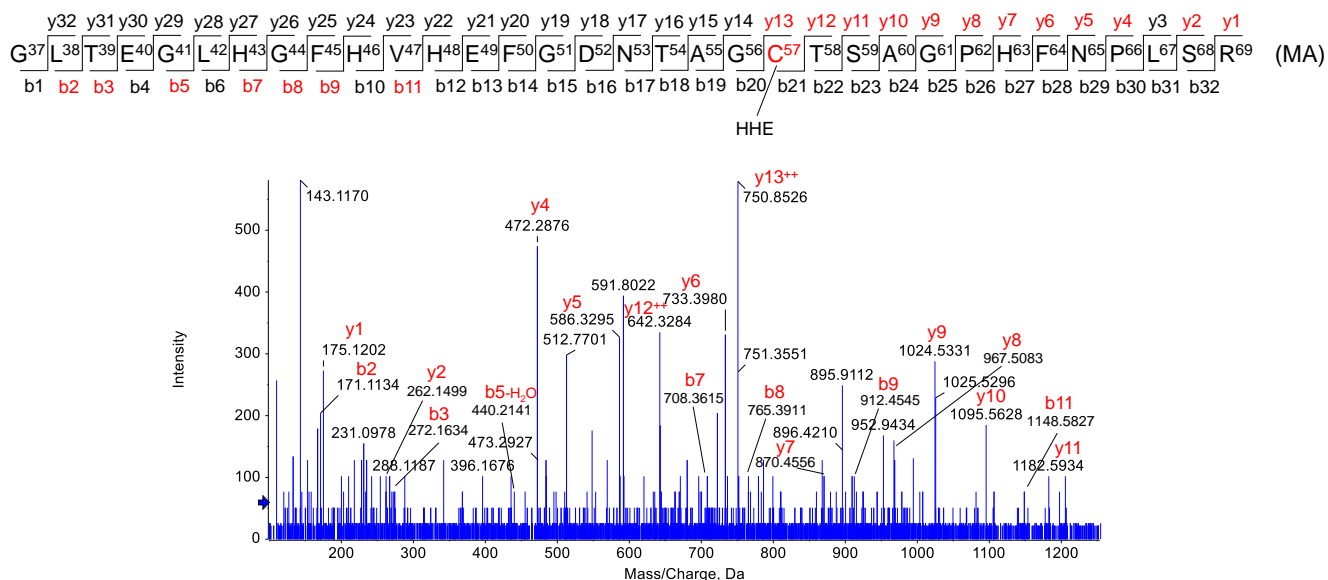


**Figure S9.** MS/MS of the peptide G<sup>37</sup>LTEGLHGFHVHEFGDNTAG CTSAGPHFNPLSR<sup>69</sup> modified by HHE at Cys57 by Michael Addition.

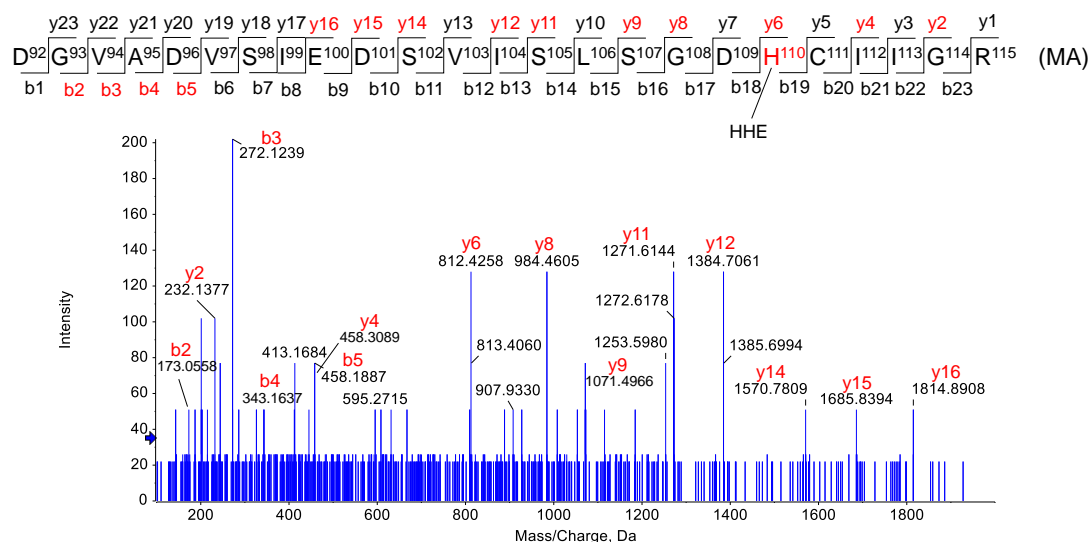


**Figure S10.** MS/MS of the peptide D<sup>92</sup>GVADSVIEDSVISLSGDHCCIIGR<sup>115</sup> modified by HHE at His110 by Michael Addition.

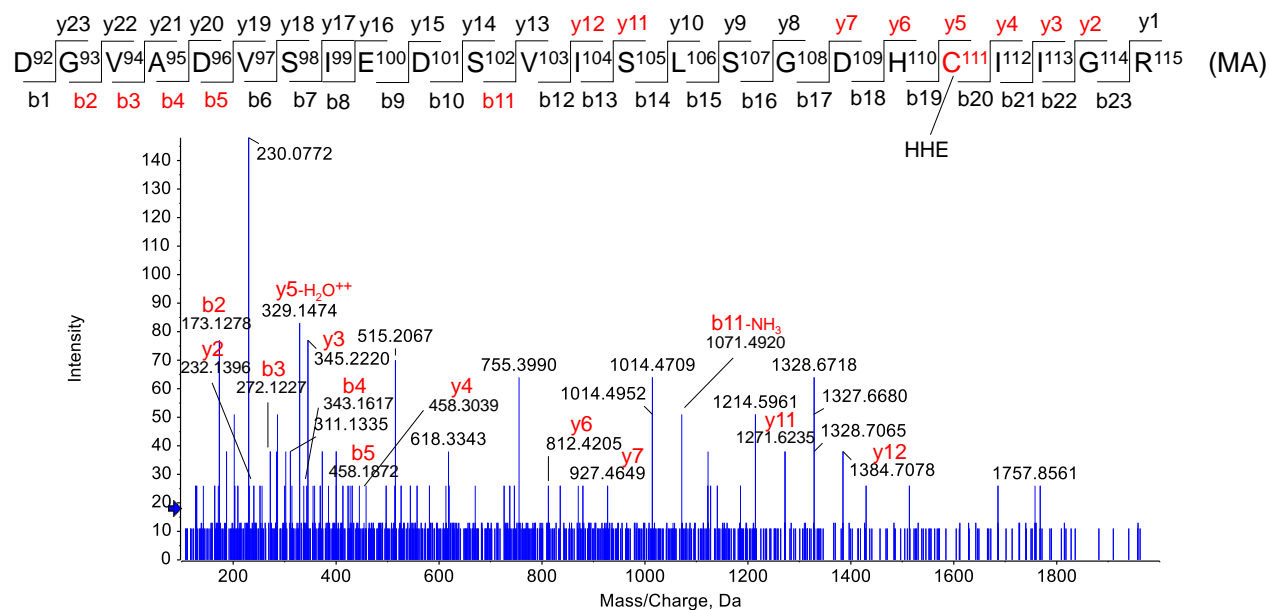


**Figure S11.** MS/MS of the peptide D<sup>92</sup>GVADVSIEDSVISLSGDHCIIGR<sup>115</sup> modified by HHE at Cys111 by Michael Addition.

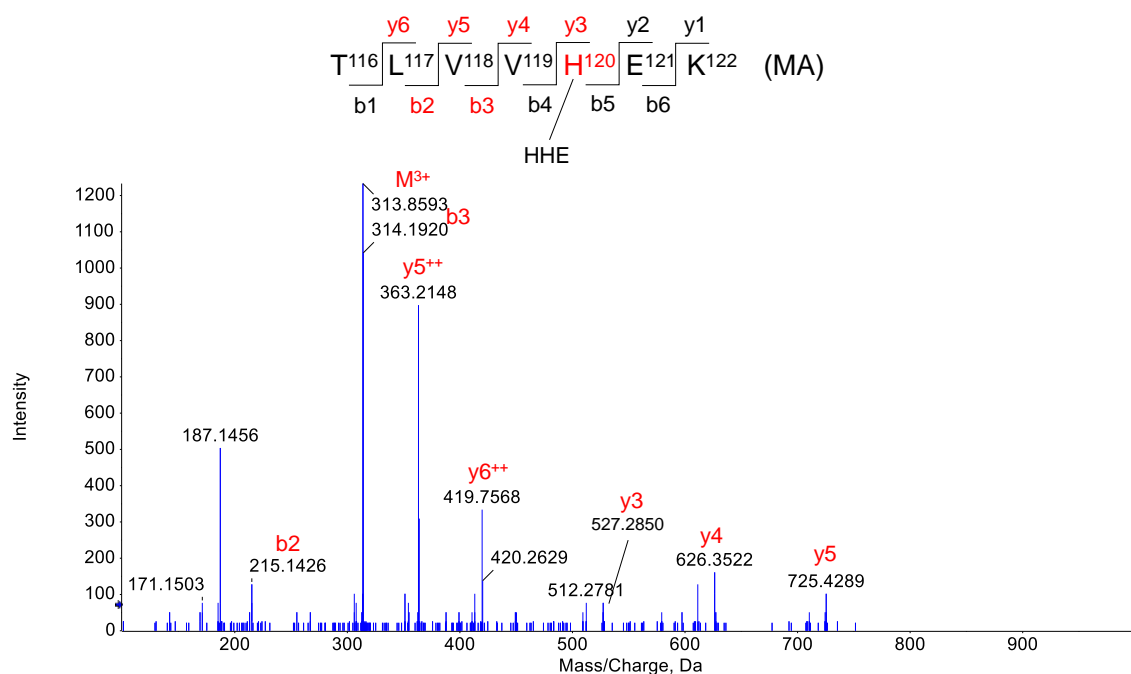


**Figure S12.** MS/MS of the peptide T<sup>116</sup>LVVHEK<sup>122</sup> modified by HHE at His120 by Michael Addition.

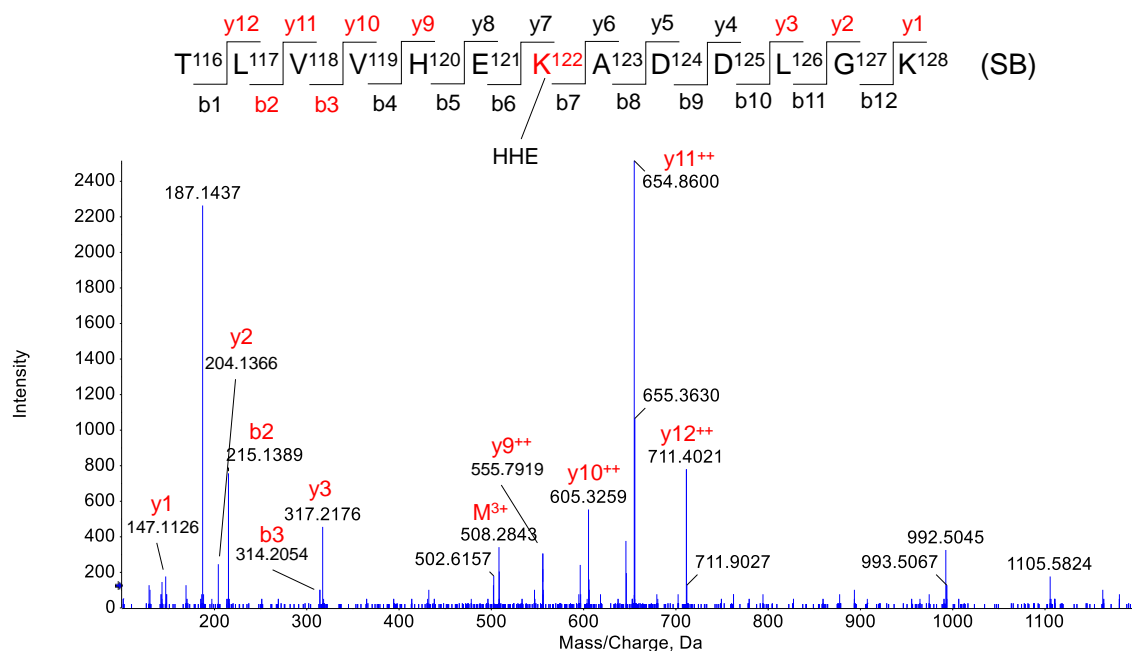


**Figure S13.** MS/MS of the peptide T<sup>116</sup>L<sup>117</sup>V<sup>118</sup>V<sup>119</sup>H<sup>120</sup>E<sup>121</sup>K<sup>122</sup>A<sup>123</sup>D<sup>124</sup>D<sup>125</sup>L<sup>126</sup>G<sup>127</sup>K<sup>128</sup> modified by HHE at Lys122 by Schiff base formation.

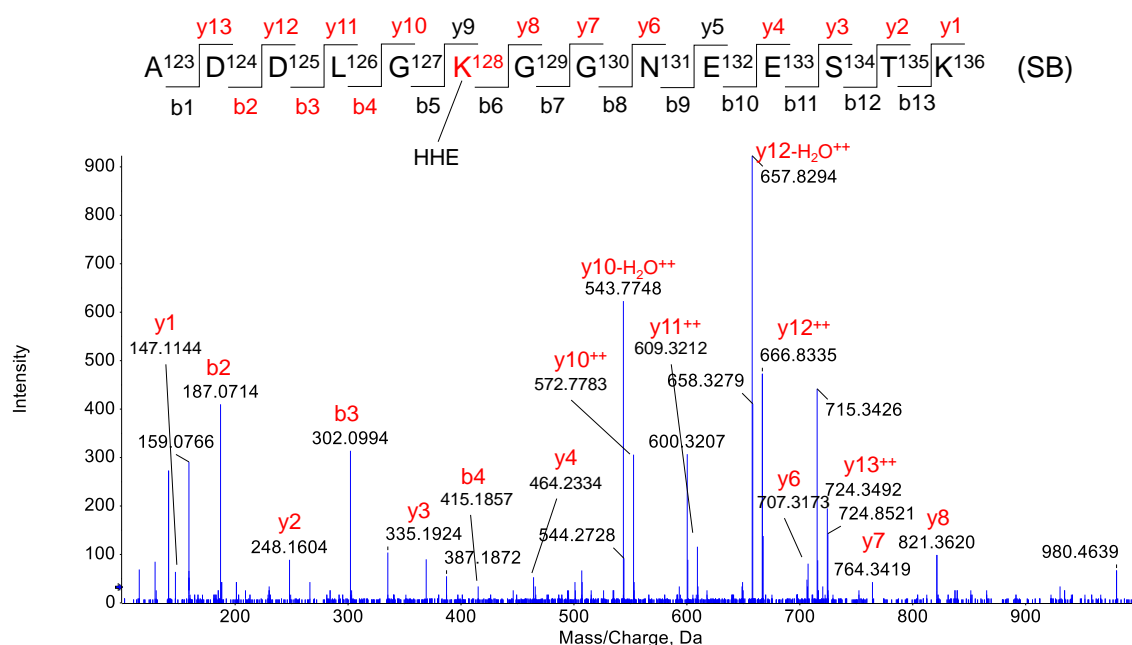


**Figure S14.** MS/MS of the peptide A<sup>123</sup>D<sup>124</sup>D<sup>125</sup>L<sup>126</sup>G<sup>127</sup>K<sup>128</sup>G<sup>129</sup>G<sup>130</sup>N<sup>131</sup>E<sup>132</sup>E<sup>133</sup>S<sup>134</sup>T<sup>135</sup>K<sup>136</sup> modified by HHE at Lys128 by Schiff base formation.



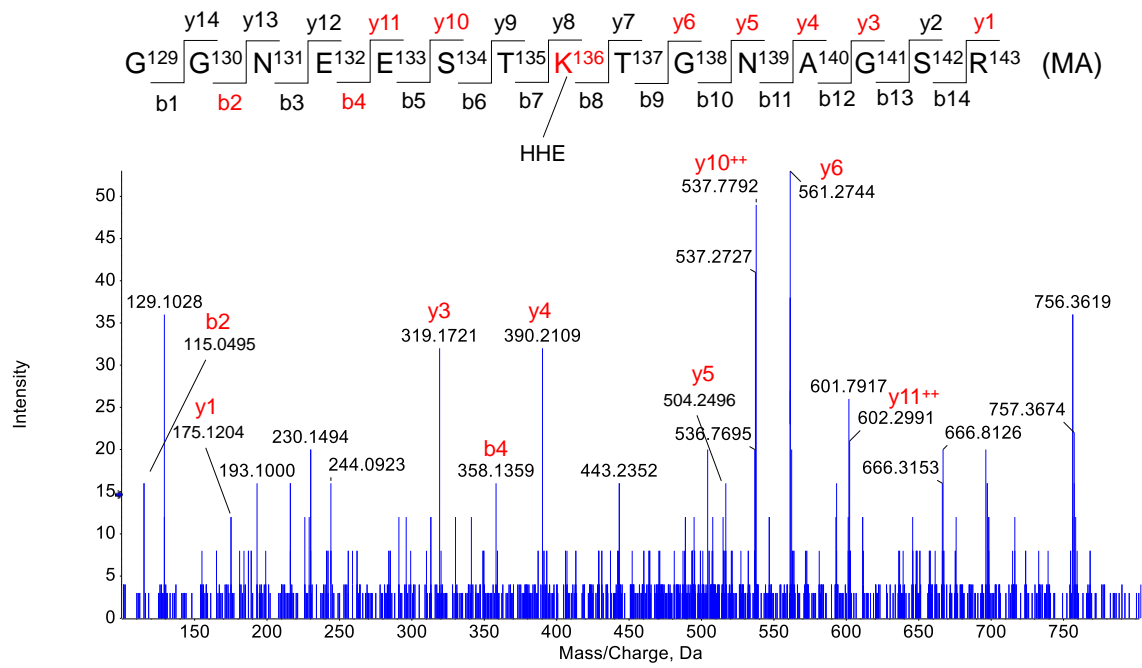


**Figure S15.** MS/MS of the peptide  $\text{G}^{129}\text{GNEESTKTGNAGSR}^{143}$  modified by HHE at Lys136 by Michael Addition.

**Table S2.** Hexenal-modified peptides identified by LC-MS/MS after digestion with trypsin.

Sequence	Residue	Unmodified (m/z)	Expected	Observed	Error (ppm)
ATK*AVC'VLK	Lys3 (SB)	330.5319 (3+)	357.8913 (3+)	357.8909 (3+)	-1.1
AVC*VLK	Cys6 (MA)	316.6936 (2+)	365.7302 (2+)	365.7299 (2+)	-0.9
AVC'VLK*GDGPVQGIINFE QK	Lys9 (SB)	724.7209 (3+)	752.0803 (3+)	752.0848 (3+)	5.9
ESNGPVK*VWGSIK	Lys30 (SB)	467.5893 (3+)	494.9487 (3+)	494.9474 (3+)	-2.6
GLTEGLHGFHVH*EFGDNT AGC*TSAGPHFNPLSR	His48 (MA) Cys57 (MA)	693.3264 (5+)	732.5557 (5+)	732.5583 (5+)	3.4
K*H*GGPKDEER	Lys70 (SB) His71 (MA)	288.8994 (4+)	333.9372 (4+)	333.9361 (4+)	-3.3
KHGGPK*DEER	Lys75 (SB)	384.8634 (3+)	412.2228 (3+)	412.2214 (3+)	-3.4
HVGD LGNVTADK*DG VAD VSIEDSVISLSGDHC*IIGR	Lys91 (SB) Cys111 (MA)	733.5642 (5+)	769.5944 (5+)	769.6004 (5+)	7.7
TLVVH*EK	His120 (MA)	413.2451 (2+)	462.2817 (2+)	462.2786 (2+)	6.6
TLVVHEK*ADDLGK	Lys122 (SB)	475.5963 (3+)	502.9557 (3+)	502.9543 (3+)	-2.8
ADDLGK*GGNEESTK	Lys128 (SB)	474.2232 (3+)	501.5826 (3+)	501.5799 (3+)	-5.4
GGNEESTK*TGNAGSR	Lys136 (SB)	488.8940 (3+)	516.2534 (3+)	516.2504 (3+)	-5.8
GGNEESTK*TGNAGSR	Lys136 (MA)	488.8940 (3+)	521.5850 (3+)	521.5874 (3+)	4.5
LAC*GVIGIAQ	Cys146 (MA)	472.7653 (2+)	521.8019 (2+)	521.8009 (2+)	-1.9

SB: Schiff Base

MA: Michael Addition

\* Aldehyde adduct

' Carbamidomethyl adduct

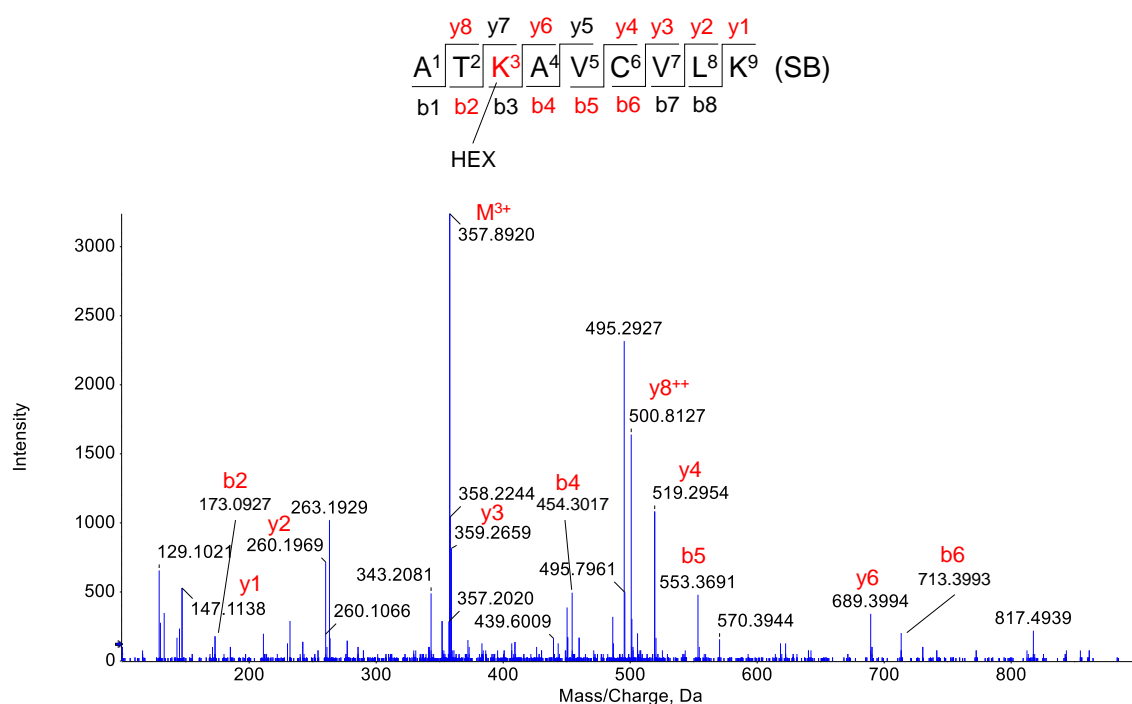


**Figure S16.** MS/MS of the peptide A<sup>1</sup>TKAVCVLK<sup>9</sup> modified by hexenal at Lys3 by Schiff base formation.

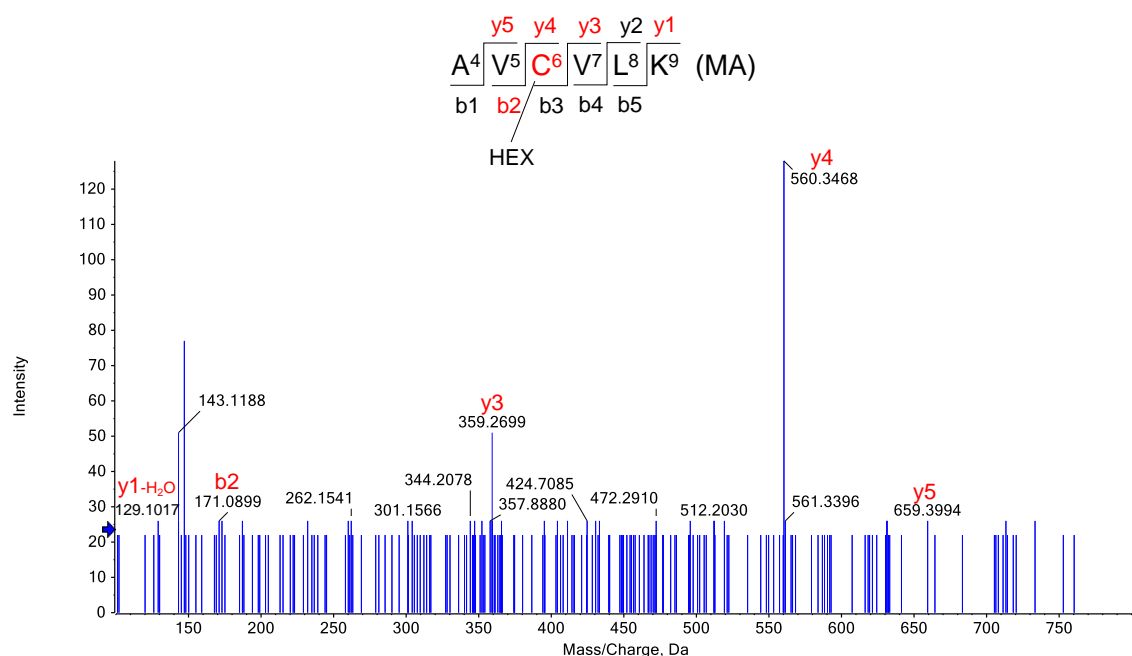


**Figure S17.** MS/MS of the peptide A<sup>4</sup>VCVLK<sup>9</sup> modified by hexenal at Cys6 by Michael Addition.

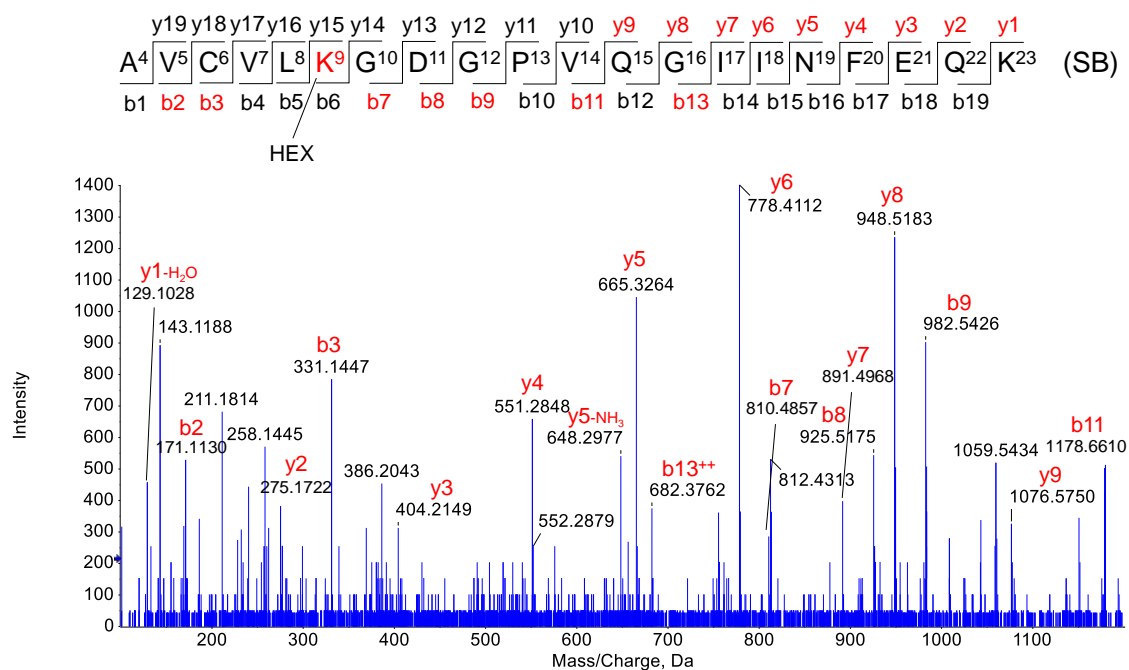


**Figure S18.** MS/MS of the peptide A<sup>4</sup>VCVLKGDGPVQGIINFEQK<sup>23</sup> modified by hexenal at Lys9 by Schiff base formation.

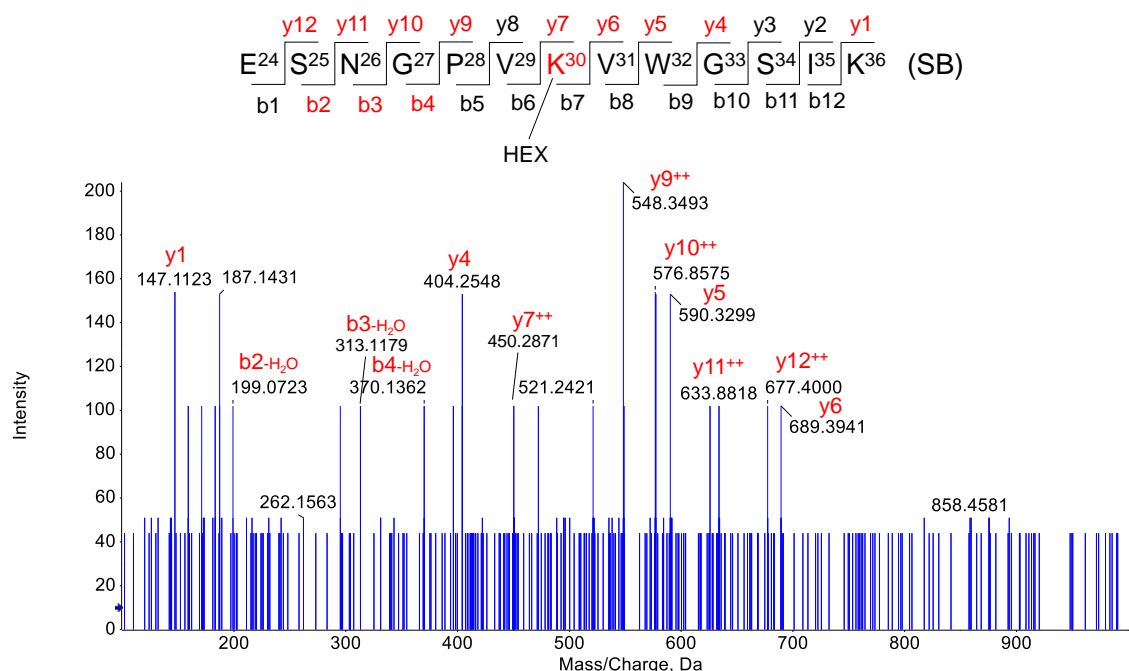


**Figure S19.** MS/MS of the peptide E<sup>24</sup>SNGPVKVWGSIK<sup>36</sup> modified by hexenal at Lys30 by Schiff base formation.

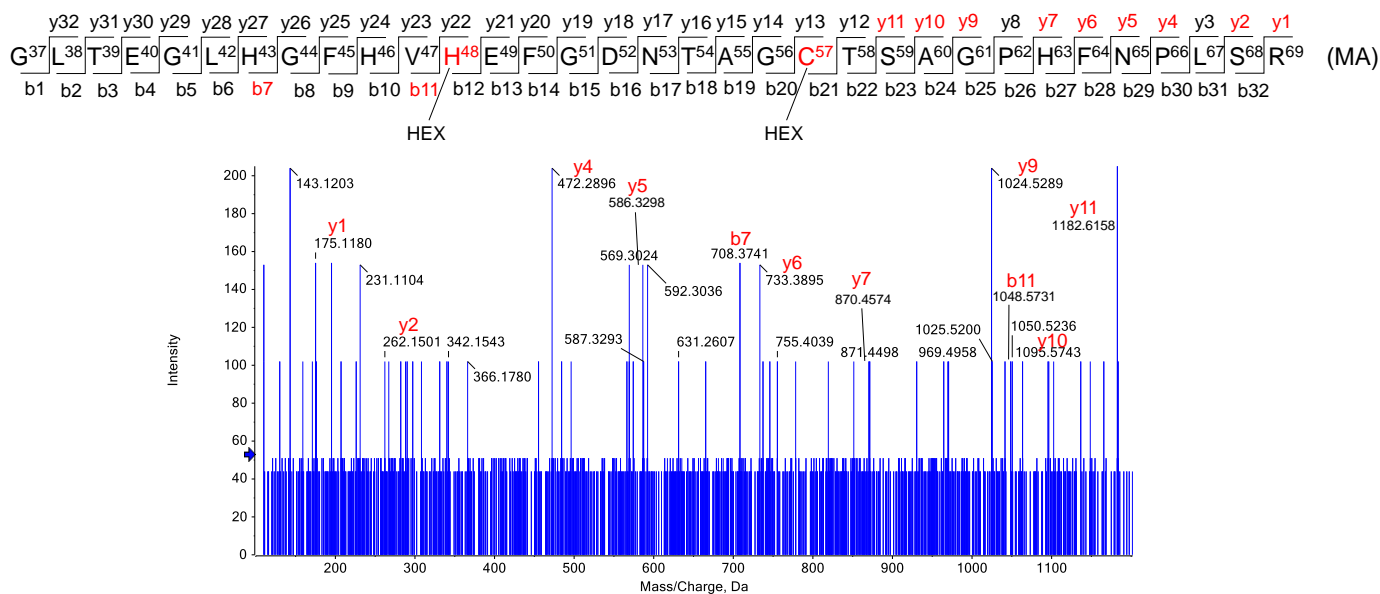


**Figure S20.** MS/MS of the peptide  $G^{37}LTEGLHGFHVHEFGDNTAGC TSAGPHFNPLSR^{69}$  modified by hexenal at His48 by Michael Addition.

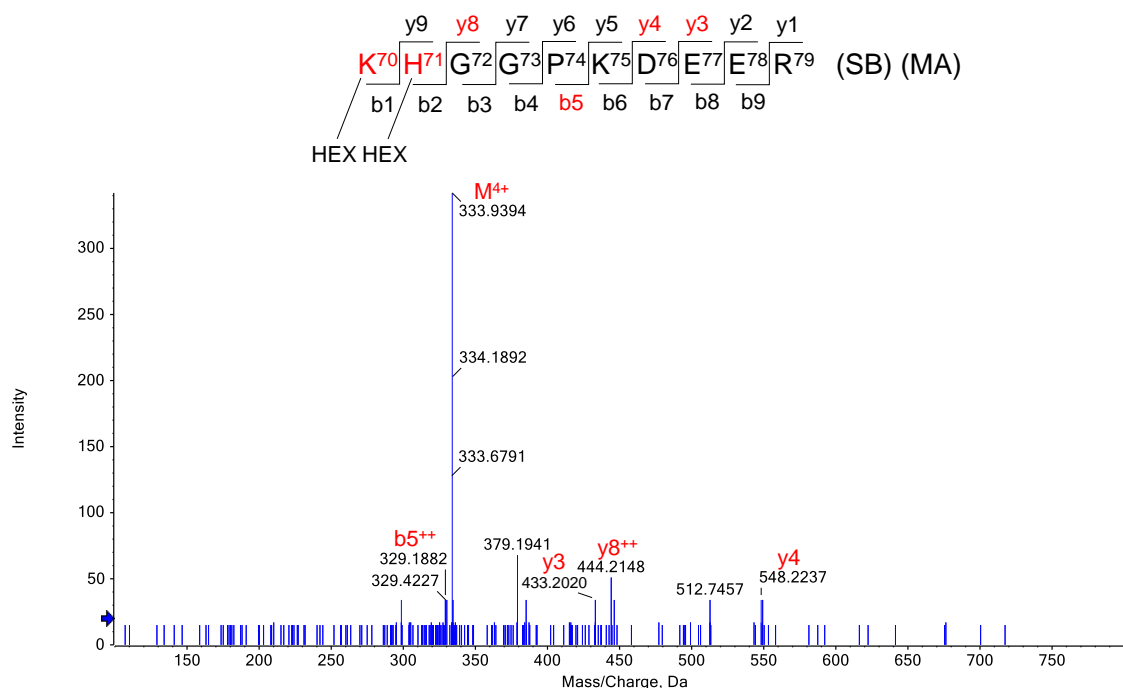


**Figure S21.** MS/MS of the peptide  $K^{70}HGGPKDEER^{79}$  modified by hexenal at Lys70 by Schiff base formation and His48 by Michael Addition.

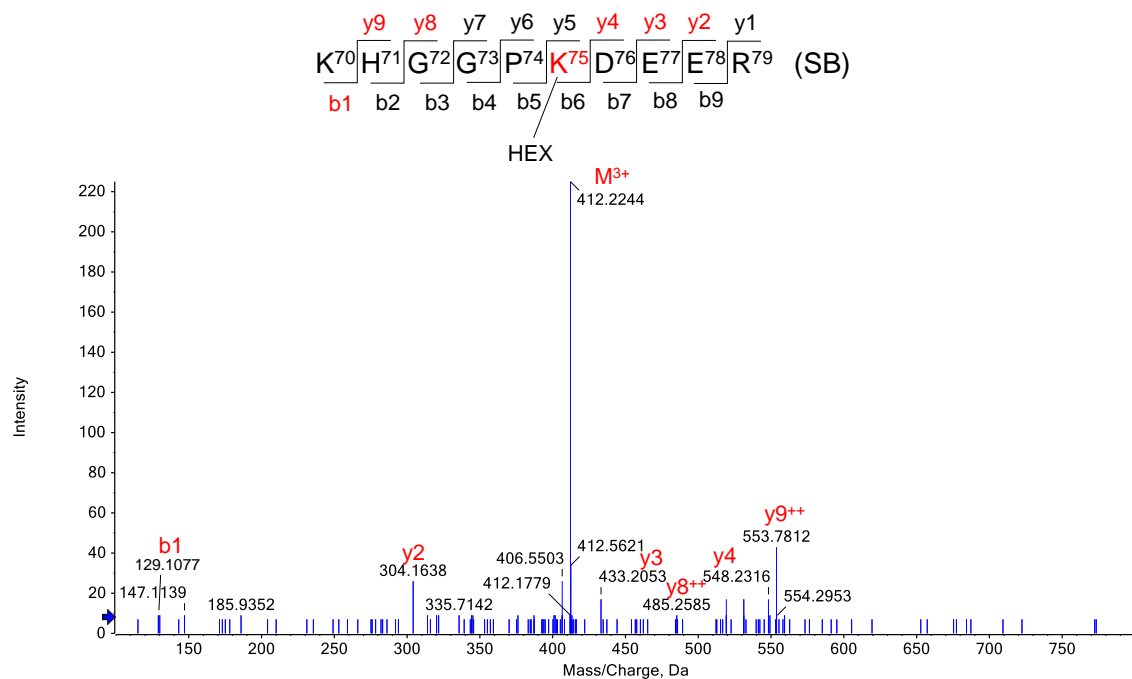


**Figure S22.** MS/MS of the peptide  $K^{70}HGPKDEER^{79}$  modified by hexenal at Lys75 by Schiff base formation.

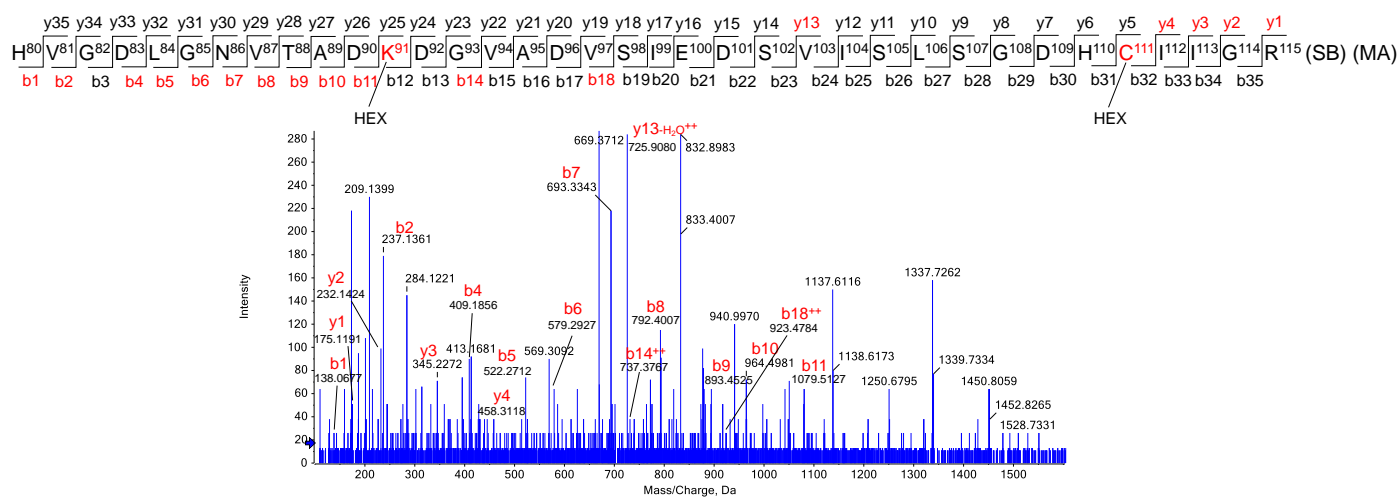


**Figure S23.** MS/MS of the peptide  $H^{80}VGDLGNVTADKDGVAADVSIEDSVISLSGDHCIIGR^{115}$  modified by hexenal at Lys91 by Michael Addition.

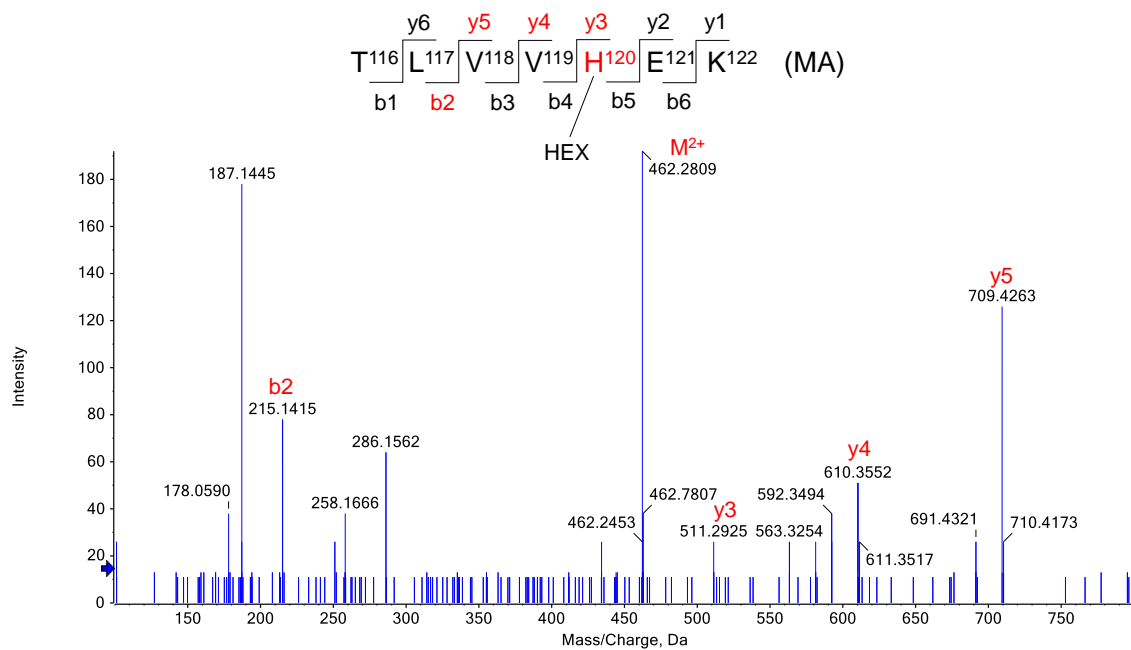


**Figure S24.** MS/MS of the peptide  $T^{116}LVVHEK^{122}$  modified by hexenal at His120 by Michael Addition.

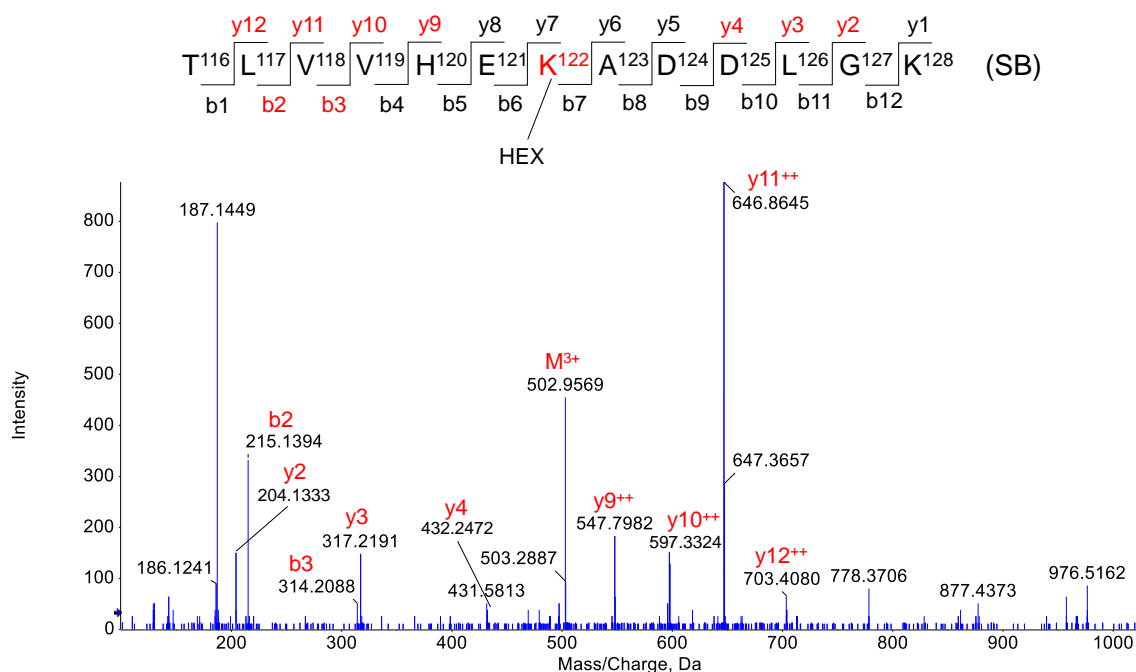


**Figure S25.** MS/MS of the peptide  $T^{116}LVVHEKADDLGK^{128}$  modified by hexenal at Lys122 by Schiff base formation.

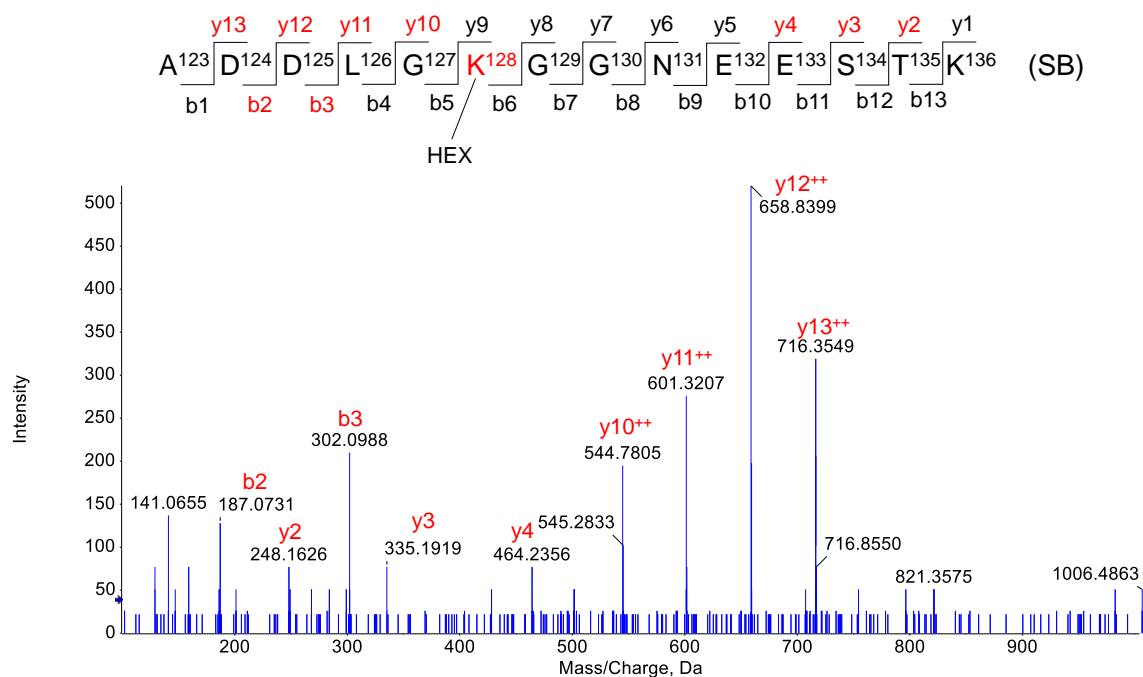


**Figure S26.** MS/MS of the peptide A<sup>123</sup>DDLGGKGGNEESTK<sup>136</sup> modified by hexenal at Lys128 by Schiff base formation.

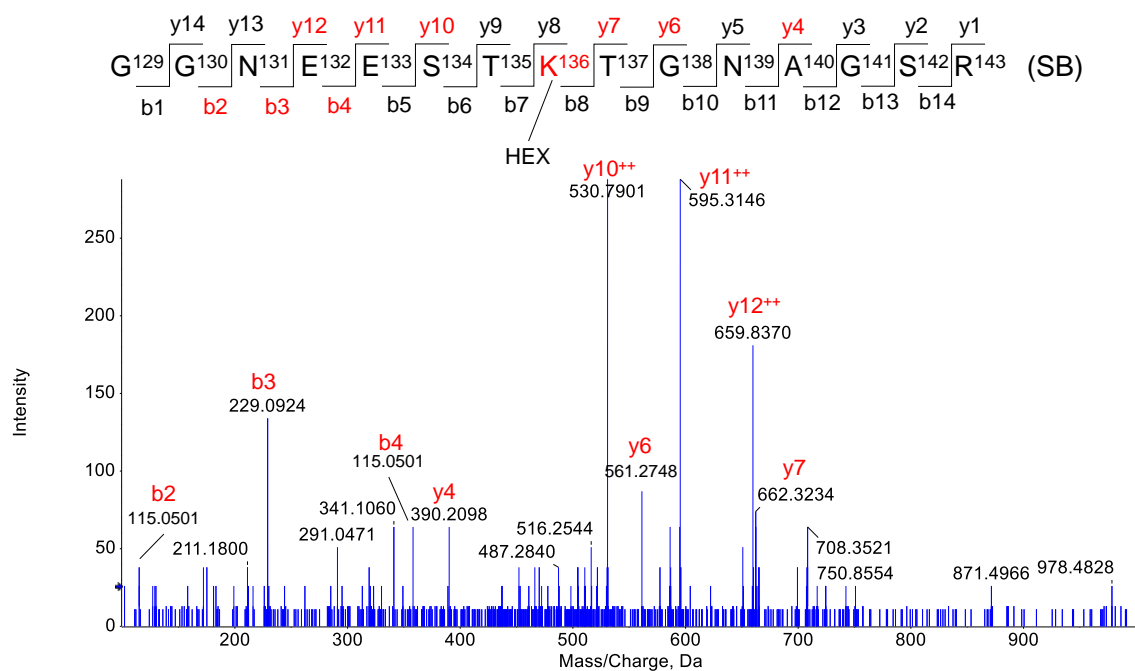


**Figure S27.** MS/MS of the peptide G<sup>129</sup>GNEESTKTGNAGSR<sup>143</sup> modified by hexenal at Lys136 by Schiff base formation.



**Table S3.** HNE-modified peptides identified by LC-MS/MS after digestion with trypsin.

Sequence	Residue	Unmodified (m/z)	Expected	Observed	Error (ppm)
ATK*AVC'VLK	Lys3 (SB)	495.2942 (2+)	565.3543 (2+)	565.3539 (2+)	-0.7
AVC'VLK*GDGPVQGII NFEQK	Lys9 (SB)	724.7209 (3+)	771.4276 (3+)	771.4302 (3+)	3.3
ESNGPVK*VWGSIK	Lys30 (SB)	467.5893 (3+)	514.2960 (3+)	514.2934 (3+)	-5.0
K*HGGPKDEER	Lys70 (SB)	384.8634 (3+)	431.5701 (3+)	431.5675 (3+)	-5.9
H*GGPKDEER	His71 (MA)	342.1651 (3+)	394.2034 (3+)	394.2056	5.5
KHGGPK*DEER	Lys75 (SB)	384.8634 (3+)	431.5701 (3+)	431.5683 (3+)	-4.6
TLVVH*EK	His120 (MA)	413.2451 (2+)	491.3026 (2+)	491.3012 (2+)	-2.8
TLVVHEK*ADDLGK	Lys122 (SB)	475.5963 (3+)	522.3030 (3+)	522.3027 (3+)	-0.5
ADDLGK*GGNEESTK	Lys128 (SB)	474.2232 (3+)	520.9299 (3+)	520.9300 (3+)	0.1
GGNEESTK*TGNAGSR	Lys136 (SB)	488.8940 (3+)	535.6007 (3+)	535.6009 (3+)	0.3
GGNEESTK*TGNAGSR	Lys136 (MA)	488.8940 (3+)	540.9323 (3+)	540.9307 (3+)	-2.9

SB: Schiff Base

MA: Michael Addition

\* Aldehyde adduct

' Carbamidomethyl adduct

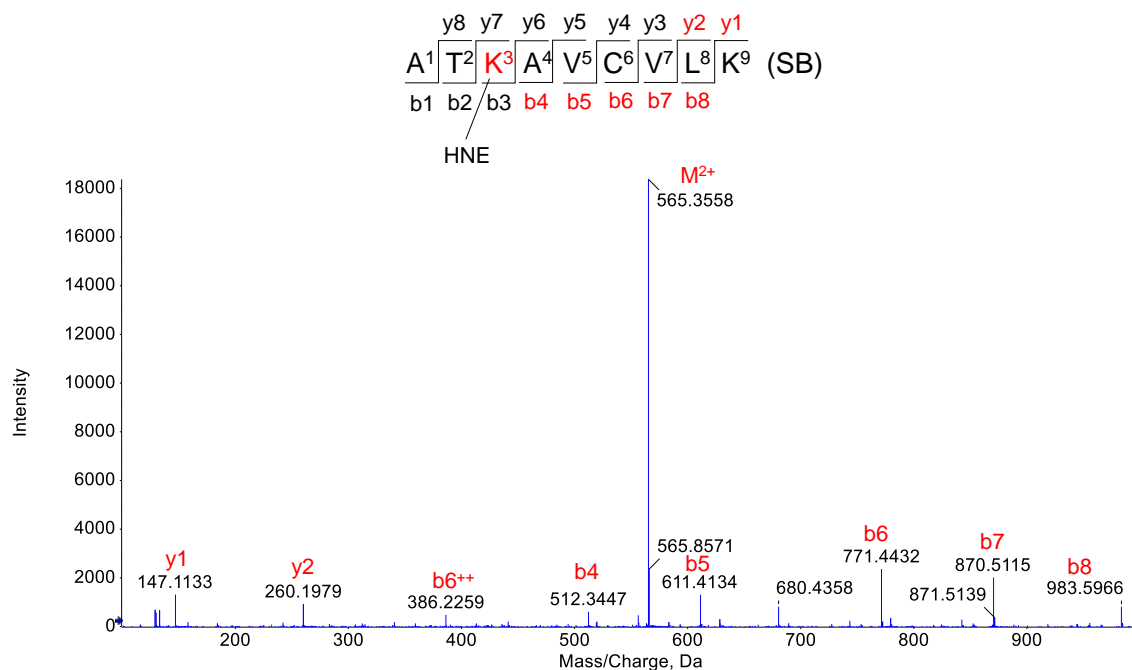


**Figure S28.** MS/MS of the peptide A<sup>1</sup>TKAVCVLK<sup>9</sup> modified by HNE at Lys3 by Schiff base formation.

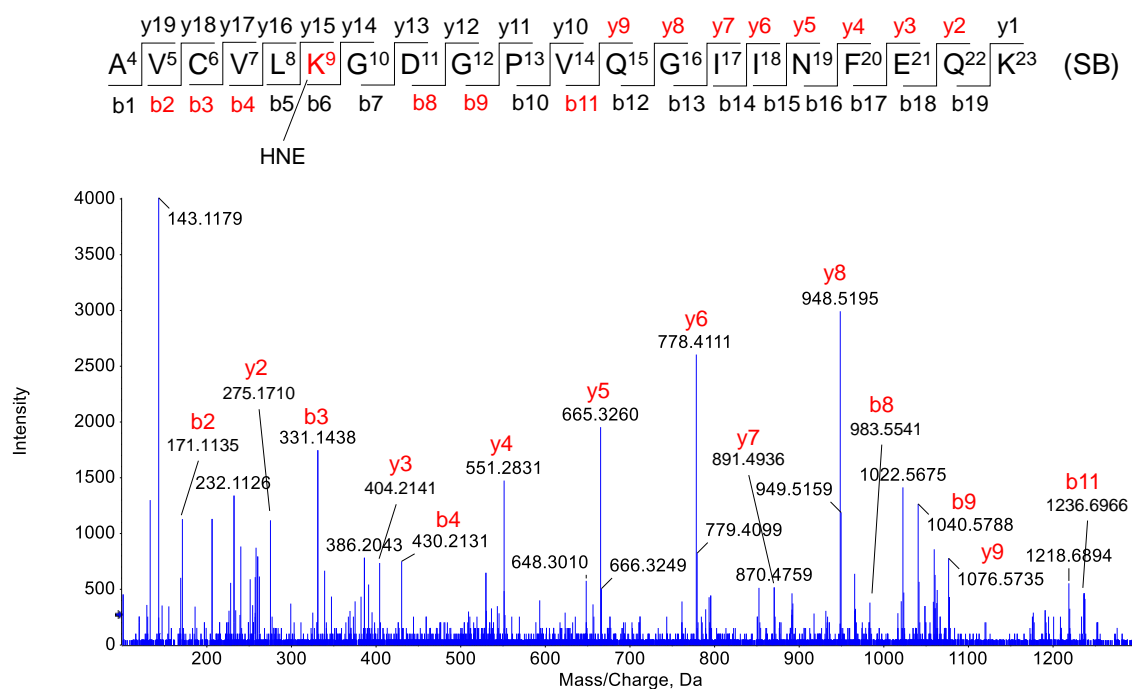


**Figure S29.** MS/MS of the peptide A<sup>4</sup>VCVLKGDGPVQGIINFEQK<sup>23</sup> modified by HNE at Lys9 by Schiff base formation.

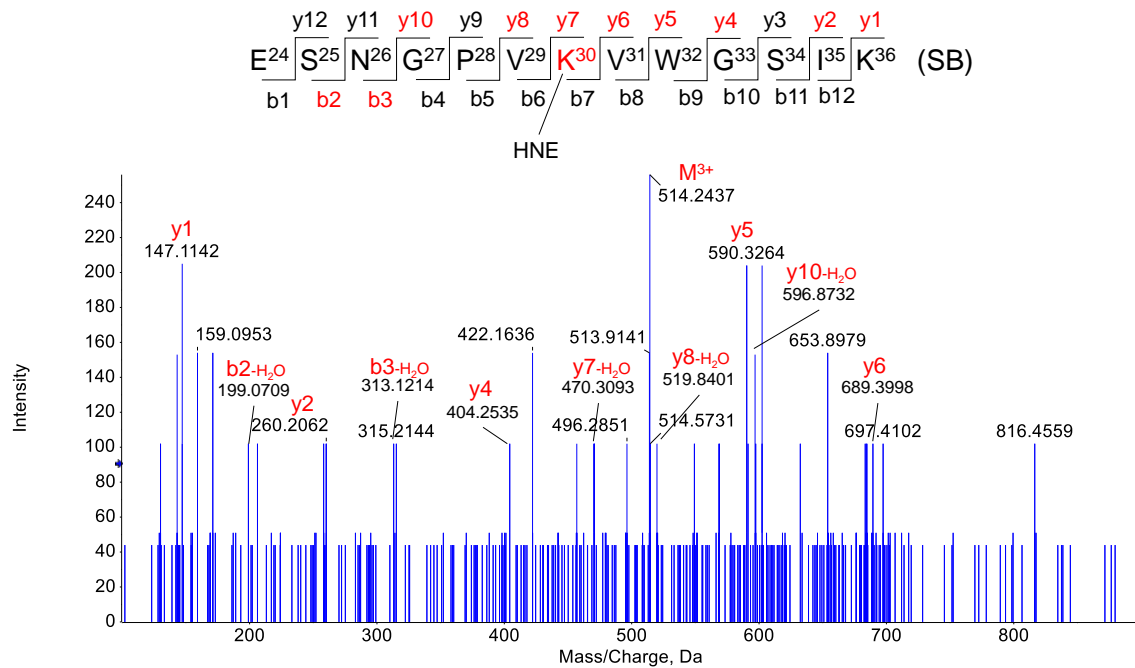


**Figure S30.** MS/MS of the peptide E<sup>24</sup>SNGPVKQVWGSIK<sup>36</sup> modified by HNE at Lys30 by Schiff base formation.

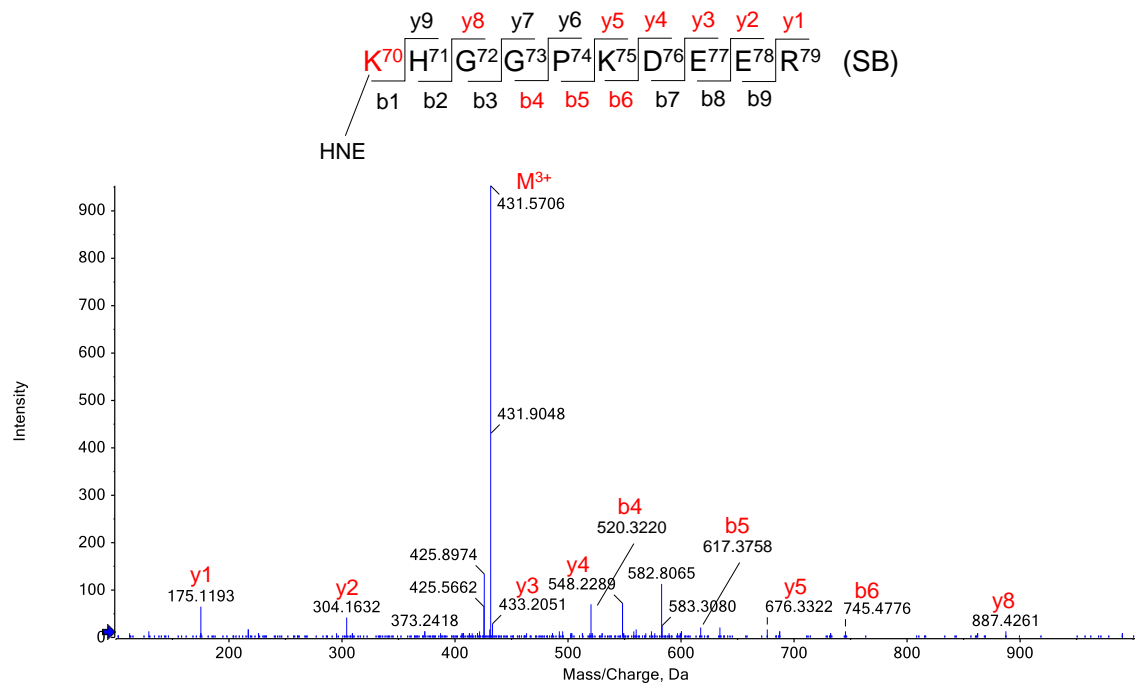


**Figure S31.** MS/MS of the peptide K<sup>70</sup>HGGPKDEER<sup>79</sup> modified by HNE at Lys30 by Schiff base formation.

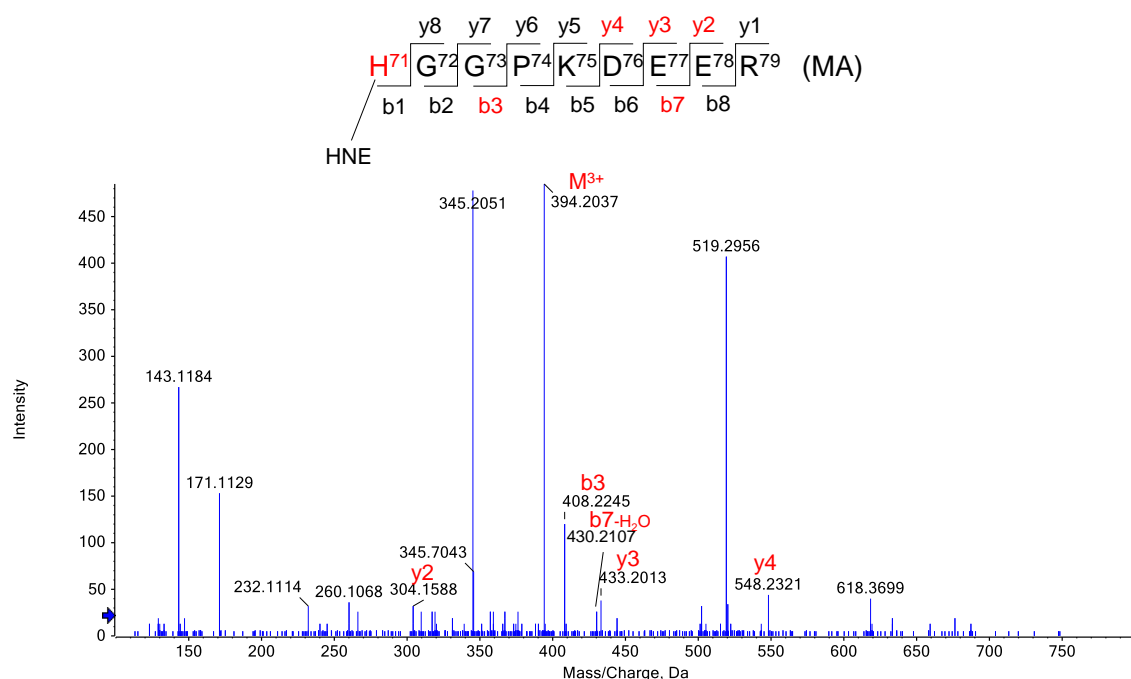


**Figure S32.** MS/MS of the peptide H<sup>71</sup>GGPKDEER<sup>79</sup> modified by HNE at His71 by Michael Addition.

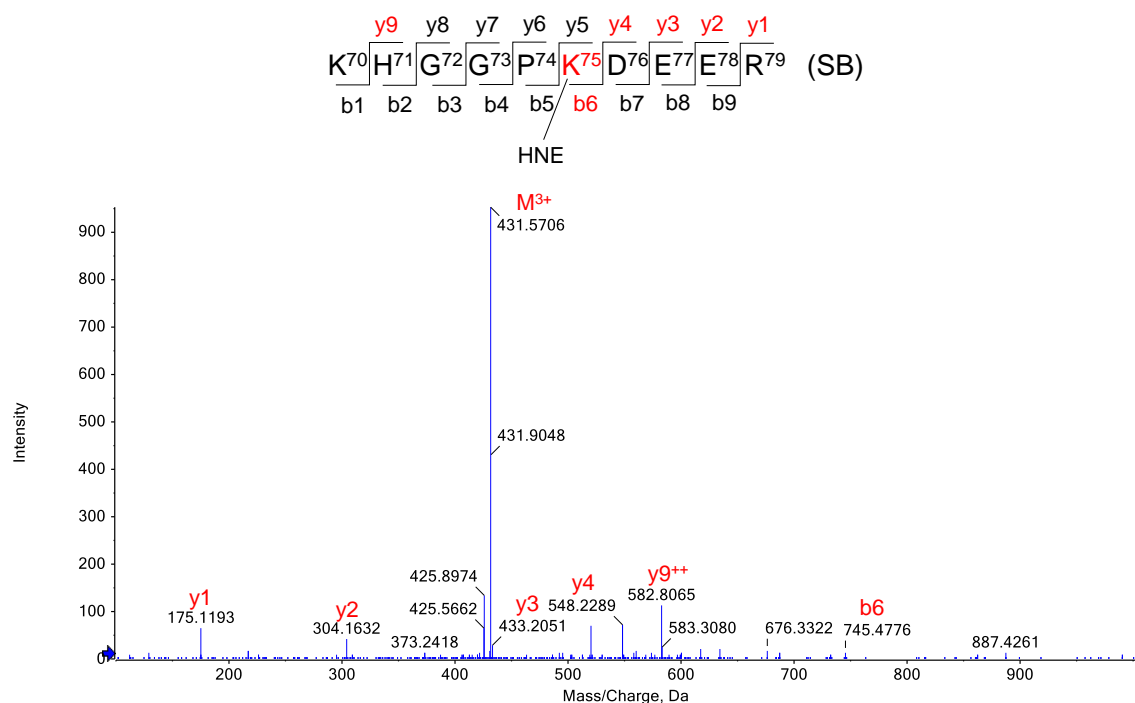


**Figure S33.** MS/MS of the peptide K<sup>70</sup>HGGPKDEER<sup>79</sup> modified by HNE at Lys75 by Schiff base formation.

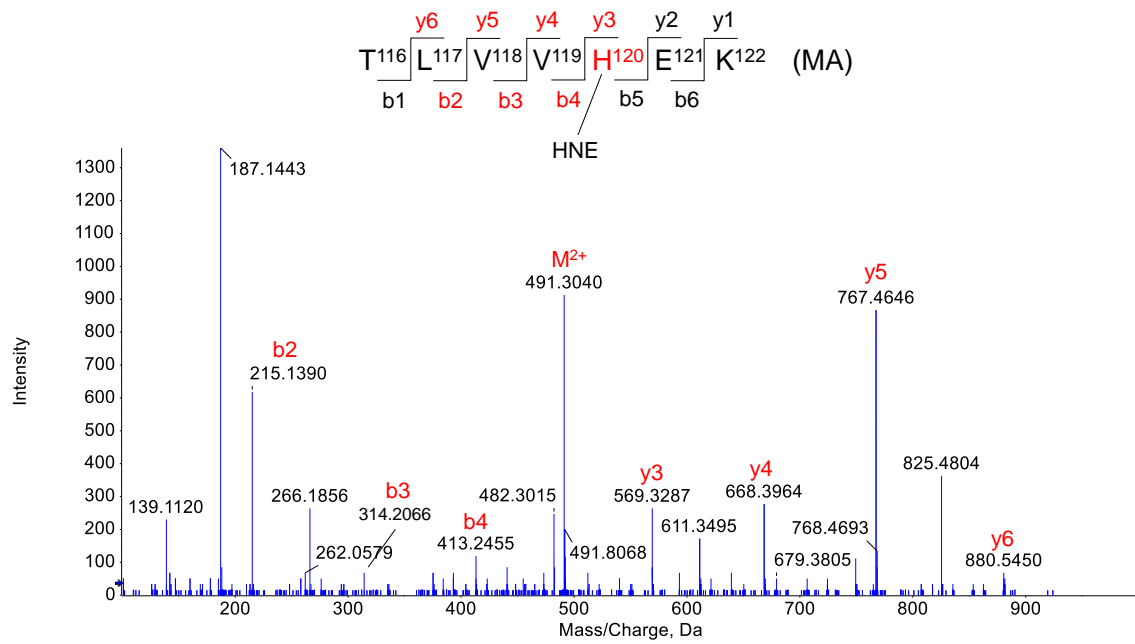


**Figure S34.** MS/MS of the peptide T<sup>116</sup>LVVHEK<sup>122</sup> modified by HNE at His120 by Michael Addition.

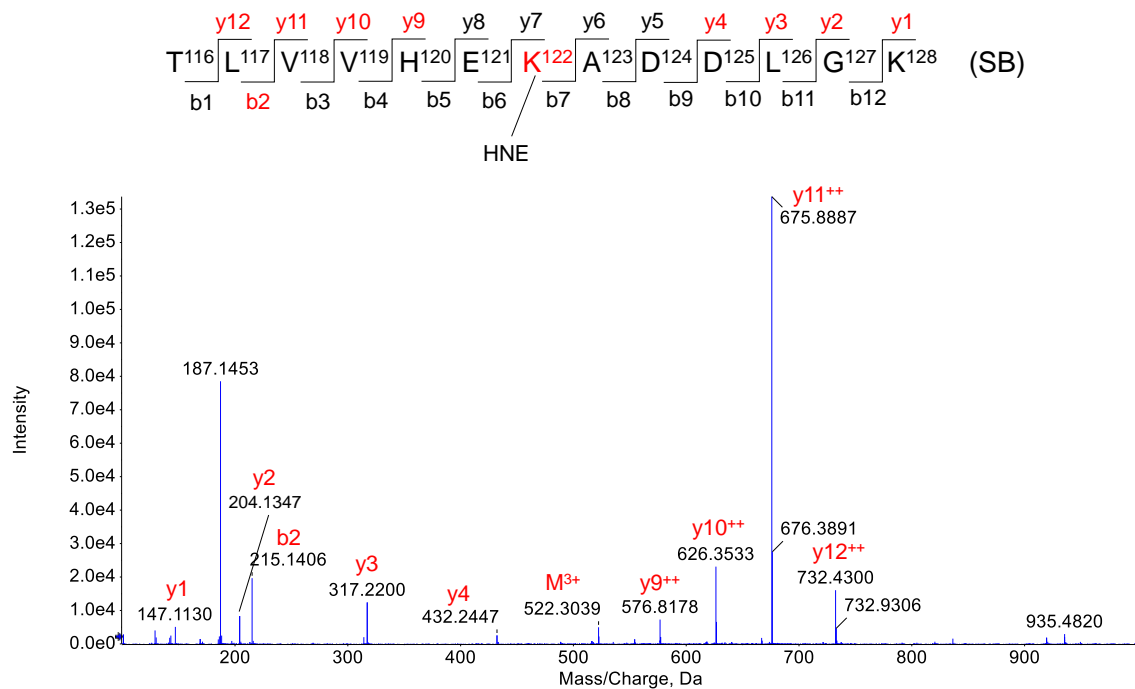


**Figure S35.** MS/MS of the peptide T<sup>116</sup>LVVHEKADDLKG<sup>128</sup> modified by HNE at Lys122 by Schiff base formation.

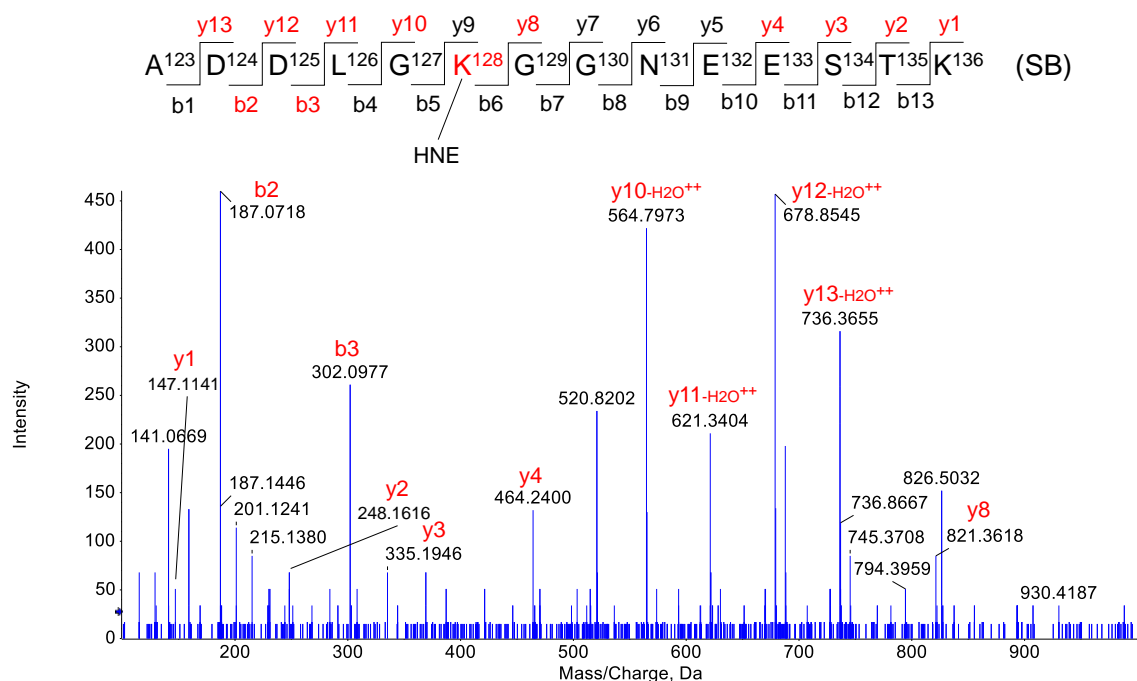


**Figure S36.** MS/MS of the peptide  $A^{123}DDLKGKGNEESTK^{136}$  modified by HNE at Lys128 by Schiff base formation.

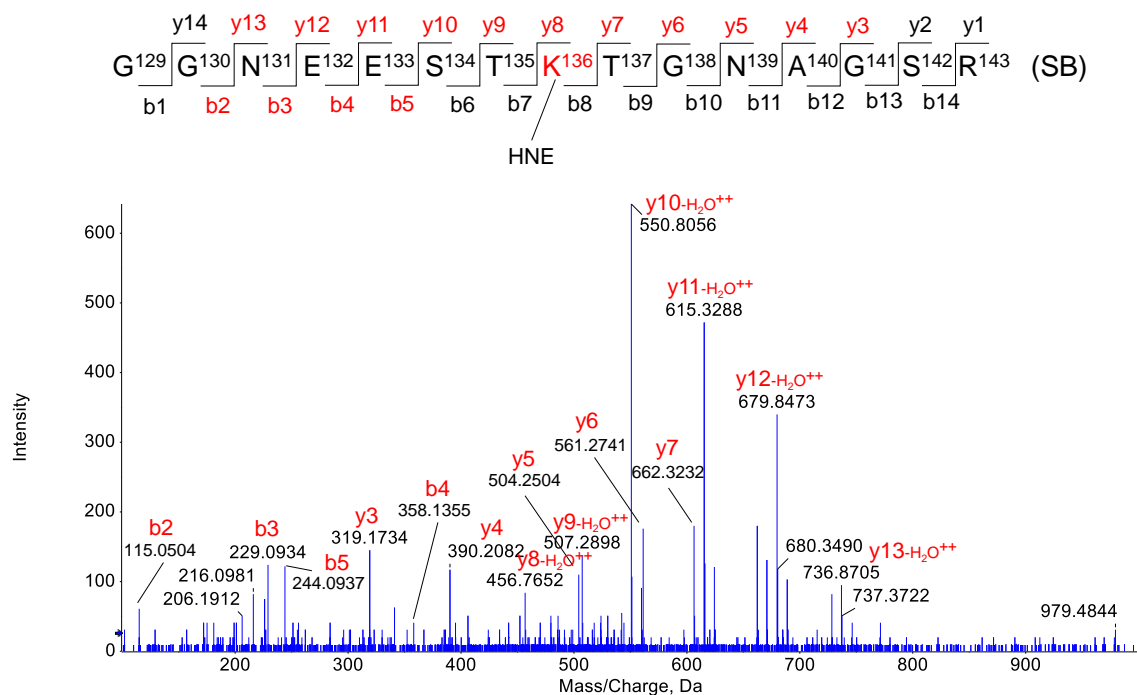


**Figure S37.** MS/MS of the peptide  $G^{129}GNEESTKTGNAGSR^{143}$  modified by HNE at Lys128 by Schiff base formation.

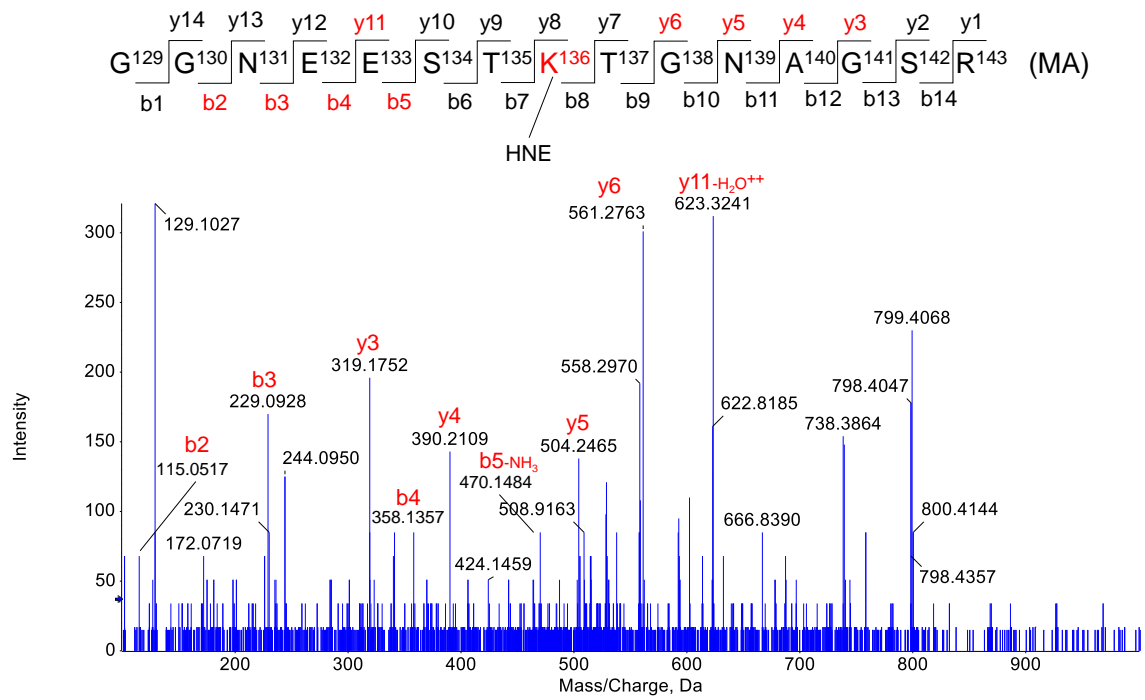


**Figure S38.** MS/MS of the peptide  $G^{129}GNEESTKTGNAGSR^{143}$  modified by HNE at Lys128 by Michael Addition.

**Table S4.** Nonadialenal-modified peptides identified by LC-MS/MS after digestion with trypsin.

Sequence	Residue	Unmodified (m/z)	Expected	Observed	Error (ppm)
ATK*AVC'VLK	Lys3 (SB)	330.5319 (3+)	371.2351 (3+)	371.2346 (3+)	-1.4
AVC*VLK	Cys6 (MA)	316.6936 (2+)	385.7459 (2+)	385.7443 (2+)	-4.1
AVC'VLK*GDGPVQGII NFEQK	Lys9 (SB)	724.7209 (3+)	765.4241 (3+)	765.4280 (3+)	5.1
ESNGPVK*VWGSIK	Lys30 (SB)	467.5893 (3+)	508.2924 (3+)	508.2908 (3+)	-3.1
TLVVH*EK	His120 (MA)	275.8325 (3+)	321.8673 (3+)	321.8661 (3+)	-3.6
TLVVHEK*ADDLGK	Lys122 (SB)	475.5963 (3+)	516.2995 (3+)	516.2966 (3+)	-5.6
TLVVHEK*ADDLGK	Lys122 (MA)	475.5963 (3+)	521.6311 (3+)	521.6304 (3+)	-1.3
ADDLGK*GGNEESTK	Lys128 (MA)	474.2232 (3+)	520.2580 (3+)	520.2607	5.1
GGNEESTK*TGNAGSR	Lys136 (SB)	488.8940 (3+)	529.5971 (3+)	529.5967 (3+)	-0.9
LAC*GVIGIAQ	Cys146 (MA)	472.7653 (2+)	541.8176 (2+)	541.8175 (3+)	-0.1

SB: Schiff Base

MA: Michael Addition

\* Aldehyde adduct

' Carbamidomethyl adduct



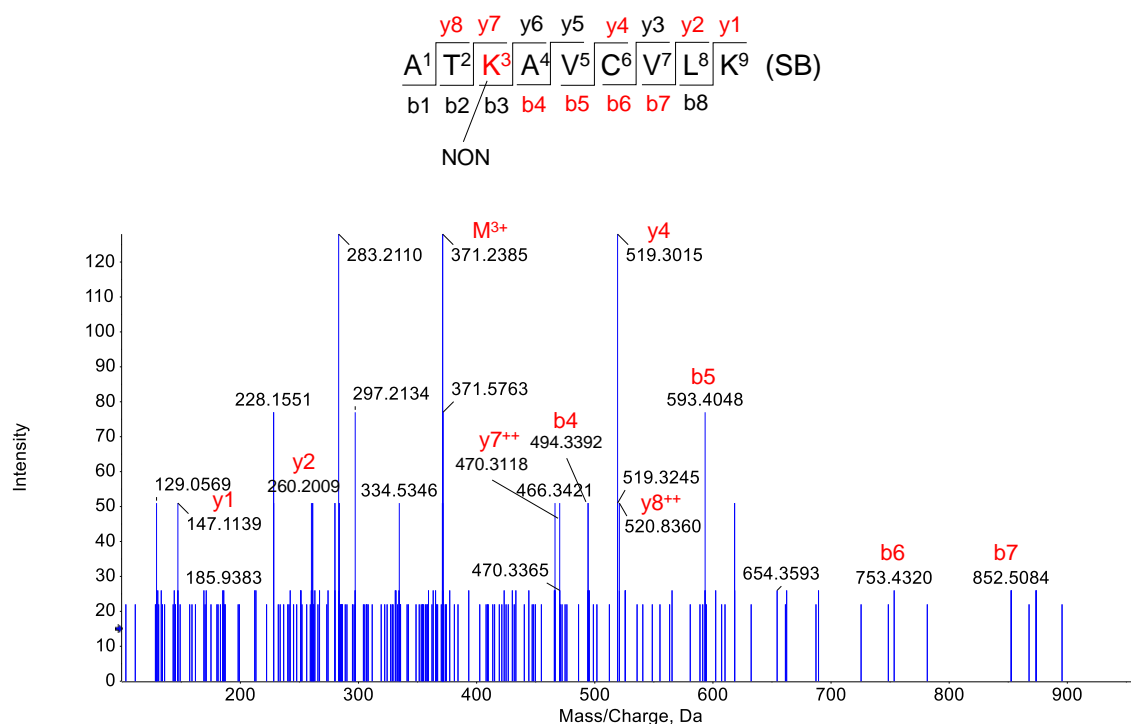


**Figure S39.** MS/MS of the peptide A<sup>1</sup>TKAVCVLK<sup>9</sup> modified by nonadial at Lys3 by Schiff base formation.

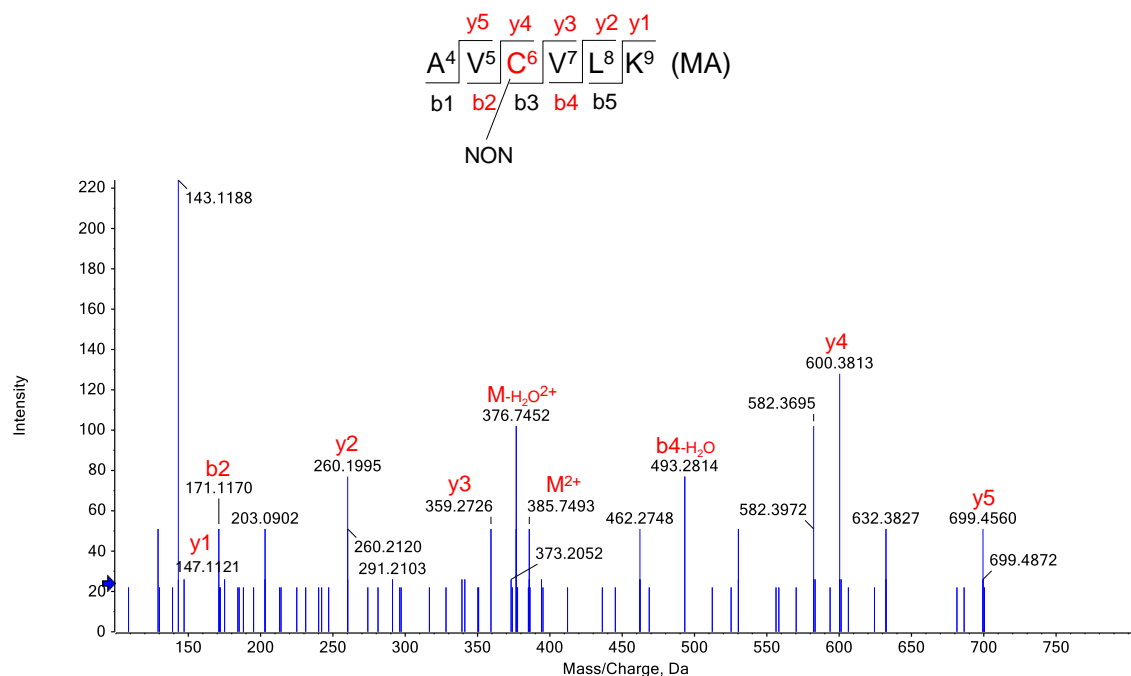


**Figure S40.** MS/MS of the peptide A<sup>4</sup>VCVLK<sup>9</sup> modified by nonadial at Cys6 by Michael Addition.

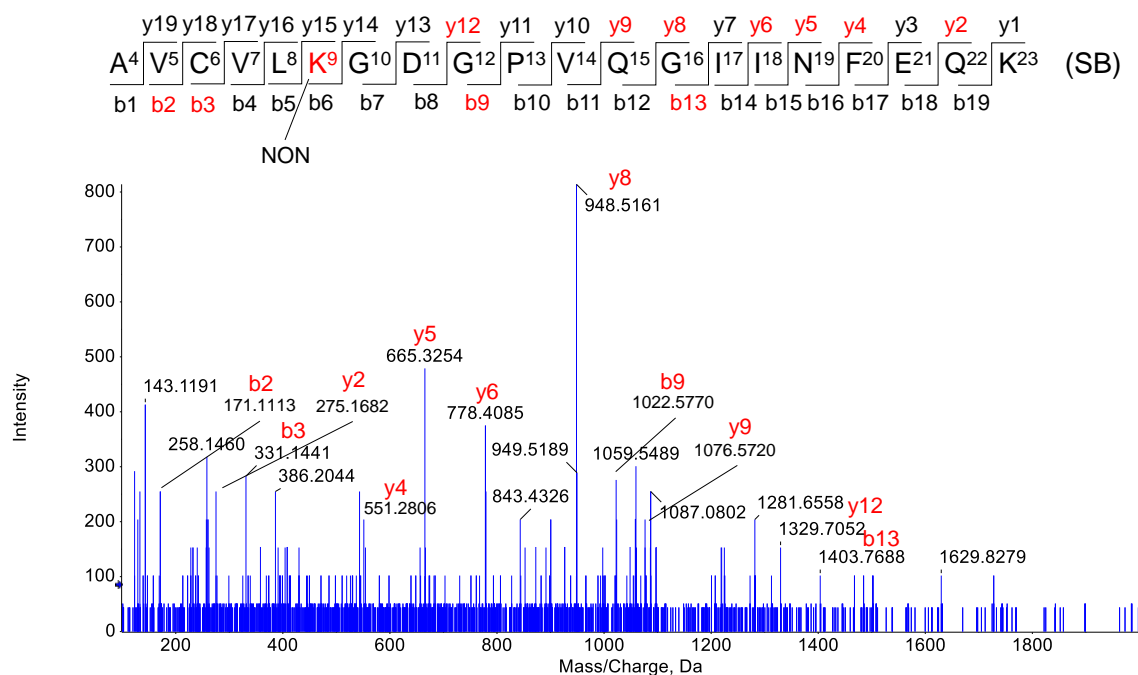


**Figure S41.** MS/MS of the peptide A<sup>4</sup>VCVLKGDGPVQGIINFEQK<sup>23</sup> modified by nonadialal at Lys9 by Schiff base formation.

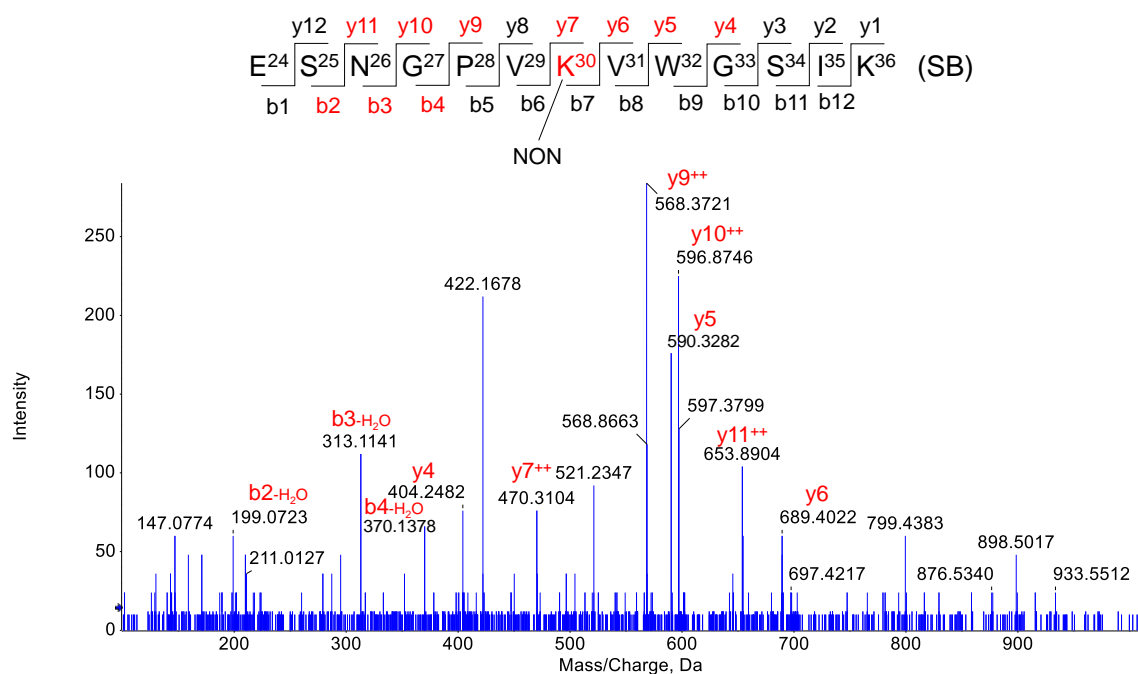


**Figure S42.** MS/MS of the peptide E<sup>24</sup>SNGPVKVWGSIK<sup>36</sup> modified by nonadialal at Lys30 by Schiff base formation.

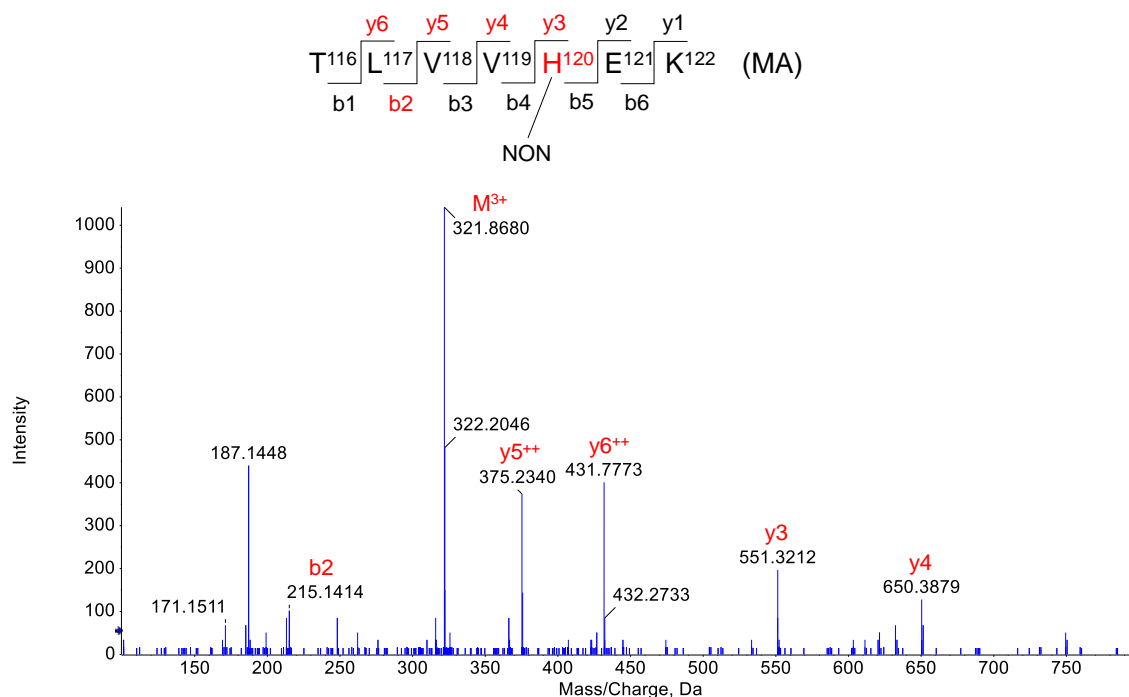


**Figure S43.** MS/MS of the peptide T<sup>116</sup>LVVHEK<sup>122</sup> modified by nonadial at His120 by Michael Addition.

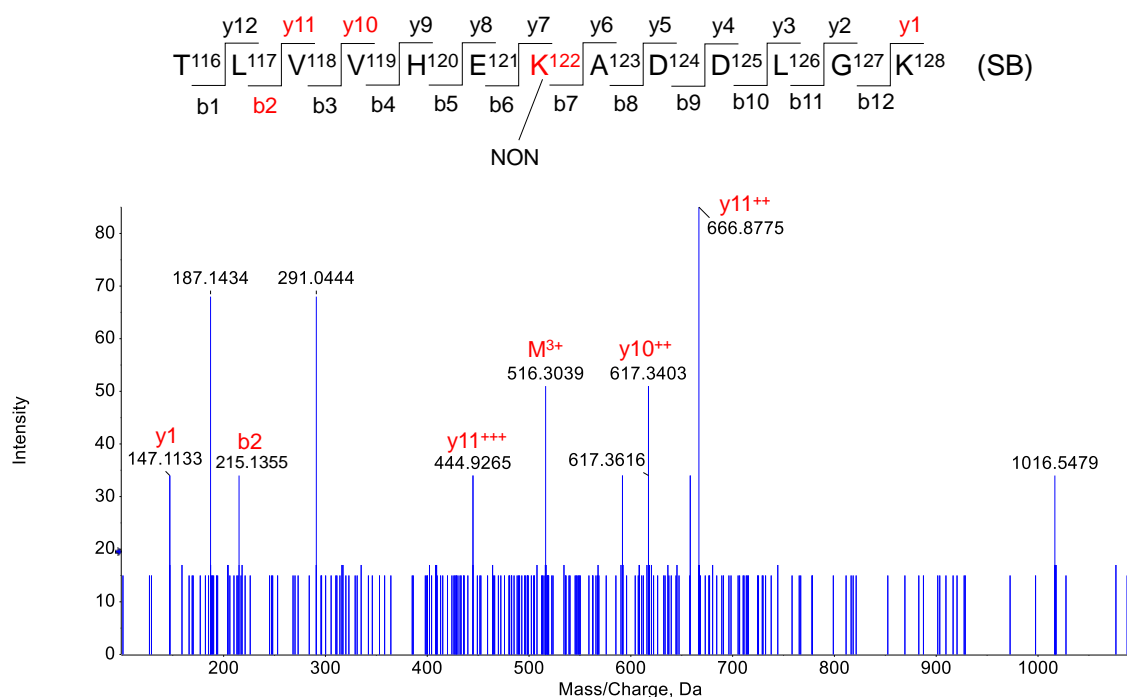


**Figure S44.** MS/MS of the peptide T<sup>116</sup>LVVHEKADDLGK<sup>128</sup> modified by nonadial at Lys122 by Schiff base formation.

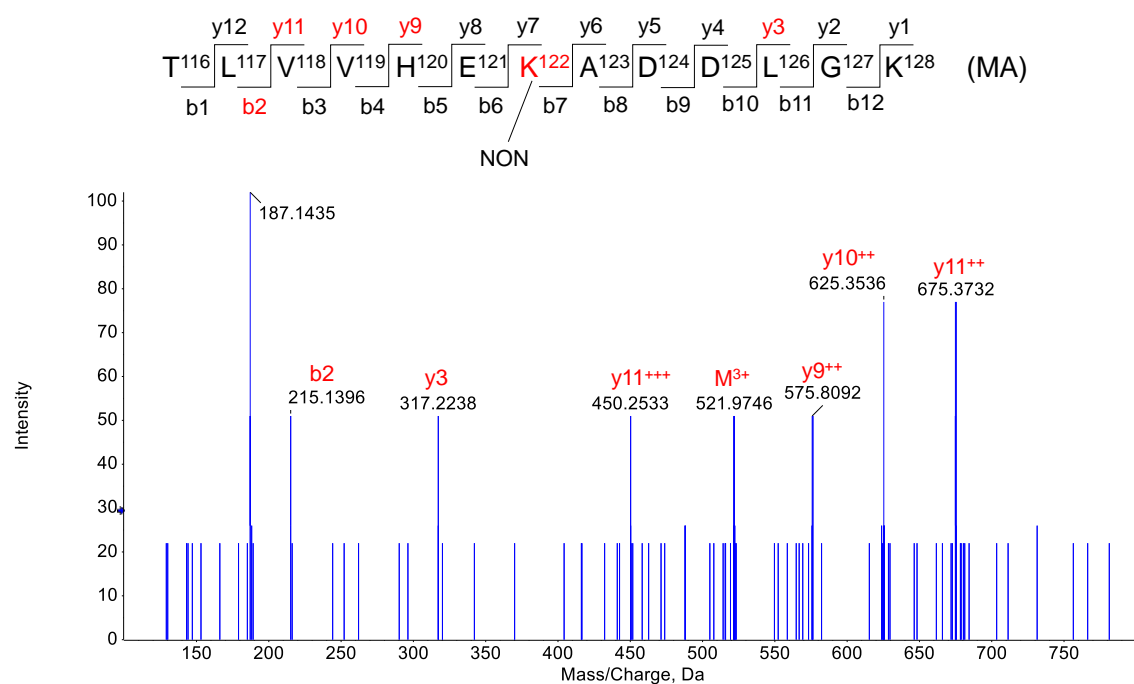


**Figure S45.** MS/MS of the peptide  $T^{116}LVVHEKADDLKG^{128}$  modified by nonadial at Lys122 by Michael Addition.

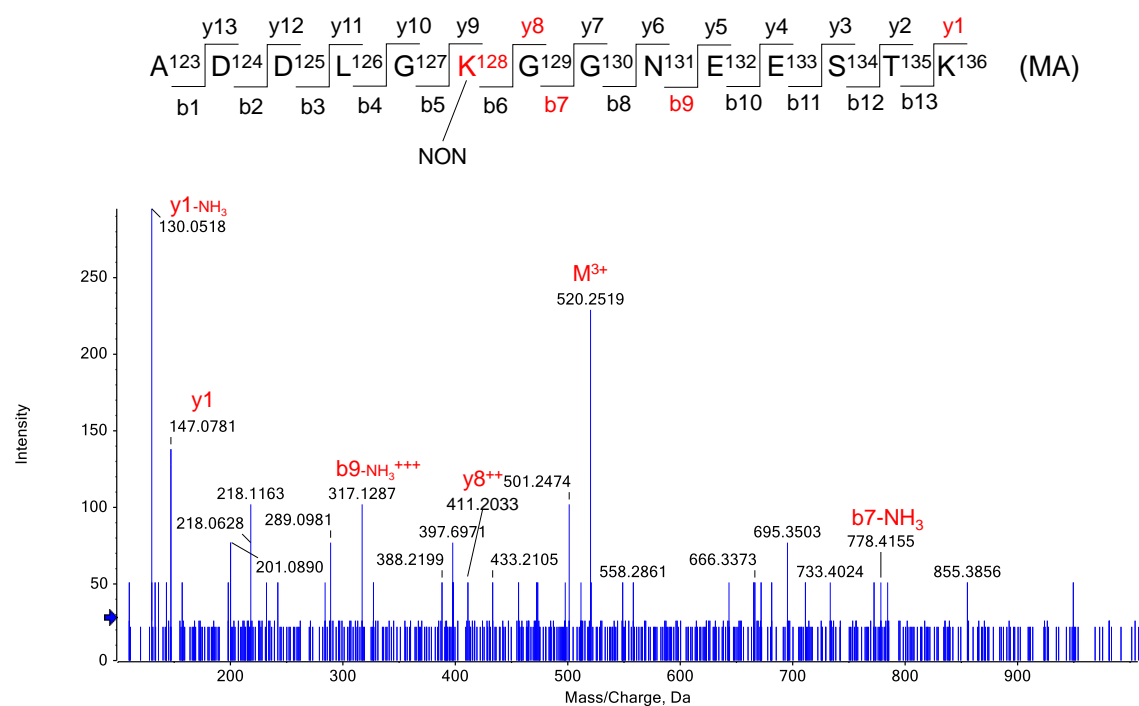


**Figure S46.** MS/MS of the peptide  $A^{123}DDLKGKGNEESTK^{136}$  modified by nonadial at Lys128 by Michael Addition.

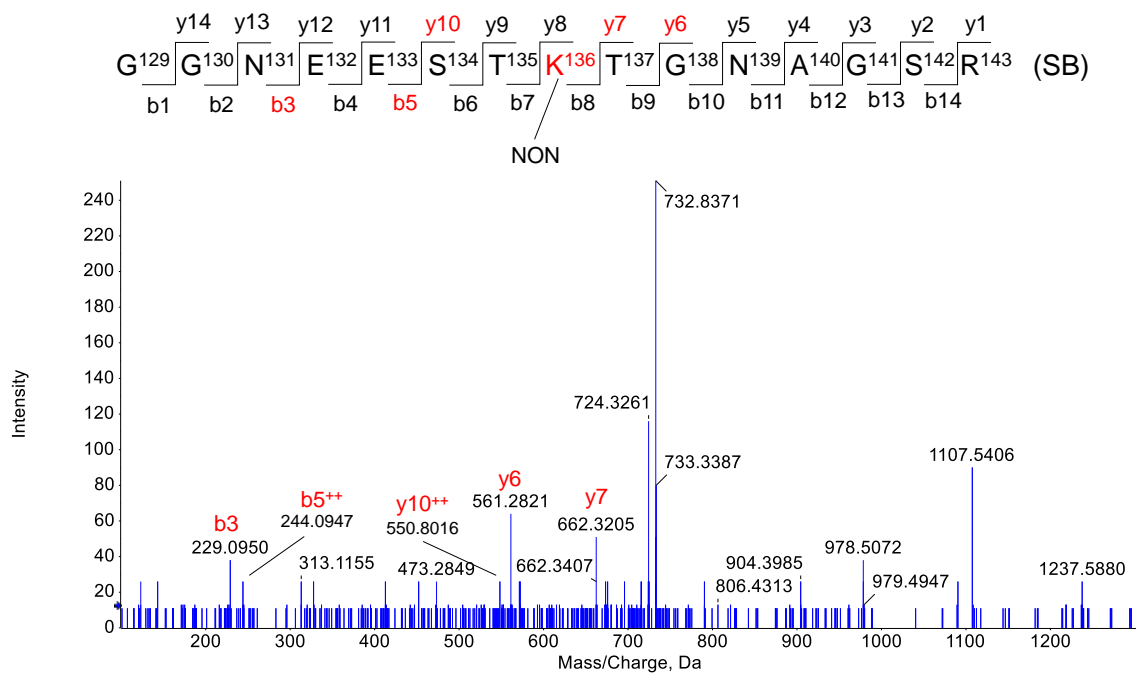


**Figure S47.** MS/MS of the peptide  $G^{129}GNEESTKTGNAGSR^{143}$  modified by nonadial at Lys136 by Schiff base formation.

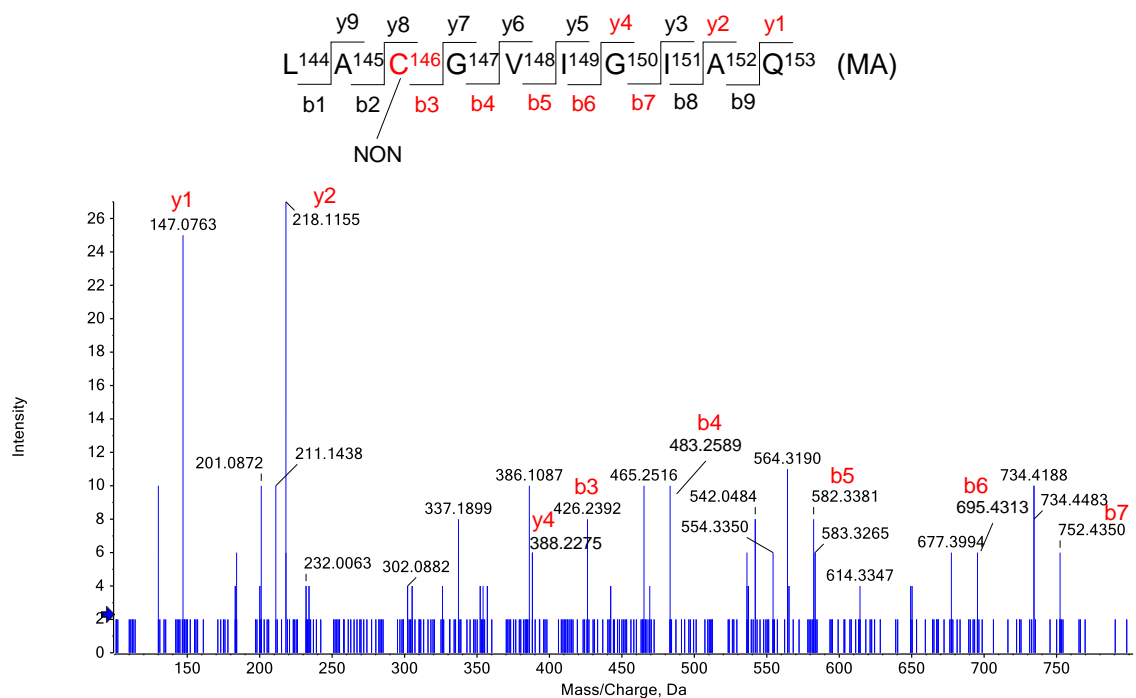


**Figure S48.** MS/MS of the peptide  $L^{144}ACGVIGIAQ^{153}$  modified by nonadial at Cys146 by Michael Addition.

**Table S5.** Decadienal-modified peptides identified by LC-MS/MS after digestion with trypsin.

Sequence	Residue	Unmodified (m/z)	Expected	Observed	Error (ppm)
ATK*AVC'VLK	Lys3 (SB)	330.5319 (3+)	375.9070 (3+)	375.9078 (3+)	2.1
AVC*VLK	Cys6 (MA)	316.6936 (2+)	392.7537 (2+)	392.7532 (2+)	-1.3
AVC'VLK*GDGPVQGIINF EQK	Lys9 (SB)	724.7209 (3+)	770.0960 (3+)	770.0940 (3+)	-2.5
AVC'VLK*GDGPVQGIINF EQK	Lys9 (MA)	724.7209 (3+)	775.4276 (3+)	775.4337 (3+)	7.8
ESNGPVK*VWGSIK	Lys30 (SB)	467.5893 (3+)	512.9643 (3+)	512.9665 (3+)	4.2
HVGDLGNVTADKDG VAD VSIEDSVISLSGDH*C'IIGR	His110 (MA)	930.9588 (4+)	968.9888 (4+)	968.9973 (4+)	8.7
TLVVH*EK	His120 (MA)	275.8325 (3+)	326.5392 (3+)	326.5389 (3+)	-1.0
TLVVHEK*ADDLGK	Lys122 (SB)	475.5963 (3+)	520.9714 (3+)	520.9729 (3+)	2.9
ADDLGK*GGNEESTK	Lys128 (SB)	474.2232 (3+)	519.5983 (3+)	519.6019 (3+)	6.9
GGNEESTK*TGNAGSR	Lys136 (SB)	488.8940 (3+)	534.2690 (3+)	534.2719 (3+)	5.4
LAC*GVIGIAQ	Cys146 (MA)	472.7653 (2+)	548.8254 (2+)	548.8232 (2+)	-3.9

SB: Schiff Base

MA: Michael Addition

\* Aldehyde adduct

' Carbamidomethyl adduct

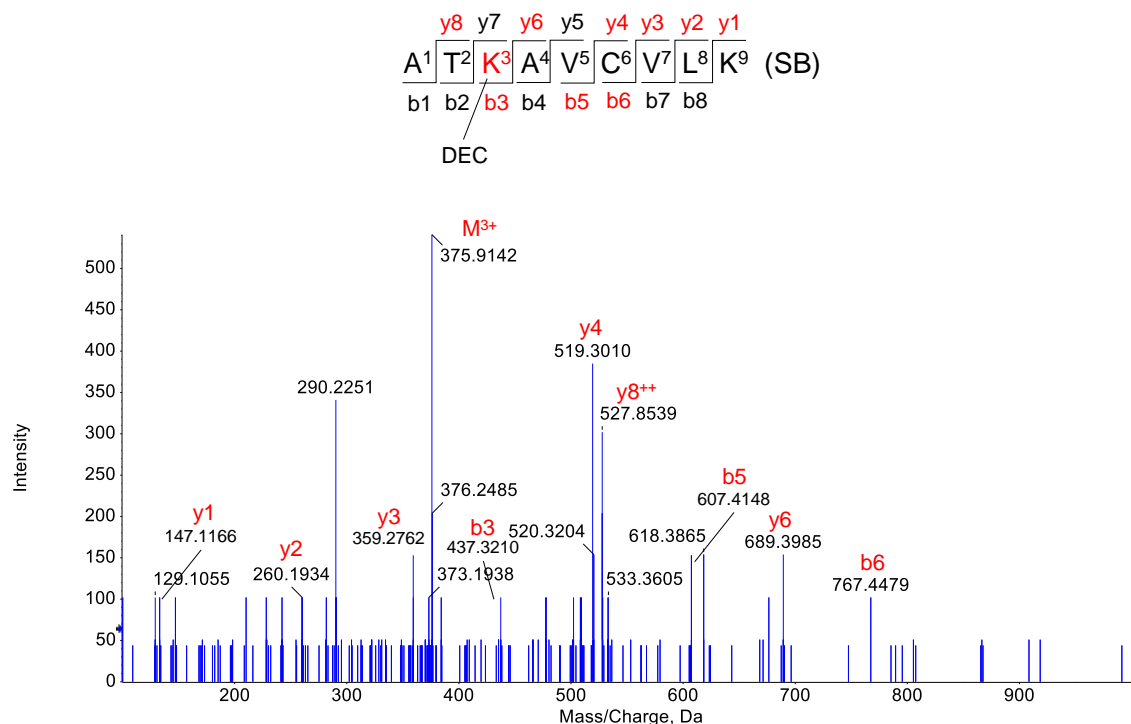


**Figure S49.** MS/MS of the peptide A<sup>1</sup>TKAVCVLK<sup>9</sup> modified by decadienal at Lys3 by Schiff base formation.

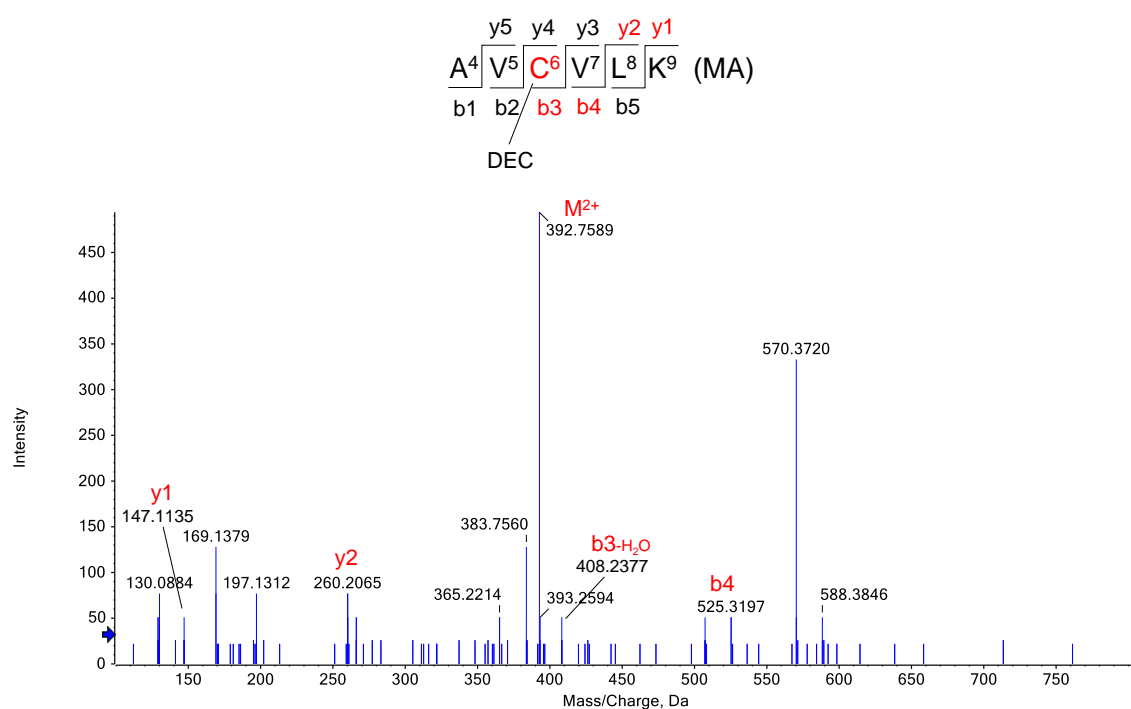


**Figure S50.** MS/MS of the peptide A<sup>4</sup>VCVLK<sup>9</sup> modified by decadienal at Cys6 by Michael Addition.

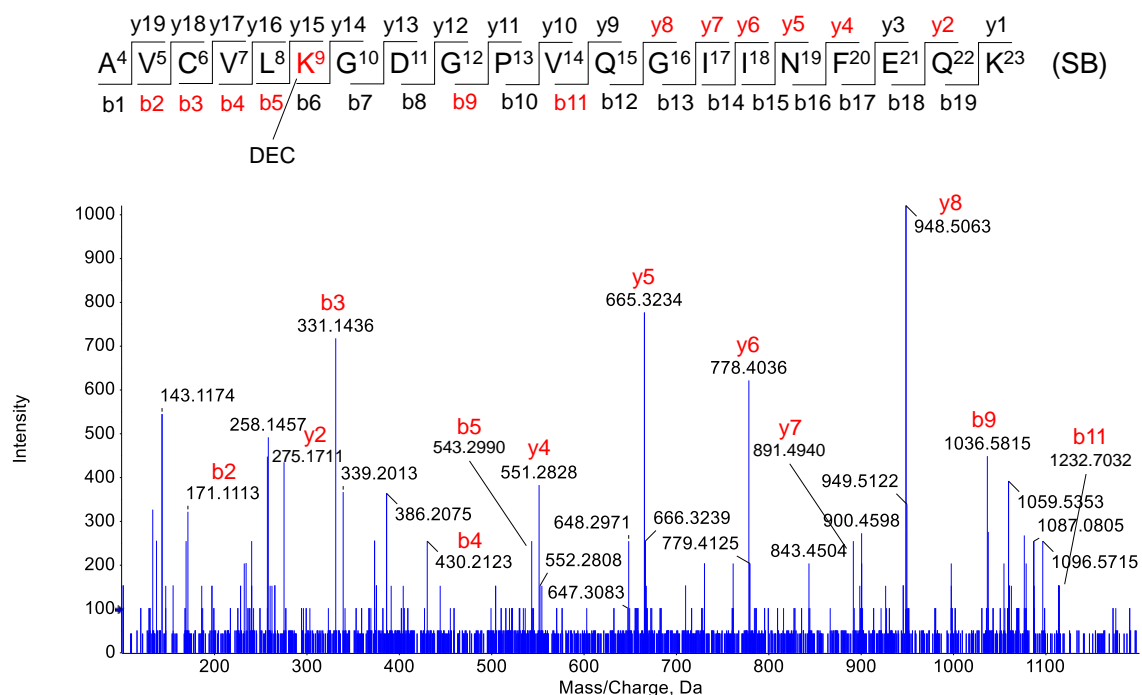


**Figure S51.** MS/MS of the peptide  $A^4VCVLKGDGPVQGIINFEQK^{23}$  modified by decadial at Lys9 by Schiff base formation.

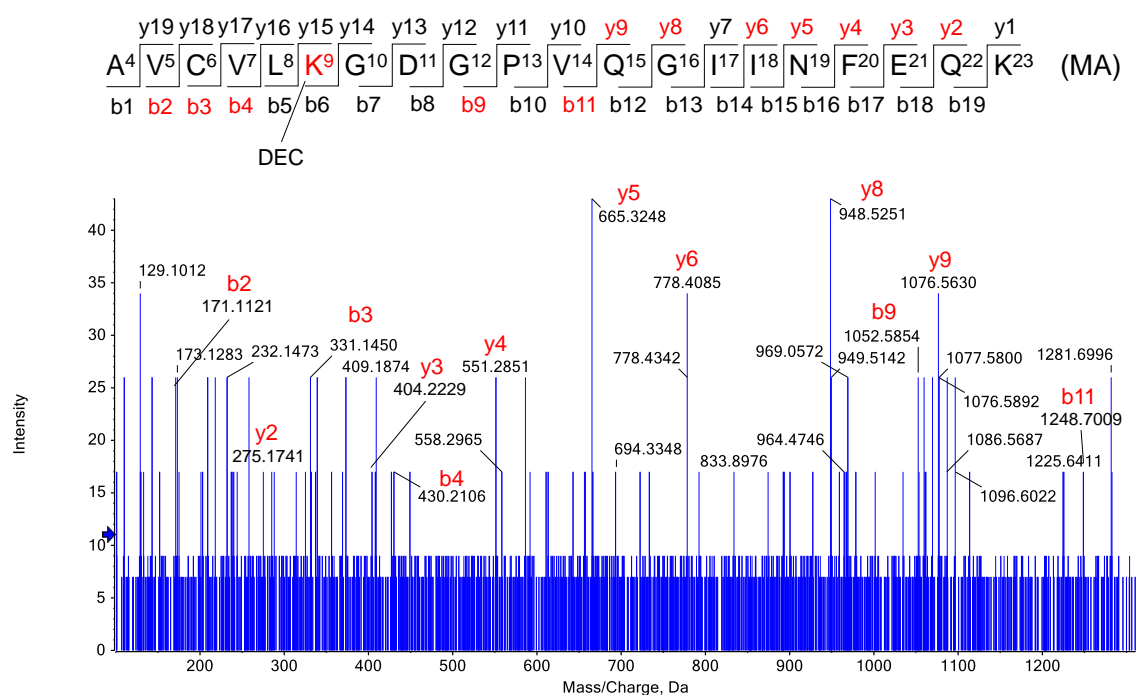


**Figure S52.** MS/MS of the peptide  $A^4VCVLKGDGPVQGIINFEQK^{23}$  modified by decadial at Lys9 by Michael Addition.



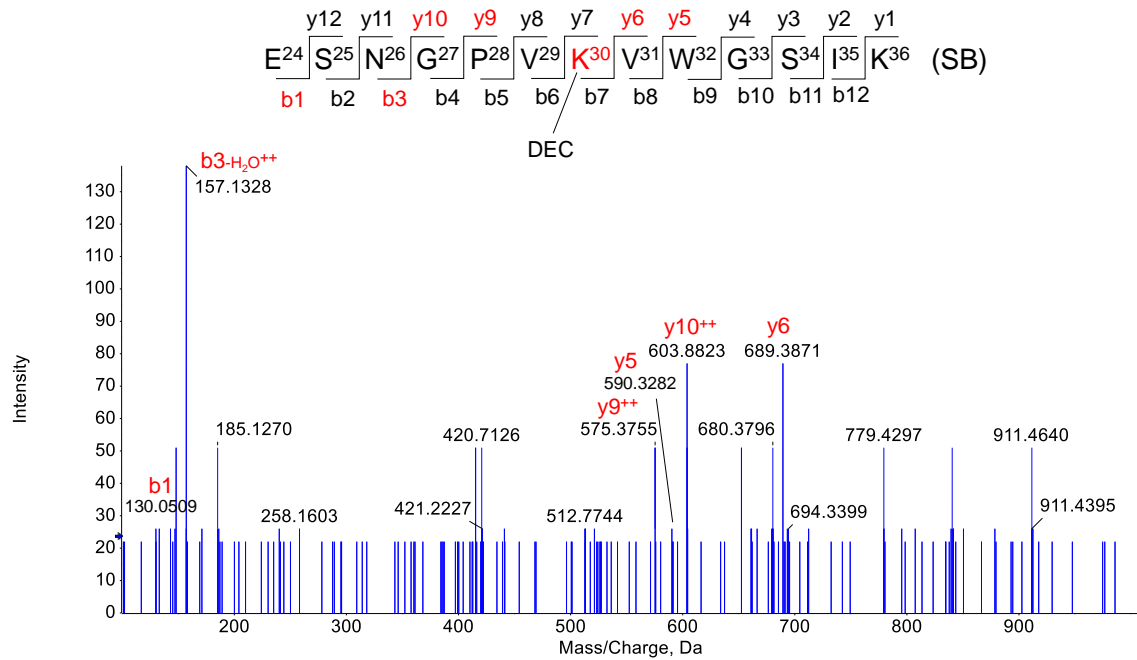


**Figure S53.** MS/MS of the peptide  $E^{24}SNGPVKVWGSIK^{36}$  modified by decadienal at Lys30 by Schiff base formation.

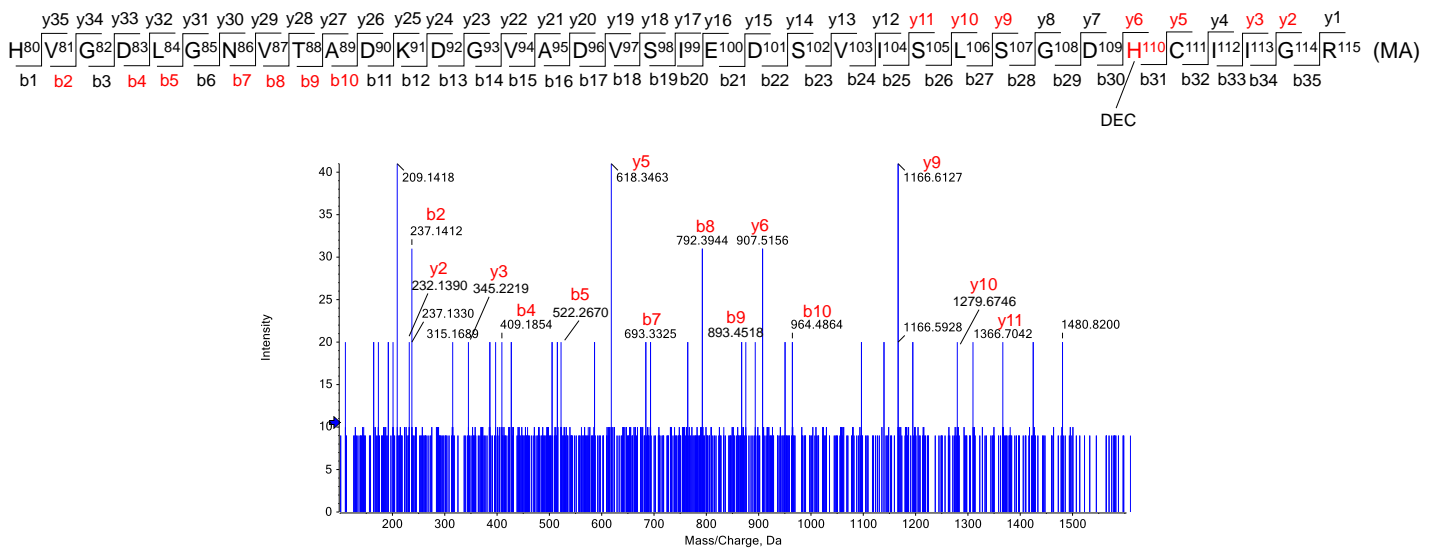


**Figure S54.** MS/MS of the peptide  $H^{80}VGDLGNVTADKDG VADVSIED SVISLSGDHCIIGR^{115}$  modified by decadienal at His110 by Michael Addition.

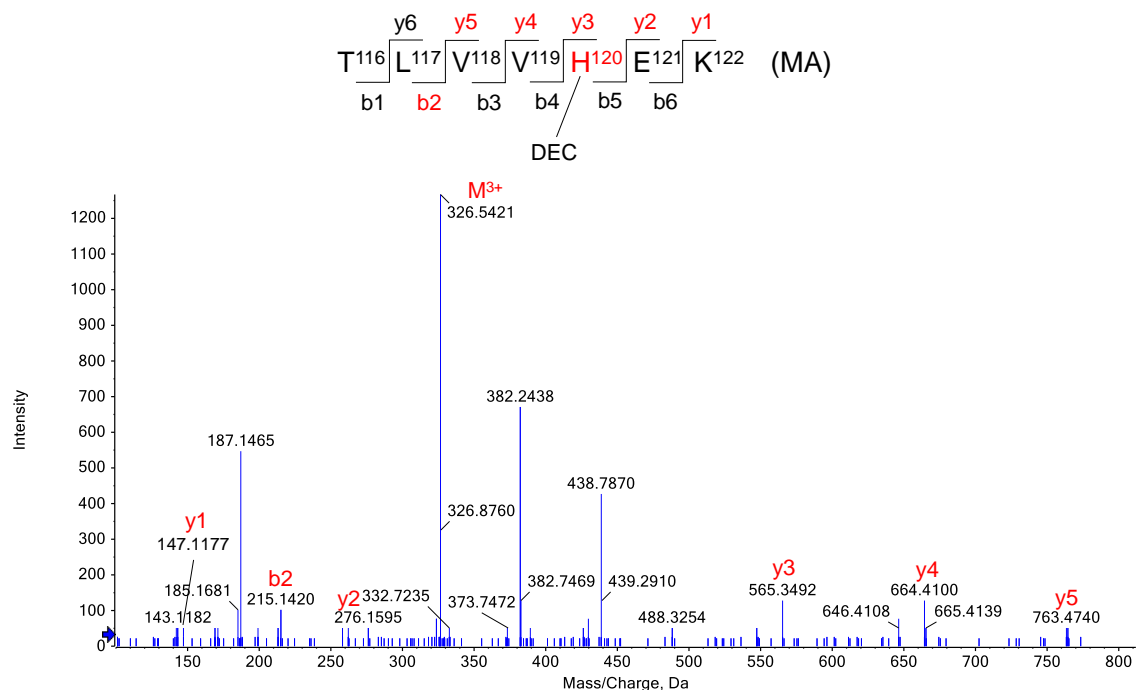


**Figure S55.** MS/MS of the peptide  $T^{116}LVVHEK^{122}$  modified by decadienal at His120 by Michael Addition.

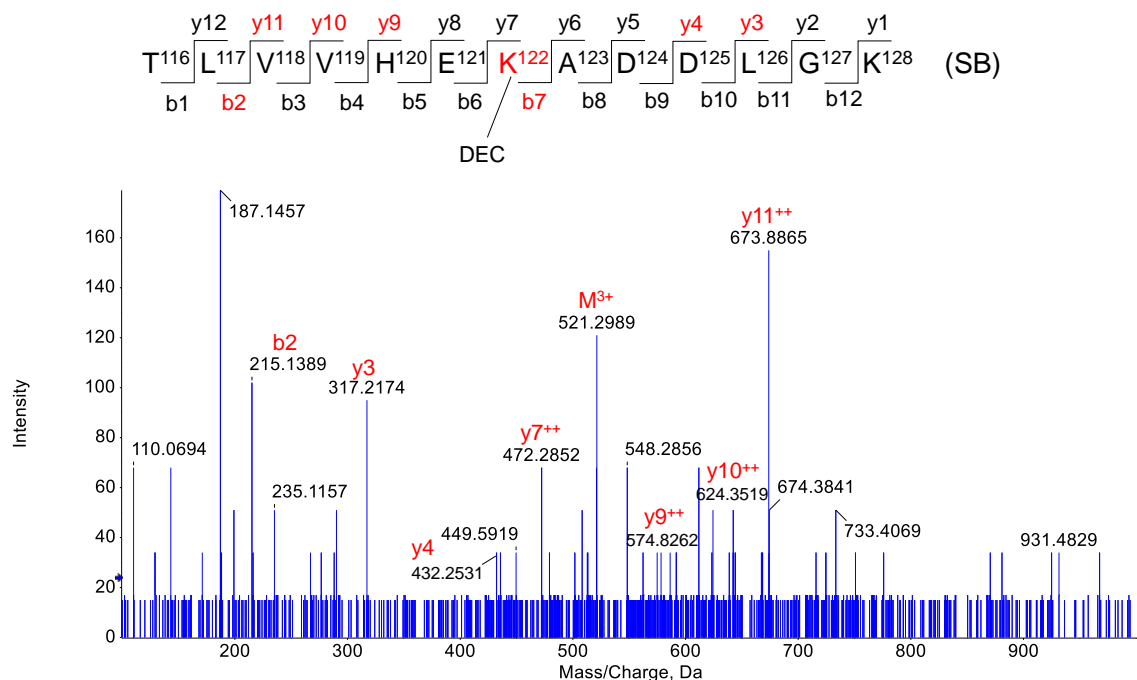


**Figure S56.** MS/MS of the peptide  $T^{116}LVVHEKADDLGK^{128}$  modified by decadienal at Lys122 by Schiff base formation.

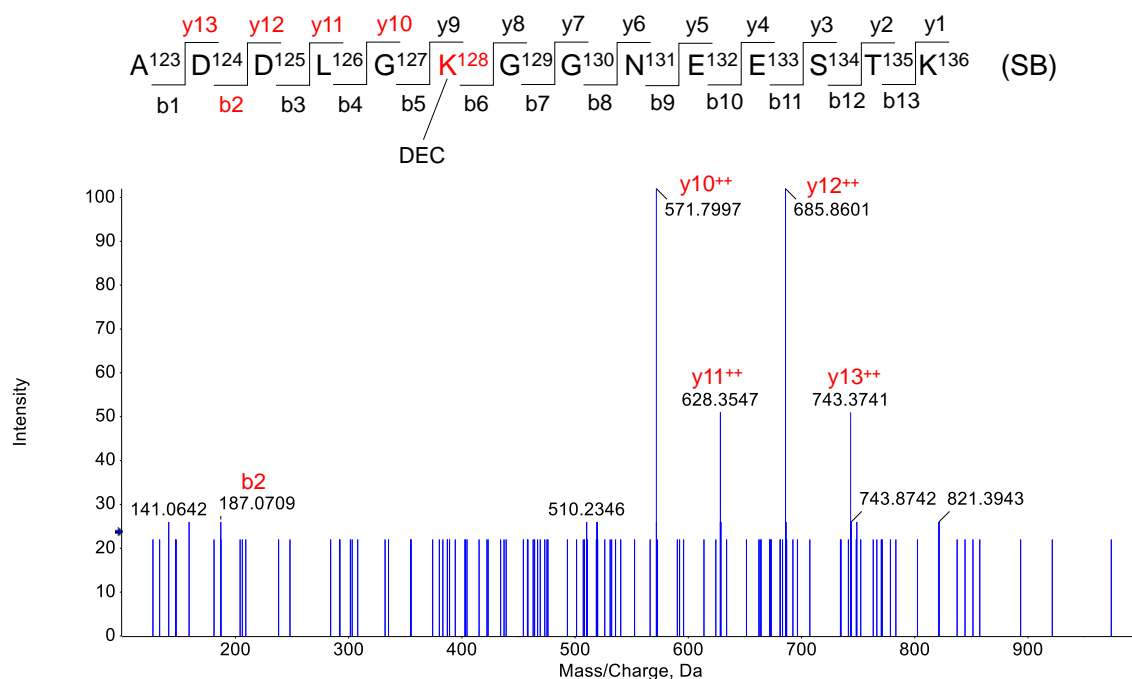


**Figure S57.** MS/MS of the peptide  $\text{A}^{123}\text{DDLGGNEESTK}^{136}$  modified by decadienal at Lys128 by Schiff base formation.

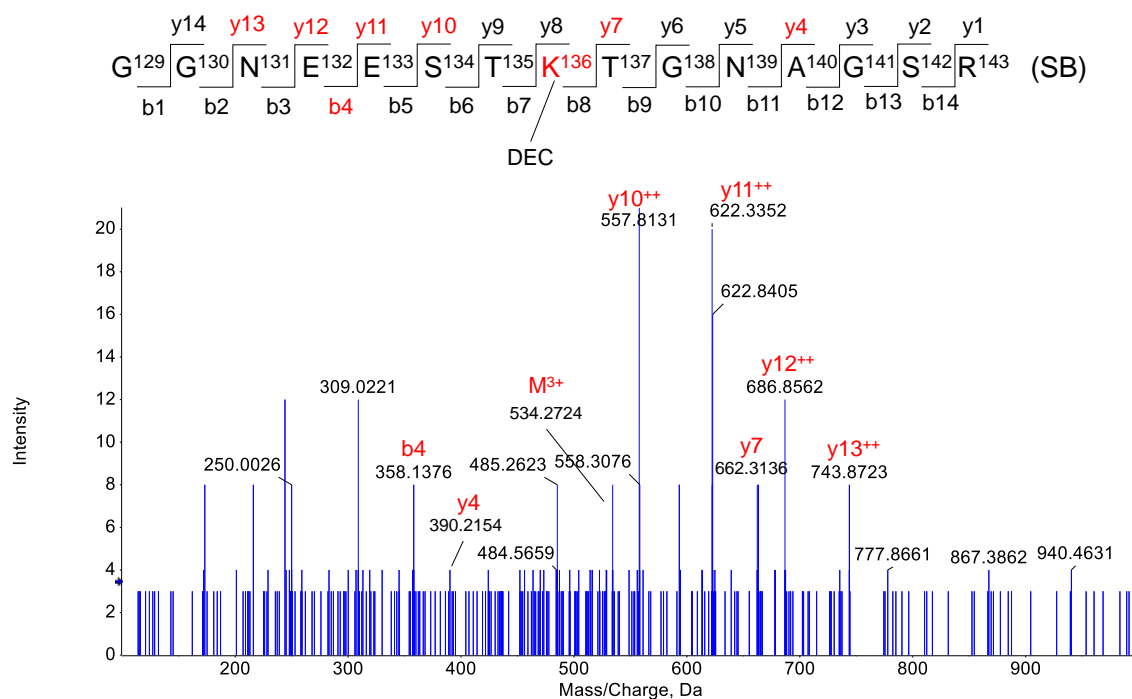


**Figure S58.** MS/MS of the peptide  $\text{G}^{129}\text{GNEESTKTGNAGSR}^{143}$  modified by decadienal at Lys136 by Schiff base formation.

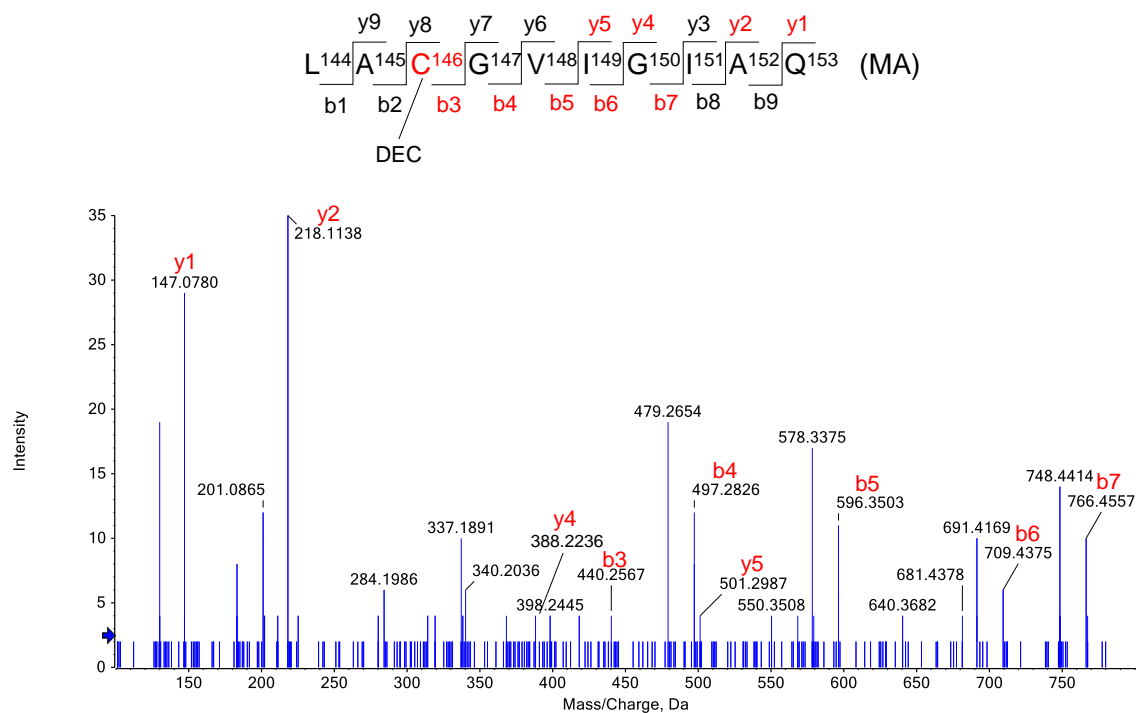


**Figure S59.** MS/MS of the peptide LACGVIGIAQ modified by decadienal at Cys146 by Michael Addition.

**Table S6.** SecoA/B-modified peptides identified by LC-MS/MS after digestion with trypsin.

Sequence	Residue	Unmodified (m/z)	Expected	Observed (Seco-A/Seco-B)	Error (ppm)
ATK*AVC'VLK	Lys3	330.5319 (3+)	464.6485 (3+)	464.6475/464.6468 (3+)	-2.1/-3.6
AVC'VLK*GDGPVQGII NFEQK	Lys9	724.7209 (3+)	858.8375 (3+)	858.8398/858.8399 (3+)	2.6/2.7
ESNGPVK*VWGSIK	Lys30	467.5893 (3+)	601.7059 (3+)	601.7057/601.7055 (3+)	-0.3/-0.6
TLVVHEK*ADDLGK	Lys122	475.5963 (3+)	609.7129 (3+)	609.7144/609.7149 (3+)	2.4/3.2
ADDLGK*GGNEESTK	Lys128	474.2232 (3+)	608.3398 (3+)	608.3398/608.3400 (3+)	0.0/0.3
GGNEESTK*TGNAGSR	Lys136	488.8940 (3+)	623.0106 (3+)	623.0132/623.0129 (3+)	4.1/3.6

SB: Schiff Base

MA: Michael Addition

\* Aldehyde adduct

' Carbamidomethyl adduct

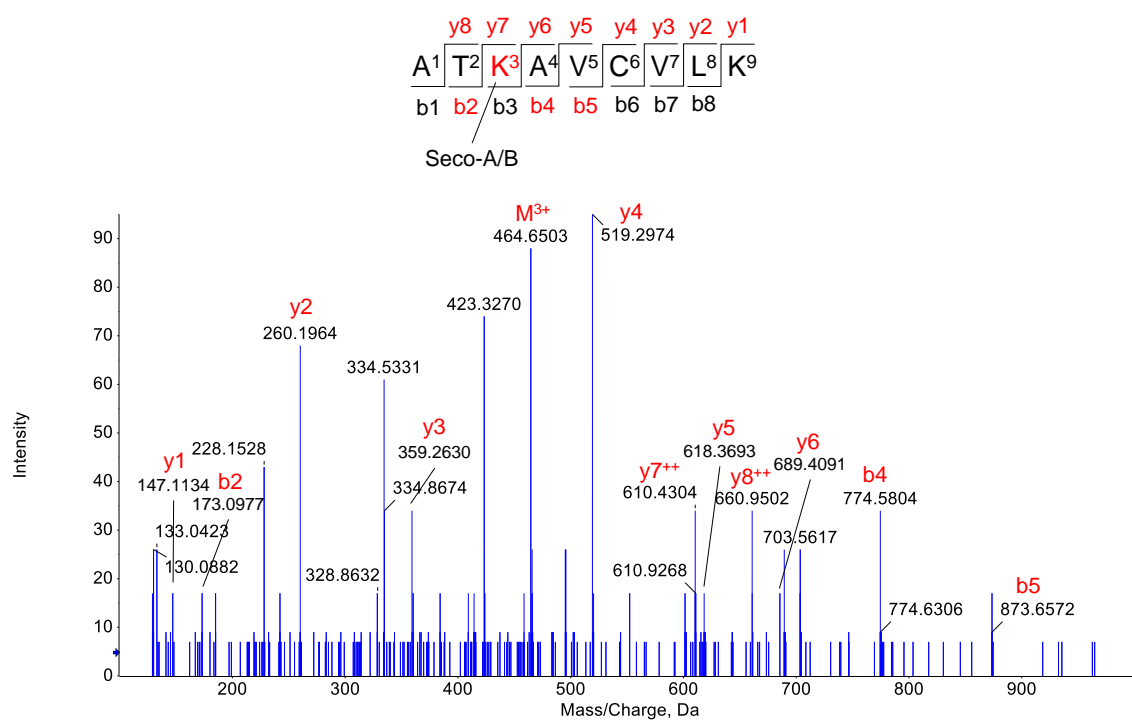


**Figure S60.** MS/MS of the peptide A<sup>1</sup>TKAVCVLK<sup>9</sup> modified by Seco-A at Lys3 by Schiff base formation.

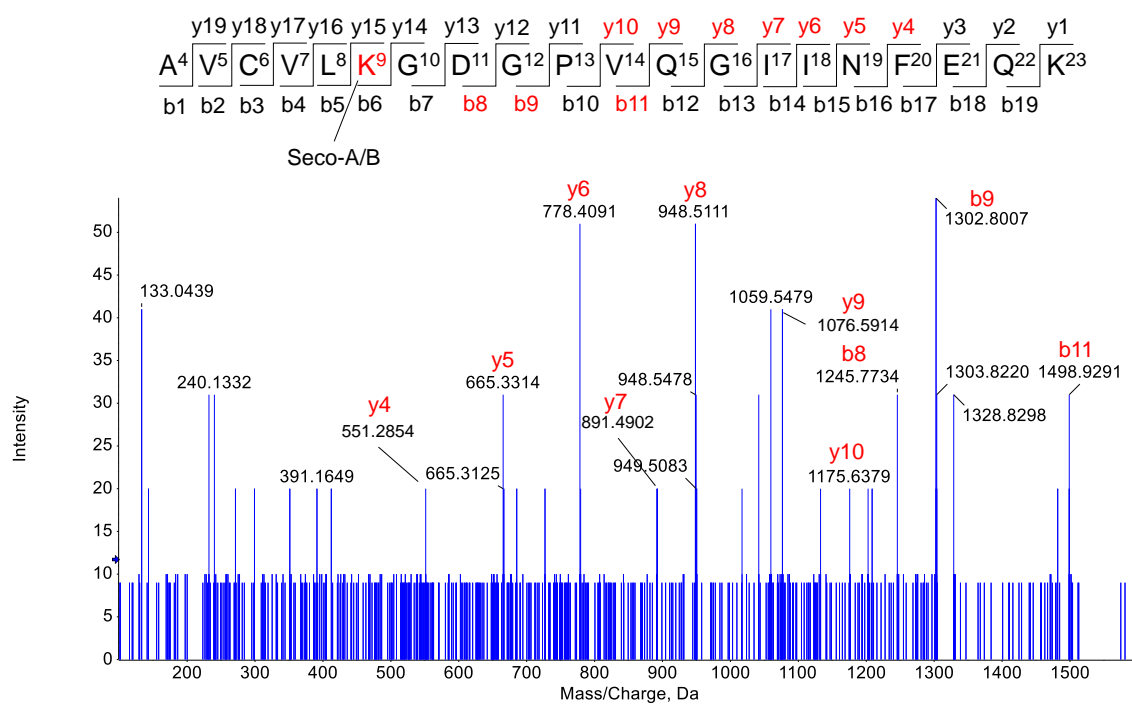


**Figure S61.** MS/MS of the peptide A<sup>4</sup>VCVLKGDGPVQGIINFEQK<sup>23</sup> modified by Seco-A at Lys9 by Schiff base formation.

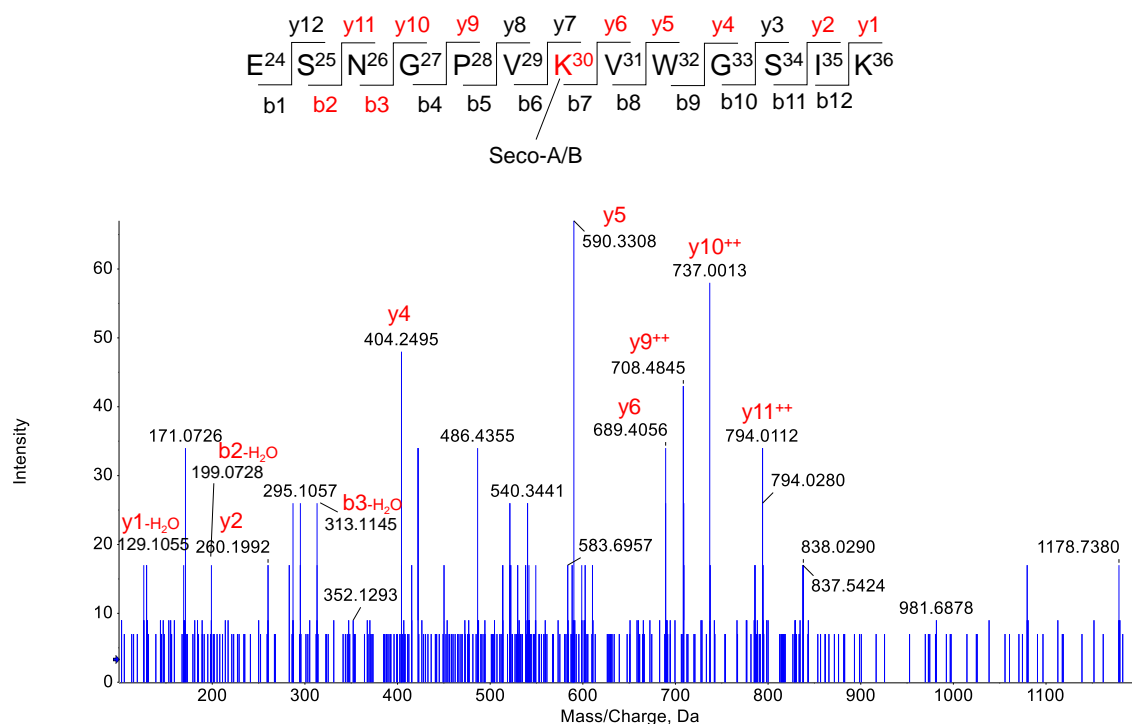


**Figure S62.** MS/MS of the peptide  $E^{24}SNGPVKVWGSIK^{36}$  modified by Seco-A at Lys30 by Schiff base formation.

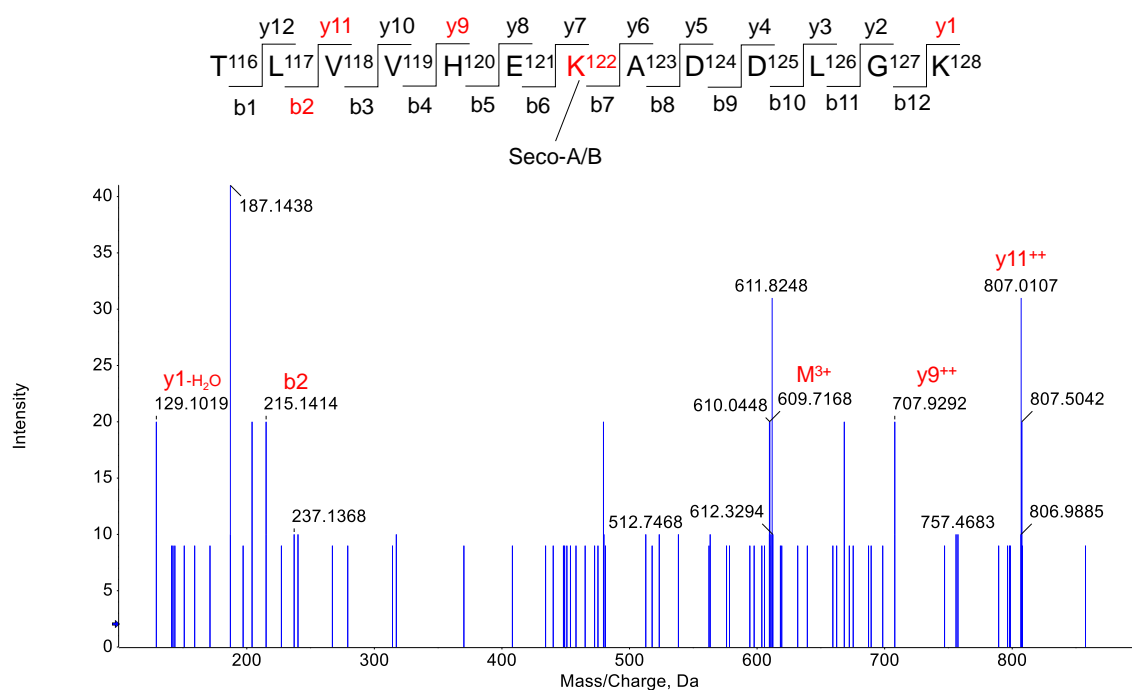


**Figure S63.** MS/MS of the peptide  $T^{116}LVVHEKADDLGK^{128}$  modified by Seco-A at Lys122 by Schiff base formation.

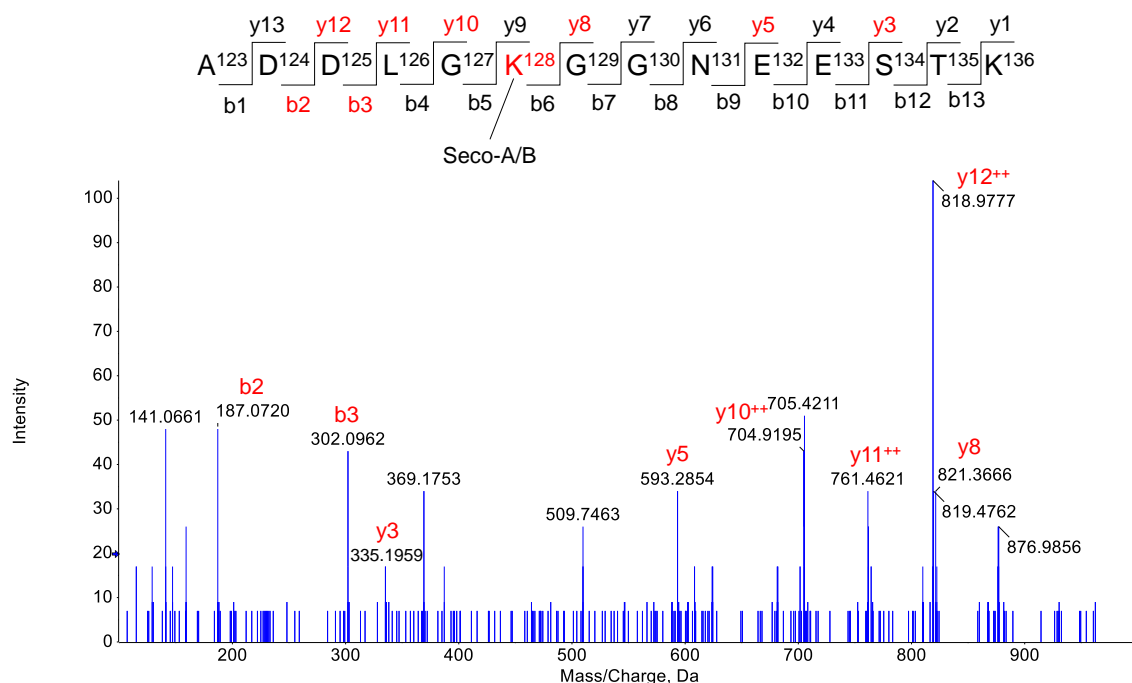


**Figure S64.** MS/MS of the peptide A<sup>123</sup>DDLGGKGNEESTK<sup>136</sup> modified by Seco-A at Lys128 by Schiff base formation.

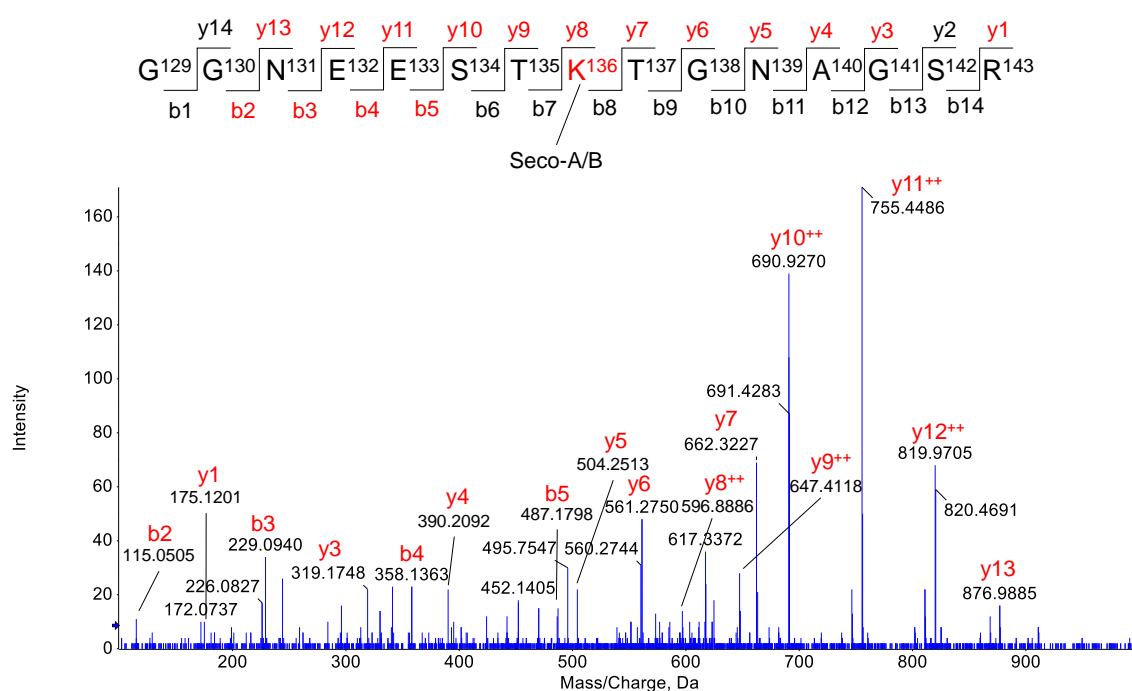


**Figure S65.** MS/MS of the peptide G<sup>129</sup>GNEESTKTGNAGSR<sup>143</sup> modified by Seco-A at Lys136 by Schiff base formation.



**Table S7a.** Covalent docking of the aldehydes with modified lysines.

				Electrostatic loop (121-142)		
	K3	K9	K30	K122	K128	K136
HHE						
HEX						
HNE						
NON						

**Table S7b.** Covalent docking of the aldehydes with modified lysines.

				Electrostatic loop (121-142)		
	K3	K9	K30	K122	K128	K136
DEC						
Seco-A						
Seco-B						

### 3. CONCLUSIONS AND FUTURE DIRECTIONS

Lipid-derived aldehydes are considered final products of lipid oxidation and are thus commonly used as biomarkers of oxidative stress. Their application has been focused on diseases involving redox pathways, such as inflammatory, metabolic and neurodegenerative diseases. Although the mechanisms leading to formation of aldehydes are not totally understood, elevated amounts of these electrophiles have been found in several tissues of patients and animal models of neurodegenerative disorders. In particular, the accumulation of lipid-derived aldehydes leading to proteins' aggregation has been suggested as direct cause and/or consequence of the neurodegenerative diseases. Thus detailed studies involving lipid aldehydes reactivity with proteins are required to better understand the role of electrophiles in the pathology of these diseases.

In the first chapter of this thesis, it was shown that secosterol aldehydes accumulate in ALS rats, suggesting elevated oxidative stress during the disease as a source of these electrophiles. In turn, secosterol aldehydes were demonstrated to covalently modify and induce aggregation of SOD1, which aggregation is directly involved in the pathology of ALS. Given that cholesterol is the most abundant lipid in the brain, secosterol aldehydes may potentially play a critical role in ALS and other neurodegenerative diseases. Additional results from chapter 1 suggest that secosterol aldehydes interaction with SOD1 may be associated with their hydrophobicity. It was then decided to test the hypothesis of whether other aldehydes modify SOD1 according to their polarities (chapter 2). The results from chapter two confirmed our hypothesis that the hydrophobicity of aldehydes is critical to the ligand-induced SOD1 aggregation. Moreover, our results highlight the elevated effect of secosterol aldehydes in SOD1 aggregation compared to other important lipid-derived electrophiles. Some of tested aldehydes, such as HHE and HNE, do not apparently affect SOD1 aggregation, although they highly modified this protein. The findings of our study also corroborate to other works which

show that SOD1 aggregation can occur when the protein is in contact with lipids and membranes.

Altogether, our results, besides presenting a possible mechanism involving lipid oxidation products and ALS, contribute to the understanding of two biochemical pathways: first, this is an additional work showing that secosterol aldehydes can play some biological effects resulting in pathological conditions. Secondly, our results help to better understand how SOD1 aggregates in presence of lipids and hydrophobic surfaces.

The future perspectives of this work may give rise to new projects in our laboratory. New approaches can be used in order to analyze the effect of secosterol aldehydes on SOD1 aggregation in some more complex environments, such as cells and animal models for ALS. Treatment of ALS model cells with secosterol aldehydes seems to be a good strategy for analyzing the induction of protein aggregation and cell viability. Furthermore, proteomics analysis of cells treated with these aldehydes could answer the question about what proteins are the main target of secosterol aldehydes. The use of alkynyl-labeled secosterol aldehydes could be an interesting strategy to select the modified proteins in a complex sample, by the use of beads that bind specifically to alkynyl groups. Another interesting experiment would be a treatment of ALS rats with a cholesterol rich diet. That would show whether the disease development would be affected by the treatment, with the possibility of quantification of oxysterols in the tissues of these animals, besides a proteomics analysis focused in identify secosterol aldehydes-modified proteins.

#### 4. REFERENCES

- [1] G.C. Burdge, P.C. Calder, Introduction to fatty acids and lipids, *World Rev. Nutr. Diet.* 112 (2015) 1–16. doi:10.1159/000365423.
- [2] H. Esterbauer, Cytotoxicity and genotoxicity of lipid-oxidation, *Am. J. Clin. Nurs.* 57 (1993) 779S–786S.
- [3] H. Yin, L. Xu, N.A. Porter, Free radical lipid peroxidation: Mechanisms and analysis, *Chem. Rev.* 111 (2011) 5944–5972. doi:10.1021/cr200084z.
- [4] A. Ayala, M.F. Muñoz, S. Argüelles, Lipid peroxidation: Production, metabolism, and signaling mechanisms of malondialdehyde and 4-hydroxy-2-nonenal, *Oxid. Med. Cell. Longev.* 2014 (2014). doi:10.1155/2014/360438.
- [5] K. Uchida, Aldehyde adducts generated during lipid peroxidation modification of proteins, *Free Radic. Res.* 49 (2015) 896–904. doi:10.3109/10715762.2015.1036052.
- [6] A. Moghe, S. Ghare, B. Lamoreau, M. Mohammad, S. Barve, C. McClain, S. Joshi-Barve, Molecular mechanisms of acrolein toxicity: Relevance to human disease, *Toxicol. Sci.* 143 (2015) 242–255. doi:10.1093/toxsci/kfu233.
- [7] D. Del Rio, A.J. Stewart, N. Pellegrini, A review of recent studies on malondialdehyde as toxic molecule and biological marker of oxidative stress, *Nutr. Metab. Cardiovasc. Dis.* 15 (2005) 316–328. doi:10.1016/j.numecd.2005.05.003.
- [8] E.K. Long, M.J. Picklo, Trans-4-hydroxy-2-hexenal, a product of n-3 fatty acid peroxidation: Make some room HNE..., *Free Radic. Biol. Med.* 49 (2010) 1–8. doi:10.1016/j.freeradbiomed.2010.03.015.
- [9] K. Uchida, 4-Hydroxy-2-nonenal: A product and mediator of oxidative stress, *Prog. Lipid Res.* 42 (2003) 318–343. doi:10.1016/S0163-7827(03)00014-6.
- [10] T.I. Williams, B.C. Lynn, W.R. Markesbery, M.A. Lovell, Increased levels of 4-hydroxynonenal and acrolein, neurotoxic markers of lipid peroxidation, in the brain in Mild Cognitive Impairment and early Alzheimer's disease, *Neurobiol. Aging.* 27 (2006) 1094–1099. doi:10.1016/j.neurobiolaging.2005.06.004.
- [11] P.R. Angelova, M.H. Horrocks, D. Klenerman, S. Gandhi, A.Y. Abramov, M.S. Shchepinov, Lipid peroxidation is essential for  $\alpha$ -synuclein-induced cell death, *J. Neurochem.* 133 (2015) 582–589. doi:10.1111/jnc.13024.
- [12] Z. Qin, D. Hu, S. Han, S.H. Reaney, D.A. Di Monte, A.L. Fink, Effect of 4-hydroxy-2-nonenal modification on  $\alpha$ -synuclein aggregation, *J. Biol. Chem.* 282 (2007) 5862–5870. doi:10.1074/jbc.M608126200.
- [13] E.-J. Bae, D.-H. Ho, E. Park, J.W. Jung, K. Cho, J.H. Hong, H.-J. Lee, K.P. Kim, S.-J. Lee, Lipid Peroxidation Product 4-Hydroxy-2-Nonenal Promotes Seeding-Capable Oligomer Formation and Cell-to-Cell Transfer of  $\alpha$ -Synuclein, *Antioxid. Redox Signal.* 18 (2013) 770–783. doi:10.1089/ars.2011.4429.
- [14] A. Ambaw, L. Zheng, M.A. Tambe, K.E. Strathearn, G. Acosta, S.A. Hubers, F. Liu, S.A. Herr, J. Tang, A. Truong, E. Walls, A. Pond, J.-C. Rochet, R. Shi, Acrolein-mediated neuronal cell death and alpha-synuclein aggregation: Implications for

- Parkinson's disease, *Mol. Cell. Neurosci.* 88 (2018) 70–82.  
doi:10.1016/j.mcn.2018.01.006.
- [15] M.I. Ellis G, Fang E, Maheshwari M, Roltsch E, Holcomb L, Zimmer D, Martinez D, Lipid oxidation and modification of amyloid- $\beta$  (A $\beta$ ) in vitro and in vivo., *J Alzheimers Dis.* 22(2) (2010) 593–607.
  - [16] K. Uchida, M. Kanematsu, Y. Morimitsu, T. Osawa, N. Noguchi, E. Niki, Acrolein Is a Product of Lipid Peroxidation Reaction, *J. Biol. Chem.* 273 (1998) 16058–16066.  
doi:10.1074/jbc.273.26.16058.
  - [17] H. Esterbauer, R.J. Schaur, H. Zollner, Chemistry and biochemistry of 4-hydroxynonenal, malonaldehyde and related aldehydes, *Free Radic. Biol. Med.* 11 (1991) 81–128. doi:10.1016/0891-5849(91)90192-6.
  - [18] J.F. Stevens, C.S. Maier, Acrolein: Sources, metabolism, and biomolecular interactions relevant to human health and disease, *Mol. Nutr. Food Res.* 52 (2008) 7–25.  
doi:10.1002/mnfr.200700412.
  - [19] M. Griesser, W.E. Boeglin, T. Suzuki, C. Schneider, Convergence of the 5-LOX and COX-2 pathways: heme-catalyzed cleavage of the 5S-HETE-derived di-endoperoxide into aldehyde fragments., *J. Lipid Res.* 50 (2009) 2455–62. doi:10.1194/jlr.M900181-JLR200.
  - [20] J. Korbecki, I. Baranowska-Bosiacka, I. Gutowska, D. Chlubek, Cyclooxygenase pathways, *Acta Biochim. Pol.* 61 (2014) 639–649.
  - [21] E.K. Long, M.J. Picklo, Trans-4-hydroxy-2-hexenal, a product of n-3 fatty acid peroxidation: Make some room HNE..., *Free Radic. Biol. Med.* 49 (2010) 1–8.  
doi:10.1016/j.freeradbiomed.2010.03.015.
  - [22] S.L. Van Lier JE, Autoxidation of cholesterol via hydroperoxide intermediates., *J Org Chem.* 35 (1970) 2627–32.
  - [23] A.W. Girotti, T. Kriska, Role of Lipid Hydroperoxides in Photo-Oxidative Stress Signaling, *Antioxid. Redox Signal.* 6 (2004) 301–310.  
doi:10.1089/152308604322899369.
  - [24] W. Kulig, L. Cwiklik, P. Jurkiewicz, T. Rog, I. Vattulainen, Cholesterol oxidation products and their biological importance, *Chem. Phys. Lipids.* 199 (2016) 144–160.  
doi:10.1016/j.chemphyslip.2016.03.001.
  - [25] I. Björkhem, G. Eggertsen, Genes involved in initial steps of bile acid synthesis., *Curr. Opin. Lipidol.* 12 (2001) 97–103. doi:10.1097/00041433-200104000-00002.
  - [26] I.A. Pikuleva, cytochromes P450 : implications, (2008) 1403–1414.
  - [27] D.M.P. Uemi M, Ronsein GE, Miyamoto S, Medeiros MH, Generation of cholesterol carboxyaldehyde by the reaction of singlet molecular oxygen [ $O_2$  (1 $\Delta$ (g))] as well as ozone with cholesterol., *Chem Res Toxicol.* 22 (2009) 875–84.
  - [28] L. Iuliano, Pathways of cholesterol oxidation via non-enzymatic mechanisms, *Chem. Phys. Lipids.* 164 (2011) 457–468. doi:10.1016/j.chemphyslip.2011.06.006.
  - [29] A.W. Girotti, Photosensitized oxidation of membrane lipids: Reaction pathways, cytotoxic effects, and cytoprotective mechanisms, *J. Photochem. Photobiol. B Biol.* 63 (2001) 103–113. doi:10.1016/S1011-1344(01)00207-X.

- [30] W. Korytowski, a W. Girotti, Singlet oxygen adducts of cholesterol: photogeneration and reductive turnover in membrane systems., *Photochem. Photobiol.* 70 (1999) 484–489.
- [31] A.D. Wentworth, B.-D. Song, J. Nieva, A. Shafton, S. Tripurenani, P. Wentworth Jr., The ratio of cholesterol 5,6-secoosterols formed from ozone and singlet oxygen offers insight into the oxidation of cholesterol in vivo, *Chem. Commun.* (2009) 3098. doi:10.1039/b821584g.
- [32] S. Tomono, N. Miyoshi, H. Shiokawa, T. Iwabuchi, Y. Aratani, T. Higashi, H. Nukaya, H. Ohshima, Formation of cholesterol ozonolysis products in vitro and in vivo through a myeloperoxidase-dependent pathway, *J. Lipid Res.* 52 (2011) 87–97. doi:10.1194/jlr.M006775.
- [33] P.D. Brinkhorst J, Nara SJ, Hock cleavage of cholesterol 5alpha-hydroperoxide: an ozone-free pathway to the cholesterol ozonolysis products identified in arterial plaque and brain tissue., *J Am Chem Soc.* 130 (2008) 12224–5.
- [34] M. Uemi, G.E. Ronsein, S. Miyamoto, M.H.G. Medeiros, P. Di Mascio, Generation of cholesterol carboxyaldehyde by the reaction of singlet molecular oxygen [O<sub>2</sub> (1Delta(g))] as well as ozone with cholesterol., *Chem. Res. Toxicol.* 22 (2009) 875–84. doi:10.1021/tx800447b.
- [35] Z.A.M. Zielinski, D.A. Pratt, Cholesterol Autoxidation Revisited: Debunking the Dogma Associated with the Most Vilified of Lipids, *J. Am. Chem. Soc.* 138 (2016) 6932–6935. doi:10.1021/jacs.6b03344.
- [36] K. Usui, J.D. Hulleman, J.F. Paulsson, S.J. Siegel, E.T. Powers, J.W. Kelly, Site-specific modification of Alzheimer's peptides by cholesterol oxidation products enhances aggregation energetics and neurotoxicity., *Proc. Natl. Acad. Sci. U. S. A.* 106 (2009) 18563–8. doi:10.1073/pnas.0804758106.
- [37] J.C. Scheinost, H. Wang, G.E. Boldt, J. Offer, P. Wentworth, Cholesterol seco-sterol-induced aggregation of methylated amyloid-β peptides - Insights into aldehyde-initiated fibrillization of amyloid-β, *Angew. Chemie - Int. Ed.* 47 (2008) 3919–3922. doi:10.1002/anie.200705922.
- [38] J. Bieschke, Q. Zhang, E.T. Powers, R.A. Lerner, J.W. Kelly, Oxidative metabolites accelerate Alzheimer's amyloidogenesis by a two-step mechanism, eliminating the requirement for nucleation, *Biochemistry.* 44 (2005) 4977–4983. doi:10.1021/bi0501030.
- [39] Q. Zhang, E.T. Powers, J. Nieva, M.E. Huff, M.A. Dendle, J. Bieschke, C.G. Glabe, A. Eschenmoser, P. Wentworth, R.A. Lerner, J.W. Kelly, Metabolite-initiated protein misfolding may trigger Alzheimer's disease., *Proc. Natl. Acad. Sci. U. S. A.* 101 (2004) 4752–7. doi:10.1073/pnas.0400924101.
- [40] D. a Bosco, D.M. Fowler, Q. Zhang, J. Nieva, E.T. Powers, P. Wentworth, R. a Lerner, J.W. Kelly, Elevated levels of oxidized cholesterol metabolites in Lewy body disease brains accelerate alpha-synuclein fibrilization., *Nat. Chem. Biol.* 2 (2006) 249–253. doi:10.1038/nchembio782.
- [41] N.K. Cygan, J.C. Scheinost, T.D. Butters, P. Wentworth, Adduction of cholesterol 5,6-seco-sterol aldehyde to membrane-bound myelin basic protein exposes an

- immunodominant epitope, *Biochemistry*. 50 (2011) 2092–2100. doi:10.1021/bi200109q.
- [42] H.G. Stewart CR, Wilson LM, Zhang Q, Pham CL, Waddington LJ, Staples MK, Stapleton D, Kelly JW, Oxidized cholesterol metabolites found in human atherosclerotic lesions promote apolipoprotein C-II amyloid fibril formation., *Biochemistry*. (2007) 5552–5561.
- [43] Y.-L. Lai, S. Tomono, N. Miyoshi, H. Ohshima, Inhibition of endothelial- and neuronal-type, but not inducible-type, nitric oxide synthase by the oxidized cholesterol metabolite secosterol aldehyde: Implications for vascular and neurodegenerative diseases, *J. Clin. Biochem. Nutr.* 50 (2011) 84–89. doi:10.3164/jcbrn.11-31.
- [44] J. Nieva, B.D. Song, J.K. Rogel, D. Kujawara, L. Altobel, A. Izharrudin, G.E. Boldt, R.K. Grover, A.D. Wentworth, P. Wentworth, Cholesterol secosterol aldehydes induce amyloidogenesis and dysfunction of wild-type tumor protein p53, *Chem. Biol.* 18 (2011) 920–927. doi:10.1016/j.chembiol.2011.02.018.
- [45] E. Wachtel, D. Bach, R.F. Epand, A. Tishbee, R.M. Epand, A product of ozonolysis of cholesterol alters the biophysical properties of phosphatidylethanolamine membranes, *Biochemistry*. 45 (2006) 1345–1351. doi:10.1021/bi0516778.
- [46] T.C. Genaro-Mattos, P.P. Appolinário, K.C.U. Mugnol, C. Bloch, I.L. Nantes, P. Di Mascio, S. Miyamoto, Covalent binding and anchoring of cytochrome c to mitochondrial mimetic membranes promoted by cholesterol carboxyaldehyde, *Chem. Res. Toxicol.* 26 (2013) 1536–1544. doi:10.1021/tx4002385.
- [47] K. Windsor, T.C. Genaro-Mattos, S. Miyamoto, D.F. Stec, H.Y.H. Kim, K.A. Tallman, N.A. Porter, Assay of protein and peptide adducts of cholesterol ozonolysis products by hydrophobic and click enrichment methods, *Chem. Res. Toxicol.* 27 (2014) 1757–1768. doi:10.1021/tx500229h.
- [48] M.C. Kiernan, S. Vucic, B.C. Cheah, M.R. Turner, A. Eisen, O. Hardiman, J.R. Burrell, M.C. Zoning, Amyotrophic lateral sclerosis, *Lancet*. 377 (2011) 942–955. doi:10.1016/S0140-6736(10)61156-7.
- [49] P.N. Leigh, L.C. Wijesekera, Motor neuron disease: Focusing the mind on ALS: updated practice parameters, *Nat. Rev. Neurol.* 6 (2010) 191–192. doi:10.1038/nrneurol.2010.33.
- [50] H. Deng, A. Hentati, J. Tainer, Z. Iqbal, A. Cayabyab, W. Hung, E. Getzoff, P. Hu, B. Herzfeldt, R. Roos, A. Et, Amyotrophic lateral sclerosis and structural defects in Cu,Zn superoxide dismutase, *Science* (80-. ). 261 (1993) 1047–1051. doi:10.1126/science.8351519.
- [51] J. Sreedharan, I.P. Blair, V.B. Tripathi, X. Hu, C. Vance, B. Rogelj, S. Ackerley, J.C. Durnall, K.L. Williams, E. Buratti, F. Baralle, J. de Bellerocche, J.D. Mitchell, P.N. Leigh, A. Al-Chalabi, C.C. Miller, G. Nicholson, C.E. Shaw, TDP-43 mutations in familial and sporadic amyotrophic lateral sclerosis., *Science*. 319 (2008) 1668–72. doi:10.1126/science.1154584.
- [52] M.B. Yim, J.H. Kang, H.S. Yim, H.S. Kwak, P.B. Chock, E.R. Stadtman, A gain-of-function of an amyotrophic lateral sclerosis-associated Cu,Zn-superoxide dismutase mutant: An enhancement of free radical formation due to a decrease in  $K_m$  for hydrogen peroxide, *Proc. Natl. Acad. Sci. U. S. A.* 93 (1996) 5709–5714.



doi:10.1073/pnas.93.12.5709.

- [53] W.A. Pryor, G.L. Squadrito, The chemistry of peroxynitrite: a product from the reaction of nitric oxide with superoxide, *Am J Physiol.* 268 (1995) L699-722. doi:10.1152/ajplung.1995.268.5.L699.
- [54] S. Miyamoto, G.R. Martinez, A.P.B. Martins, M.H.G. Medeiros, P. Di Mascio, Direct Evidence of Singlet Molecular Oxygen [  $O_2(1\Delta g)$  ] Production in the Reaction of Linoleic Acid Hydroperoxide with Peroxynitrite, 2 (2003) 4510–4517.
- [55] J. Magrané, G. Manfredi, Mitochondrial Function, Morphology, and Axonal Transport in Amyotrophic Lateral Sclerosis, *Antioxid. Redox Signal.* 11 (2009) 1615–1626. doi:10.1089/ars.2009.2604.
- [56] D. Bonnefont-Rousselot, L. Lacomblez, M. Jaudon, S. Lepage, F. Salachas, G. Bensimon, C. Bizard, V. Doppler, J. Delattre, V. Meininger, Blood oxidative stress in amyotrophic lateral sclerosis., *J. Neurol. Sci.* 178 (2000) 57–62. doi:S0022510X00003658 [pii].
- [57] A. Baillet, V. Chantepedrix, C. Trocmé, P. Casez, C. Garrel, G. Besson, The role of oxidative stress in amyotrophic lateral sclerosis and Parkinson's disease, *Neurochem. Res.* 35 (2010) 1530–1537. doi:10.1007/s11064-010-0212-5.
- [58] J.S. Valentine, P.A. Doucette, S. Zittin Potter, Copper-Zinc Superoxide Dismutase and Amyotrophic Lateral Sclerosis, *Annu. Rev. Biochem.* 74 (2005) 563–593. doi:10.1146/annurev.biochem.72.121801.161647.
- [59] R. Rakhit, P. Cunningham, A. Furtos-Matei, S. Dahan, X.F. Qi, J.P. Crow, N.R. Cashman, L.H. Kondejewski, A. Chakrabartty, Oxidation-induced misfolding and aggregation of superoxide dismutase and its implications for amyotrophic lateral sclerosis, *J. Biol. Chem.* 277 (2002) 47551–47556. doi:10.1074/jbc.M207356200.
- [60] Y.J. Kim, R. Nakatomi, T. Akagi, T. Hashikawa, R. Takahashi, Unsaturated fatty acids induce cytotoxic aggregate formation of amyotrophic lateral sclerosis-linked superoxide dismutase 1 mutants, *J. Biol. Chem.* 280 (2005) 21515–21521. doi:10.1074/jbc.M502230200.
- [61] L. Banci, I. Bertini, M. Boca, S. Girotto, M. Martinelli, J.S. Valentine, M. Vieru, SOD1 and amyotrophic lateral sclerosis: Mutations and oligomerization, *PLoS One.* 3 (2008) 1–8. doi:10.1371/journal.pone.0001677.
- [62] L. Banci, I. Bertini, A. Durazo, S. Girotto, E.B. Gralla, M. Martinelli, J.S. Valentine, M. Vieru, J.P. Whitelegge, Metal-free superoxide dismutase forms soluble oligomers under physiological conditions: a possible general mechanism for familial ALS., *Proc. Natl. Acad. Sci. U. S. A.* 104 (2007) 11263–11267. doi:10.1073/pnas.0704307104.
- [63] L. Banci, I. Bertini, M. Boca, V. Calderone, F. Cantini, S. Girotto, M. Vieru, Structural and dynamic aspects related to oligomerization of apo SOD1 and its mutants., *Proc. Natl. Acad. Sci. U. S. A.* 106 (2009) 6980–6985. doi:10.1073/pnas.0809845106.
- [64] G. De Franceschi, E. Frare, L. Bubacco, S. Mammi, A. Fontana, P.P. de Laureto, Molecular Insights into the Interaction between  $\alpha$ -Synuclein and Docosahexaenoic Acid, *J. Mol. Biol.* 394 (2009) 94–107. doi:10.1016/j.jmb.2009.09.008.
- [65] I. Choi, H.D. Song, S. Lee, Y.I. Yang, J.H. Nam, S.J. Kim, J.J. Sung, T. Kang, J. Yi,

- Direct observation of defects and increased ion permeability of a membrane induced by structurally disordered cu/zn-superoxide dismutase aggregates, *PLoS One*. 6 (2011) 1–10. doi:10.1371/journal.pone.0028982.
- [66] P.P. Appolinário, D.B. Medinas, A.B. Chaves-Filho, T.C. Genaro-Mattos, J.R.R. Cussiol, L.E.S. Netto, O. Augusto, S. Miyamoto, Oligomerization of Cu,Zn-superoxide dismutase (SOD1) by Docosahexaenoic acid and its hydroperoxides in vitro: Aggregation dependence on fatty acid unsaturation and thiols, *PLoS One*. 10 (2015) 1–15. doi:10.1371/journal.pone.0125146.
- [67] R.M. Adibhatla, J.F. Hatcher, Role of lipids in brain injury and diseases, *Future Lipidol*. 2 (2007) 403–422. doi:10.2217/17460875.2.4.403.
- [68] B.A. Tsui-Pierchala, M. Encinas, J. Milbrandt, E.M. Johnson, Lipid rafts in neuronal signaling and function, *Trends Neurosci*. 25 (2002) 412–417. doi:10.1016/S0166-2236(02)02215-4.
- [69] R.S. Yadav, N.K. Tiwari, Lipid Integration in Neurodegeneration: An Overview of Alzheimer's Disease, *Mol. Neurobiol*. 50 (2014) 168–176. doi:10.1007/s12035-014-8661-5.
- [70] A.H. Bhat, K.B. Dar, S. Anees, M.A. Zargar, A. Masood, M.A. Sofi, S.A. Ganie, Oxidative stress, mitochondrial dysfunction and neurodegenerative diseases; a mechanistic insight, *Biomed. Pharmacother*. 74 (2015) 101–110. doi:10.1016/j.biopha.2015.07.025.
- [71] R. Thanan, S. Oikawa, Y. Hiraku, S. Ohnishi, N. Ma, S. Pinlaor, P. Yongvanit, S. Kawanishi, M. Murata, Oxidative stress and its significant roles in neurodegenerative diseases and cancer, *Int. J. Mol. Sci*. 16 (2014) 193–217. doi:10.3390/ijms16010193.
- [72] N.A. Simonian, J.T. Coyle, Oxidative Stress in Neurodegenerative Diseases, *Annu. Rev. Pharmacol. Toxicol*. 36 (1996) 83–106. doi:10.1089/ars.2006.8.1971.
- [73] E. Mariani, M.C. Polidori, A. Cherubini, P. Mecocci, Oxidative stress in brain aging, neurodegenerative and vascular diseases: An overview, *J. Chromatogr. B Anal. Technol. Biomed. Life Sci*. 827 (2005) 65–75. doi:10.1016/j.jchromb.2005.04.023.
- [74] R. Sultana, M. Perluigi, D.A. Butterfield, Lipid peroxidation triggers neurodegeneration: A redox proteomics view into the Alzheimer disease brain, *Free Radic. Biol. Med*. 62 (2013) 157–169. doi:10.1016/j.freeradbiomed.2012.09.027.
- [75] L.T. McGrath, B.M. McGleenon, S. Brennan, D. McColl, S. McILroy, a P. Passmore, Increased oxidative stress in Alzheimer's disease as assessed with 4-hydroxynonenal but not malondialdehyde., *QJM*. 94 (2001) 485–490. doi:10.1093/qjmed/94.9.485.
- [76] M.A. Lovell, C. Xie, W.R. Markesbery, Acrolein is increased in Alzheimer's disease brain and is toxic to primary hippocampal cultures, *Neurobiol. Aging*. 22 (2001) 187–194. doi:10.1016/S0197-4580(00)00235-9.
- [77] a Yoritaka, N. Hattori, K. Uchida, M. Tanaka, E.R. Stadtman, Y. Mizuno, Immunohistochemical detection of 4-hydroxynonenal protein adducts in Parkinson disease., *Proc. Natl. Acad. Sci. U. S. A*. 93 (1996) 2696–2701. doi:10.1073/pnas.93.7.2696.
- [78] R.J. Castellani, G. Perry, S.L. Siedlak, A. Nunomura, L.M. Sayre, M.A. Smith, Hydroxynonenal adducts indicate a role for lipid peroxidation in neocortical and

- brainstem Lewy bodies in humans, 319 (2002) 25–28.
- [79] J. Agar, H. Durham, Relevance of oxidative injury in the pathogenesis of motor neuron diseases, *Amyotroph. Lateral Scler. Other Mot. Neuron Disord.* 4 (2003) 232–242. doi:10.1080/14660820310011278.
  - [80] E.P. Simpson, Y.K. Henry, J.S. Henkel, R.G. Smith, S.H. Appel, Increased lipid peroxidation in sera of ALS patients A potential biomarker of disease burden, 41303 (2004).
  - [81] M. Perluigi, H.F. Poon, K. Hensley, W.M. Pierce, J.B. Klein, V. Calabrese, C. De Marco, D.A. Butterfield, Proteomic analysis of 4-hydroxy-2-nonenal-modified proteins in G93A-SOD1 transgenic mice - A model of familial amyotrophic lateral sclerosis, *Free Radic. Biol. Med.* 38 (2005) 960–968. doi:10.1016/j.freeradbiomed.2004.12.021.
  - [82] N. Shibata, S. Yamada, K. Uchida, A. Hirano, S. Sakoda, H. Fujimura, S. Sasaki, M. Iwata, S. Toi, M. Kawaguchi, T. Yamamoto, M. Kobayashi, Accumulation of protein-bound 4-hydroxy-2-hexenal in spinal cords from patients with sporadic amyotrophic lateral sclerosis, *Brain Res.* 1019 (2004) 170–177. doi:10.1016/j.brainres.2004.05.110.
  - [83] Y. Cai, C. Lendel, L. Österlund, A. Kasrayan, L. Lannfelt, M. Ingelsson, F. Nikolajeff, M. Karlsson, J. Bergström, Changes in secondary structure of  $\alpha$ -synuclein during oligomerization induced by reactive aldehydes, *Biochem. Biophys. Res. Commun.* 464 (2015) 336–341. doi:10.1016/j.bbrc.2015.06.154.
  - [84] Q. Liu, J. Zhang, Lipid metabolism in Alzheimer's disease, *Neurosci. Bull.* 30 (2014) 331–345. doi:10.1007/s12264-013-1410-3.
  - [85] C. Colombelli, M. Aoun, V. Tiranti, Defective lipid metabolism in neurodegeneration with brain iron accumulation (NBIA) syndromes: not only a matter of iron, *J. Inherit. Metab. Dis.* 38 (2014) 123–136. doi:10.1007/s10545-014-9770-z.
  - [86] V. Leoni, C. Caccia, Study of cholesterol metabolism in Huntington's disease, *Biochem. Biophys. Res. Commun.* 446 (2014) 697–701. doi:10.1016/j.bbrc.2014.01.188.
  - [87] J. Zhang, Q. Liu, Cholesterol metabolism and homeostasis in the brain, *Protein Cell.* 6 (2015) 254–264. doi:10.1007/s13238-014-0131-3.
  - [88] H. Kölsch, R. Heun, A. Kerksiek, K. V. Bergmann, W. Maier, D. Lütjohann, Altered levels of plasma 24S- and 27-hydroxycholesterol in demented patients, *Neurosci. Lett.* 368 (2004) 303–308. doi:10.1016/j.neulet.2004.07.031.
  - [89] D. Lütjohann, a Papassotiropoulos, I. Björkhem, S. Locatelli, M. Bagli, R.D. Oehring, U. Schlegel, F. Jessen, M.L. Rao, K. von Bergmann, R. Heun, Plasma 24S-hydroxycholesterol (cerebrosterol) is increased in Alzheimer and vascular demented patients., *J. Lipid Res.* 41 (2000) 195–8.
  - [90] L. Puglielli, G. Konopka, E. Pack-Chung, L.A. Ingano, O. Berezovska, B.T. Hyman, T.Y. Chang, R.E. Tanzi, D.M. Kovacs, Acyl-coenzyme A: cholesterol acyltransferase modulates the generation of the amyloid beta-peptide, *Nat Cell Biol.* 3 (2001) 905–12.
  - [91] B. Hutter-Paier, H.J. Huttunen, L. Puglielli, C.B. Eckman, D.Y. Kim, A. Hofmeister, R.D. Moir, S.B. Domnitz, M.P. Frosch, M. Windisch, D.M. Kovacs, The ACAT inhibitor CP-113,818 markedly reduces amyloid pathology in a mouse model of

- Alzheimer's disease, *Neuron*. 44 (2004) 227–238. doi:10.1016/j.neuron.2004.08.043.
- [92] M. Doria, L. Maugest, T. Moreau, G. Lizard, A. Vejux, Contribution of cholesterol and oxysterols to the pathophysiology of Parkinson's disease, *Free Radic. Biol. Med.* 101 (2016) 393–400. doi:10.1016/j.freeradbiomed.2016.10.008.
- [93] J. Abdel-Khalik, E. Yutuc, P.J. Crick, J.-Å. Gustafsson, M. Warner, G. Roman, K. Talbot, E. Gray, W.J. Griffiths, M.R. Turner, Y. Wang, Defective cholesterol metabolism in amyotrophic lateral sclerosis, *J. Lipid Res.* 58 (2017) 267–278. doi:10.1194/jlr.P071639.
- [94] R.G. Cutler, J. Kelly, K. Storie, W.A. Pedersen, A. Tammara, K. Hatanpaa, J.C. Troncoso, M.P. Mattson, Involvement of oxidative stress-induced abnormalities in ceramide and cholesterol metabolism in brain aging and Alzheimer's disease, *Proc. Natl. Acad. Sci.* 101 (2004) 2070–2075. doi:10.1073/pnas.0305799101.
- [95] X. Han, D. Holtzman, D.W. McKeel, J. Kelley, J.C. Morris, Substantial sulfatide deficiency and ceramide elevation in very early Alzheimer's disease: Potential role in disease pathogenesis, *J. Neurochem.* 82 (2002) 809–818. doi:10.1046/j.1471-4159.2002.00997.x.
- [96] S.K. Abbott, H. Li, S.S. Muñoz, B. Knoch, M. Batterham, K.E. Murphy, G.M. Halliday, B. Garner, Altered ceramide acyl chain length and ceramide synthase gene expression in Parkinson's disease, *Mov. Disord.* 29 (2014) 518–526. doi:10.1002/mds.25729.
- [97] M.M. Mielke, W. Maetzler, N.J. Haughey, V.V.R. Bandaru, R. Savica, C. Deuschle, T. Gasser, A.K. Hauser, S. Gräber-Sultan, E. Schleicher, D. Berg, I. Liepelt-Scarfone, Plasma Ceramide and Glucosylceramide Metabolism Is Altered in Sporadic Parkinson's Disease and Associated with Cognitive Impairment: A Pilot Study, *PLoS One*. 8 (2013) 1–6. doi:10.1371/journal.pone.0073094.
- [98] S.K. Abbott, A.M. Jenner, A.S. Spiro, M. Batterham, G.M. Halliday, B. Garner, Fatty acid composition of the anterior cingulate cortex indicates a high susceptibility to lipid peroxidation in Parkinson's disease., *J Park. Dis.* 5 (2015) 175–85.
- [99] T. Fraser, H. Tayler, S. Love, Fatty acid composition of frontal, temporal and parietal neocortex in the normal human brain and in Alzheimer's disease, *Neurochem. Res.* 35 (2010) 503–513. doi:10.1007/s11064-009-0087-5.
- [100] R. Nitsch, A. Pittas, J.K. Blusztajn, B.E. Slack, J.H. Growdon, R.J. Wurtman, Alterations of phospholipid metabolites in postmortem brain from patients with Alzheimer's disease., *Ann N Y Acad Sci.* 640 (1991) 100–3.
- [101] Z. Li, J. Zhang, H. Sun, Increased plasma levels of phospholipid in Parkinson's disease with mild cognitive impairment, *J. Clin. Neurosci.* 22 (2015) 1268–1271. doi:10.1016/j.jocn.2015.02.013.
- [102] Y. Xiang, S.M. Lam, G. Shui, What can lipidomics tell us about the pathogenesis of Alzheimer disease?, *Biol. Chem.* 396 (2015) 1281–1291. doi:10.1515/hsz-2015-0207.
- [103] D. Touboul, M. Gaudin, Lipidomics of Alzheimer's disease., *Bioanalysis.* 6 (2014) 541–61.
- [104] H. Blasco, C. Veyrat-Durebex, C. Bocca, F. Patin, P. Vourc'H, J. Kouassi Nzoughe, G. Lenaers, C.R. Andres, G. Simard, P. Corcia, P. Reynier, Lipidomics Reveals

- Cerebrospinal-Fluid Signatures of ALS, *Sci. Rep.* 7 (2017) 1–10. doi:10.1038/s41598-017-17389-9.
- [105] J.M. Dietschy, S.D. Turley, *Thematic review series: Brain Lipids*. Cholesterol metabolism in the central nervous system during early development and in the mature animal, *J. Lipid Res.* 45 (2004) 1375–1397. doi:10.1194/jlr.R400004-JLR200.
- [106] R.G. Cutler, W.A. Pedersen, S. Camandola, J.D. Rothstein, M.P. Mattson, Evidence that accumulation of ceramides and cholesterol esters mediates oxidative stress - Induced death of motor neurons in amyotrophic lateral sclerosis, *Ann. Neurol.* 52 (2002) 448–457. doi:10.1002/ana.10312.
- [107] M. V. Dupuis L, Corcia P, Fergani A, Gonzalez De Aguilar JL, Bonnefont-Rousselot D, Bittar R, Seilhean D, Hauw JJ, Lacomblez L, Loeffler JP, Dyslipidemia is a protective factor in amyotrophic lateral sclerosis., *Neurology.* 70 (2008) 1004–9.
- [108] J. Dorst, P. Kühnlein, C. Hendrich, J. Kassubek, A.D. Sperfeld, A.C. Ludolph, Patients with elevated triglyceride and cholesterol serum levels have a prolonged survival in amyotrophic lateral sclerosis, *J. Neurol.* 258 (2011) 613–617. doi:10.1007/s00415-010-5805-z.
- [109] B. a. Golomb, E.K. Kwon, S. Koperski, M. a. Evans, Amyotrophic Lateral Sclerosis-Like Conditions in Possible Association with Cholesterol-Lowering Drugs, *Drug Saf.* 32 (2009) 649–661. doi:10.2165/00002018-200932080-00004.
- [110] S. Kim, M. Noh, H. Kim, S. Cheon, K. Mi, J. Lee, E. Cha, K.S. Park, K. Lee, S.H. Kim, 25-Hydroxycholesterol is involved in the pathogenesis of amyotrophic lateral sclerosis, 8 (2017) 11855–11867. doi:10.18632/oncotarget.14416.
- [111] L.L. Smith, Review of progress in sterol oxidations: 1987-1995, *Lipids.* 31 (1996) 453–487. doi:10.1007/BF02522641.
- [112] V. Mutemberezi, O. Guillemot-Legris, G.G. Muccioli, Oxysterols: From cholesterol metabolites to key mediators, *Prog. Lipid Res.* 64 (2016) 152–169. doi:10.1016/j.plipres.2016.09.002.
- [113] W.J. Griffiths, Y. Wang, An update on oxysterol biochemistry: New discoveries in lipidomics, *Biochem. Biophys. Res. Commun.* (2018) 1–6. doi:10.1016/j.bbrc.2018.02.019.
- [114] L.L. Smith, J.I. Teng, M.J. Kulig, F.L. Hill, Sterol metabolism. 23. Cholesterol oxidation by radiation-induced processes, *J Org Chem.* 38 (1973) 1763–1765. [http://www.ncbi.nlm.nih.gov/entrez/query.fcgi?cmd=Retrieve&db=PubMed&dopt=Citation&list\\_uids=4709674](http://www.ncbi.nlm.nih.gov/entrez/query.fcgi?cmd=Retrieve&db=PubMed&dopt=Citation&list_uids=4709674).
- [115] A.W. Girotti, New trends in photobiology. Photosensitized oxidation of cholesterol in biological systems: Reaction pathways, cytotoxic effects and defense mechanisms, *J. Photochem. Photobiol. B Biol.* 13 (1992) 105–118. doi:10.1016/1011-1344(92)85050-5.
- [116] P. Wentworth, J. Nieva, C. Takeuchi, R. Galve, A.D. Wentworth, R.B. Dilley, G.A. DeLaria, A. Saven, B.M. Babior, K.D. Janda, A. Eschenmoser, R.A. Lerner, Evidence for ozone formation in human atherosclerotic arteries., *Science.* 302 (2003) 1053–6. doi:10.1126/science.1089525.

- [117] A. Okado-Matsumoto, I. Fridovich, Subcellular distribution of superoxide dismutases (SOD) in rat liver. Cu,Zn-SOD in mitochondria, *J. Biol. Chem.* 276 (2001) 38388–38393. doi:10.1074/jbc.M105395200.
- [118] L.A. Sturtz, K. Diekert, L.T. Jensen, R. Lill, V.C. Culotta, A fraction of yeast Cu,Zn-superoxide dismutase and its metallochaperone, CCS, localize to the intermembrane space of mitochondria. A physiological role for SOD1 in guarding against mitochondrial oxidative damage, *J. Biol. Chem.* 276 (2001) 38084–38089. doi:10.1074/jbc.M105296200.
- [119] J.P. Crow, J.B. Sampson, Y. Zhuang, J. a Thompson, J.S. Beckman, Decreased zinc affinity of amyotrophic lateral sclerosis-associated superoxide dismutase mutants leads to enhanced catalysis of tyrosine nitration by peroxynitrite., *J. Neurochem.* 69 (1997) 1936–1944. doi:10.1046/j.1471-4159.1997.69051936.x.
- [120] K.A. Trumbull, J.S. Beckman, A role for copper in the toxicity of zinc-deficient superoxide dismutase to motor neurons in amyotrophic lateral sclerosis., *Antioxid. Redox Signal.* 11 (2009) 1627–39. doi:10.1089/ars.2009.2574.
- [121] I. Choi, Y. In Yang, H.D. Song, J.S. Lee, T. Kang, J.J. Sung, J. Yi, Lipid molecules induce the cytotoxic aggregation of Cu/Zn superoxide dismutase with structurally disordered regions, *Biochim. Biophys. Acta - Mol. Basis Dis.* 1812 (2011) 41–48. doi:10.1016/j.bbadis.2010.09.003.
- [122] H. Karube, M. Sakamoto, S. Arawaka, S. Hara, H. Sato, C.H. Ren, S. Goto, S. Koyama, M. Wada, T. Kawanami, K. Kurita, T. Kato, N-terminal region of  $\alpha$ -synuclein is essential for the fatty acid-induced oligomerization of the molecules, *FEBS Lett.* 582 (2008) 3693–3700. doi:10.1016/j.febslet.2008.10.001.
- [123] K. Broersen, D. Van Den Brink, G. Fraser, M. Goedert, B. Davletov,  $\alpha$ -Synuclein Adopts an  $\alpha$ -Helical Conformation in the Presence of Polyunsaturated Fatty Acids To Hinder Micelle Formation, *Biochemistry.* 45 (2006) 15610–15616. doi:10.1021/bi061743l.

## CURRICULUM VITAE

### **Personal data**

**Name:** Lucas Souza Dantas

**Birth and place:** April 5 1990, in São Paulo (Brazil)

**E-mail:** lucassouza\_farma@usp.br

**Current occupation:** PhD student – Biological Sciences (Biochemistry), Universidade de São Paulo (São Paulo, SP), with scholarship from Conselho Nacional de Desenvolvimento Científico e tecnológico (CNPq).

### **Education**

**2013 – present:** PhD student – Biological Sciences (Biochemistry), Universidade de São Paulo (São Paulo, SP). Advisor: Dra. Sayuri Miyamoto

**2008 – 2013:** Bachelor in Pharmacy. Universidade Federal de Sergipe (Aracaju, SE).

### **Complementary education**

**2016 - 2016:** XI Curso de Inverno Temas Avançados em Bioquímica. (Carga horária: 40h). Instituto de Química - USP, IQ, Brasil.

**2014 – 2014:** 1ª Escola Brasileira de Espectrometria de Massas – BrMASS. Natal, Brasil.

**2014 – 2014:** Processos Redox em Biomedicina. (Carga horária: 6h). Sociedade Brasileira de Bioquímica e Biologia Molecular, SBBQ, Brasil.

**2014 - 2014:** IX Curso de Inverno Temas Avançados em Bioquímica. (Carga horária: 40h). Instituto de Química - USP, IQ, Brasil.

**2012 - 2012:** Extensão universitária em Estágio: Lab. de Pesquisa em Lipídeos Modificados. (Carga horária: 80h). Instituto de Química - USP, IQ, Brasil.

**2012 – 2012:** Curso Básico sobre HPLC. (Carga horária: 9h). Universidade Federal de Sergipe, UFS, Brasil.

**2009 – 2013:** Iniciação científica. Universidade Federal de Sergipe, UFS, Brasil.

### **Awards**

**2016:** Travel Award, Society for Redox Biology and Medicine. San Francisco, CA. Poster presentation: *"Cholesterol secosterol aldehydes are increased in amyotrophic lateral sclerosis rat model and induce covalent modification and aggregation of Cu,Zn-superoxide dismutase."*

**2015:** Travel Award, Society for Redox Biology and Medicine. Boston, MA. Poster presentation: *"Lipid-derived electrophiles induce covalent modification and aggregation of Cu,Zn-superoxide dismutase in a hydrophobicity-dependent manner."*

**2010:** Menção Honrosa, X Reunião Regional Nordeste da Sociedade Brasileira de Bioquímica e Biologia Molecular - SBBq. Poster presentation: *"Evaluation of inhibition of lipid peroxidation and antioxidant activity of Angico de caroço (Anadenanthera macrocarpa) stem bark extract."*

### **Publications**

1. Bispo, Vanderson S.; Dantas, Lucas S.; Chaves-Filho, Adriano B.; Pinto, Isabella F.D.; Silva, Railmara P.; Otsuka, Felipe A.M.; Santos, Rodrigo B.; Santos, Aline C.; Trindade, Danielle J.; Matos, Humberto R. Reduction of the DNA damages, Hepatoprotective Effect and Antioxidant Potential of the Coconut Water, Ascorbic and Caffeic Acids in Oxidative Stress Mediated by Ethanol. Anais da Academia Brasileira de Ciências, v. 89, p. 1095-1109, 2017.



2. Pinto, Isabella F.D.; Silva, Railmara P.; Chaves-Filho, Adriano B.; Dantas, Lucas S.; Bispo, Vanderson S.; Matos, Isaac A.; Otsuka, Felipe A.M.; Santos, Aline C.; Matos, Humberto R. Study of Antiglycation, Hypoglycemic, and Nephroprotective Activities of the Green Dwarf Variety Coconut Water (*Cocos nucifera* L.) in Alloxan-Induced Diabetic Rats. *Journal of Medicinal Food*, v. 18, p. 802-809, 2015.

3. Santos, João L.A.; Bispo, Vanderson S.; Chaves-Filho, Adriano B.; Pinto, Isabella F.D.; Dantas, Lucas S.; Vasconcelos, Daiane F.; Abreu, Fabíula F.; Melo, Danilo A.; Matos, Isaac A.; Freitas, Florêncio P.; Gomes, Osmar F.; Medeiros, Marisa H.G.; Matos, Humberto R. Evaluation of Chemical Constituents and Antioxidant Activity of Coconut Water (*Cocos nucifera* L.) and Caffeic Acid in Cell Culture. *Anais da Academia Brasileira de Ciências*, v. 85, p. 1235-1247, 2013.

### **Participation in scientific events**

**2017** - 15th Euro Fed Lipid Congress and Expo (Suécia).

**2017** - Tsukuba Global Science Week. (Japão)

**2016** - 23rd Annual Meeting of Society for Redox Biology and Medicine (Estados Unidos).

**2016** - XI Congresso do Departamento de Bioquímica do IQ-USP (Brasil).

**2015** - 22nd Annual Meeting of Society for Redox Biology and Medicine (Estados Unidos).

**2014** - Mini-Symposium on Singlet Oxygen. (Brasil).

**2014** - XLIII Annual Meeting of Brazilian Society for Biochemistry and Molecular Biology (SBBq) (Brasil).

**2013** - Antioxidants and Redox Process in Health (Brasil).

**2013** - XLII Annual Meeting of The Brazilian Biochemistry and Molecular Biology Society (SBBq) (Brasil).

**2012** - XLI Annual Meeting of The Brazilian Biochemistry and Molecular Biology Society (SBBq) (Brasil).

**2011** - 21º Encontro de Iniciação Científica da Universidade Federal de Sergipe (Brasil).

**2011** - II Curso de Semiologia Farmacêutica (Brasil).

**2010** - VI Semana Farmacêutica da Universidade Federal de Sergipe (Brasil).

**2010** - X Reunião Regional Nordeste Sociedade Brasileira de Bioquímica e Biologia Molecular - SBBq (Brasil).

**2009** - V Semana Farmacêutica da Universidade Federal de Sergipe (Brasil).

**2008** - IV Semana Farmacêutica da Universidade Federal de Sergipe (Brasil).